

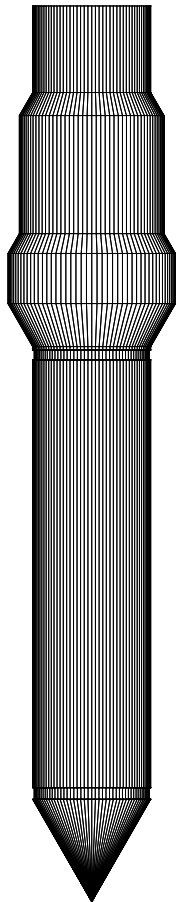
**FINAL REPORT**  
**September 2003**

---

Geotechnical Engineering Research Report No. BC-354  
UF Project No. 4504-724-12  
Contract No. BC-354, RPWO #10

---

**DESIGN, CONSTRUCTION AND EVALUATION OF**  
**A**  
**DUAL TIP PENETROMETER**



FDOT Technical Coordinator: Peter Lai, P.E.



UF Principal Investigator: David Bloomquist, P.E.  
Graduate Research Assistant: Jaime Velez, E.I.



Department of Civil and Coastal Engineering  
College of Engineering  
University of Florida  
Gainesville, Florida 32611

---

1. Report No.  10	2. Government Accession No.	3. Recipient's Catalog No.	
4. Title and Subtitle  <b>DESIGN, CONSTRUCTION AND EVALUATION OF A DUAL TIP PENETROMETER</b>		5. Report Date  September 30, 2003	
		6. Performing Organization Code	
		8. Performing Organization Report No.	
7. Author(s) David Bloomquist P.E. and Jaime Andres Velez, E.I.T.		10. Work Unit No. (TRAIS)  99700-	
9. Performing Organization Name and Address  University of Florida Department of Civil and Coastal Engineering 365 Weil Hall / P.O. Box 116580 Gainesville, FL 32611-6580		11. Contract or Grant No.  BC-354, RPWO #10	
		13. Type of Report and Period Covered  FINAL REPORT September 1, 2002, to September 30, 2003	
12. Sponsoring Agency Name and Address  Florida Department of Transportation 605 Suwannee Street, MS 30 Tallahassee, FL 32399 (850) 414-4615		14. Sponsoring Agency Code	
		15. Supplementary Notes  Prepared in cooperation with USDOT and FHWA	
16. Abstract  This final report discusses the testing of the Dual Tip Penetrometer device that was developed at the University of Florida. A calibration chamber was set up for testing the Dual Tip Penetrometer in clean fine sand and artificially cemented sand. In addition to the calibration chamber tests, field tests were performed and compared with standard cone penetration tests performed at the same locations. The Dual Tip Penetrometer and Cone Penetrometer were then used at the West Bay Bridge in West Bay, Florida where driven pile data was available. The DTP results were then used in an attempt to predict pile capacities for the dynamically loaded test piles. These comparisons were then compared with the capacities determined from Pile Driving Analysis data. Data reduction software developed for the Dual Tip Penetrometer is also discussed. In the near future, the University of Florida along with the Florida Department of Transportation will perform additional Dual Tip Penetrometer soundings and analysis.			
17. Key Words  Cone Penetrometer, Cemented sands		18. Distribution Statement  No restrictions. This document is available to the public through the National Technical Information Service, Springfield, VA, 22161	
19. Security Classif. (of this report)  Unclassified	20. Security Classif. (of this page)  Unclassified	21. No. of Pages  165	22. Price

# TABLE OF CONTENTS

<b>DRAFT - FINAL REPORT .....</b>	<b>1</b>
<b>JULY 2003 .....</b>	<b>1</b>
<b>CHAPTER 1: CEMENTED SANDS .....</b>	<b>1</b>
INTRODUCTION .....	1
CEMENTATION .....	1
GEOTECHNICAL ISSUES IN CEMENTED SANDS .....	2
PREVIOUS RESEARCH .....	3
DUAL TIP PENETROMETER.....	4
PURPOSE AND SCOPE OF RESEARCH .....	6
<b>CHAPTER 2: TIP RATIO EFFECTS.....</b>	<b>7</b>
FACTORS THAT AFFECT TIP 1 AND TIP 2 BEARING .....	7
Soil Relative Density ( $D_r$ ) .....	8
Cementation .....	11
Effective Confining Stresses ( $\sigma'_v$ and $\sigma'_h$ ) .....	13
Chamber to Penetrometer Diameter Ratio ( $R_d$ ) and Boundary Conditions .....	17
Heterogeneous Soil Effects .....	19
SUMMARY OF TRENDS .....	19
<b>CHAPTER 3: PLAXIS ANALYSIS .....</b>	<b>22</b>
PLAXIS: FINITE ELEMENT CODE FOR SOIL AND ROCK ANALYSIS .....	23
Introduction .....	23
Purpose .....	23
Process .....	23
Geometry Input .....	23
Interfaces .....	25
Loads & Prescribed Displacements .....	26
Material Properties .....	26
Calculations Program .....	26
PLAXIS RESULTS .....	26
DTP/CPT Modeling Analysis .....	27
Pipe Diameter Analysis .....	29
Comment on PLAXIS .....	30
<b>CHAPTER 4: FIELD TEST RESULTS.....</b>	<b>31</b>
CLEAN FINE SANDS AT ARCHER LANDFILL IN ARCHER, FLORIDA .....	31
CEMENTED CALCAREOUS SANDS IN ORLANDO, FLORIDA & WEST BAY, FLORIDA .....	36
UCF in Orlando, Florida .....	36
West Bay Bridge Near Panama City, Florida .....	40
MIXED SOILS AND SOFT SOILS .....	43
REPEATABILITY OF DTP PARAMETERS IN HOMOGENEOUS AND HETEROGENEOUS SOILS .....	49
<b>CHAPTER 5: CALIBRATION CHAMBER TEST RESULTS .....</b>	<b>51</b>
CALIBRATION CHAMBER HISTORY AND DESIGN .....	51
DRY SAND TESTING .....	54
RESULTS OF CALIBRATION CHAMBER TESTING IN DRY SAND .....	60
CALIBRATION CHAMBER SETUP FOR THE CEMENTED SAND TESTS .....	67
RESULTS OF THE CALIBRATION CHAMBER TESTING .....	70

SUMMARY OF FIELD RESULTS AND CHAMBER TESTS .....	77
<b>CHAPTER 6: SOIL CLASSIFICATION AND DTP 2002 SOFTWARE</b> .....	<b>79</b>
SOIL CLASSIFICATION .....	79
DTP 2002 SOFTWARE .....	80
DTP2002 USER'S GUIDE .....	81
<b>CHAPTER 7: WEST BAY BRIDGE PILE CAPACITY EVALUATION</b> .....	<b>83</b>
USING THE DTP TO DETERMINE PILE CAPACITIES .....	83
WEST BAY BRIDGE TEST PILE CAPACITIES .....	83
<b>CHAPTER 8: CONCLUSIONS AND RECOMMENDATIONS .....</b>	<b>94</b>
CONCLUSIONS .....	94
RECOMMENDATIONS .....	96
<b>REFERENCES.....</b>	<b>97</b>
<b>APPENDIX A.....</b>	<b>99</b>
<b>APPENDIX B.....</b>	<b>141</b>
<b>APPENDIX C.....</b>	<b>158</b>

## **CHAPTER 1: CEMENTED SANDS**

### **Introduction**

One of the more challenging types of soil for geotechnical engineers to work with is cemented sand. While cementation in sands improves its static strength, this strength gain is tenuous at best, since energy imparted into a cemented soil mass (e.g., via pile driving, blasting or earthquake) can sever the interstitial bonds, resulting in a weakened condition. For this reason, identification of as well as the degree of cementation is very important to designers who must weigh the effect of this in their design calculations. The degree of the bond strength in the cemented sands should be considered when designing foundations on or in cemented sands.

### **Cementation**

When a geotechnical analysis of a site is performed, an engineer can encounter rock or a variety of soil types including clay, silt, sand and gravel. The soil encountered may also be a conglomerate of these main soil types. These soil types can also change from one type to another due to geological processes and time. For example, a rock can turn into sediment through weathering by wind, water or ice. Conversely, sediment such as sand can turn into a rock (i.e. sandstone or limestone) after deposition due to packing of the particles and cementation of the grains. The cementing process consists of the chemical precipitation of a mineral phase such as calcite, dolomite or quartz into a pore space (Randazzo, 1997). Cemented sand is the general term given to sand when it is in the cementation phase.

Cemented sands exist in many areas of the United States including California, Texas, Florida, and along the banks of the lower Mississippi River, as well as in parts of Norway, Australia, Canada, and Italy (Puppala et al. 1995). The calcareous cemented soils are also a feature of warm water seas mainly due to the sedimentation of the skeletal remains of marine organisms (Lunne et al. 1997). The skeletal remains are a source of calcium carbonate, the acting cement in these cemented soils. Other natural cements include hydrous iron oxides, hydrous silicates, gypsum and silica (Clough et al., 1981).

The term “cemented sand” can be a very general term used for a wide variety of soils. King proposed a classification system for a variety of cemented carbonate soils (Table 1.1).

		FINE GRAINED				MEDIUM-COARSE GRAINED							
		INCREASING GRAINSIZE											
		0.002mm	0.006mm	0.02mm	0.06mm	0.2mm	0.6mm	2mm	6mm	20mm	60mm	DEGREE OF CEMENTATION	CONE RESISTANCE $q_c$ MN/m <sup>2</sup>
SOIL	VERY WEAKLY INDURATED	0-2										VERY WEAKLY CEMENTED	0-2
	WEAKLY INDURATED	2-4		CARBONATE MUD	CARBONATE SILT	CARBONATE SAND <small>clastic/bioclastic/oolitic</small>			CARBONATE GRAVEL <small>clastic/bioclastic</small>			WEAKLY CEMENTED	2-4
	FIRMLY INDURATED	4-10										FIRMLY CEMENTED	4-10
	WELL INDURATED	>10		CALCILUTITE <small>(carb mudstone)</small>	CALCISILTITE <small>(carb siltstone)</small>	CALCARENITE <small>(carb sandstone)</small> <small>clastic/bioclastic/oolitic</small>			CALCIRUDITE <small>(carb congl. or breccia)</small> <small>clastic/bioclastic</small>			WELL CEMENTED	>10
ROCK				FINE GRAINED LIMESTONE		DETRITAL LIMESTONE <small>clastic/bioclastic/oolitic</small>			CONGLOMERATE LIMESTONE <small>clastic/bioclastic</small>				
				CRYSTALLINE LIMESTONE		CRYSTALLINE LIMESTONE							

Classification of Carbonate Sediments (90-100% carbonate)  
(modified after Clark and Walker, 1977)

Table 1.1: Classification system for Calcareous Soils proposed by King et al. (Lunne et al. 1997).

### Geotechnical Issues in Cemented Sands

The degree of cementation in sands can be an issue for geotechnical engineers. For dense cemented sands the strength is high and usually not a concern. However, if the sand is weakly cemented then a breakdown in cohesion can occur from a disturbance such as that of an earthquake or pile driving. One such example is when the Loma Prieta San Francisco earthquake caused slope failures along the cemented northern Daly City bluffs (Puppala et al. 1995). Other similar slope failures have occurred due to earthquakes and heavy rains (Rad and Clough 1980; Rad and Tumay, 1986).

Pile capacities can also be affected by the presence of weakly cemented sands. If Cone Penetration Test (CPT) results are used to determine the pile capacity in cemented sands then the tip and frictional capacity for the pile could be overestimated. Cementation has been

found to increase CPT tip bearing and friction sleeve readings (Puppala et al. 1995) and therefore can be a problem for pile capacity determination. If the sands found with a CPT test are not known to be cemented then the high bearing readings may be misinterpreted as being due to high relative densities. This can lead to an underestimation of the liquefaction potential of the soil. The pile friction capacity can also be overestimated. The pile side friction capacities assessed from CPT tests for piles at two sites -- North Rankin offshore Australia and Matinlock Platforms in the Philippines -- were grossly over predicted compared to the actual values (Lunne et al. 1997). An overestimation of pile tip bearing can also result in the necessary splicing of additional pile length in order to reach a high enough tip resistance.

### **Previous Research**

Much research has been performed on cemented sands in an effort to better understand their properties and behavior. Many different tests have been performed on both naturally and artificially cemented sands including CPT tests, unconfined compressive strength tests, triaxial tests and plate load tests.

Some researchers have performed laboratory tests on cemented soils obtained in the field. Both Clough et al. and Puppala et al. (1998) have tested naturally cemented sands in triaxial tests and unconfined compressive tests. The cemented sands were obtained by trimming block samples. The sampling of the weakly cemented sands was tricky since the bonds tended to break easily under light finger pressure.

Due to the difficulty in sampling cemented sands insitu testing has become a more popular method of testing the natural cemented sands. The CPT test is a popular device for testing the cemented sands. The CPT test has been used to test both naturally occurring cemented sands in the field (Puppala et al., 1998) and artificially cemented sands in calibration chambers (Rad & Tumay, 1986; and Puppala et al. 1995). In both the 1985 and 1996 calibration chamber studies Monterrey no. 0/30 sand was cemented with 1% and 2% Portland cement. An attempt was made to relate the tip bearing and friction sleeve values to the sand properties including cement content, relative density, confining stress and friction angle.

Puppala (1991 and 1995) did this by using the bearing capacity equations of Durgunoglu & Mitchell (1973) and Janbu & Senneset (1974). To get the effect of cementation or cohesion on the tip bearing the other parameters that affect the tip bearing, mainly relative density and confining stress, needed to be known and put into the equations proposed by Puppala.

Since the main concern in weakly cemented sands is the effect of cohesion on tip bearing resistance then maybe its effect could be removed from the tip bearing resistance. It may then be possible to get more accurate bearing predictions. One way to do this would be to design an insitu device that could measure the bearing strength of the cemented sands after the cohesive bonds have been broken up. This is the idea behind the Dual Tip Penetrometer developed at the University of Florida.

### **Dual Tip Penetrometer**

The Dual Tip Penetrometer (DTP) is a device designed to measure broken up cemented sand bearing resistance. The DTP is similar to the standard electronic cone penetration test except for an additional bearing annulus located just above the friction sleeve. The annulus is a floating member that measures upward bearing resistance. The annulus has the same 60° slope and bearing area (10 cm<sup>2</sup>) as the bottom tip (Tip 1 in Figure 1.1). The idea was that tip 1 would break down the cohesive bonds of the cemented sand while the upper tip would measure the residual or broken up bearing resistance.



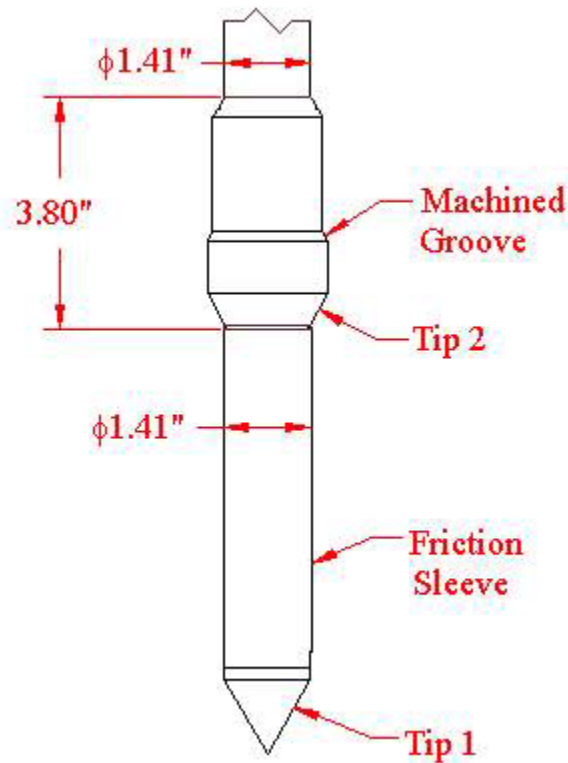


Figure 1.1: Dual Tip Penetrometer

The DTP is the latest version of a series of devices developed at the University of Florida intended for use in cemented sands. Daniel Hart developed the first version of the device in 1996. This device had a lip welded onto the top of the friction sleeve. However, this meant that the bearing reading measured by the lip was added to the frictional component measured by the friction sleeve strain gauge. The lip also made it difficult to remove the cone from the ground. In 1998, Randell Hand eliminated the welded lip and instead welded a bearing annulus onto the friction reducer coupler. The annulus was therefore located about 20 inches above the top of the friction sleeve of the cone. Strain gages were used to measure resistance in an aluminum cylinder. The voltage output was translated into a second “ $q_c$ ” reading. Steve Kiser and Hogentogler & Co. Inc. in 1999 improved on the old design and came up with the new Dual Tip Penetrometer.

### **Purpose and Scope of Research**

The purpose of this research was to test the Dual Tip Penetrometer and then attempt to use it to predict pile tip capacity in cemented sand. To do this a calibration chamber was set up for testing clean fine sand and artificially cemented sand. In addition to the calibration chamber tests, field tests were performed and compared with standard cone penetration tests performed at the same locations. The DTP and CPT tests were then used at the West Bay Bridge in West Bay, Florida where driven pile data were available. The DTP results were then used to predict pile capacities for comparison with the capacities determined from Pile Driving Analysis data. Also, data reduction software was developed for the DTP.

## CHAPTER 2: TIP RATIO EFFECTS

The Dual Tip Penetrometer acquires three primary sounding values: the tip 1 bearing (T1), the friction reading (F) and finally a tip 2 bearing (T2). The DTP also monitors probe inclination and is capable of measuring pore pressures with the insertion of a porous plastic annulus directly behind T1. The tip ratio  $T2/T1$  is of particular interest, since this relationship helps determine whether the soil resistance increases or decreases between tip 1 and tip 2. For example, if  $T2/T1 < 1$ , then the local bearing strength of the soil has decreased after being “failed” by tip 1 and the trailing friction sleeve (5 inches in length). Conversely, if  $T2/T1 > 1$  then the bearing strength has increased. Of course, this interpretation requires that the bearing areas of tip 1 and 2 be equal, and the Wheatstone bridge calibration factors for both tips are similar.

### Factors That Affect Tip 1 and Tip 2 Bearing

Prior to analyzing the  $T2/T1$  ratio, those factors that affect tip 1 and tip 2 should be examined in greater detail. The tip 1 bearing strength value is identical to the  $q_c$  bearing strength of the standard cone penetrometer and hence is affected by several soil properties and insitu conditions. These include:

1. Relative Density  $D_r$  – for sand and cemented sands (Lunne et al. 1997).
2. Cohesion or Cementation – clays and silts (Puppala et al.)
3. Over Consolidation Ratio OCR – clays (Lunne et al. 1997).
4. Insitu Effective Stresses - ( $\sigma'_h$  and  $\sigma'_v$ )
5. Undrained Shear Strength  $s_u$  – in Undrained Soils (Teh)
6. Rigidity Index  $G/s_u$  in Undrained Soils (Teh)
7. Chamber Diameter to Penetrometer Diameter Ratio -  $R_d$  (Puppala et al.)
8. Boundary Conditions of a Calibration Chamber (BC1, BC2, BC3 and BC4 to be defined later)

Since these parameters affect the tip 1 bearing reading, it is reasonable to assume that they would also affect the tip 2 readings. Hence, if these variables change due to the penetration disturbance of tip 1, then one would expect a decrease (or in some cases, increase) in tip 2 bearing strength. In fact, even if all of the relevant parameters cited above were to remain unchanged after tip 1 passage, it is still reasonable to postulate that the rearrangement of the soil particles after this induced failure would somehow alter the bearing strength of tip 2. Regardless of the causal effects, the soil characteristics measured by tip 2 are always “disturbed” by the passage of tip 1. Hence understanding the attributes of this disturbance is crucial in a rational analysis of a DTP’s sounding test results.

Accordingly, this chapter examines parametric effects of items 1, 2, 4, 7 and 8 referred to above. Since one of the original objectives for the development of the DTP was cemented sand identification, the undrained shear strength, rigidity index and overconsolidation ratio effects are not considered. However, based on the results of this research, it was determined that when DTP sounding in soft clays, the T2/T1 ratio is very low. While additional scrutiny regarding the field-testing results will be discussed in the next chapter, this observation provides the user with an unintended benefit of the DTP, i.e., the probe appears to provide a remolded versus undisturbed cohesive soil relationship. Thus, pending additional testing, this device may augment or even supplant the traditional vane shear test.

### Soil Relative Density ( $D_r$ )

The relative density of a soil relates its current particle packing state (either insitu or laboratory prepared) to its most dense condition. Relative density is also a parameter related to a cohesionless soil’s strength, since the two are directly correlated. To obtain  $D_r$ , the maximum and minimum void ratios of the sand must first be determined from laboratory tests. The actual void ratio is then measured and related to the maximum and minimum void ratios. However, the existing “undisturbed” void ratio is usually only accurately known in prepared soil specimens, since it is difficult to determine insitu.

In triaxial tests, it is observed that dense sands exhibit greater strength than loose sands (Lambe and Whitman). CPT sand tests performed in large calibration chambers have also revealed that  $q_c$  readings increase with greater relative densities (Figure 2.3). However,

when sands fail during drained triaxial tests, they typically exhibit a volume change within the failure zone. Loose sands display only minor changes (there may be some slight contraction of particles), whereas dense sands tend to increase in volume (dilate) until the soil particles are sufficiently loose to shear. As one would expect, the volume increase diminishes as confining stresses increase. These trends also appear to hold true for cemented sands (Abdulla et al. and Clough 1997). Clough found that weakly and moderately cemented sands tend to dilate during drained triaxial tests. The dilational effect in cemented sands also decreases with increased confining stress (similar to non-cemented sands).

Dilation appears to occur in silty fine sands as well. Compressible fine silty sand from Taiwan (Mai Lao Sand), was tested under drained conditions in a triaxial apparatus and found to dilate under low confining stresses (49 KPa or 1,023 psf - Huang 1999). However, under increased confining stresses, the soil appeared to compress (a volume decrease) during shearing at high axial strains up to 25%. This volume decrease would indicate an increase in relative density. Therefore, the confining stress conditions to some extent, dictate which mechanism will occur during a shear failure.

It is important to note that volume changes primarily occur under drained conditions. Saturated fine-grained soils with low permeability (clays and some silts) respond as undrained material (pore pressure dissipation does not keep up with the deviator stress application) and usually will not dilate – especially under high strain rate loading.

It is reasonable to assume that what occurs in the triaxial test also occurs when a CPT or DTP tip fails the soil. However, the failure geometry is more complex for the soil adjacent to the tip than it is for a cylindrical triaxial test sample. For the DTP, the majority of soil particles in the vicinity of the tip are totally rearranged during failure. There does not appear to be a distinct failure shear plane, but rather a zone of plastic deformation as the soil is force down and away from the penetrometer. This pushing action is a complicated mechanism, in which shearing between sand particles along with some fracturing occurs, resulting in a thorough rearrangement of soil particles. For penetration depths greater than one to two feet (above this depth, shoving or heaving of the soil typically occurs), the failure mechanism is a compression of the soil beneath the penetrometer tip, including soil arching and grain crushing (Durgunoglu & Mitchell 1975). The soil failure adjacent to the tip differs from

triaxial shearing, since failure in the triaxial chamber is obtained by increasing the deviatoric principal stress until failure occurs. However, the cone tip also adds a shear stress to the soil at the tip and along the friction sleeve. The reaction to these stresses can be seen in Figure 2.1.

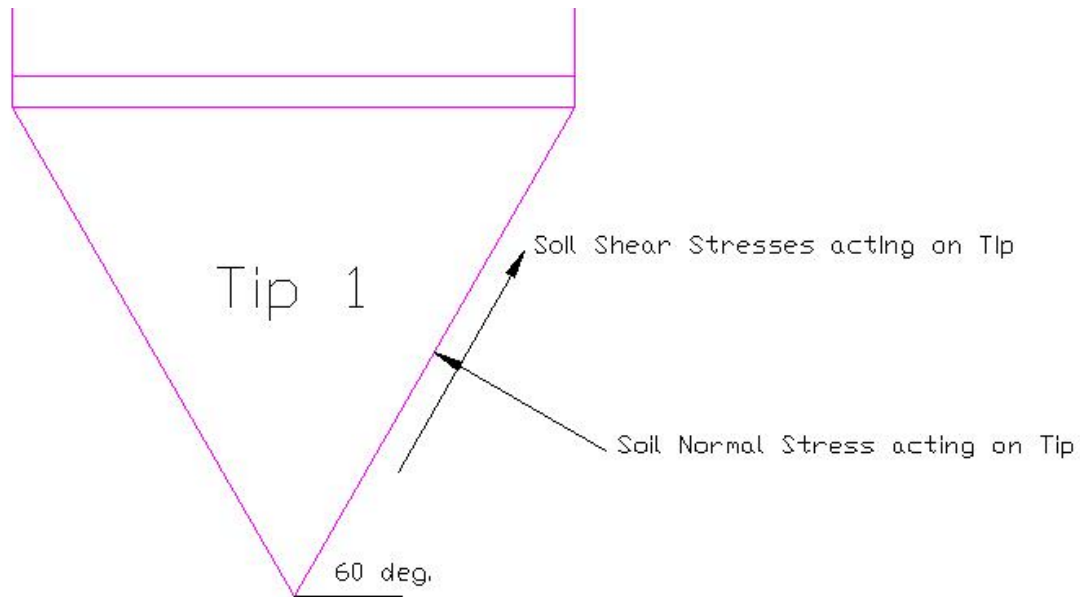


Figure 2.1: Stresses acting on tip 1

Although there are differences between the failure of a triaxial soil sample and a DTP, it is customary to assume that dilative soils will also dilate when failed by the DTP. For the dense sand particles to shift away from the advancing cone, they must interact (shear) with adjacent particles. This action, whereby they slide or rotate over one another creates dilation of the soil volume. On the other hand, in a low  $D_r$  soil, the particle-to-particle contact occurs at their respective asperities (soil tips), hence this contractive soil will typically densify during tip penetration. As the DTP's tip 1 penetrates, it strains the soil at a rapid rate (2 cm/sec), inducing large localized deformations and bearing capacity failures. For this rapid loading condition, it is assumed that saturated silt does not react as in a drained case, therefore little or no density change should occur between tips 1 and 2. Whether or not cemented sands exhibit drained material characteristics, is difficult to ascertain. It is expected that the presence of cementing agents (calcium carbonate, silicates, etc.) within the

soil voids decrease the permeability by partially occluding the capillary pores. However, when the cement bonds break, fracturing occurs and the permeability may increase significantly. Without a substantial laboratory effort to quantify this phenomenon, it must be tacitly assumed that cemented sands (from lightly to heavily cemented and from fine to coarse gradation) indeed act as a drained material. However, as described above, this assumption no doubt will complicate the DTP analysis, since the soil response is diametrically opposite for the two described conditions. Based on this conjecture, it is therefore expected that volume/density changes will have an effect on tip 1 and tip 2 in sands, cemented sands, and dry (or partially saturated) silts.

When the DTP is operated in dense sands and or cemented sands at relatively shallow depths, dilation and an increase in void ratio is expected. This increase in void ratio would then result in a decreased tip 2 bearing strength ( $T_2/T_1 < 1$ ). This phenomenon may also be viewed as a brittle failure mode. In this case, a brittle response is defined as a condition in which the peak strength is greater than the residual, large strain shear strength. Thus, if tip 1 fails the soil to the point where the peak strength is exceeded, then tip 2 will only experience the residual strength (the lower strength at large shear strains). This condition should dissipate with depth, since increasing confining stresses mitigate this effect.

In addition, if there is a compressible soil stratum, such as dry silty sand at significant depths, there may in fact be a volume decrease resulting in a relative density increase. This scenario would be similar to that of a very ductile soil. In this case, the strains produced by tip 1 would be insufficient to mobilize its peak strength; hence tip 2 would continue straining this highly compressible soil resulting in a higher resistance.

### Cementation

The influence of cementation in sands in triaxial and cone penetration tests can be very important. In both venues, cementation has been found to increase the strength of the soil. The increase is proportional to the cement content. In triaxial tests at UF as well as Clough et al. and Schniad et al. found that cementation produces an effect similar to a cohesion intercept and not greatly affecting the friction angle of the soil. The strength increase due to cementation appears to decrease with increased confining stresses. These trends were

observed for calibration chamber cone penetration tests performed in artificially cemented sands (Puppala et al. 1995 and 1998). A plot of CPT  $q_c$  bearing strength due to cementation divided by the uncemented  $q_c$  bearing strength with respect to vertical effective stress (normalized by atmospheric pressure) is shown in Figure 2.2.

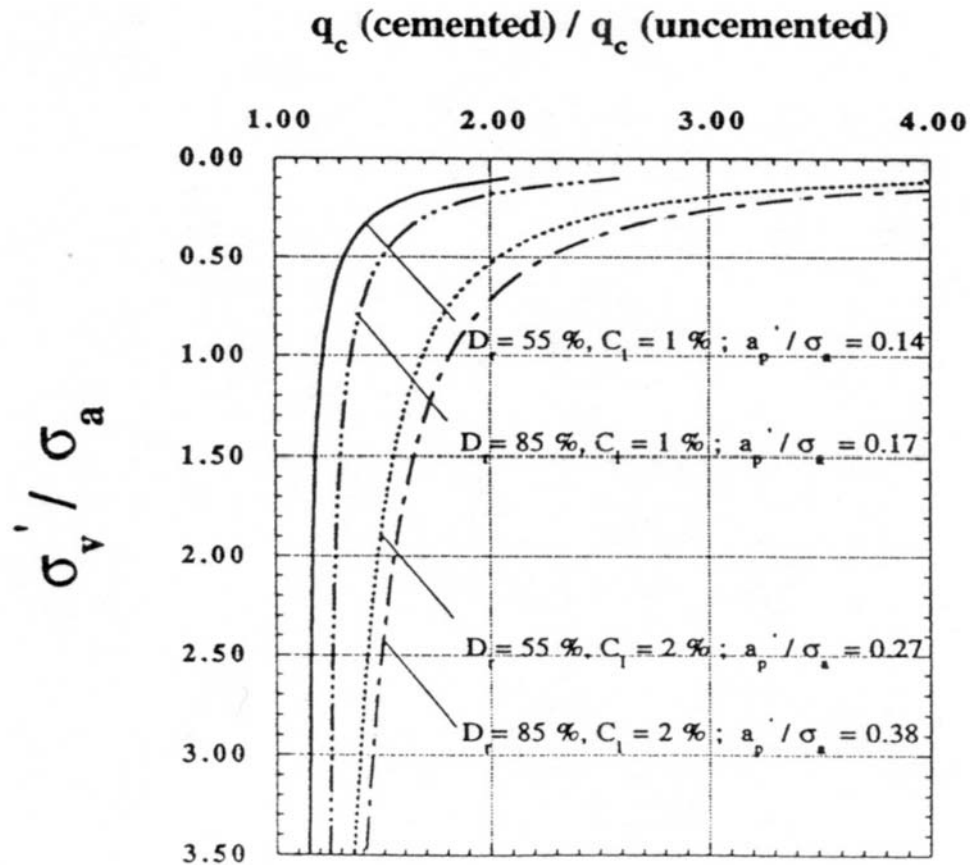


Figure 2.2: Relative Effect of Weak Cementation (1% and 2%) on Tip Resistance in Monterey No. 0/30 Sand (Puppala et al. 1995)

Figure 2.2 illustrates that, although the influence of cementation decreases with depth, the increase in strength appears to reach a constant value at deeper depths (approximately 1.2 for the 1% cement content and 1.4 for a 2% cement content).

It is assumed that as the DTP tip 1 penetrates a cemented sand, the interstitial bonds rupture which in turn will manifest itself at tip 2 as a lower bearing strength value. This effect should be proportional to the degree of cementation. Higher cement content should produce a greater tip 1 bearing, but due to its greater brittleness, the decrease at tip 2 will also be



greater. One major assumption in this line of reasoning is that all of the cement bonds are broken within a reasonable distance away from the tip. While it is logical to expect the majority bonds to be broken contiguous to the actual tip, it is not known to what extent spatially this disturbed zone extends. Indeed, it is quite possible that if only the soil in the immediate vicinity of tip 1 is affected, then tip 2 may be sensing a combination of this broken bond soil with some still-cemented material. Again, this would complicate the analysis of the DTP results, since the degree of cementation may in fact alter this zone of influence. Also, at higher cementation contents, the soil will behave more as rock and may not be penetrable by the DTP or CPT.

Effective Confining Stresses ( $\sigma'_v$  and  $\sigma'_h$ )

The effects of confining stresses in triaxial specimens are well known. It is generally acknowledged that the larger confining stresses resist the applied shearing forces in the failure zone, thereby increasing a soils' resistance. This also holds true in the cone penetration test (Figure 2.3).

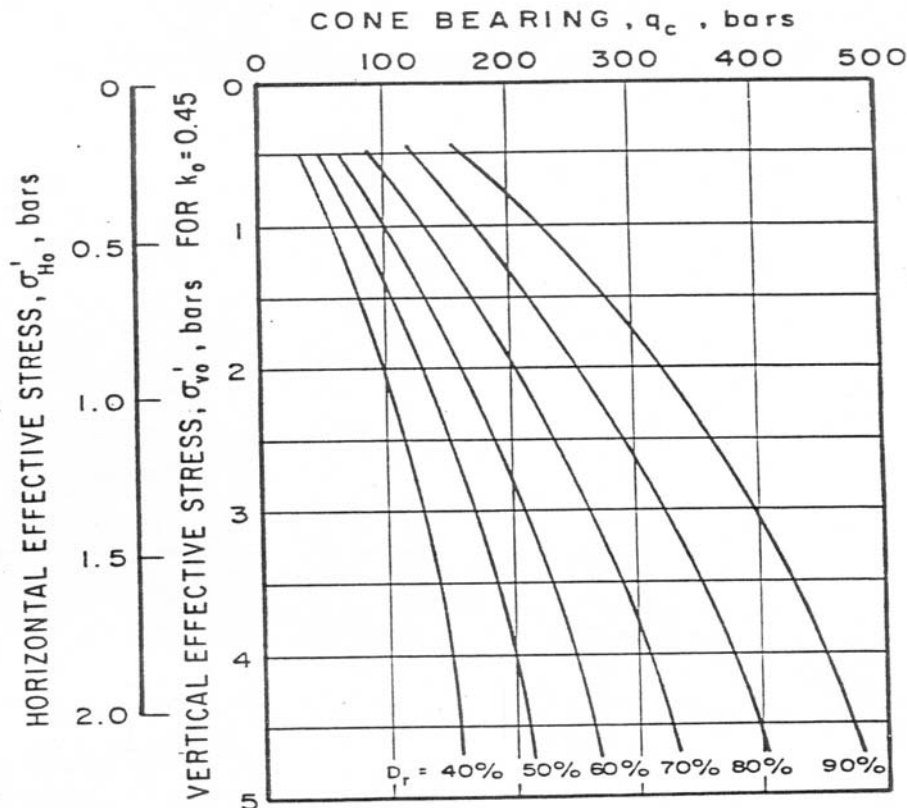


Figure 2.3:  $D_r$  and  $\sigma'_h$  Relationship for Uncemented Unaged Quartz Sand (Baldi et al.)

There is a difference between the DTP and the CPT in regards to the effective confining stresses. For a particular depth, it is difficult to verify that the soil confining stresses (at failure) are identical at tip 2 and tip 1. It is quite possible that the disturbance of the soil from the penetration of tip 1 may cause a change in the effective stresses, thereby influencing the tip 2 resistance. In addition, tip 2 may be influencing the confining stress of the soil that is being failed by tip 1 (i.e., the tip 2 annulus may increase  $\sigma'_v$  and  $\sigma'_h$  for the soil at tip 1). However, such an affect (tip 2 on tip 1) has not been observed during testing. As will be reiterated in Chapter 3, the tip 1 bearing and the  $q_c$  bearing values from the CPT are virtually identical at similar sites and soil conditions.

The question then arises, “Does tip 1 penetration increase or decrease the effective stresses in the soil being failed by tip 2?” To attempt to answer this question, two research articles on modeling of CPT penetration will be discussed.

Salgado et al. attempted to model the cone penetration test as a cylindrical cavity expansion problem (Figure 2.4). In this analysis, the cone penetrometer movement is modeled as a cavity expanding from zero to a final radius equal to the radius of the penetrometer. This expansion will cause plastic zones (where the soil has failed and non-recoverable strains observed), nonlinear elastic zones and linear elastic zones within the soil. In the elastic zone it is determined that the final radial normal stress  $\sigma_r$  increases to a value greater than the initial/insitu radial stress.

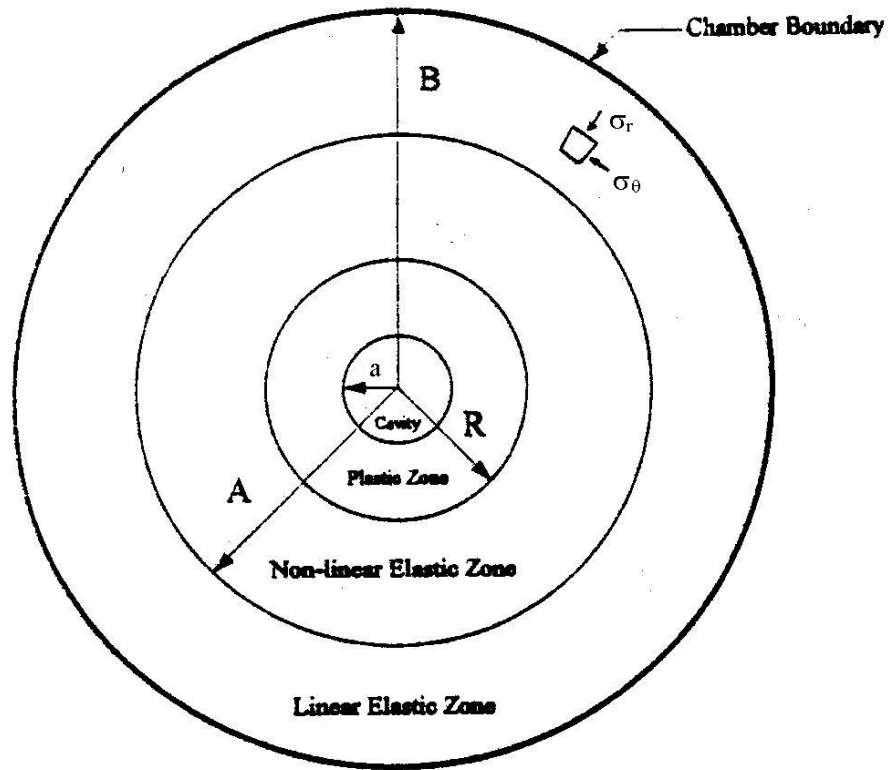


Figure 2.4: Cavity Expansion Theory, generating Plastic, Nonlinear Elastic and Elastic Zones (Salgado et al.)

In another research project, Teh performed an analytical study of the cone penetration test in undrained clays. The cone penetration process was analyzed as a stationary cone tip with soil flowing up and around it. The soil was modeled as an inviscid fluid using the strain path method to determine the stresses and strains acting around the cone. Figure 2.5 shows the stress variations for a stream of soil located a distance  $r/R = 1.2$  from the center of the cone tip where  $R$  is the radius of the cone. The analysis was done using cylindrical coordinates. The radial stress is noted as  $\sigma_{rr}$  and the vertical stress is shown as  $\sigma_{zz}$ . The x-axis is the normalized value of stresses (stress divided by undrained shear strength). The initial stresses in all directions were taken to be zero. The plot shows that the stresses increase to a maximum value at the cone shoulder and then decrease. However, the values do not return to zero.

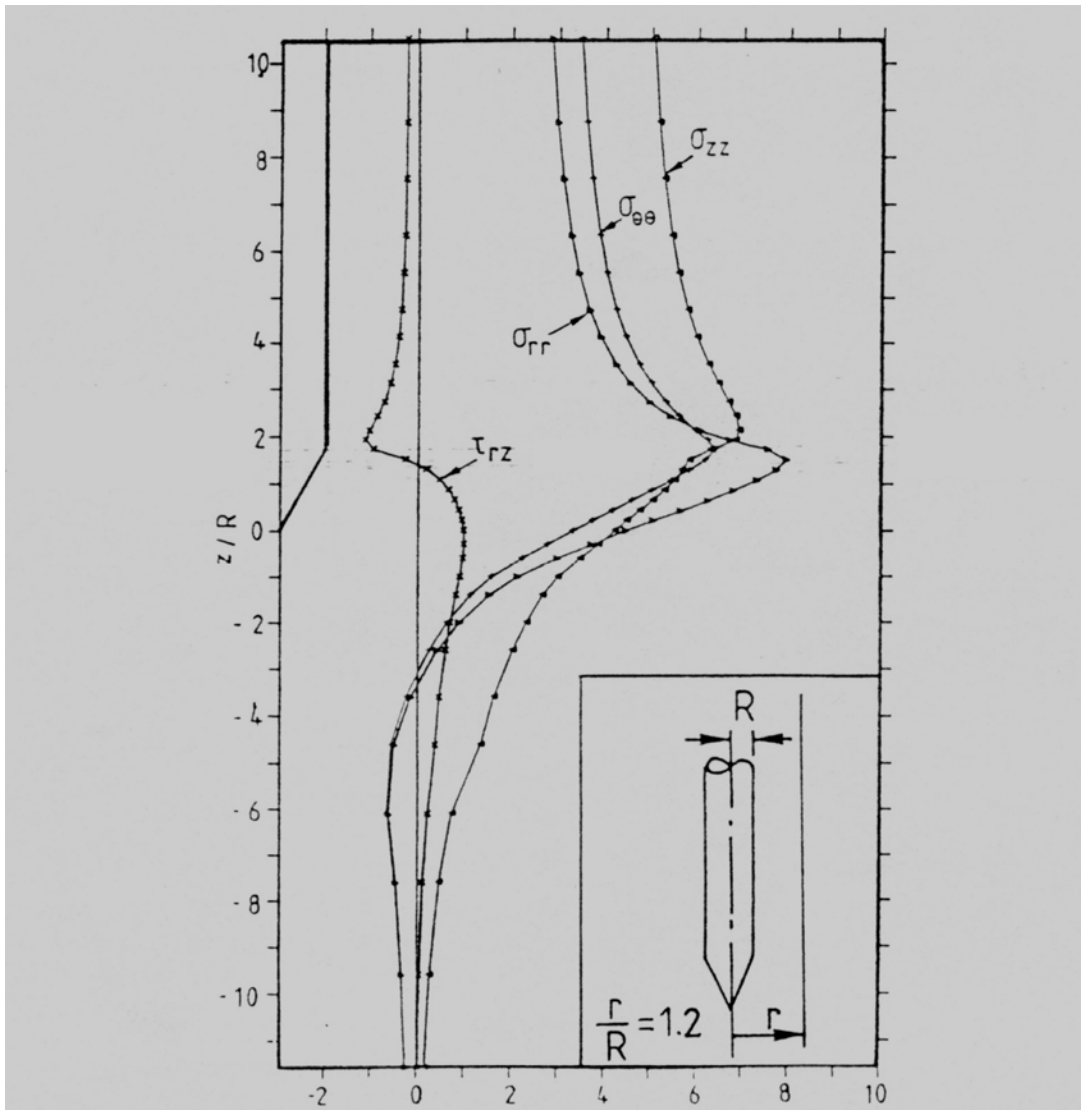


Figure 2.5: Stress Variation along a Vertical Grid Line (Teh 1987).  
 Note: the x-axis is stress/ $S_u$

The results presented above suggest that during cone penetration, the horizontal effective stresses in the soil may increase during tip 1 penetration to values above the initial insitu values. If the effective confining stresses in the soil increase after the penetration of tip 1, then the soil resistance at the tip 2 annulus would be greater than tip 1 discounting any effect of cementation,  $D_r$  changes, etc.

### Chamber to Penetrometer Diameter Ratio ( $R_d$ ) and Boundary Conditions

Calibration chambers are designed to create controlled testing conditions in soils of known density and confining stresses. For DTP testing purposes, a modified calibration chamber (no lateral pressure control) was constructed and filled with layers of clean and artificially cemented sand. Additional details regarding the calibration chamber and test results will be discussed in Chapter 4. However, when utilizing a calibration chamber it is important to determine to what extent tip 1 (or CPT tip) is affected by the boundary conditions imposed by a finite chamber diameter.

The effect of chamber diameter on cone bearing has been investigated many times. Sweeney and Clough attempted to analyze the effect based on an extensive literature search. Puppala et al. 1995 normalized the  $q_c$  readings with respect to atmospheric pressure and effective vertical stress (Figure 2.6). The research showed that for small chamber to cone diameter ratios  $R_d$ , there is a reduction in  $q_c$  values in very dense sands compared to field results (analogous to an infinite diameter). This bearing decrease is less pronounced as  $R_d$  gets larger and the soil gets looser. What is interesting in this study is that one would expect the penetration resistance to increase as the diameter ratio decreased. However, it is plausible that the induced lateral stresses would be transmitted through the dense material into the confining stress media (air or water), thereby dissipating more readily. Regardless, this treatise only reinforces the assertion that bi-modal soil-structure interaction is indeed a complex phenomenon.

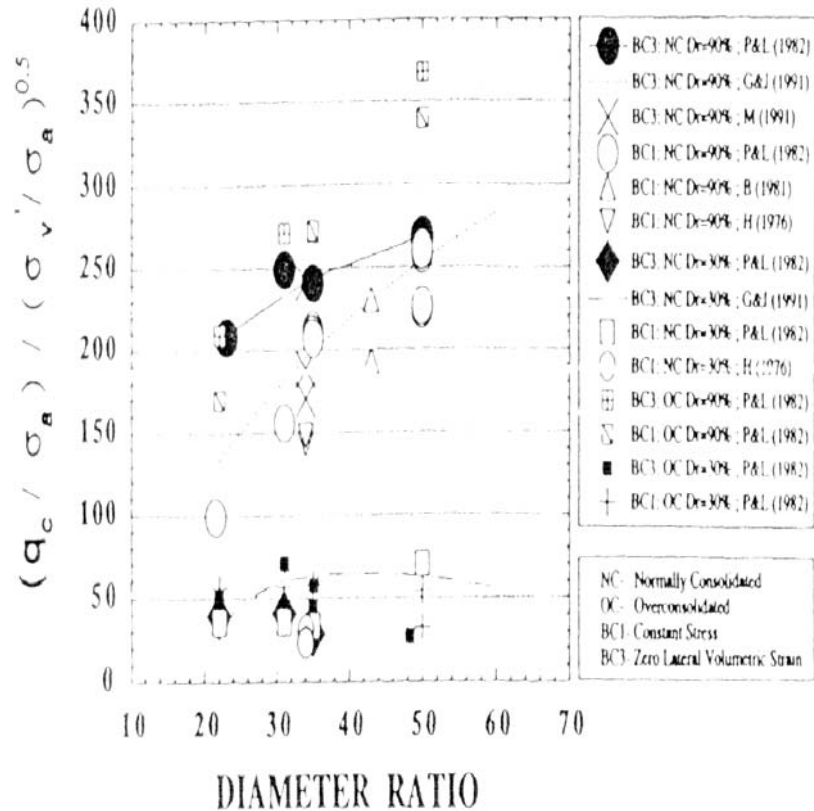


Figure 2.6: Effect of Chamber Size and Boundary Condition on Tip Resistance in various calibration chamber studies  
 (Note: P&L = Parkin and Lunne; G&J = Ghionna and Jamiolkowski; M = Manassero; B = Baldi et al.; and H = Harman) from Puppala et al. 1995

The final parameter to consider is the testing chamber boundary condition (BC). The four boundary conditions mentioned previous are defined as:

1. BC 1 – Constant horizontal and vertical stresses
2. BC 2 – No vertical displacement, average lateral displacement - zero
3. BC 3 – No lateral volumetric strain, constant vertical stress
4. BC 4 – No vertical displacement, constant lateral stress

The effect of boundary condition 3 (BC 3) is also shown in Figure 2.6. Since the calibration chamber used in this research is constructed of high-density polyethylene, zero lateral

displacements are expected (BC 3). The stress at the top of the soil is atmospheric so that boundary condition 3 is maintained as well. Puppala (1995) suggests that assuming boundary condition 3 will have a negligible effect on low  $R_d$  readings. In addition, for this research, soil stress cells were placed on the calibration chambers walls, thereby slightly decreasing  $R_d$  at the elevation of the pressure cell. The results of the above will be further discussed in Chapter 4.

### Heterogeneous Soil Effects

In addition to the parameters conferred above, it is possible that heterogeneous soils may result in T2 being larger than T1. If we assume that tip 2 has influence zones (plastic and elastic) that extend further in the radial direction than the influence zones of tip 1, then stiffer soil (or rocks or other objects) that may be present to increase T2. Of course, the opposite effect may also occur, i.e., a weak zone could cause T2 to decrease.

The heterogeneous soils may affect tip 2 in yet another way. At the beginning of this chapter it was mentioned that the tip ratio analysis (ratio of T2/T1) requires that the bearing areas and strain gage calibration factors of tips 2 and 1 be equal. During calibration of the Dual Tip Penetrometer, Hogentogler Inc. discovered that the tip 2 bearing readings might change if exposed to large uneven bearing stresses. It was observed that the tip 2 readings were most consistent when the load was uniform across the surface of the tip 2 annulus. Soils that are extremely heterogeneous may cause a large uneven bearing resistance on the tip 2 annulus and therefore decrease or increase the tip 2 reading. Hence, this effect is an artifact of the probe's design, which is not alterable. However, it is felt that additional data will provide insight into this effect and eventually lead to a better understanding of the probes performance characteristics.

### **Summary of Trends**

In summary, three of the four parameters mentioned previously tend to cause T2 to be lower than T1: Relative density decreases due to dilation, cementation break up and  $R_d$  changes. The possible increase in confining stresses or increase in relative density (loose dry silt) may

increase the T2 to a value greater than T1. The heterogeneous soil effects could have both increasing and decreasing affects on the tip ratio.

There also may be other unexpected conditions that can affect the T2/T1 ratio. As was mentioned previously, there is the possibility that for larger size particles, a rearrangement of them caused by tip 1 penetration might result in superior interlocking (not necessarily denser, albeit more effective particle orientation). This would make it more difficult for tip 2 to penetrate this “rearranged” soil.

A tentative equation can be written to account for the parameters mentioned in this report. If necessary, Equation 2.1 can be modified with additional factors as more data becomes available.

$$T2/T1 = 1 \pm C_d - C_c \pm C_{clay} \pm C_{he} - C_{Rd} + C_{\Delta\sigma_h} \quad (\text{eqn. 2.1})$$

Where:

- $C_d$  is a factor that depends on soil dilation (loosening) or contraction (densification), and is contingent on soil type, soil state and effective confining stresses
- $C_c$  accounts for the effect of cementation content, extent of cementation bond breakage and confining stresses
- $C_{clay}$  is a possible factor depending on changes in undrained shear strength, over consolidation ratio, rigidity index and/or clay sensitivity
- $C_{Rd}$  is a correction factor that is based on  $R_d$  – only used during calibration chamber testing
- $C_{\Delta\sigma_h}$  depends on horizontal or vertical soil stress changes (assumed positive)
- $C_{he}$  is a factor to account for the heterogeneity of the soil

In Chapters 3 and 4 the results of the Dual Tip Penetrometer tests in the field and in the calibration chamber will be discussed. However, attempting to quantify this equation with its various factors at this stage of the research is premature. For this reason, in the future, FDOT



will continue to use the DTP, thereby generating valuable data. It is expected that eventually, the DTP results will provide geotechnical engineers with a fullness of subsurface information that was not possible presently. In the interim, the most interesting factor to study in equation 2.1 is the cementation break up factor,  $C_c$ , since this is the strength loss that could occur in cemented sands.

## CHAPTER 3: PLAXIS ANALYSIS

As requested by the FDOT, we were to study relative densities using the DTP. Hence, the next objective was to attempt to find a correlation between relative density in sands and DTP tip results. Relationships have been made previously between relative density and  $q_c$  resistance (Schmertmann, 1976; Villet and Mitchell, 1981; Baldi et al., 1982). The correlation will be achieved by running a controlled testing of the DTP.

The controlled testing proposed may also be used to correlate the DTP over CPT friction reading increase with sand relative density. That is to say, for dense sand, the additional confining stress induced from Tip 2 should result in an increase in friction reading. On the other hand loose sand should have little effect on side friction since the sand has void space in which to densify during penetration.

The proposed testing will consist of DTP penetration soundings being performed in the center of a large diameter HDPE (High Density Polyethylene) pipe full of sand at various densities. The pipe will be placed on the ground and then filled with sand. The test will be done 2 to 3 times on a loose sand (non densified) and 2 to 3 times on a dense sand (densified with a vibrator plus a surcharge). By knowing the weight of sand placed in the pipe and the volume occupied the unit weight of the sand can be calculated. If a specific gravity is assumed then the void ratio can also be calculated. The maximum/minimum void ratio tests can be performed on the sand and relative density can be obtained. A relationship between cone performance and relative density will then be attempted.

The length of the pipe was chosen as 8 feet so that it could fit with little protrusion into a test pit at the new Department of Transportation Pavement Evacuation Site in Gainesville, Florida. However, due to accessibility concerns with the cone truck the controlled test will likely be performed in the Weil Hall structures lab at the University of Florida.

Due to strength and size concerns, HDPE was chosen as the material. The thickness of the pipe will be 1.108 inches to retain a diameter to thickness ratio (SDR ratio) of 32.5. The SDR ratio of 32.5 will ensure strength of 50 psi or 7200 psf. This is more than enough to hold 8 feet of sand [creating approximately 800 psf of vertical pressure at the bottom of the pipe].

The diameter of the pipe must be large enough so that boundary effects do not influence the DTP readings. In the placement of piles it has been found that a spacing of 3 diameters (center to center) is adequate for negligible pile-to-pile interaction. If this convention is used for determining the diameter of the pipe then a radius of 6 inches ( $3 * 2.0$  inches DTP diameter) should be sufficient. However, intuitively this seems to be too small. Therefore the finite element program PLAXIS was used to analyze the effects of pipe diameter and resulting boundary effects.

## PLAXIS: Finite Element Code for Soil and Rock Analysis

### Introduction

Plaxis is a finite element program used to measure deformations and soil mass displacements. First, a geometry input of an object is drawn into a grid. The program then analyzes the movement of this object within a soil type (or material). It analyzes the object on soil movement by using different soil models such as the linear-elastic model, the Mohr-Coulomb Model or the Hardening-Soil Model (similar to Hyperbolic Duncan & Chang Model).

### Purpose

There are two purposes for using PLAXIS in this report. The first purpose is to model the movement of the DTP and CPT results. These results will be compared to the actual field results. It must be noted that the PLAXIS program cannot analyze dynamic or failure conditions within soil. However, this program can be used to analyze the stresses acting on an object “settling” within a body of soil.

The second purpose of PLAXIS is to find a diameter of pipe that is appropriate for performing a controlled relative density test with the DTP.

### Process

PLAXIS uses triangulation techniques to split up an object or geometry into finite elements for analysis. PLAXIS then uses either a specified object displacement or a specified loading on an object to analyze the overall system.

The following section describes the process used to model the movement of the standard CPT and the DTP.

### Geometry Input

The first step was to create a geometric input file. After starting the input program the *New* option was selected under the *File* sub-menu. Immediately following this selection, the *General Settings* window appeared. Two tab sheets could then be chosen under the *General Settings - Project and Dimensions*. The *Project* sub-menu could also be used to open a saved file. Under the *General* sub-menu, the option for a 15-node elemental analysis was chosen. The number of elements was selected as 15 instead of 6 to increase accuracy. The axisymmetric input model option was chosen so that only half of the cone would have to be analyzed (the CPT and DTP are cylindrical so that half of the cone had to be drawn). The accelerations in the representative x and y-directions were both set to zero. In order to simulate the penetration into the soil stratum, a prescribed displacement was used. Through a process of trial and error a prescribed displacement of 0.10 inches was used. It seemed that large displacements would not work in PLAXIS because some soils would fail before reaching displacements greater than 0.10 inches. After the *Project* sub-menu is completed, the *Dimensions* sub-menu must be selected to specify the *Units*, *Geometry dimensions*, and

*Grid dimensions.* In order to facilitate the creation of the input file, English units were chosen in the *Dimensions* submenu. The boundaries for which the soil and penetration devices would be drawn were a 625 sq.in. two dimensional area. In other words, the coordinates of each corner were as follows (X,Y):

0,0  
 0,25  
 25,0  
 25,25.

Within the options under grid dimensions, a spacing of .05 inches at a total of 100 space intervals was used. Once these parameters were specified, the geometry model could be created.

A typical geometry model or object is made up of points, lines, and clusters. The points and lines are used to draw the object. Lines can be drawn by selecting the *Geometry Line* option from the second tool bar or by selecting the appropriate option from the *Geometry* tool bar. After drawing the object the program then automatically creates the clusters necessary to complete the object. Two separate input files were made (one for the CPT and another for the DTP). By knowing the actual dimensions of the CPT and DTP, drawings of the penetrometers were made. As stated before, both cone penetrometers were modeled axisymmetrically within a volume of soil. The coordinates for each point of the CPT/DTP are as follows (the units are inches):

Table 3.1: Coordinates of CPT/DTP points in the PLAXIS grid

CPT (coordinates)		DTP (coordinates)	
X (in)	Y (in)	X (in)	Y (in)
0	24.8	0	25
0.705	24.8	0.705	25
0.705	19.814	0.705	23.75
0.705	14.554	0.9	23.45
0.705	14.071	0.9	21.55
0	12.85	1	21.4
		1	20.55
		0.705	20.05
		0.705	14.754
		0.705	14.271
		0	13.05

Material layers, loading conditions, and boundary conditions can then be specified. Here, the user must specify the general stratification of the soil into layers, where and how the loads are applied, and the location of the physical boundaries and their significance. The following figures show the CPT/DTP and the soil boundaries.

Figure 3.1: DTP Geometrical Input

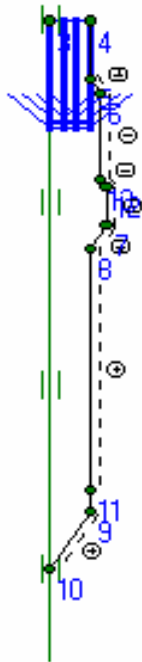
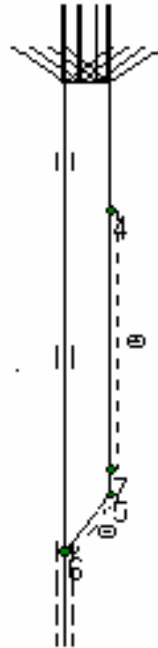


Figure 3.2: CPT Geometrical Input



### Interfaces

The next step was to specify the interfaces where the soil and structures/objects meet or interact. Interfaces are used to analyze surface interactions between a soil and a surface (made of either steel, wood, another soil stratum or even some other material given the material properties). Stresses, deformations, displacements, strains and incremental strains along an interface are then calculated and saved to an output file.

Clicking on the Interfaces option in the Geometry sub-menu makes an interface. The interface appears as a dashed line (see Figures 1 and 2 above) lying just outside a geometry/object line to represent the interaction between that object and the surrounding soil. In the CPT model, interfaces were placed along the friction sleeve and the tip. In the DTP model, interfaces were created along the surface of the friction sleeve, Tip #1, and Tip #2.

### Loads & Prescribed Displacements

The next step was to specify loads and boundary conditions. The *Loads* sub-menu contains the options to introduce distributed loads, point forces, or prescribed displacements. As stated before, a prescribed displacement of 0.1 inches downward for both penetrometers was used because it would more accurately model the actual penetrating movement of the cone. A more accurate way of modeling the cone would be to give it a constant rate of movement because the actual cone is a quasi-static tool that moves into the ground at a speed of 2 cm/sec. Unfortunately, this type of movement cannot be specified using PLAXIS.

After choosing the prescribed displacements icon the user must double-click on the surface in which the displacement is to be applied. The displacement was applied to the top of the cone but since it is steel the whole cone would move the same amount. The value of displacement must then be chosen [-1 unit was used (negative sign is used to simulate a downward movement)].

### Material Properties

The DTP and CPT models were placed in six different soil types: silt, clay, loose sand, dense sand, clayey sand, and silty sand (unfortunately cemented sand is not an available option). The properties (unit weight, soil behavior, soil model, permeability etc.) of each of these soil types and other materials were already stored in a database within the input program. The Mohr-Coulomb soil model was chosen for all of the test runs. Besides soil, three other data sets are available to the user: beams, geotextiles, and anchors. These data sets can be assigned to soil clusters or to any other structural object within the PLAXIS diagram.

No water table was given in any of the analyses.

### Calculations Program

Once all the input variables and meshes were created the calculations program within PLAXIS could be started. Within the calculations program the user can choose to load the object in one stage or multiple stages. There are also multiplier options. These options allow the user to change the amount of displacement, loading, and moment arms in the vertical and horizontal directions. The moments and loads were set to zero while the displacement was set at 0.10 inches.

## **Plaxis Results**

As stated before, the main results given by PLAXIS in the output are displacements, stresses, strains and incremental stresses at interfaces. The following section describes the results obtained from PLAXIS and compares them with the field results.

## DTP/CPT Modeling Analysis

Table 2 on the following page gives the average shear and normal stresses along Tip 1 for both penetrometers. The vertical components of these stresses must be calculated in order to obtain the theoretical bearing tip pressures, which can then be compared to the  $q_c$  values of a CPT or DTP test (see Figures B-1 and B-2 in Appendix B).

Table 3.2: PLAXIS Tip 1 Comparisons between Penetrometers

Soil Type	CPT (Tip 1)			DTP (Tip 1)		
	Average Shear Stresses (KPa)	Average Normal Stresses (KPa)	Theor. Bearing $q_c$ (KPa)	Average Shear Stresses (KPa)	Average Normal Stresses (KPa)	Theor. Bearing $q_c$ (KPa)
Silt	128.5	451.1	<b>336.8</b>	122.8	418.0	<b>315.4</b>
Loose Sand	147.6	509.9	<b>382.7</b>	67.2	210.7	<b>163.6</b>
Dense Sand	337.6	1392	<b>988.3</b>	302.1	1299.9	<b>911.5</b>
Clayey Sand	252.9	813.3	<b>625.7</b>	242.2	813.1	<b>616.3</b>
Silty Sand	129.4	451.8	<b>337.9</b>	95.8	318.7	<b>242.3</b>
Clay	18.4	191.5	<b>111.7</b>	10.1	133.97	<b>75.7</b>

Table 3.2 shows that Tip 1 theoretical bearing values between penetrometers matched one another closely. The soils with the greatest difference were silty sand and loose sand where the DTP Tip 1 was 0.72 and 0.43 times smaller than CPT Tip 1 respectively. The relationships between shear forces on the DTP and CPT Tip 1's can also be seen in Figure B-3 in Appendix B. This figure plots the DTP shear stress distribution along Tip 1 against the CPT shear stress distribution along Tip 1 in six different soil types. The plots are close to straight lines on a 45-degree angle. This shows that the distribution of shear stresses along the Tip 1 does not change much between penetrometers (i.e. the Tip 1 resistances between penetrometers are equal for a given soil). This result was also found in the field (see generalized results section).

Table 3.3: PLAXIS Average Friction Sleeve Resistances between Penetrometers

Soil Type	CPT (fs)	DTP (fs)
	Average Shear Stresses (KPa)	Average Shear Stresses (KPa)
Silt	19.4	21.9
Loose Sand	20.3	3.7
Dense Sand	23.1	4.1
Clayey Sand	47.1	56.3
Silty Sand	19.4	13.4
Clay	19.7	15.2

The values in the table above provide average shear stresses on the friction sleeve. The average values are given because the stress distributions vary (slightly) along the length of the sleeve (see Figures B-4 to B-8 and Table B-10 in Appendix B).

According to Table 3.3 above, the CPT had smaller friction sleeve readings than the DTP in silts and clayey sands. The friction sleeve readings for clay, silty sand, clayey sand and silt do not have large variations (agrees with field results). However, the friction sleeve readings for the CPT in loose and dense sands are about 6 times greater than those values in the DTP readings. This is contrary to the results in the field. In the field the DTP had greater friction values than the CPT (up to 4 times as large at its peak).

The discrepancy from the PLAXIS results could be due to the small movement that the penetrometer moves (0.1 inches downward). This small movement is not great enough to induce a failure condition in the soils. As stated before, PLAXIS cannot be used to analyze quasi-static conditions.

Table 3.4: PLAXIS DTP Tip 1 and Tip 2 results

Soil Type	DTP (Tip 1)			DTP (Tip 2)		
	Average Shear Stresses (KPa)	Average Normal Stresses (KPa)	Theor. Bearing T1 (KPa)	Average Shear Stresses (KPa)	Average Normal Stresses (KPa)	Theor. Bearing T2 (KPa)
Silt	122.8	418	<b>315.4</b>	39.3	104.6	<b>86.3</b>
Loose Sand	67.2	210.7	<b>163.6</b>	5.4	11.5	<b>10.4</b>
Dense Sand	302.1	1299.9	<b>911.5</b>	54.8	191.0	<b>143</b>
Clayey Sand	242.2	813.1	<b>616.3</b>	102.4	269.3	<b>223.3</b>
Silty Sand	95.8	318.7	<b>242.3</b>	24.2	58.9	<b>50.4</b>
Clay	10.1	134.0	<b>75.7</b>	24.4	43.5	<b>42.9</b>

According to PLAXIS the Tip 2 bearing should decrease in all types of soil (see Table 4). The decrease in theoretical bearing is greater for the sand (about 90% reduction) than it is for the other soil types (40% to 80% tip bearing reduction). This is a similar trend to that found in the field (see generalized results section). In the Archer Landfill the residual Tip 2 bearing in sands was about half of that of Tip 1. No noticeable decrease in tip bearing was found for the other soil types.

Table 3.5: PLAXIS Tip 2 Residual Strength

Soil Type	Tip 2 Percentage Strength Reduction
Dense Sand	84%
Loose Sand	94%
Silty Sand	79%
Clayey Sand	65%
Silt	73%
Clay	43%



A general summary of relations between PLAXIS results and field results are presented in Table 6.

Table 3.6: Summary of PLAXIS Results vs. Field Results

Type of Relation	Comments on Trends
Tip 1 Similarities between DTP and CPT	Good agreement for all soils (DTP tip 1 $\approx$ CPT tip 1) except in Silty Sands and Loose Sands (PLAXIS: DTP tip 1 > CPT tip 1; Field Results: DTP tip 1 $\approx$ CPT tip 1)
Friction Sleeve Similarities between DTP and CPT	PLAXIS and Field Results agree for almost all soils (DTP Friction $\approx$ CPT Friction) No agreement for sands (PLAXIS: DTP Friction < CPT Friction; Field Results: DTP Friction > CPT Friction)
Tip 2 Bearing vs. Tip 1 Bearing	Acceptable agreement (Larger reduction in Tip 2 bearing in sands then in soils with greater fines content)

### Pipe Diameter Analysis

As stated earlier in this report the second purpose of PLAXIS was to help determine the minimum diameter HDPE pipe that can be used in the proposed controlled density test with negligible boundary effects on the DTP penetration.

This purpose was achieved by adding a flexible membrane to the main DTP file. The flexible membrane was placed vertically a variable distance from the cone. The magnitude of membrane movement during analysis would be indicative of the amount of boundary influence on the cone (i.e. the more the membrane moves the more it will affect the cone results).

In the testing scheme for relative density, the flexible membrane was designed as a beam with a large flexibility. The program was run 5 times in loose sand and once in dense sand (see Figures B-8 to B-13). Each time the test was run with the membrane a different distance from the DTP. The program was run each time with the cone moving down 0.19 inches (0.04 inches for the dense sand run). The amount that the membrane moved was then recorded. From this information a ratio of downward cone movement to lateral membrane movement was made. This ratio was then multiplied by 8 feet (96 inches) to get a predicted membrane movement of the HDPE pipe wall during the actual test. The resulting displacement ratios and predicted membrane movements are shown in Table 7 on the following page.

Table 3.7 PLAXIS DTP Boundary Influence Effects

Dist. from Cone Center	Max. Membrane movement	Ratio of membrane movement to cone movement	Test Pipe Diameter	Maximum Predicted Membrane movement
(in.)	(in.)		(in.)	(in.)
8	$1.56 \times 10^{-3}$	$9.28 \times 10^{-3}$	16	0.891
10	$1.02 \times 10^{-3}$	$6.07 \times 10^{-3}$	20	0.583
12	$7.23 \times 10^{-4}$	$4.30 \times 10^{-3}$	24	0.413
15	$4.42 \times 10^{-4}$	$2.63 \times 10^{-3}$	30	0.253
18	$1.81 \times 10^{-4}$	$1.08 \times 10^{-3}$	36	0.103
18*	$6.75 \times 10^{-5}$	$1.86 \times 10^{-3}$	36	0.178

\*Test run in Dense Sand

According to the table above the maximum membrane movement of a 36-inch diameter flexible pipe will be only 0.1 inches for loose sand and 0.18 inches for dense sand. This suggests that there will be very little influence by the pipe wall on the penetrometer at this distance.

A pipe diameter of 36 inches will be chosen. This diameter should be large enough for boundary effects by the wall to be negligible (as long as the test is performed in the center of the pipe). This diameter will also be many times larger than the 3 diameter spacing used in pile placement design.

#### Comment on PLAXIS

As mentioned before, the PLAXIS results had some variation with the field results. This difference is likely due to the method of analysis. PLAXIS is a program best suited for analyzing soil body interactions in a settling state, not during failure.

## CHAPTER 4: FIELD TEST RESULTS

The Dual Tip Penetrometer was evaluated at various field locations. Several different soils, including clean fine sands, cemented calcareous sands and mixed soils were tested. The majority of the soundings were performed in conjunction with the standard cone penetrometer for comparison purposes. All DTP testing was performed with one or more of the following DTP probes: CSC 765 TC (2000), CSC 782 TC (2001), CSC 830 TC (2002) or CSC 829 TC (2002). The soil types and test locations include:

Clean Fine Sands: Archer Landfill; Archer, Florida

Cemented Calcareous Sand: Orlando & West Bay, Florida

Mixed Soils: Vilano, Gainesville & Vilano Beach, Florida

Soft Soils: Vilano & Green Cove Springs, Florida

Shelly Sands: Port Orange, Florida

### **Clean Fine Sands at Archer Landfill in Archer, Florida**

One of the first sites used for DTP testing was the Archer landfill, an excellent site for initial scrutiny. Located in Archer, Florida, this site contains a very clean fine sand deposit peripheral to the outside of the clay liner boundary. This area has been used for many years as a borrow area, where clean sands were mined for daily cover of the landfill debris.

Four DTP and one CPT tests were performed at this site. However, one of the DTP tests was approximately about 25 feet away from the CPT comparison test where landfill operators had equipment parked at the original location and hence was not directly compared to its CPT counterpart.

The first observation was the fact that the tip 1 measurements for the DTP were identical to those of the CPT at the same site. This trend was discerned at all the sites tested and suggested that the presence of the second tip has virtually no effect on the tip 1 bearing readings. Recall that there was an initial concern that tip 2 might influence tip 1 via an

extended stress bulb, these tests belied that notion. The tip 1 bearing values ranged from zero to 30 MPa for the three DTP soundings. The tip 1 readings can be seen in Figure 3.1 below.

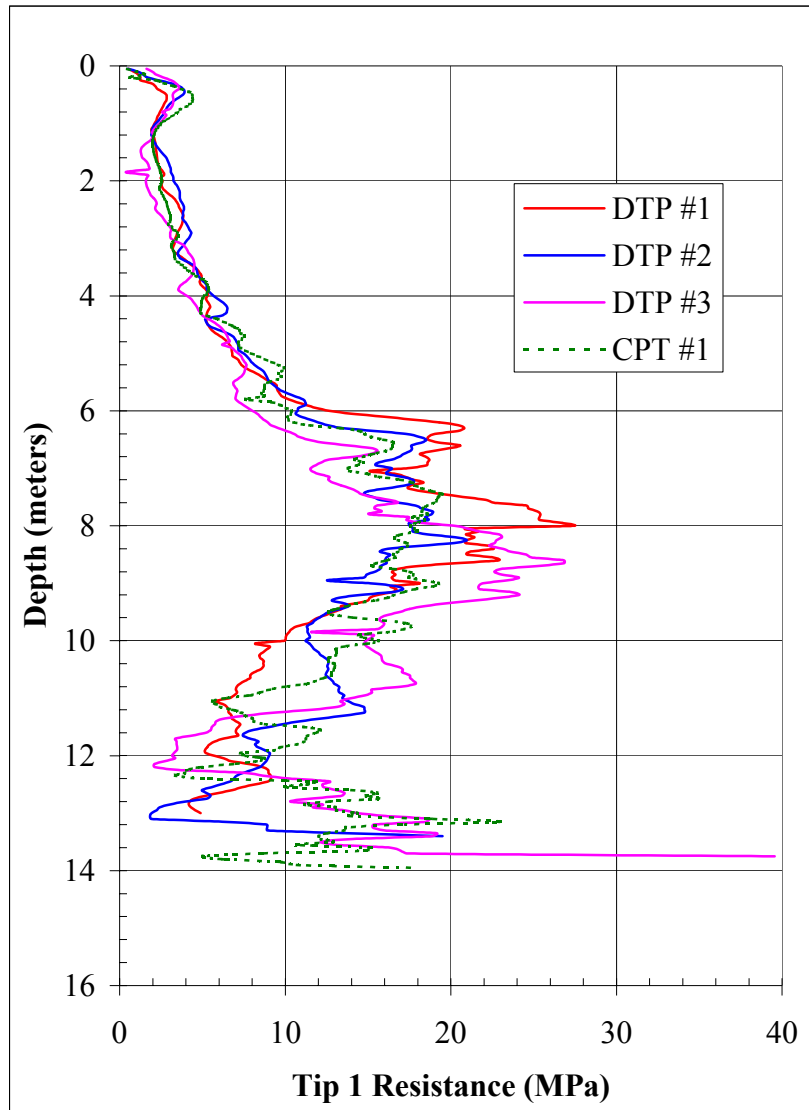


Figure 3.1: Archer Landfill Tip 1 vs. Depth

The friction ratio readings vary between the CPT and DTP in these clean fine sands. While the CPT friction ratio was consistently near 0.8 % the DTP friction ratios ranged between 2% and 3%. The friction ratios can be seen in Figure 4.2. The larger friction ratios are due to the tip 2 producing an increase in vertical and therefore horizontal stresses near the friction sleeve. This increased horizontal stress will then result in a larger shear resistance.

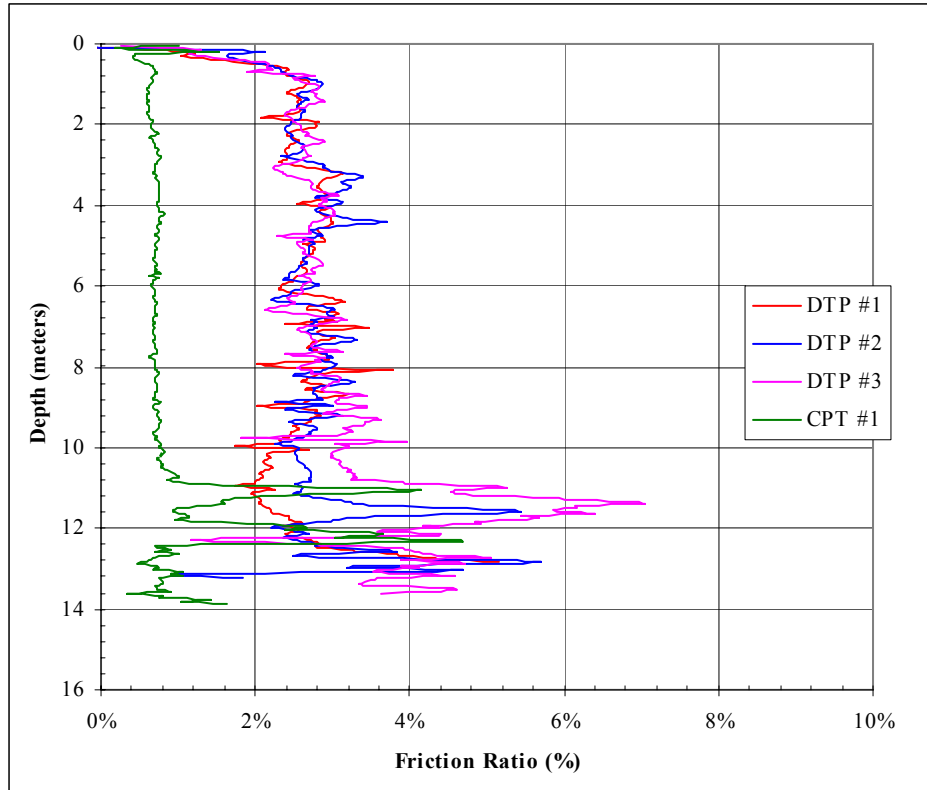


Figure 4.2: Archer Landfill Friction Ratio Comparison

While on initial inspection this observation might be a cause for concern, the uniform nature of the offset simply means that a correction factor should be used to “adjust” the values. Another alternative would be to reduce the length of the friction sleeve by approximately 10%. Since the stress bulb affects the end of the sleeve (adjacent to tip 2) the most, inserting a floating ring spacer at this location would reduce the surface area of the modified friction sleeve. This alteration would result in lower friction readings, which would then coincide with the CPT values. However, it is interesting to note just how much more sensitive the DTP friction readings are compared to the CPT. Additional soundings may provide an insight into this observation and in fact lead to a new taxonomy. For example, the oscillating waveform pattern might indicate that some of the soil grains are being subject to crushing (as opposed to only shearing) since this energy release would be erratic. Regardless, this is an interesting observation that will be monitored.

The T2/T1 or tip ratios were consistent in the clean fine sands as can be seen in Figures 4.3 and 4.4.

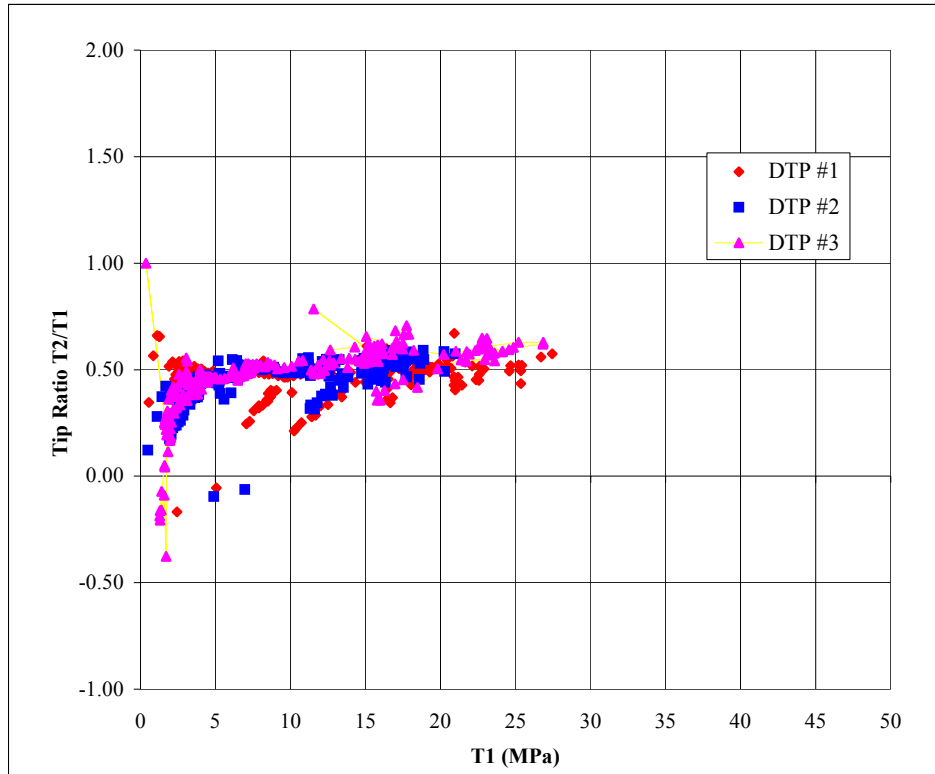


Figure 4.3: Archer Landfill T2/T1 vs. T1

The tip ratios ranged between 0.4 and 0.6 for the clean fine sands. This appeared to be the case in the high and low tip 1 bearing areas (in the denser and looser regions of the fine sand). It also appears from Figure 4.4 that tip ratio increases slightly with increasing depth or increasing stresses  $\sigma'_h$  and  $\sigma'_v$ .

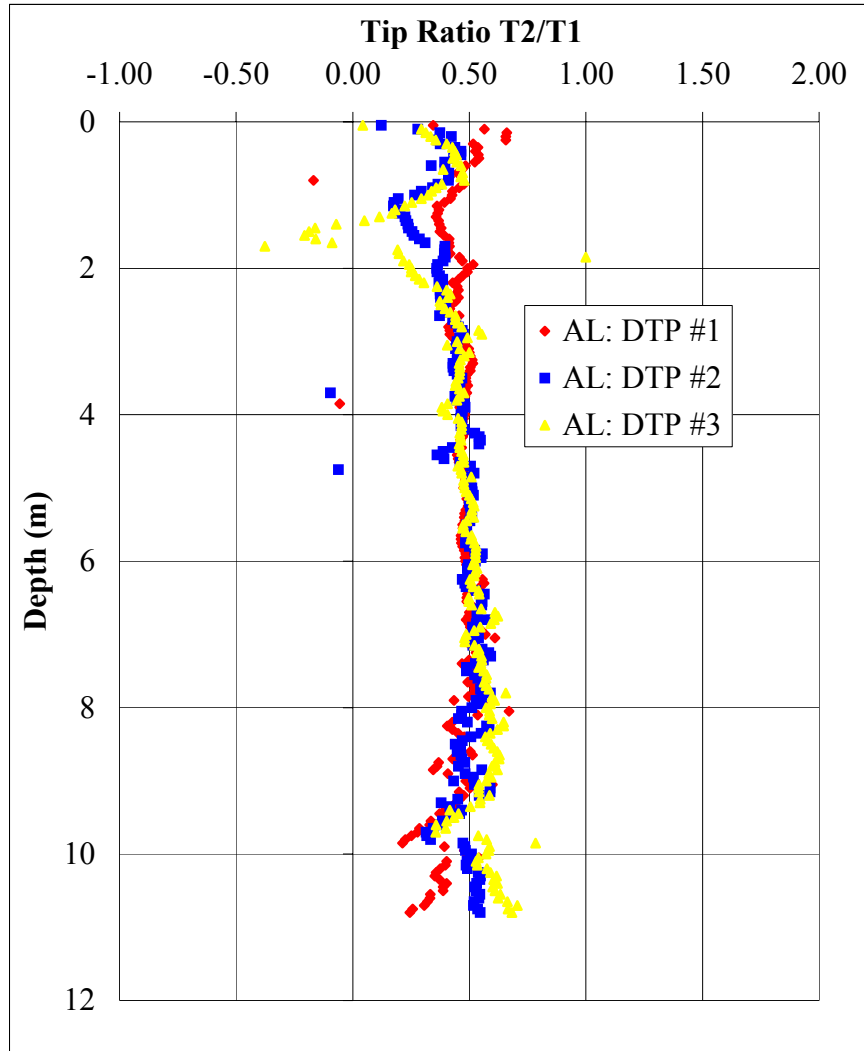


Figure 4.4: Archer Landfill (AL) T2/T1 vs. Depth

Based on these results, Equation 2.1 from Chapter 2 can be simplified by assuming that the soil was not cemented (numerous tests at this site confirm this - hence no cementation reduction factor) and that there was no  $C_{he}$  factor (i.e., soil sampled with a Shrew Sampler was indeed homogeneous). Equation 4.1 for clean fine sands is given below.

$$T2/T1 = 1 \pm C_d + C_{\Delta\sigma_h} \quad (\text{eqn. 4.1})$$

The results from the Archer Landfill tests show that the tip ratio ( $T_2/T_1$ ) is less than one (near 0.5) for this sand, suggesting that the dilational effect is positive and dominates any contribution from the increase in horizontal stress with depth.

### **Cemented Calcareous Sands in Orlando, Florida & West Bay, Florida**

#### UCF in Orlando, Florida

The University of Central Florida (UCF) in Orlando, Florida has developed a site on campus that is reserved for insitu testing and may also be used for future deep foundations research. In 2002, a series of insitu tests were performed. In addition to pressuremeter and dilatometer tests, UF performed 5 CPT and 4 DTP soundings at this site. These were performed in pairs such that the two penetration tests adjacent to each other, were given the same number (i.e. CPT 1 and DTP 1 were 1 meter apart as were CPT 2 and DTP 2 and so forth). Standard Penetration Tests (SPT) were also performed by the Florida Department of Transportation. All tests were performed to a depth of 19 meters.

The test results indicated very consistent soil profiles. The first 10 meters ranged from fine sand to sandy, clayey silt interspersed with two thin clay layers. From 10 to 16 meters, a variable layer of clayey silt with shell was present. Below 14 meters the bearing strength steadily increases from 2 MPa to 20 MPa. The readings become more erratic at these depths. The CPT classification (based on Robertson and Campanella) categorized the erratic soils from 16 to 18.5 meters (termination depth) as being sands to silty sands. However, the SPT samples recovered from these depths showed a heterogeneous mix of slightly clayey sandy gravel. The gravel component was found, on closer inspection, to be gray-cemented calcareous sand (Firmly to Well Cemented Calcareous according to Table 1.1). The calcite content appeared to be increasing with depth since the cemented sands were found just below the initial presence of clayey shells (the presumed source of calcite).

The depth between 16 and 19 meters is of interest due to the presence of cemented sands. The penetrometer readings at this depth are very erratic, typical of readings in weak limestone. This variability however, is rational, since calcareous cemented sands typically reside at the transition zone between calcareous sands and the sedimentary rock limestone.



Within the cemented zones (below 16 meters) the DTP tests showed that tip 2 bearing was as erratic as tip 1 bearing. At times the tip 2 readings were above the tip 1 readings and at other times they were equal to or less than the tip 1 readings. However, the peaks and valleys of the tip 2 readings usually coincided rather well with those of tip 1. The tip 1 and tip 2 readings for DTP 3 are shown in Figure 4.5.

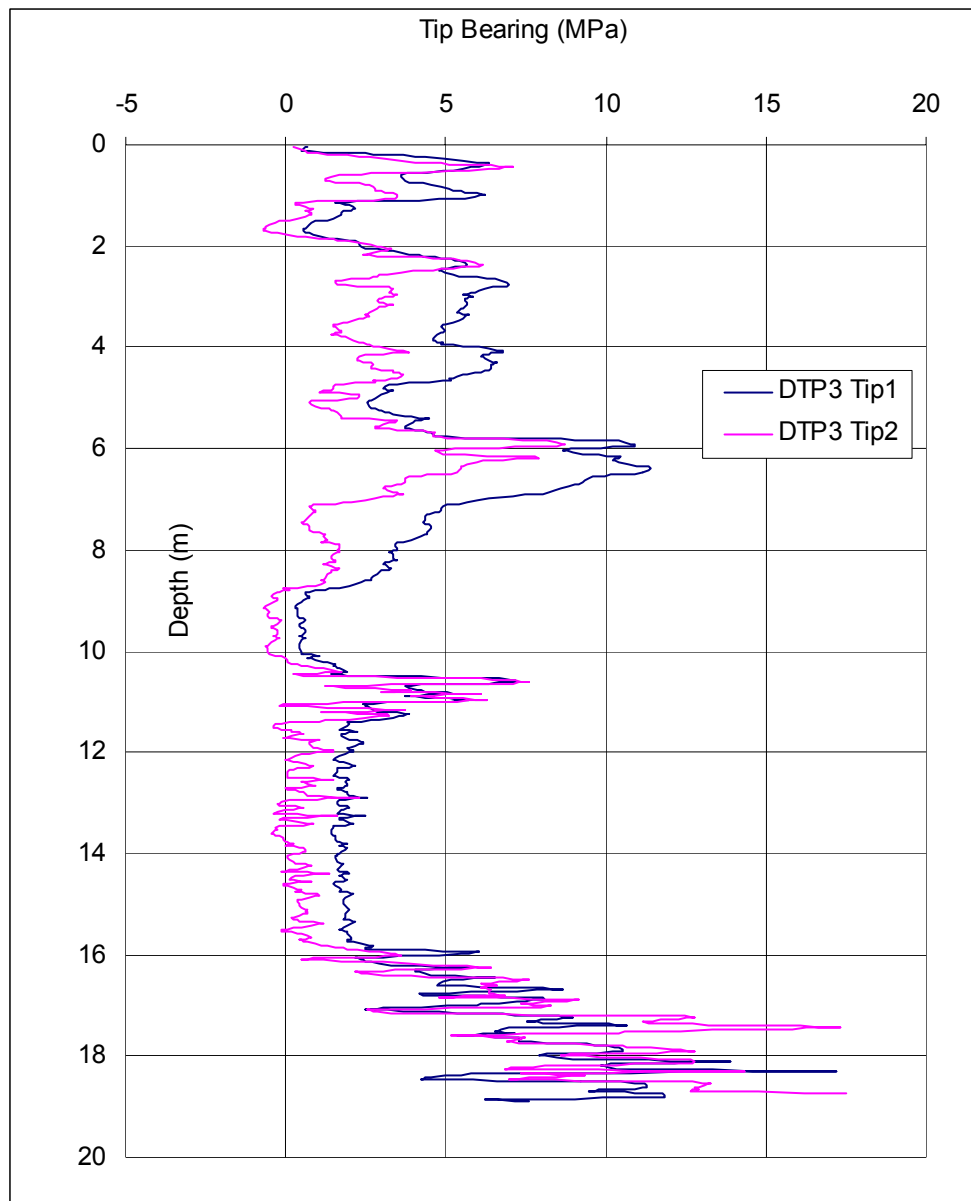


Figure 4.5: UCF Site DTP #3 Tip 1 and Tip 2 Bearing vs. Depth

The erratic nature of the readings may be due to one or both of the following possibilities. First, the trends may be visualized as a series of strength tests on brittle rocks or cemented sands. When one layer of weak rock/cemented sand fractures the strength decreases rapidly

until the underlying intact rock/cemented sand begins to take the stresses of the tip. The bearing then goes up until the new rock/cemented sand fractures. The cycle appears to repeat itself up to 5 times (Bearing readings go up and down 4 to 5 times) for every meter of penetration within this type of material. The second possible mechanism is that the erratic effects may be due to the heterogeneous nature of the degree of cementation within the sands. The SPT samples obtained at these depths show bits of cemented sands with calcareous clayey sands. The calcareous clayey sand may be present in the valleys of the tip bearings while the harder cemented sands may be present at the peaks.

Figure 4.6 below shows the friction ratios for DTP #3 and CPT #3. In the upper sand layers we see that the friction ratio is larger for the DTP than the CPT (just as it is at the Archer Landfill Site). However, within the medium cemented calcareous sand the friction ratios are equal for the DTP and CPT.

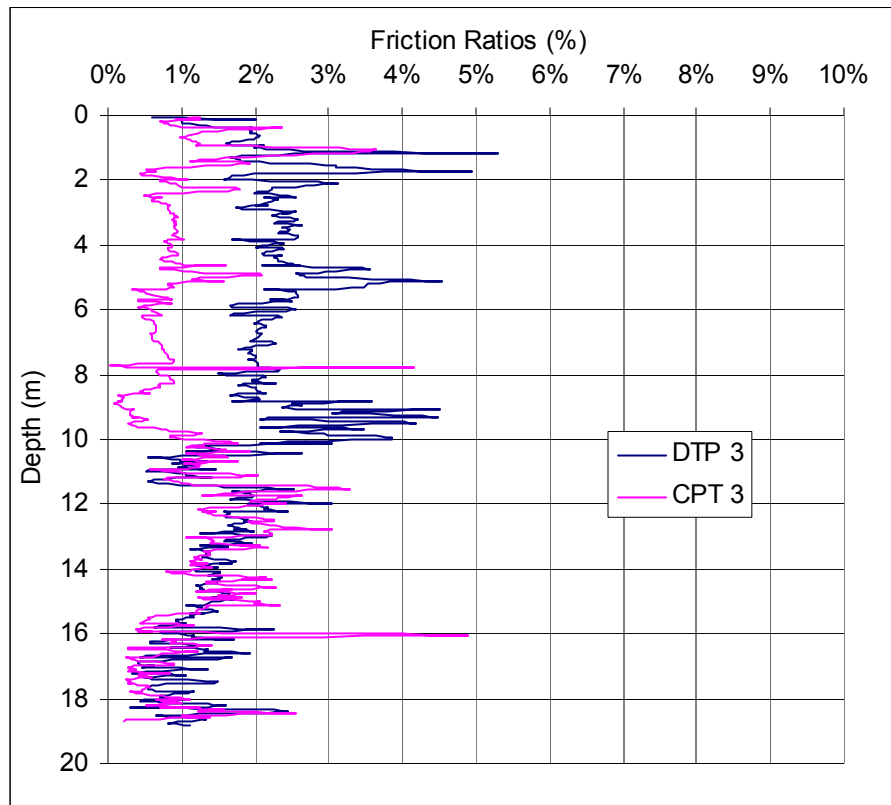


Figure 4.6: UCF Site CPT #3 and DTP #3 Friction Ratio Comparisons

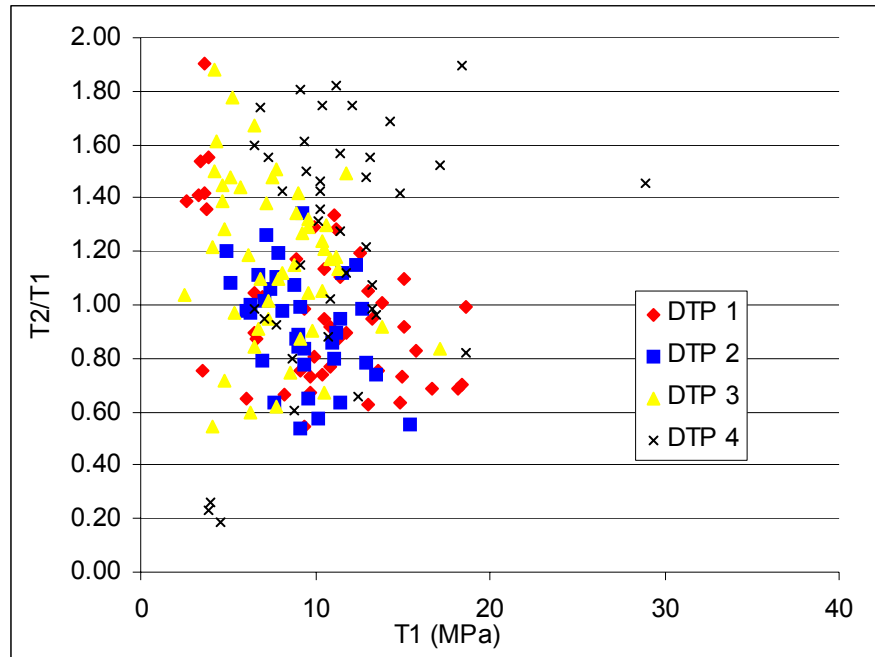


Figure 4.7: UCF Site T2/T1 vs. T1 for Medium Cemented Calcareous Sands (depth between 16 and 18.5 meters)

Figure 4.7 shows the T2/T1 values obtained for DTP soundings 1 to 4 at the depths where cemented sands were present. These values are significantly higher than the values of the Archer Landfill clean fine sands.

In addition to the visual inspection of the SPT cemented sand samples the samples were tested to determine calcite content, silica sand content and clay content. Three small samples of the gray-cemented sand were tested in an improvised acid test. The samples were first oven dried and then crushed, weighed and placed into 3 separate glass containers. A concentrated amount of hydrochloric acid solution was added to the samples to dissolve all of the calcite. The byproducts of the reaction with calcite were water, carbon dioxide gas and calcium ions. When it was believed that all the calcite had dissolved the remaining solution was poured into a small glass bottle. The remaining solution had to be discarded because the calcium ions within the solution could precipitate out as calcite if the solution were allowed to simply evaporate. The fine particles in the solution (clay) were screened out with filter paper. The sediment that remained on the filter paper and in the initial jar was silica fine sand and clay. After the samples were dried, the silica sand and clay amounts were weighed.

The results of the three samples showed rather consist concentrations of material (see Table 4.1).

Component	Estimated Percentage of Material
Calcium Carbonate (Calcite)	60 to 65%
Silica Quartz Sand	25 to 30%
Clay	10 to 15%

Table 4.1: UCF Site Cemented Sand Components from Acid Test

According to the Calcite content, the visual inspection of the cemented samples found in the SPT samples and the classification from Table 1.1, we could assume that the degree of cementation was medium to high. Also, if it were a weakly cemented sand sample it would likely have completely broken down during SPT sampling.

#### West Bay Bridge Near Panama City, Florida

The West Bay Bridge is a site where cemented sands were believed to be present. At this site 6 DTP tests and 3 CPT tests were performed. The DTP test results were used to attempt to predict pile capacities for Test Piles that had been installed in the early 1990's. The pile capacities are discussed in Chapter 6. However, DTP tests #5 and #6 were performed in cemented sand/limestone and therefore will be discussed next.

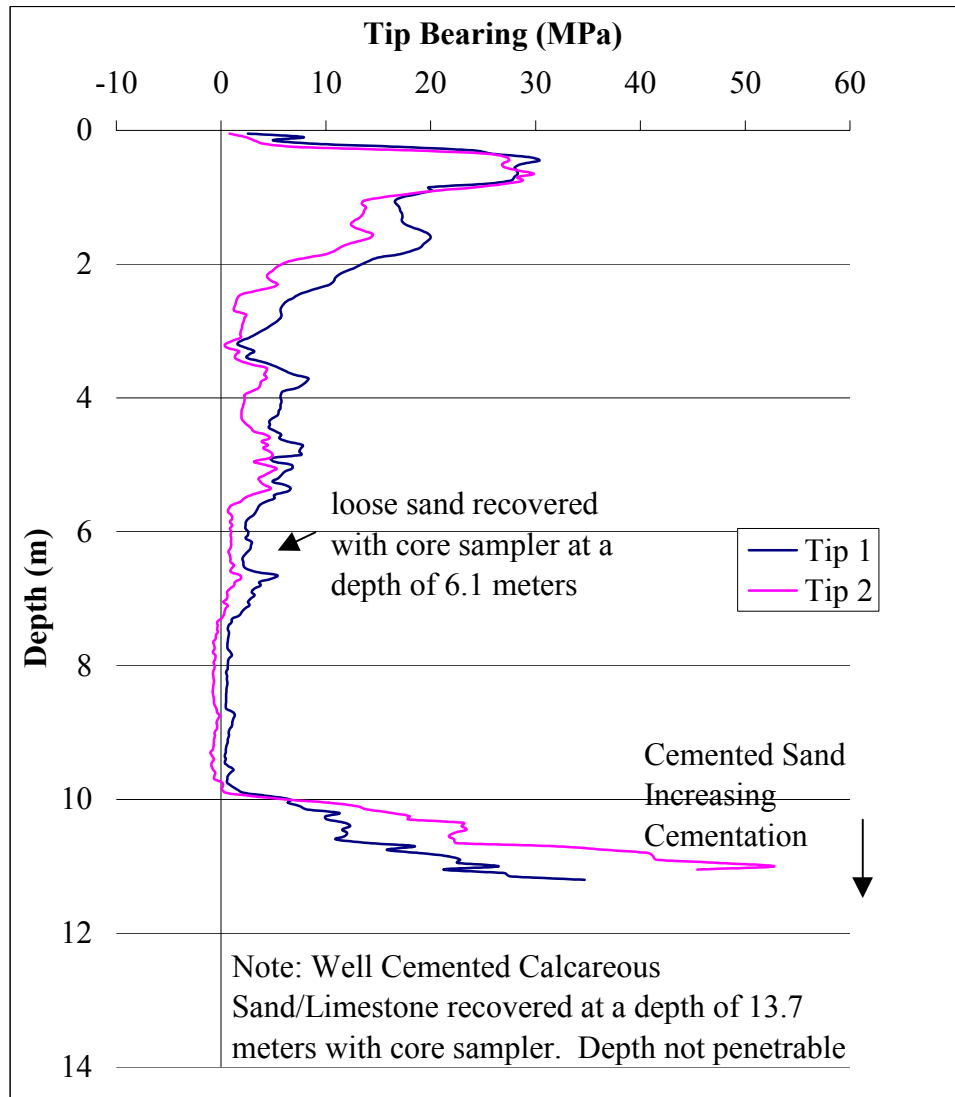


Figure 4.8: West Bay Bridge DTP 5 Tip Bearings vs. Depth (15 feet from DTP 6)

Although there appeared to be cemented sands of varying cementation at different locations across the West Bay Bridge two DTP tests were performed in the immediate vicinity where an actual coring of well cemented sand/limestone was obtained. The borehole where the core sample was obtained was located at DTP 6 down to a depth of 50 ft. or 15.25 m. Within the borehole two core samples were obtained, one at 20 ft. (6.1 m) and one at 45 ft. (13.71 m). Loose sand was obtained at 6.1 m while well-cemented calcareous sand or limestone was obtained at 13.7 m. The hole was then backfilled with sand and DTP 6 performed within it. Therefore, DTP 6 showed virtually no resistance to a depth of almost 10 m. DTP 5 was

performed about 15 ft. from DTP 6. Neither sounding was able to penetrate completely into the limestone.

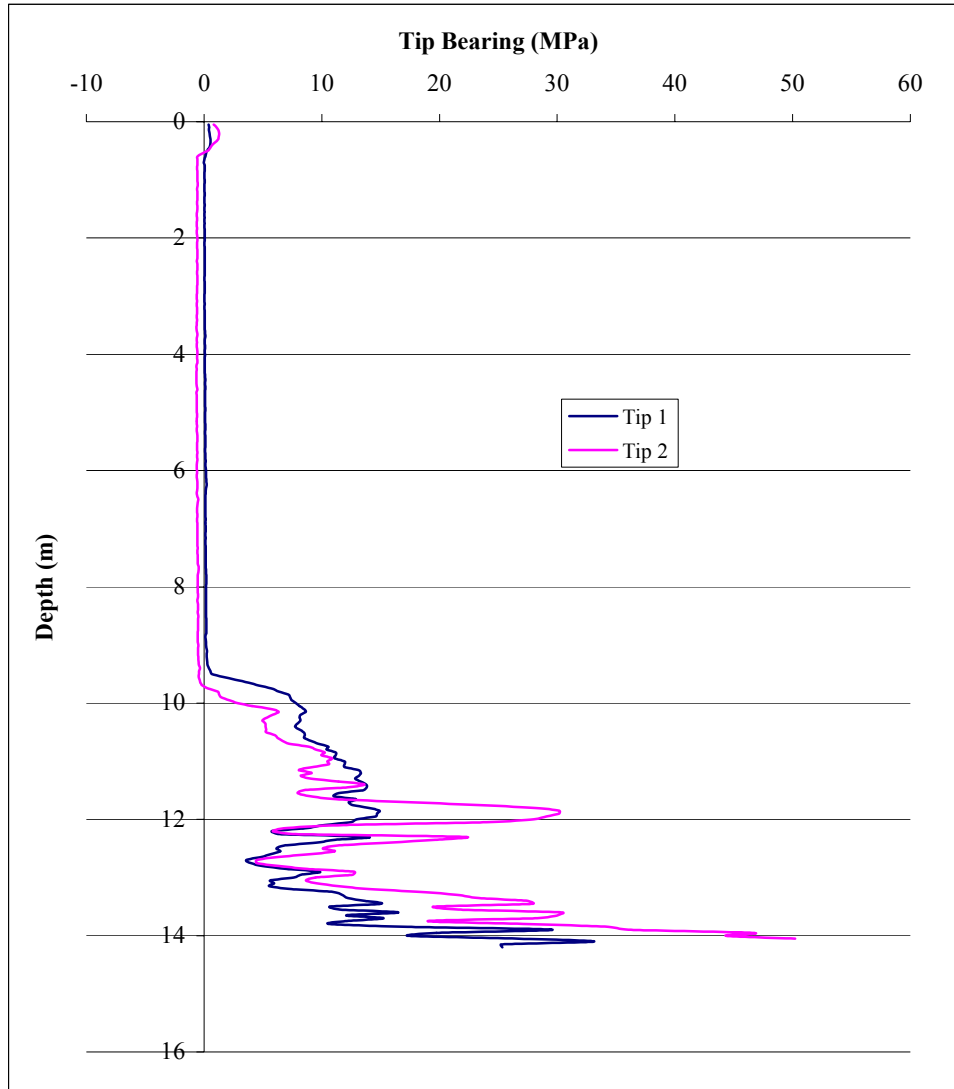


Figure 4.9: West Bay Bridge DTP 6 Tip Bearings vs. Depth (performed within Borehole after backfilling with sand)

In both Figures 4.8 and 4.9 we see high tip ratios in the depths where cemented sands were likely present. The cemented sand was likely to be present just above the point where refusal is encountered (from 10 to 11 m for DTP 5 and from 13 to 14 meters for DTP 6). Within these depths the tip ratios are between 1.5 and 2.5 while tip 1 values are between 10 and 35 MPa. These values are just slightly higher than those seen at the UCF site (between 0.6 and

1.8). However, there is good consistency between both cemented sand sites. Also, the bearing readings for DTP 6 are erratic like those soundings at UCF, while the readings for DTP 5 were not erratic.



Figure 4.10: West Bay Bridge Samples Obtained from Borehole

Figure 4.10 shows the sample of limestone obtained at 45 ft. The top of the sample (45 ft.) could barely be broken up with finger pressure. The bottom of the sample however (50 ft.) could not be broken up with finger pressure giving the impression that cementation was increasing with depth.

### **Mixed Soils and Soft Soils**

Many of the DTP tests performed in the field were performed in different mixed soils including silty fine sands and clayey sands. Table 4.2 shows the test locations and the number of tests that were performed at those sites. No soil sampling was performed at these sites with the exception of the Lake Alice West Bank site where auger bored samples of soil were visually inspected down to a depth of 6 feet. Since little soil sampling was performed, the conclusions drawn come from the comparison of the DTP and CPT results.

Site Name	Number of CPT Tests	Number of DTP Tests
Vilano Beach – Vilano, Fl	2	5
Vilano Bridge West – Vilano, Fl	1	1
South West Recreation Center – Gainesville, Fl	1	5
Lake Alice West Bank – Gainesville, Fl	1	1
Applied Foundations Testing – Green Cove Springs, Fl	1	1

Table 4.2: Sites where Mixed Soils and Soft Soils were present



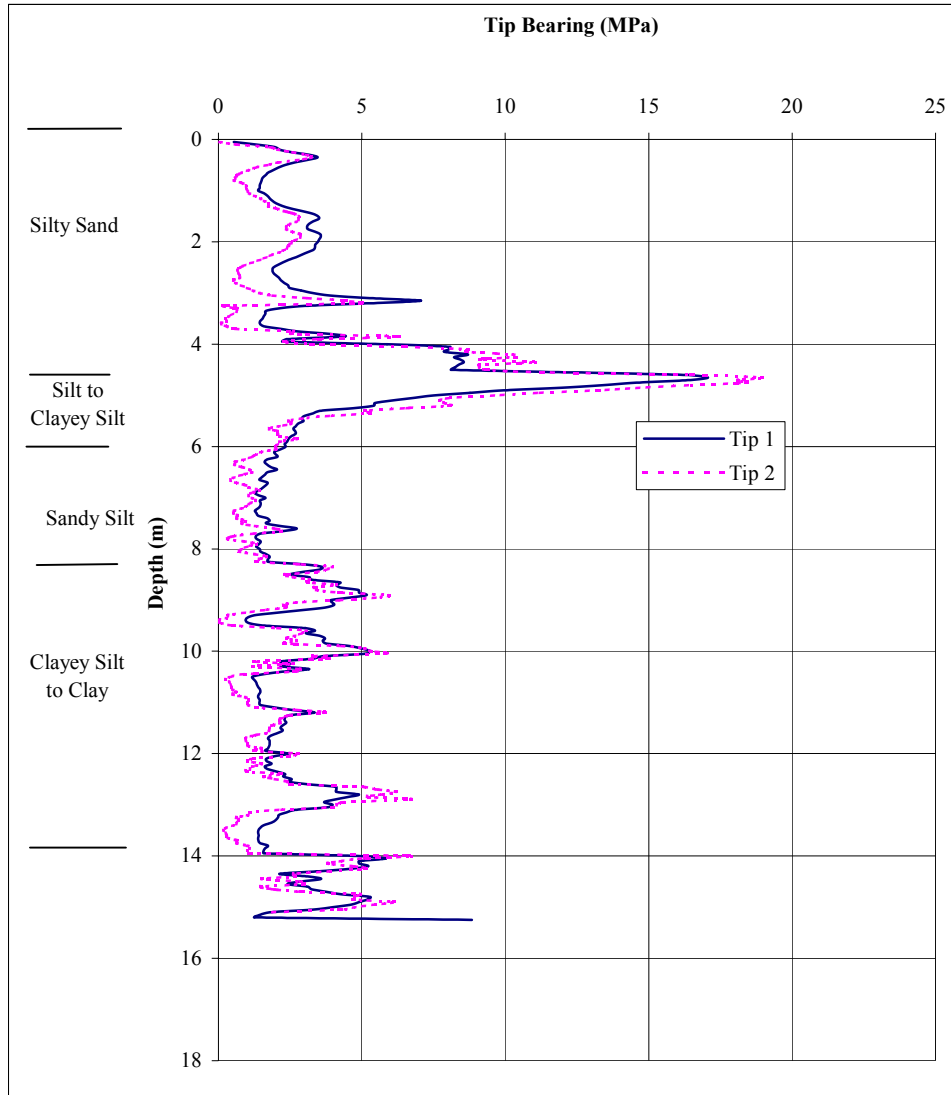


Figure 4.11: Lake Alice West DTP 1 Tips vs. Depth

As mentioned previously the Archer Landfill was a site where clean fine sands were known to be present. Sands and silty sands were also found at Vilano Beach and at the west bank of Lake Alice in Gainesville, Florida. The T2/T1 ratios in the silty sands were greater than those at the Archer Landfill. While the tip ratios at the Archer Landfill fine sands were between 0.4 and 0.6 (Figure 4.3) the tip ratios at Lake Alice went from less than 0.4 to over 1.0 (Figure 4.11). The tip ratios are higher at Lake Alice possibly due to the high silt contents.

At the locations where the sands had large silt contents and clay contents the tip ratios varied greatly increasing as high as 2.0. It is not clear what could be causing the soils to behave this way. In Chapter 2 we discussed the possibility of a compressible silty soil being densified causing a larger tip 2 reading. It may also be possible that there are more heterogeneous soil effects occurring.

Some soft soil was present in Green Cove Springs and Vilano, Florida. These soils showed a low tip ratio, similar to the clean fine sands. These soils were so weak that tip 2 had virtually no resistance acting on it. This can be seen in Figures 4.12 and 4.14 where the tip 2 readings are zero or slightly negative. The slightly negative readings may be due to the variability of the tip 2 baseline or the tip 2 annulus straining unevenly. Also in Figure 4.13 we see that there is still a difference in friction ratio between the DTP and the CPT in the soft clay (below a depth of 7 meters), however the difference is smaller than in the upper sand layers.

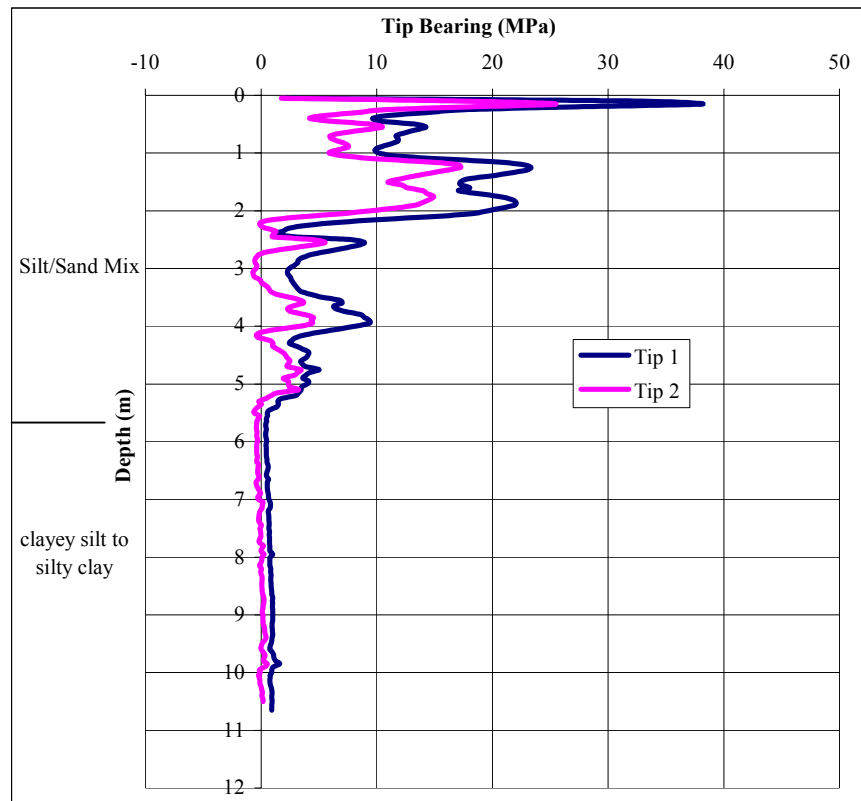


Figure 4.12: Green Cove Springs DTP Tips vs. Depth

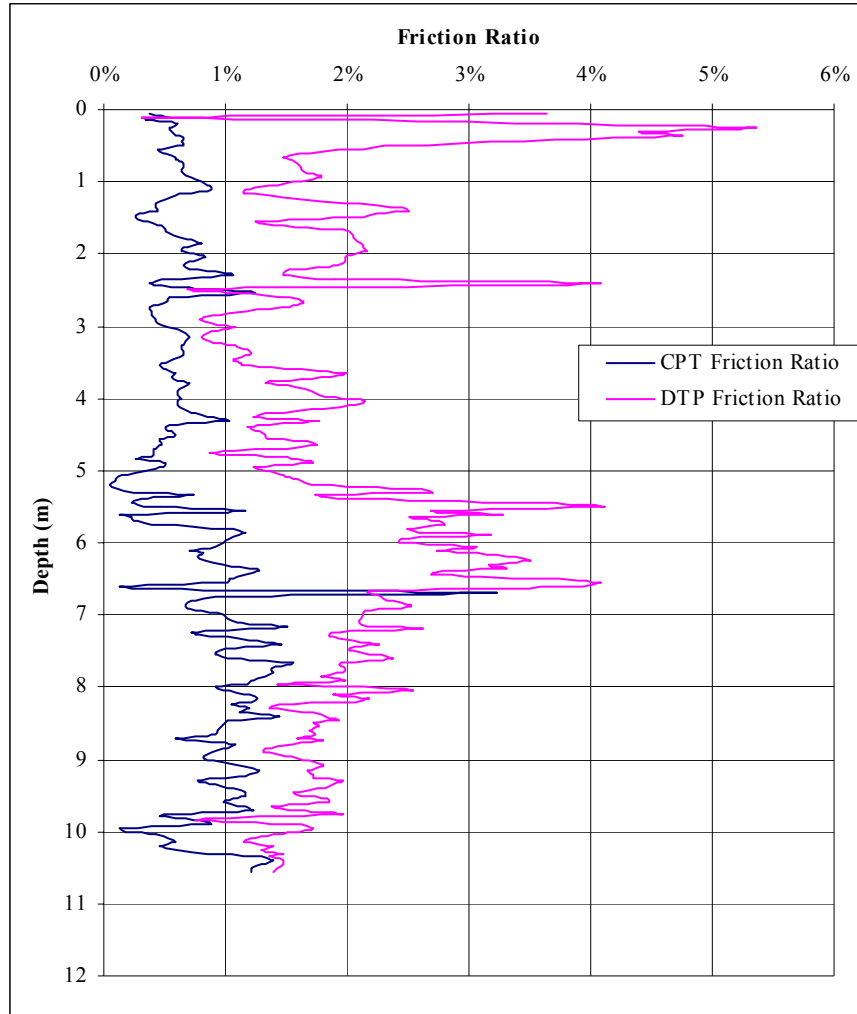


Figure 4.13: Green Cove Springs DTP #1 and CPT #1 Friction Ratios

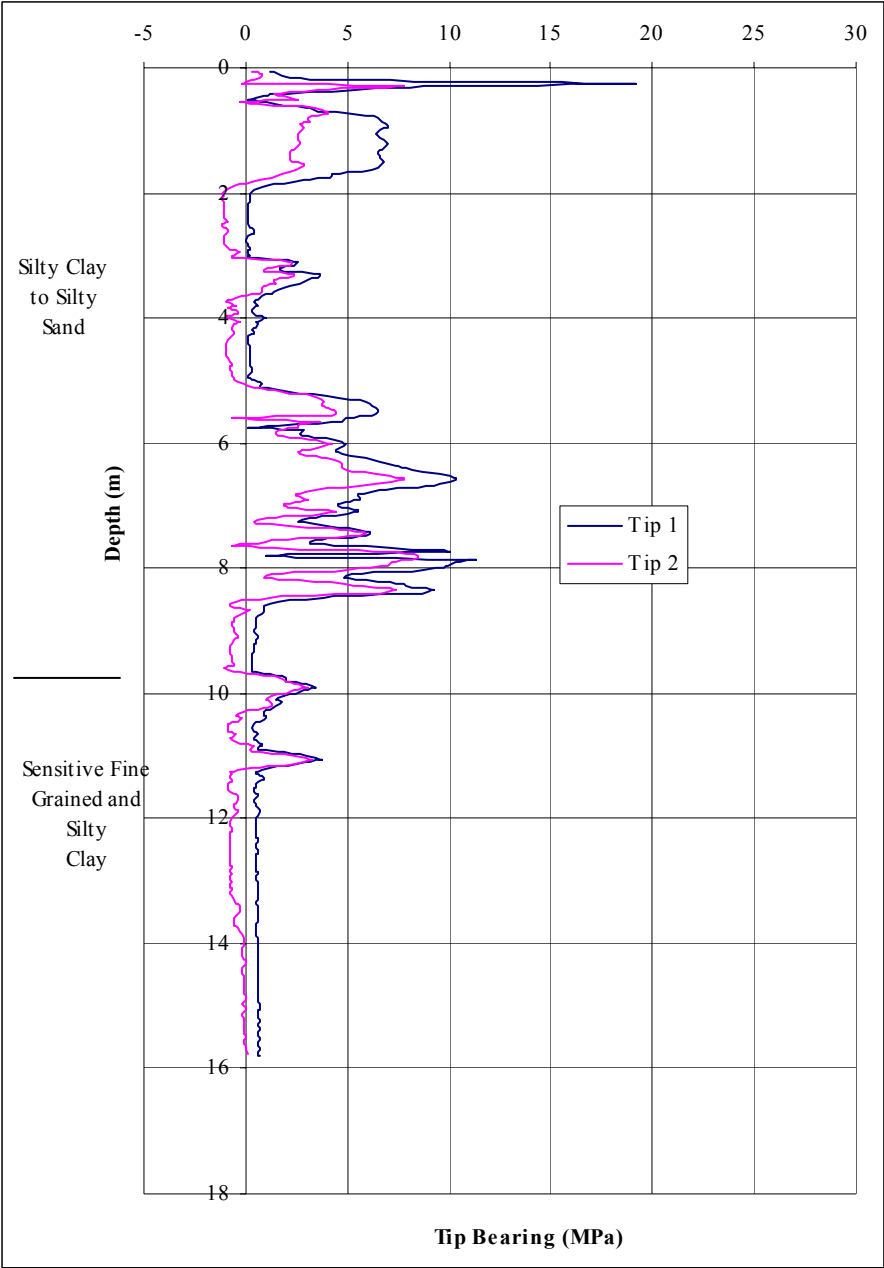


Figure 4.14: Vilano Beach West DTP #1 Tips vs. Depth

## **Repeatability of DTP parameters in Homogeneous and Heterogeneous Soils**

In Chapter 2 the possible effects of heterogeneous soils on tip ratio were discussed. During cone calibration it was seen that the tip 2 annulus shows the most consistent results when a load is uniform on the bearing annulus. Non-uniform stresses, due to penetrating heterogeneous soils, could strain the element un-evenly and cause false readings. Homogeneous soils should give us better results.

The homogeneous fine sands at Archer landfill where tests showed rather repeatable DTP results (namely tip ratio and friction ratio). The three CPT soundings were performed in the same vicinity. The DTP friction ratios and tip ratios were seen to be consistent between the three soundings (Appendix Figures A-5 to A-10).

Heterogeneous soils such as those present near the western end of the Port Orange causeway in Port Orange, Florida show less repeatable tip ratio readings between nearby DTP soundings (Appendix Figures A-80 to A-82). At this site 6 DTP soundings were performed with three of the four presently available Dual Tip Penetrometers: CSC 830 TC (2002), CSC 829 TC (2002) and CSC 782 TC (2001). Each of these penetrometers were used for two soundings. The soundings were done in the same location with 1 meter apart. Standard Penetration tests previously performed at this site showed grey shelly silty clayey sands. At this site the friction ratios are rather consistent between soundings (Figures A-77 to A-79) as they were in the homogeneous soils of the Archer landfill. However, the tip ratios show variability in magnitude between soundings although they are consistent in their trends (Appendix Figures A-80 to A-82). The tip ratios increase and decrease at nearly the same depths for each sounding.

The tip ratio magnitudes therefore appear to be more consistent in homogeneous soils rather than heterogeneous soils.

The next chapter will discuss the results from the Calibration Chamber tests in sand. These tests will be compared with the field results. The results will be used to develop a soil classification system based on the DTP data.

## CHAPTER 5: CALIBRATION CHAMBER TEST RESULTS

In addition to the DTP field-testing, a calibration chamber was designed and assembled for testing clean fine sand and artificially cemented sand. This chapter describes the design, set up and results of the testing program.

### Calibration Chamber History and Design

The cone penetration test has been used for insitu testing for over 40 years. However, during its initial stages of design, researchers were quickly forced to conduct laboratory controlled CPT tests on artificially prepared samples as opposed to field trials. This was, in large measure, due to subsurface spatial variability that would invariably complicate any tentative theories derived from the probe. The laboratory tests consisted of placing soils of known properties, usually cohesionless material, into large calibration chambers and inserting cone penetrometers under a variety of boundary conditions. Many of the CPT interpretation methods for determining soil properties are based on these calibration chamber tests in conjunction with triaxial test data (Lunne et al. 1997).

The standard calibration chamber is similar to a very large triaxial device, in which confining stresses are controlled via a piston and fluid filled membranes. However, due to fiscal and time constraints (i.e., this testing program was not included in the original research plan), the system used at the University of Florida for DTP testing was less elaborate. The rigid wall chamber, without boundary stress control, was constructed and installed at Weil Hall on the UF campus. The traditional calibration chamber also has a sophisticated raining system that allows provides for a uniform deposition of material at user prescribed relative densities. Again, since the objective of this chamber is to compare a cemented sand to a non-cemented one, the necessary raining system and appurtenances could not be justified. However, the sands' relative density was controlled via a measuring system that allowed for reasonably accurate ranges. Figures 5.1 and 5.2 illustrate the chamber design and set up.

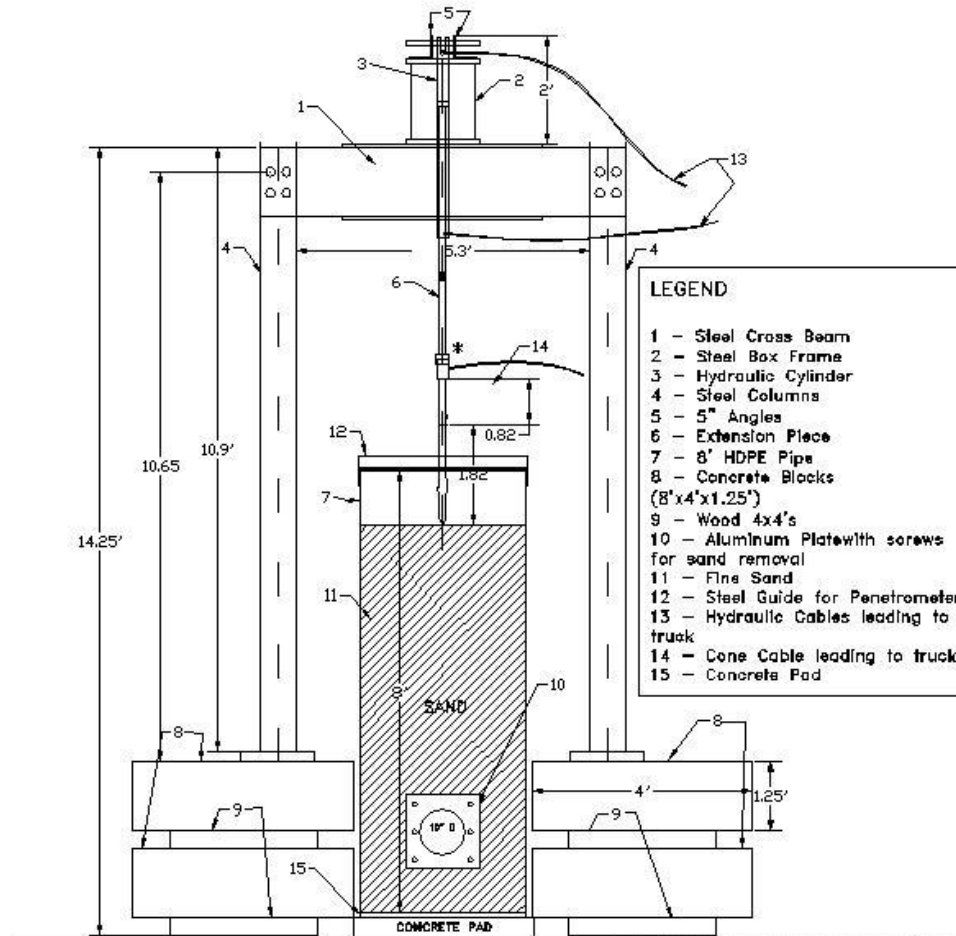


Figure 5.1 Calibration Chamber Set Up for Fine Sand Testing

The testing device consists of an 8 ft. tall, 36-inch diameter high-density polyethylene pipe. The pipe has a circular insert at the bottom to contain the sand. There is also a 10 in. diameter hole near the bottom of the pipe for sand removal. When in use, this access panel is covered by an aluminum plate and secured with screws and two large restraining straps (not shown). During the initial set-up, the pipe was first placed on a fresh concrete base that would conform to the pipe's O.D. dimensions. After curing, the pipe was hoisted up and a load cell attached to a steel bearing plate was placed over the cured concrete base to serve as a weighing mechanism. Unfortunately, the load cell was damaged during filling of the chamber due to disproportionate eccentric loads exerted on the plate.





Figure 5.2 Exterior View of DTP Calibration Chamber

The pipe and base are positioned between 4 concrete blocks and a steel reaction frame. The reaction frame consists of two steel columns approximately 11 ft. tall linked together by two 7 ft. long steel channels. The gap between the channels, in turn, houses a reaction plate bolted to them in which a 3,000-psi hydraulic ram is located. This ram is used to thrust the penetrometers (CPT and DTP) into the sand-filled chamber. The columns were connected to the concrete blocks in order to maintain sufficient clearance height for the hydraulic cylinder as well as providing reaction for the ram.

The first series of tests were performed in dry fine sand. The sand chosen was a silica sand mined at Edgar, Florida. This material had been used for over 20 years at UF on previous research projects.

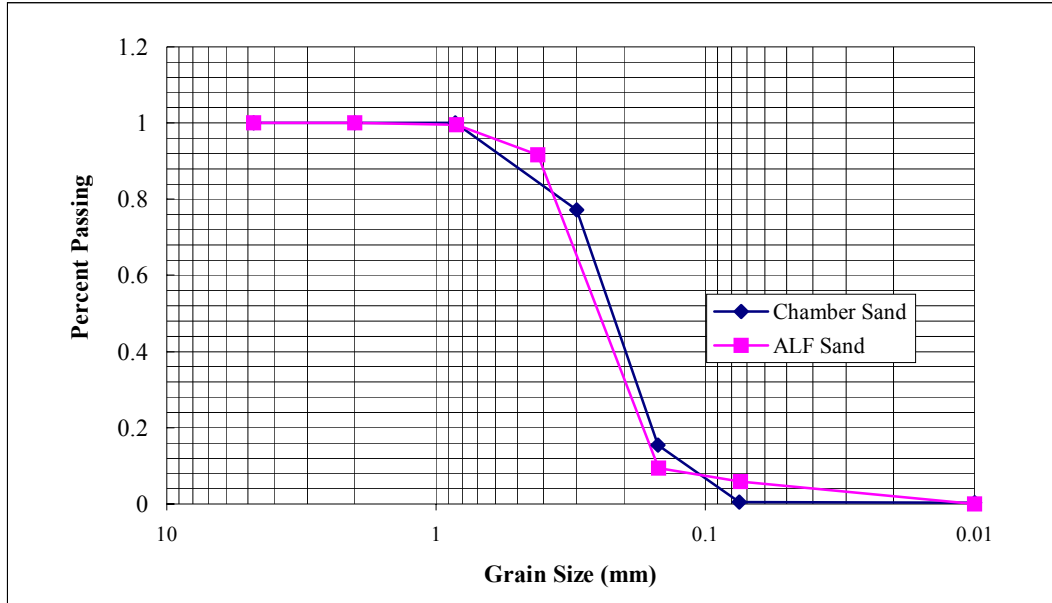


Figure 5.3: Grain Size Distribution Curve for Edgar Fine (Glass) Sand and Archer Landfill Sand

Figure 5.3 presents the soil distribution curves for both the Edgar and Archer landfill site. Both curves are very similar, therefore it was expected that the results would be comparable. The maximum and minimum void ratios measured for the Edgar sand were 0.91 and 0.65 respectively and its specific gravity, 2.63.

### Dry Sand Testing

The goal of the first series of DTP tests was to see if there were any differences in T2/T1 ratios between loose and dense sands. To do this the chamber would be used to hold dense and loose sand. The lower layers of sand were compacted while the top layers of sand were left loose. The pipe was filled in lifts of 8-inch thickness on average. The first 6 lifts were compacted with a 30 lb concrete falling weight. The weight was allowed to fall evenly onto the surface of the sand from a height of about 2 feet. The following 5 lifts needed to fill the pipe were not compacted. The result was a 43-inch thick dense layer overlain by a 43-inch thick loose layer of sand. The following table describes the lift number, top of lift elevation and degree of compaction. For simplification purposes the elevation datum zero was set to refer to the bottom of sand lift 1. The layers can also be seen in Figure 5.7.

Sand Lift	Top of Layer	Lift Thickness (in.)	Degree of Compaction
-----------	--------------	----------------------	----------------------

Number	Elevation (in.)		
1	8	8	12 tamps + compaction w/concrete vibrator
2	16.9	8.9	12 tamps
3	24.9	8	12 tamps
4	32.6	7.7	13 tamps
5	38.9	6.3	20 tamps
6	43.2	4.3	20 tamps
7	52	8.8	0
8	59.9	7.9	0
9	68.8	8.9	0
10	77.8	9	0
11	86.3	8.5	0

Table 5.1: Sand Lifts for Calibration Chamber Fine Sand Testing Series

After filling the pipe, steel flat bars and bolts (Figure 5.4) were used to attach the two concrete blocks under the steel columns together to add 12,000 lbs of reaction to the frame. The hydraulic ram was then put in place within the beam and the hydraulic assembly was set up for testing (Figure 5.4). The flow valves in the hydraulic circuit were adjusted so that the penetrating rate of the ram would be near 3 cm/sec. The rate was greater than the standard 2 cm/sec in case the soil resistance were to slow down the penetration rate slightly. There is little difference in penetration resistance when the penetration rate is between 1 and 3 cm/sec. A pressure relief valve and two pressure gauges were placed in the circuit to help make sure the pressure would not exceed 3000 psi.

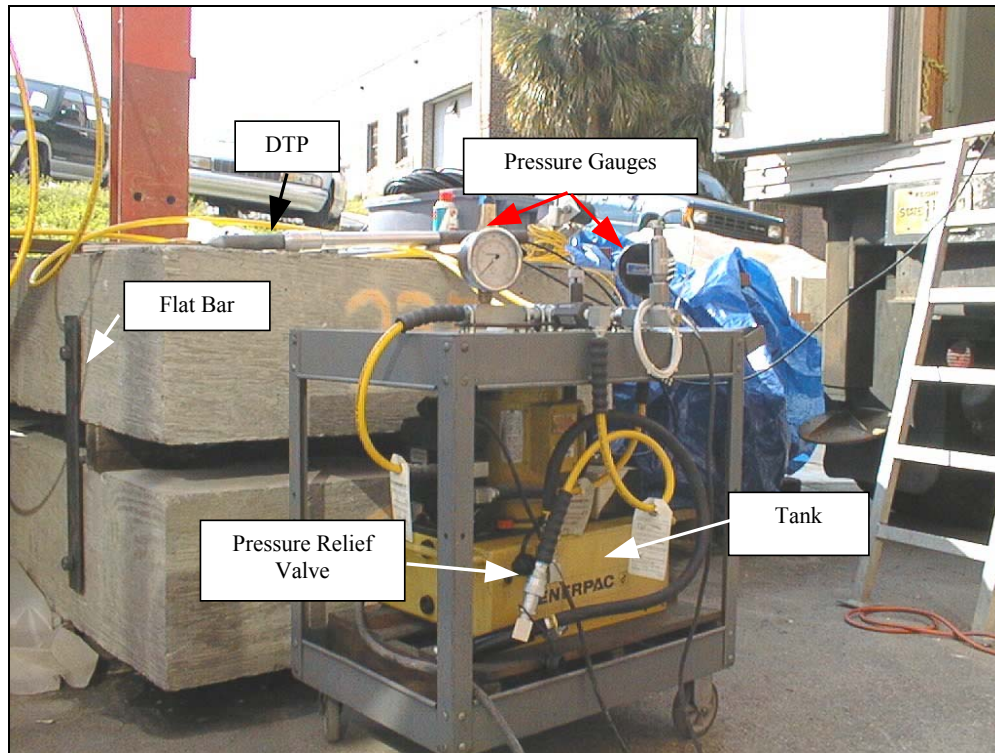


Figure 5.4: Hydraulic System and Reaction Frame Blocks

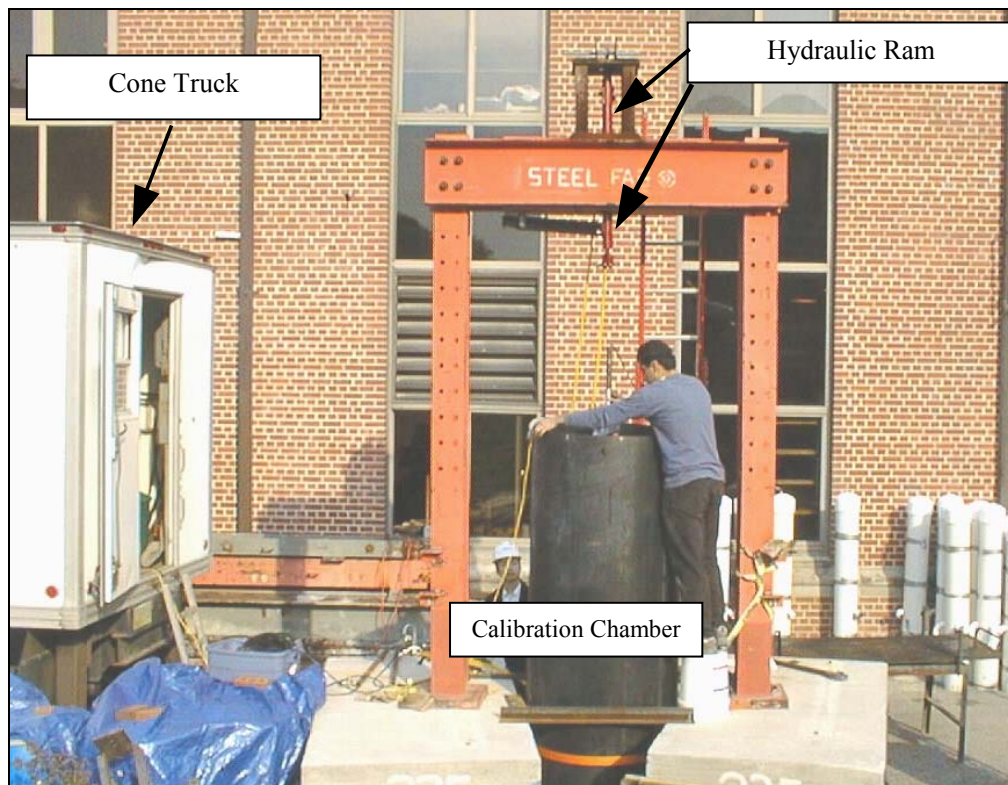


Figure 5.5: Calibration Chamber Prior to Testing

After checking the hydraulic set up, the cone truck computer was set up and turned on. A separate cone cable was threaded through two rods and the penetrometer/rod coupler. The cable was connected to the penetrometer and the coupler was screwed onto the penetrometer. The cone cable had already been tested and found to be operating properly. The penetrometer was allowed to warm up for a period of about 15 minutes.

After the warm-up period, the cone was placed through the steel guide and/or wooden guide and then through the depth counter (Figure 5.6). Since the testing would not be performed within the cone truck, a separate depth counter was needed to trigger the computer to take readings. When a CPT or DTP test is taken in the field three sensors would have to be active for the computer to take readings: the head load sensor, the hydraulics switch (there must be pressure in the hydraulic line) and the depth sensor (which activates at every 5 cm of penetration). The computer allows the option of bypassing the head load and hydraulic line triggers so that only the depth sensor would trigger readings to occur. This was done in the Calibration Chamber testing.

Due to difficulties with keeping the DTP vertical Tests 1 and 3 were not performed into the dense sand layer. The other DTP tests and the two CPT tests were performed nearly to the bottom of the pipe with the help of a wooden guide. The wooden guide was made up of two wood 2 by 4's nailed together in a cross. The wooden guide had a 1.5 inch diameter hole drilled into it that was just large enough for the push rods to go through (threaded push piece would not fit). The wooden guide was snug against the push rods.

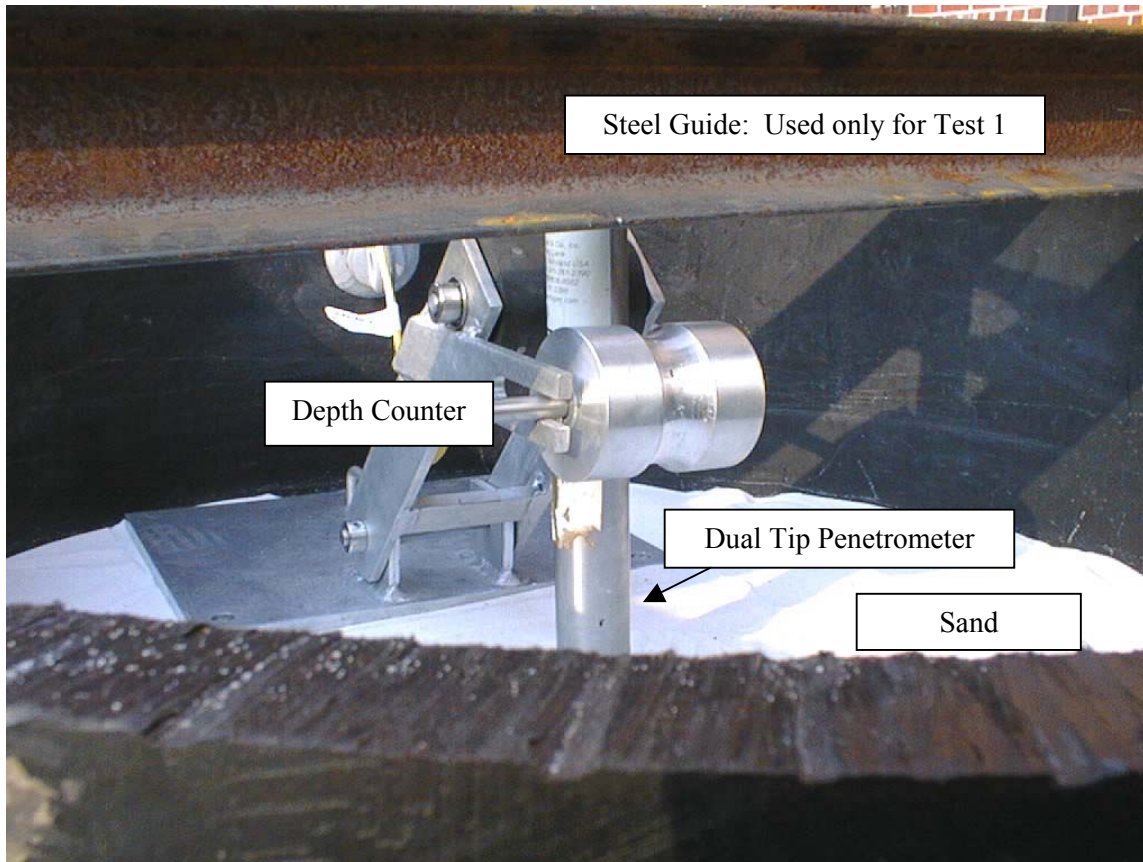


Figure 5.6: Depth Counter and Penetrometer during Test # 1

Due to the above-mentioned difficulties in keeping the penetrometer vertical, the tests were interrupted several times due to errors that needed to be corrected. Also, 450 lbs of sand had to be removed from the pipe in order to have room for the wooden guide and for an efficient pushing scheme so that the penetration would not have to be stopped too often. The removal of the sand brought down the surface elevation to 80 inches for Tests 2 and 3. More sand was removed which brought down the surface elevation to 75 inches for Tests 4 through 9 (Figure 5.7).

The discontinuous nature of the tests performed is a problem because the bearing readings are smaller when the soil is not completely failed. If the test is interrupted and the load is removed the soil will need to yield more after resuming the test in order to get a correct reading. The soil must yield a certain distance before the bearing and frictional resistance are fully mobilized by the soil. This effect is seen in regular cone penetration tests often when the test is stopped for placement of another rod. If the depth counter triggers too soon after

resuming advancement then the reading will be lower than it should be. This is seen when abnormally low  $q_c$  bearing readings are noticed at one-meter intervals. Regular cone penetration tests are usually corrected for these effects.

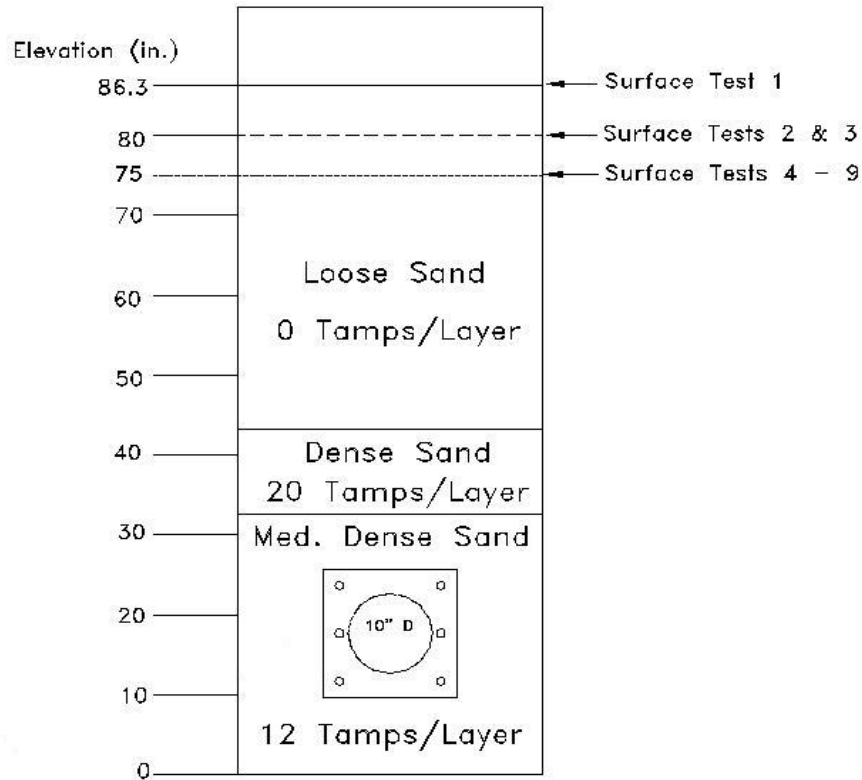


Figure 5.7 Pipe Sand layers

Besides the discontinuities in testing there were times during the calibration chamber tests, the depth counter was accidentally triggered during a pause. This resulted in near zero tip 1 readings and negative or zero tip 2 readings. It was therefore necessary to correct the readings. All figures and plots presented in this chapter on the calibration chamber data contain only the corrected data.

It should be noted that the ideal test in the calibration chamber would have 4 interruptions. These would be due to twice adding a cone rod and twice adding a longer push piece. The longer push piece must be added since the stroke of the ram is 36 inches and not long enough to push the 1-meter long rod.

### Results of Calibration Chamber Testing in Dry Sand

A total of 9 penetration tests were performed in the clean fine sand, 7 with the Dual Tip Penetrometer (DTP) and 2 with the Cone Penetrometer. Each test was performed in the same location within the chamber. This could be done since the sand was dry and the cavity formed would close up after the retraction of the penetrometer. Although the soil is “disturbed” after the first test, testing the same spot again would allow us to see if the tip ratio was dependent on the sand particles (which is constant) or on density (which can vary after each penetration).

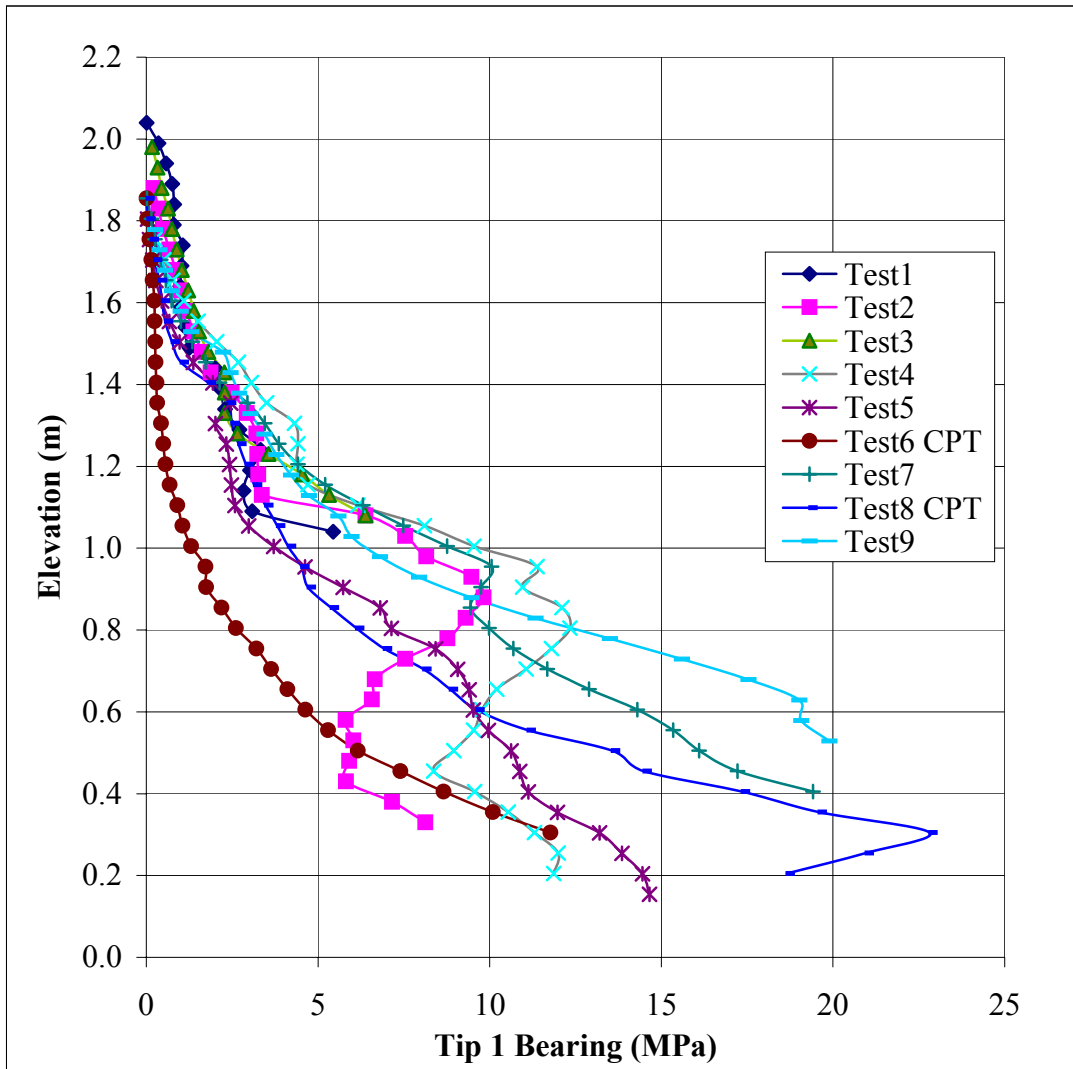


Figure 5.8a: Calibration Chamber Tests in Fine Sand Tip 1 Bearing vs. Elevation



The results for tip 1 bearing and  $q_c$  bearing for Tests 1 through 9 are shown in Figure 5.8a above. The figure has many tests shown and can be confusing to view, therefore the figure is shown again on the following pages with only the relevant tests plotted. Since Tests 1 and 3 could not be continued into the dense sand due to problems with the guide they will not be discussed here. From the tip 1 bearing plot 3 points of interest come up.

1. First, for Tests 2 and 4 -- the first two tests to penetrate the dense sand -- the tip 1 bearings are consistent with the layering described in Figure 5.7, i.e. loose sand over dense sand over medium dense sand. Near the surface of the sand tip 1 bearing increases slowly. At an elevation of about 1.4 meters the rate of increase starts to rise due to the presence of the dense sand layer. The tip 1 bearing reaches a peak in the dense layer at 0.85 meters. The bearing then starts to decrease to a relative minimum at 0.4 meters (medium dense layer). The bearing then increases again possibly due to the nearing of the bottom of the pipe.

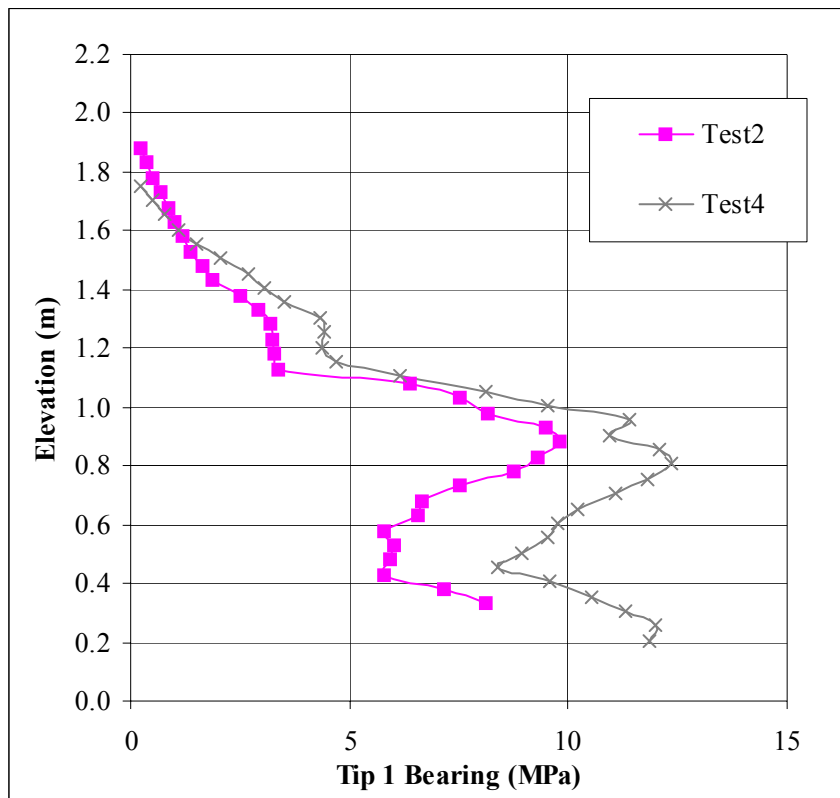


Figure 5.8b: Calibration Chamber Tests 2 and 4 in Fine Sand Tip 1 Bearing vs. Elevation

- The second point of interest is that with repeated testing the soil begins to lose its loose and dense layer characteristics and instead displays a uniform density (Figure 5.8c). There seems to be little change in density in the upper loose layer. However, the bottom sand becomes denser with each test. At an elevation of 0.6 meters Test 9 shows more resistance for tip 1 than Test 7, which shows more resistance than Test 5. Tests 9 shows a consistent increase in bearing suggesting that the sand has achieved a rather uniform density with respect to depth.

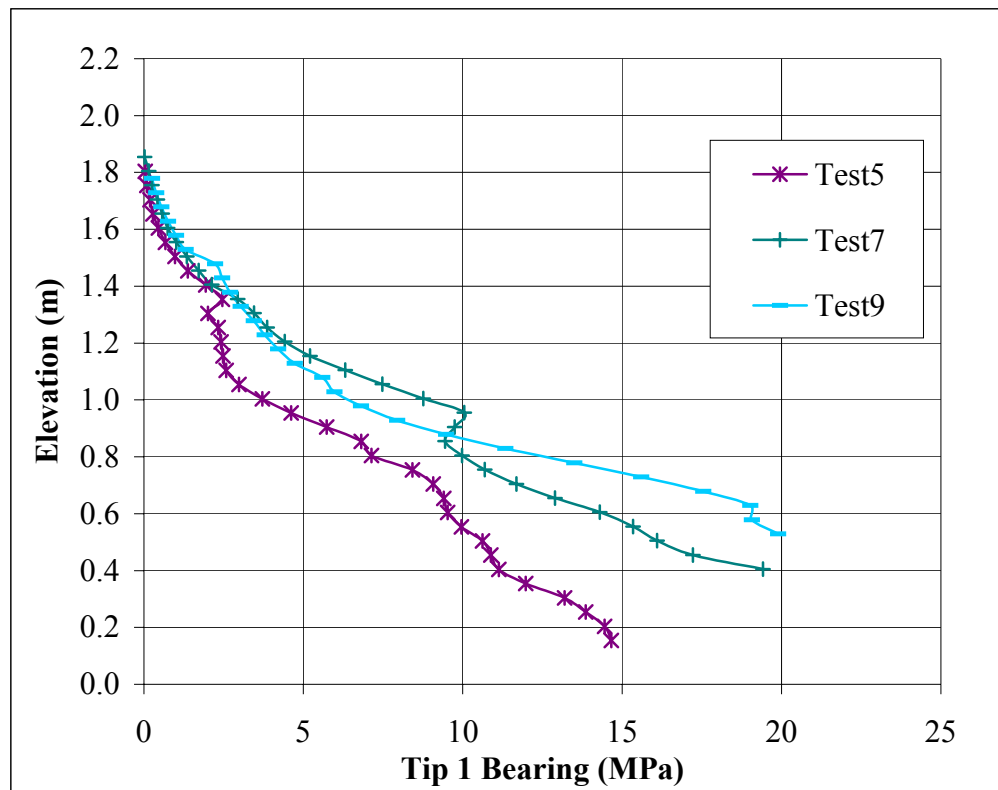


Figure 5.8c: Calibration Chamber Tests 5, 7 & 9 in Fine Sand Tip 1 Bearing vs. Elevation

- The third point of interest is that the two CPTs show lower bearings than the DTP tests (Figure 5.8d). This was odd since in the field it was noticed that tip 1 bearing values do not change from DTP to CPT at the same site. Perhaps this effect could be attributed to the boundary conditions of the chamber. However, in the plot of inclination versus depth (Figure 5.9) the CPTs appear to have greater fluctuations in inclination during penetration than do the DTP tests. It seems that the CPT cone tip moved more probably to find a path of least resistance. The second wedge on the DTP may help eliminate some of this effect in the DTP. It is also important to note

that Test 8 (2<sup>nd</sup> CPT test) shows greater bearing values than Test 6 (1<sup>st</sup> CPT test) meaning that the above-mentioned densification (point 2) is still noticed in the CPT tests.

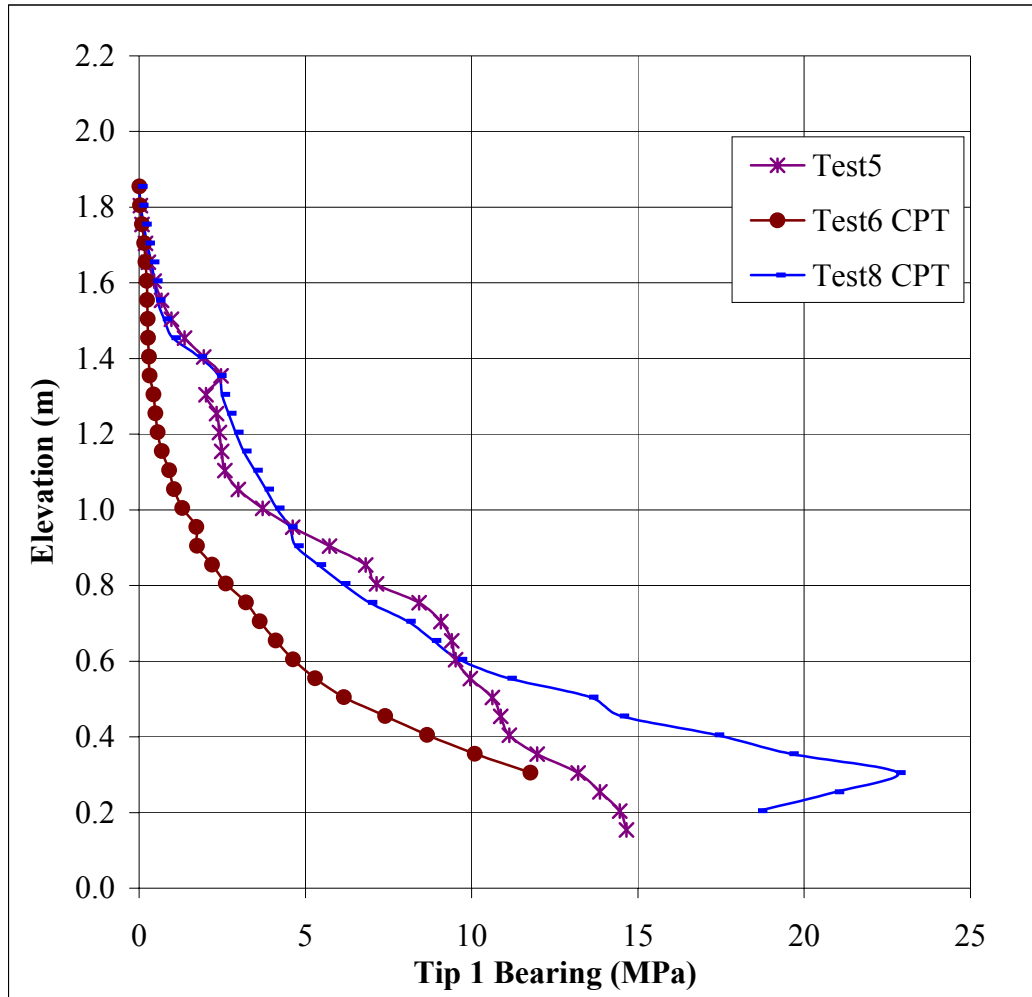


Figure 5.8d: Calibration Chamber Tests 5, 6 and 8 in Fine Sand Tip 1 Bearing vs. Elevation

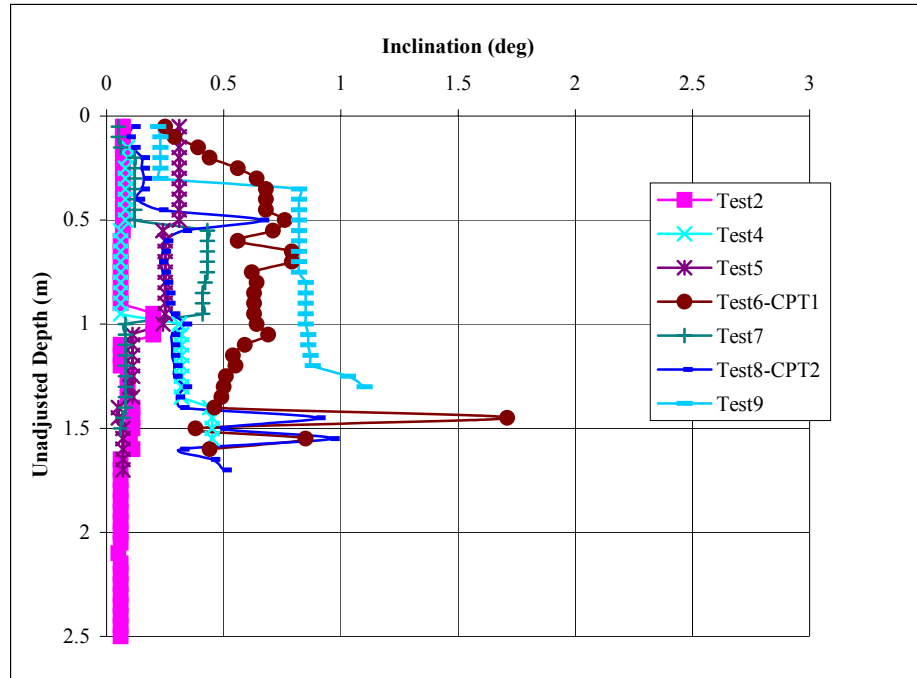


Figure 5.9: Calibration Chamber Tests in Fine Sand Inclination vs. Depth

In previous in-situ testing it was noticed that there were differences in the friction ratio values between the DTP and CPT in fine sands. The friction sleeve readings and friction ratios for the calibration chamber results are presented below in Figures 5.10 and 5.11. The friction sleeve readings show the same characteristics as the tip 1 plots in Figures 5.8a to 5.8d. However, the friction ratio plot shows much variability especially near the surface. This may be because tip 1 is not deep enough to develop a full failure zone. The “critical relative depth” – normalized by tip diameter B as the parameter  $(D/B)_{cr}$  -- is on the order of 5 to 10 for loose sands and 20 to 25 for dense sands (Durgunoglu et al.). The friction ratio values for the DTP tests appear to converge with depth to a value between 1.5% and 2.5%. The CPT friction ratio readings are more consistent and converge to about 0.8%. These results are consistent with what was found in the field. It appears that the tip 2 annulus increases the vertical and horizontal stresses on the sand near the friction sleeve, which in turn increases the shear resistance on the sleeve.

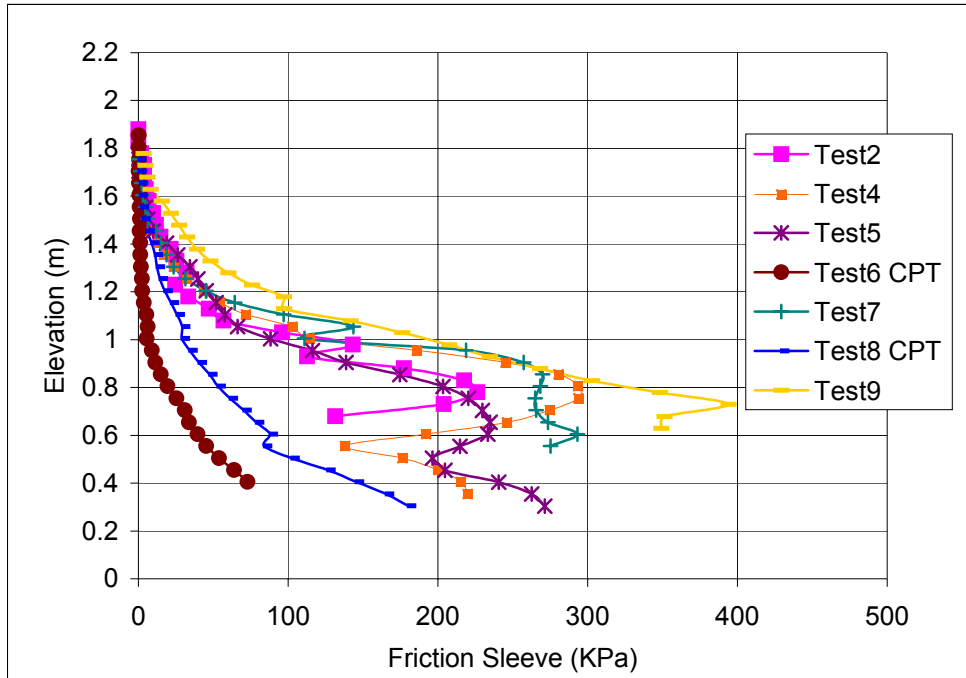


Figure 5.10: Calibration Chamber Tests in Fine Sand Friction Sleeve Readings vs. Elevation

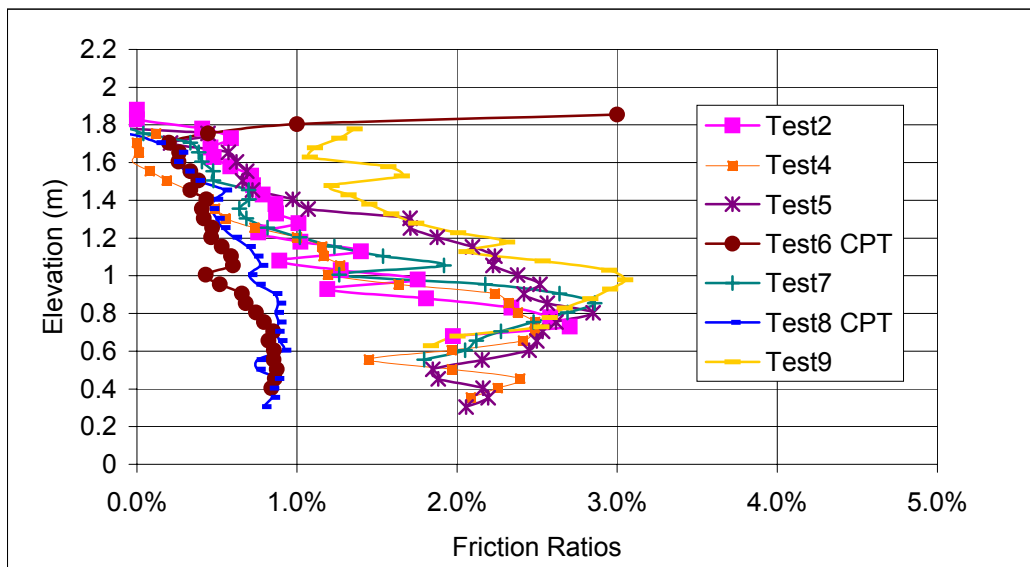


Figure 5.11: Calibration Chamber Tests in Fine Sand Friction Ratios vs. Elevation

The T2/T1 ratios with respect to depth are shown in Figure 5.12. The tip ratio showed large variability near the surface, probably also due to the “critical relative depth” parameter

$(D/B)_{cr}$  not being reached. However, at an elevation below 0.8 meters the tip ratio converges to a range between 0.4 and 0.7. This range was similar to what was seen at the Archer Landfill clean fine sands. The tip ratio didn't appear to be as sensitive to the changes in density as the tip 1 bearings were.

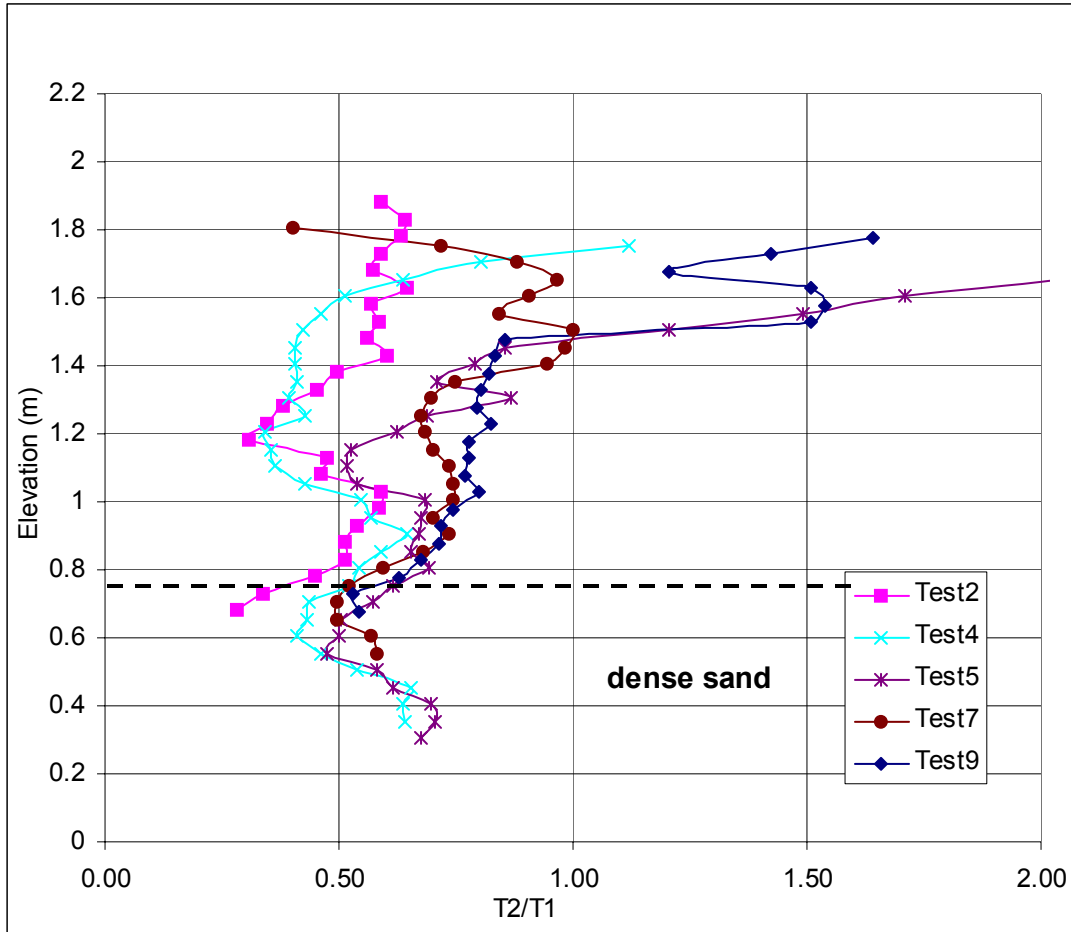


Figure 5.12: Calibration Chamber Tests in Fine Sand  $T2/T1$  vs. Elevation

### Calibration Chamber Setup for the Cemented Sand Tests

For the next series of tests, the chamber was filled with a 29-inch thick layer of loose sand overlain by a 43-inch layer of weakly cemented sand (Figure 5.14) for DTP testing.

To observe the boundary effects of the chamber walls on probe penetration, two earth pressure cells were purchased and attached along the inside chamber wall. These Geokon units have a pressure range of 0 to 15 psi and a faceplate diameter of 9 inches. The center of Cell 901 was set at an elevation of 0.61 meters (in the loose sand) and the center of Cell 902 was placed at an elevation of 1.22 meters (in the cemented sand).

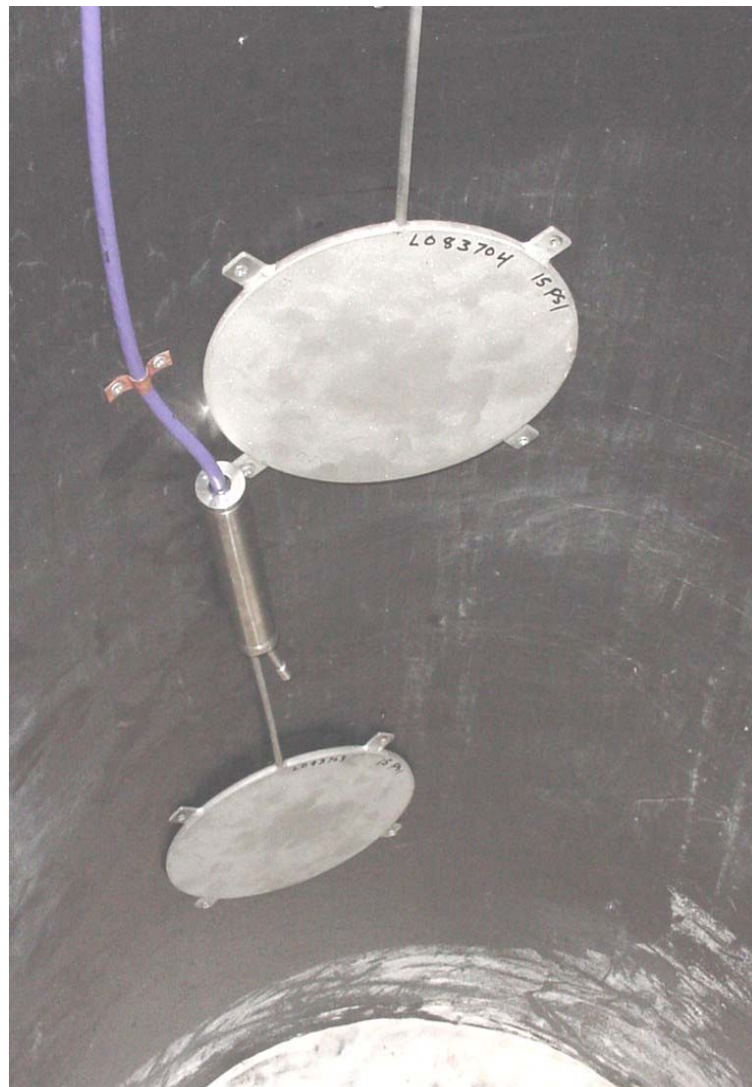


Figure 5.13: Geokon Pressure Cells inside Calibration Chamber

After installing the cells, the chamber was filled with 29 inches of loose fine sand in the same manner previously described (i.e., in multiple lifts). After placement, a plastic liner material was positioned over the loose sand in an effort to keep the water in the water-cement-sand mixture from seeping into the lower dry sand zone. The cement-sand mix was then placed into the chamber in nominal lifts. For the first lift, 25 lbs of sand was mixed with 1.5% (by weight) Portland cement and water using a portable mixer. However, since the wet mix did not dispense easily into the chamber it was decided that ensuing lifts would be mixed slightly moist (in order for the cement particles to adhere to the sand yet not segregate or agglomerate) and then saturated the material “insitu” (within the pipe). One hundred pounds of this material was subsequently spread into the chamber and carefully saturated. In order to minimize washing of the material and possible compaction from the water flow, the flow nozzle was set to spray as a gentle mist. This method of filling was repeated until the chamber was full. The cemented sand was allowed to cure for 30 days before DTP testing commenced.

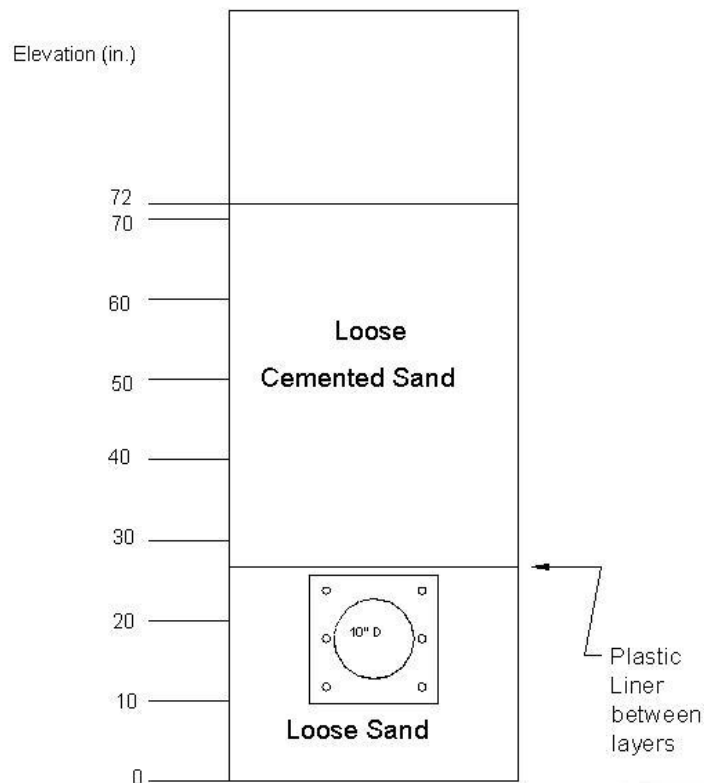


Figure 5.14: Layers for Testing Series 2



The testing scheme was similar to that used for the dry sand tests. However, a second person assisted in monitoring the pressure cell readings. The cells' outputs needed to be monitored during actual DTP penetration since this was a pseudo-dynamic event. The interest in this aspect of the testing was whether the rigid boundaries of the chamber contributed any quantifiable effect on the DTP results. That is to say, if little or no pressure fluctuations were observed during penetration testing, this would suggest that the zone of soil-straining in cemented sands is very localized, i.e., it remains contiguous to the probe itself. In fact, this potentially is extremely important since one observation noted from the numerous field tests is that while tip 1 fails the cemented sand bonds; tip 2 appears to encounter not only this weakened material, but a peripheral zone of relatively intact cemented sand. This could account for the observation that tip 2 was equal to or in some cases larger than tip 1 in several of the field soundings. In fact, this calibration data suggests that for weakly cemented sands, tip 2 values are lower compared to tip 1 which infers that the cementation zone of influence (the volume of soil in which the cement bonds are broken) extends further out into the surrounding soil. Thus, tip 2 is only measuring the residual strength of the cemented sand. However as the degree of cementation increases, the zone appears to shrink towards the probe resulting in tip 2 being subjected to the disturbed material adjacent to the probe as well as intact-cemented material further away. While this is a preliminary finding, further data should prove or disprove this supposition. If correct, then this device will be able to qualitatively determine the degree of cementation, based on the above premise.

The following table summarizes the similarities and differences between the first and second test series in the calibration chamber.

<b>Test Series</b>	<b>Series One</b>	<b>Series Two</b>
Dates Performed	3-5-02 4-2-02 4-25-02 5-1-02 5-3-02	10-8-02 11-10-02
# DTP Tests Performed	7 including: Cone CSC 765 TC (2000) and CSC 782 TC (2001)	3 including: Cone CSC 782 TC only
# CPT Tests	2	1
Sand Type	Edgar Fine Sand	Edgar Fine Sand
Layering	Loose Sand over Dense Sand over Medium Dense Sand	1.5 % Loose Cemented Sand over Loose Sand
Pressure Cells Present	NO	YES
Plastic Lining Present	NO	YES
Water Present	NO	During Saturation Surface Dry @ time of Testing
Confining Stresses	Atmospheric at Surface No Induced Boundary Stresses	Atmospheric at Surface No Induced Boundary Stresses
Point Tested	Center of Chamber	Center of Chamber

Table 5.2: Similarities and Differences between Test Series 1 and 2

The initial test in this material was the most important, since the cement bonds were broken during penetration. However, useful information was gleaned from the subsequent tests by filling the cavity formed from Test 1 with fine sand and retested to observe the zone of influence effect. This was repeated after Test 2 and Test 3. In total, three DTP tests were performed in this series followed by one CPT.

### **Results of the Calibration Chamber Testing**

This section first presents the results from the pressure cell readings during DTP testing. Next, the DTP parameters including tip 1, tip 2, tip ratio and friction ratio are examined.

Figure 5.15 shows the pressure readings for each pressure cell with respect to tip 1 depth. The figure only portrays the results for the first cemented sand test. The three breaks in the plot indicated penetration stops for adding push rods. During these pauses there is a decrease in the pressure experienced by the pressure cells. This may be due to soil rebound as the load

is removed to change the push rod. The figure shows that a maximum difference of 2.6 kPa was felt by pressure cell 902 and 6.6 kPa for pressure cell 901 during DTP penetration. These pressure changes are quite low when compared to tip 1 and tip 2 bearing values that extend into the MPa range.

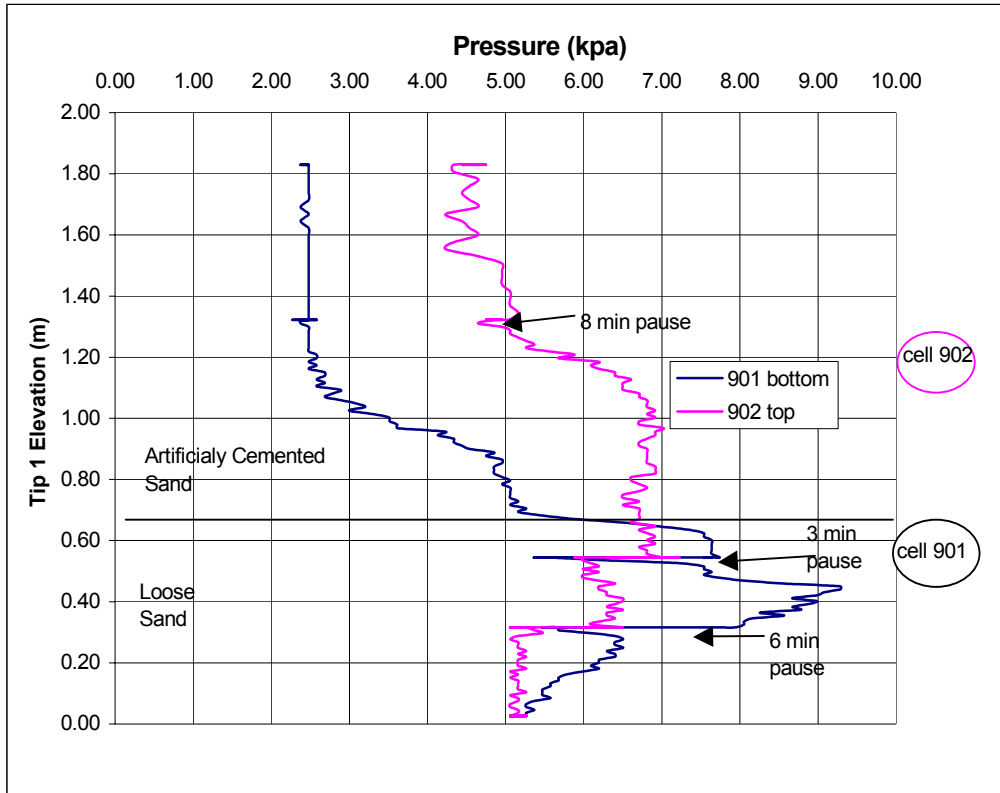


Figure 5.15: Artificially Cemented Sand Test 1- Pressure Cell Readings vs. Tip 1 Elevation

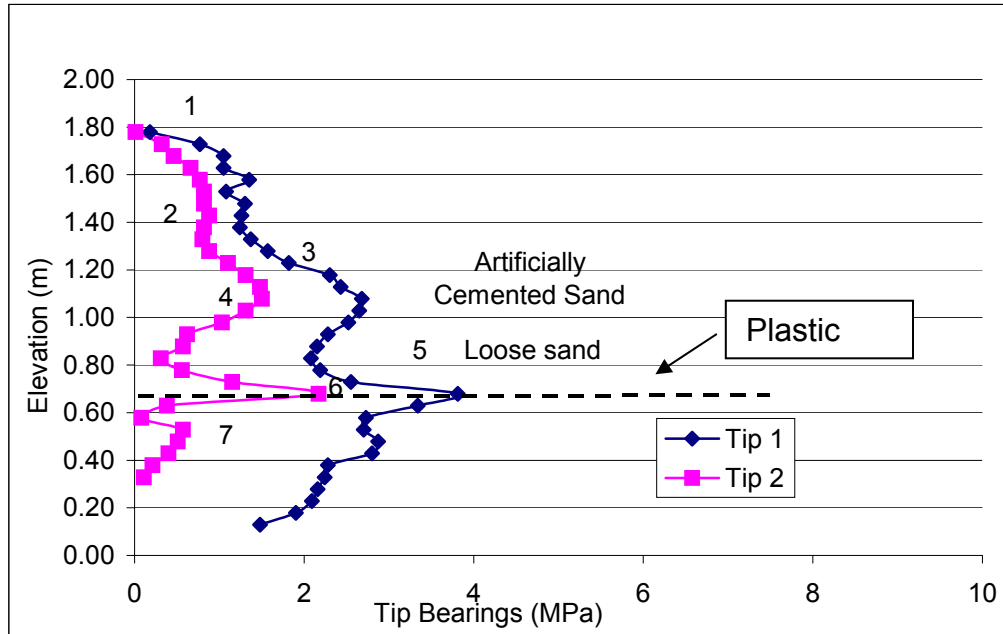


Figure 5.16: Artificially Cemented Sand - Test 1 DTP Tip Bearings vs. Depth

Figure 5.16 above shows tip 1 and tip 2 bearing readings with respect to depth for the first cemented sand test. Both tip 1 and tip 2 show similar trends in bearing but with different magnitudes. The dashed line in the above figure denotes the boundary between layers and the elevation of the thin plastic liner dividing the two layers. The following are possible explanations for the observed trends (listed by trend number on Figure 5.16):

1. An initial increase in bearing occurs until the cone tip is deep enough to develop a full failure zone. The  $(D/B)_{cr}$  is unknown for lightly cemented sand in a confined boundary chamber. It appears that the  $(D/B)_{cr}$  is just beginning to be reached by point 3.
2. The slight decrease in bearing may be due to the presence of pressure cell 902. The faces of pressure cells 901 and 902 are located approximately 1.0 to 1.5 inches from the inside surface of the chamber. This means that the effective chamber diameter decreases at that elevation. According to Puppala et al., and Sweeney et al., as the chamber diameter to cone diameter ratio reduces slightly, it translates into a slightly lower  $q_c$  bearing.

3. Since point 3 is below the pressure cell and hence close to  $(D/B)_{cr}$  this may be the zone that is most representative of tip 1, tip 2 and friction ratio values for the artificially cemented sand. Below this point, bearing decreases, ostensibly due to the loose soil underlying the cemented sand (point 4).
4. At point 5, the soil bearing increases sharply. This may be due to the plastic liner that was placed between the two layers. The liner may be restricting the failure of the soil so that the cemented sand is forced to shear along its surface, rather than failing and mixing into the loose sand below.
5. Trend point 6 shows the decrease in bearing possibly due to the combined effect of tip 1 entering the loose sand and the presence of Pressure Cell 901 (see Trend point 2).
6. The bearing increases slightly and then drops. This is likely due to a small volume of soil that was slightly more compacted than the surrounding loose sand.

Figure 5.17 shows the same trend in tip 1 bearing as was seen in the first testing series, that is, for each test, tip 1 bearing increases as the loose sand increases in density.

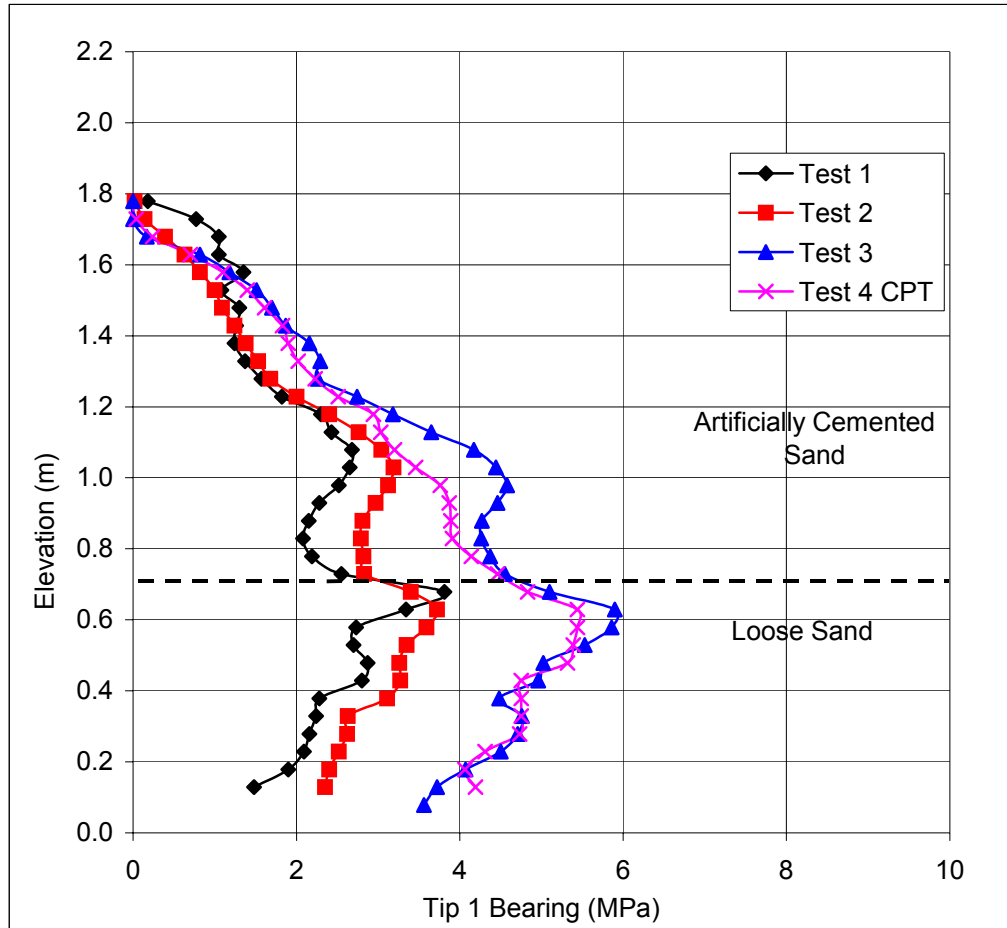


Figure 5.17: Artificially Cemented Sand Tip 1 Bearings vs. Elevation

The tip ratios for each of the three DTP tests are shown in Figure 5.18. While there is some variability observed in these three tests, the obvious reason is that much of the cementation is lost after Test 1. While it was thought that several tests could be performed in this material by offsetting the probe, the restricted effective diameter of the chamber would affect the readings and hence would complicate any observed response. As mentioned above, elevation 1.1 m is the most representative depth for the cemented sand. The tip ratio at this point is 0.56 and within the range of tip ratios observed in the first testing series for the fine dense sand (between 0.4 and 0.7).

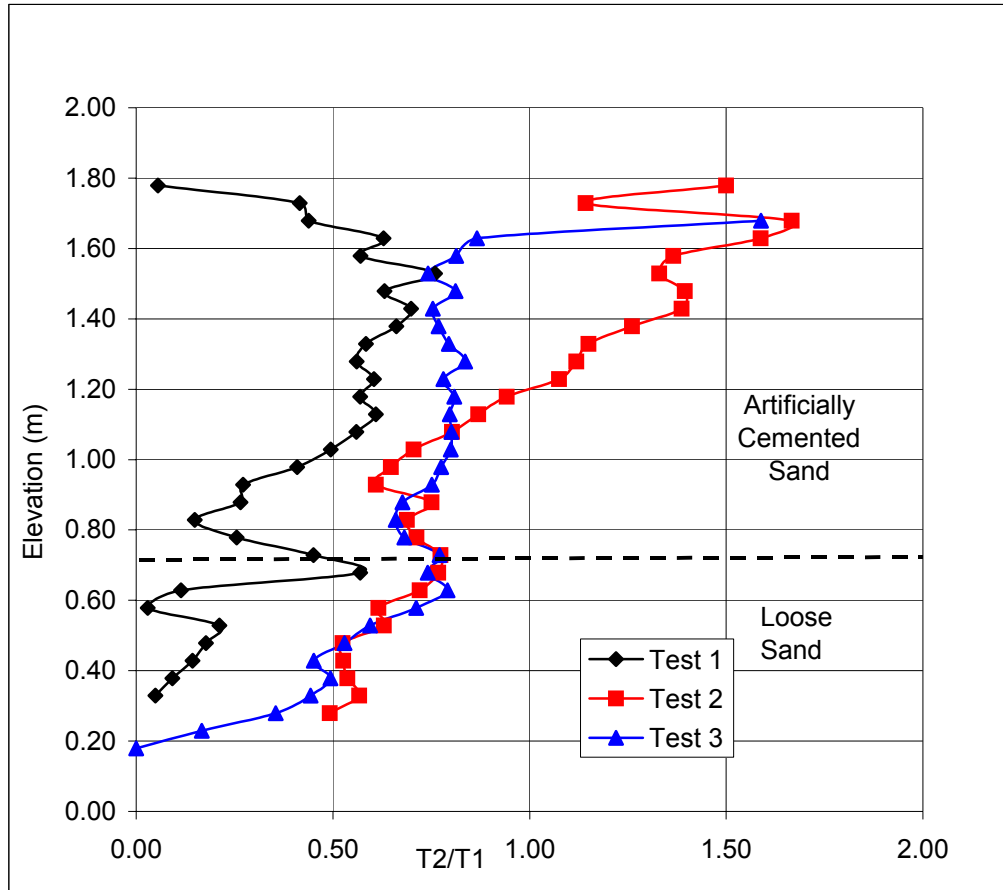


Figure 5.18: DTP T2/T1 vs. Elevation

In Figure 5.19, the friction ratios are presented. The results are very similar to the fine sand series, i.e., approaching 2.5% for the cemented sand and between 2% and 3% in the fine sand. On reflection, this finding would be expected, since the soil that is creating the shear stress on the sleeve is no longer cemented, having been broken up by the passage of tip 1.

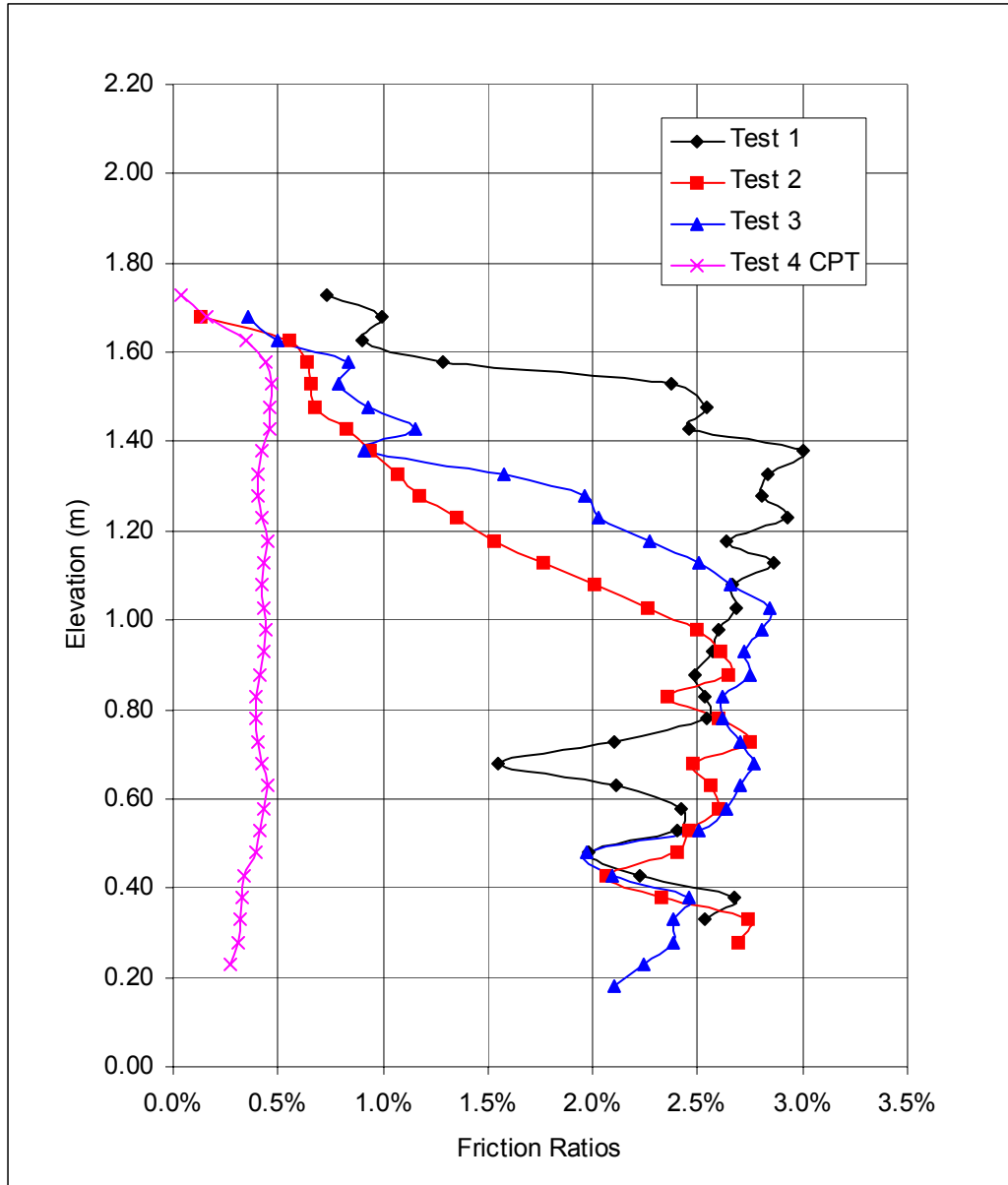


Figure 5.19: Artificial Cemented Sand Friction Ratios vs. Elevation



## Summary of Field Results and Chamber Tests

Although a significant effort was made to fill the chamber with a homogeneous mix of fine sand and weakly cemented fine sand, the testing results showed that tip ratio (T2/T1) and friction ratio vary little between fine sand and the same fine sand mixed with 1.5 % Portland cement. This may be due in part to a lower than expected degree of cementation. These results however maybe influenced by the fact that:

1. Critical relative depth not being achieved earlier in the sounding.
2. Peaks in tip readings due to the plastic liner.
3. Pressure cells decreasing the effective chamber diameter.

The DTP showed similar tip and friction ratios in fine sands in the field and in the calibration chamber. However, the tip and friction ratios for the cemented sands varied over those from the field tests. The field results indicated slightly higher tip ratios and lower friction ratios than the chamber results. This is most likely due to the degree of cementation in the field being higher than what was created in the chamber. Hence, a preliminary observation, that will be confirm as more data becomes available, is that as the degree of cementation increases, so does the tip ratio. This trend can then be cross-correlated by the fact that the friction ratio also reduces as the cementation level increases.

Although the degree of cementation appears to affect the tip and friction ratios in an observable pattern, variability in the data still makes it difficult to differentiate between the cementation magnitudes versus relative density. Equation 2.1 was simplified for the cemented sand field case by removing the  $C_{\text{clay}}$  and  $C_{\text{Rd}}$  terms. Nevertheless, there are still 4 unknowns to quantify. While it is anticipated that additional field data should ultimately provide this capability, at the current stage of the data analysis, only perfunctory suggested trends are possible.

$$T2/T1 = 1 \pm C_d - C_c \pm C_{he} + C_{\Delta\sigma_h} \quad (\text{Eqn. 5.1 Cemented sand tip ratio})$$

From the results to date, a definitive coefficient of cementation reduction factor  $C_c$  remains elusive. This is primarily due to the fact that while both the non-cemented and artificially cemented sand gave slightly different tip ratios, the differences were not consistently large enough to warrant a conclusion. However, it is important to state that, upon subsequent review of the data, it does appear that the frequency (or more aptly, wavelength) of the tip data are definitively higher in cemented sands as opposed to dense sands. Therefore, with additional sounding data, it is very likely that this area of focus will lead to a quantifiable  $C_c$  value.

Regardless at this junction, the DTP may still be able to:

1. Identification of soil types including possible cemented sands
2. Predict driven pile capacities (including potential cemented sands).

From the results presented in this chapter and Chapter 3, a general Soil Classification for DTP based on tip ratio, friction ratio and tip 1 bearing magnitude can be developed. Since the results indicate that the DTP friction ratios are higher than the CPT ratios, it is not reasonable to use the traditional soil classification method based on CPT friction ratios and  $q_c$  bearing values. In addition, since a pore pressure stone can be inserted into the DTP it may be possible to use a soil classification method based partially on the pore pressure ratio  $B_q$  (Lunne et al. 1997). The soil classification for the DTP will be presented in Chapter 5 along with the DTP 2002 software, which uses this soil classification theory. Chapter 6 discusses an attempt to use the DTP for predicting driven pile capacity in cemented sands.

## CHAPTER 6: SOIL CLASSIFICATION AND DTP 2002 SOFTWARE

### Soil Classification

After concluding all field and chamber testing a tentative soil classification system was developed based on the most relevant test data. This was then programmed into the DTP 2002 software for FDOT use. The soil classification is based on the following DTP parametric trends:

#### 1. Sand:

$$\begin{array}{l} 0.3 < T2/T1 < 0.7 \\ 1.5\% < FR_{DTP} < 3.0\% \\ 2.0 < T1 < 40 \text{ MPa} \end{array}$$

#### 2. Gravelly-Possibly Cemented Sand:

$$\begin{array}{l} 0.7 < T2/T1 < 2.1 \\ 0.2\% < FR_{DTP} < 1.5\% \\ 5.0 < T1 < 35 \text{ MPa} \end{array}$$

#### 3. Loose or Soft Granular Material:

$$\begin{array}{l} T2 \geq 0 \text{ MPa} \\ T1 < 2 \text{ MPa} \end{array}$$

#### 4. Silt/Sand/Clay Mixture:

$$\text{When none of the above criteria are met and } T1 < 40 \text{ MPa}$$

The soil classification is meant to provide the user with general soil types by limiting them to one of the above four soils. The program first checks to see if the material is a soil type 1 (sand). If the soil does not qualify as sand it is then checked as being a gravelly-possibly cemented sand (soil type 2). If the soil does not exhibit DTP parameters that are consistent with soil type 2 then the parameters are compared with those of soil type 3 (loose or soft

granular material). Finally, if the soil does not meet any of the first 3 soil types it is classified as a silt/sand/clay mixture.

### **DTP 2002 Software**

One of the tasks included in this research project is to create a computer program to provide the FDOT with a quick and easy way to reduce the DTP data. The software was written with Microsoft Visual Basic 6.0 Professional Edition code to directly utilize the output DTP sounding file.

The DTP 2000 program was first written to read the DTP (\*.cpd) output sounding files for data reduction. However, the method of soil identification used in the program was based on the traditional CPT soil type charts. Therefore, it was necessary to update the program with the new soil classification DTP method mentioned above.

The updated program is known as DTP 2002. The overall goal of DTP 2002 was a user-friendly interface to display the magnitude of the DTP readings in a Microsoft Excel-type format, a soil identification chart, and an interactive graph in which the user could select which property to include.

The ability to print the DTP tabular readings, soil identification layering chart, and each graph, was also included in DTP2002. The data in the program came directly from the output file of the DTP. This feature eliminates the creation of new files or manipulation of the original file, and allows the user to access the data reduction portion of the sounding immediately after penetration is completed.

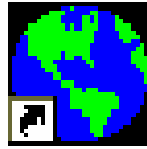
The program also has the added feature of automatically adjusting low readings attributed to the unloading of the probe for placement of new rods. If the output file has one line of data where the tip 1, friction sleeve and tip 2 readings are unusually low, then the program will replace those values with the average of the previous and subsequent lines of data, once penetration resumes. This removes the erratic readings at rod changes - typical of CPT software now in use.

## DTP2002 User's Guide

DTP2002 is a simple, user-friendly version of software that allows the user to reduce the data from a cone penetration sounding using the Dual Tip Penetrometer, developed for the FDOT at the University of Florida. The following is a user's guide for the new software, after it has been installed on a computer. This has been delivered to FDOT and installed on their new Cone Penetrometer rig along with 3 new DTP probes. It is important to note: **DO NOT USE THIS SOFTWARE FOR A STANDARD CONE (CPT) PENETRATION SOUNDING.**

**Step 1: Double click the DTP 2002 icon to start the program.** The opening screen should appear with information about the development of the software, and it asks the user to open a DTP sounding file.

The DTP2002 icon:



**DTP 2002**

**Step 3: From the File menu, choose the Open command. Knowing the location of the DTP file (with extension \*.cpd), find and select the file name by clicking, then click the Open button. Do NOT attempt to open a standard cone penetration-sounding file with DTP2002.**

**Step 4: A pop up window will ask if pore pressure readings were taken with the DTP sounding file selected. Choose yes or no.**

**Step 5: Scan the file contents shown in the text box (the top two lines of the text box containing sounding test information including location and date), and be sure to select the correct file.**

**Step 6: Click on the tab with the title “Data Grid”. The grid should display the depth, tip 1 resistance, tip 2 resistance, friction sleeve readings, friction ratio, inclination, tip ratio, soil identification and pore pressure readings.**

The initial display should be in metric units(  $\text{kN/m}^2$ ). The units can be switched to English tons per square foot (tsf) if desired. The units selection will carry over into the graphs as well. Due to the depth of some soundings, vertical and horizontal scroll bars might be necessary to view all of the data. To print the grid, press the “Print the Grid” button. Upon clicking the “Print the Grid” button, the friction sleeve readings will not be included in the subsequent printout (friction ratio WILL be included, however).

**Step 7: Once the grid has been thoroughly explored, click on the tab with the title “Data Plots”.** The initial screen should show pull-down menus with “X Axis” and “Y Axis” titles displayed for the graphs. To display the desired plot, select the data series of interest from the pull down menus. The plot will not change until both the x- and y-axis data series have been selected. To print the graph, click the “Print the Selected Graph” button. The graph (with no sounding information) will be printed.

## **CHAPTER 7: WEST BAY BRIDGE PILE CAPACITY EVALUATION**

### **Using the DTP to Determine Pile Capacities**

This chapter discusses the development of a procedure for using the DTP to determine driven pile capacities. The procedure is based on the new soil classification system, in conjunction with the DTP tip bearing data and an established pile capacity CPT prediction method.

In the previous chapter the program “DTP 2002” was introduced. After a DTP sounding is performed at the location of interest, the DTP 2002 program can be used to reduce the sounding data and display the soil classification for the particular site.

The next step is to identify whether or not gravelly/possible cemented sands are present. If the program determines that cemented sands are not present, then the tip 1 bearing can be used to predict pile capacity with an established CPT method such as the Bustamante & Gianeselli (LCPC method) or the De Ruiter & Beringen (Lunne et al. 1997). However, in fine sands the friction sleeve readings would have to be reduced by a factor of 3.5. If, however, DTP 2002 identifies gravelly/possible cemented, then a soil sample should be taken at the location of interest to prove that cemented sands are indeed present. One of the above CPT methods can then be used twice: once by substituting T1 as  $q_c$  and again by substituting T2 as  $q_c$ . The predicted pile capacities can then be adjusted by a reduction factor that will result in a more accurate prediction. As was mentioned in Chapter 1, cemented sands have a tendency to over predict bearing capacities for driven piles when traditional CPT methods are used.

### **West Bay Bridge Test Pile Capacities**

In Chapter 3, two of the DTP tests performed at the West Bay Bridge were discussed. The West Bay Bridge is located several miles north of Panama City, Florida. The bridge was completed in the early 1990's. The Florida Department of Transportation supplied bridge information including Standard Penetration Test boring data, Cone Penetration Test Data, Pile Driving Analysis data and static pile load test information. Cemented sands were believed to be responsible for many of the piles at the site requiring splices in order to

achieve sufficient axial resistance. In addition, several of the Standard Penetration Test samples obtained were identified as gray-cemented sand with shell.

A total of 3 static compressive load tests were performed on test piles at the site. However, due to accessibility constraints, the DTP tests could not be performed close to one of these piles. Although, static load tests provide the most accurate results for ultimate capacity determination, the dynamic test results (also conducted there) will be treated as the near true values for comparison purposes. This compromise in site selection resulted in DTP tests being performed near 3 different dynamically tested piles.

A total of 6 DTP tests and 3 CPT tests were performed at the West Bay Bridge. However, due to errors with the prototype DTP model CSC 782 TC, the tip 2 bearing readings cone (DTP Tests 1 and 2) were not used. Table 6.1 presents the data that were available for Test Piles 4, 5 and 12. The test piles were 30-inch square pre-stressed concrete piles with 18-inch diameter center voids cast the full length of the pile (in case pressure jetting was needed for installation). The required ultimate compressive capacities for these test piles (and most of the piles at the site) varied around 750 kips. The DTP tests were performed approximately 15 to 20 feet from the piers where the test piles were located.



	<b>Test Pile 4</b>	<b>Test Pile 5</b>	<b>Test Pile 12</b>
<b>Location</b>	Pier 4 (Station 86.66)	Pier 6 (Sta. 88.98)	Pier 16 (Sta. 102.8)
<b>SPT Tests</b>	SPT 3 (Station 87)	SPT 4 (Sta. 89) SPT 5 (Sta. 90)	SPT 19 (Sta. 102) SPT 20 (Sta. 104)
<b>CPT Tests</b>	CPT 3	CPT 2	CPT 1
<b>DTP Tests</b>	DTP 3 (only performed to 6 meters, stopped due to high inclinations) and DTP 4 (performed to 33 meters)	DTP 2 (only tip 1 readings used in B & G method)	DTP 1 (only tip 1 used in B & G Method)

Table 7.1: Information for Test Piles 4, 5 and 12

The CPT pile capacity prediction method developed by Bustamante and Gianceselli (1982) (Lunne et al. 1997). was used by substituting into the CPT  $q_c$  term either the tip 1 bearing or tip 2 bearing. This method only requires the CPT  $q_c$  term, not the friction sleeve values for determining pile capacities. However, only tip 1 should be used in determining the “nature of soil” for use in Figures 7.1 and 7.2. Lunne et al describe the Bustamante and Gianceselli method as follows:

*The equivalent average cone resistance,  $q_{ca}$ , at the base of the pile used to compute the pile unit end bearing,  $q_p$ , is the mean  $q_c$  value measured along two fixed distances ( $a = 1.5D$ , where  $D$  is the pile diameter (- $a$ ) and below (+ $a$ ) the pile tip. The author suggests to calculate  $q_{ca}$  in three steps, as shown in Figure 6.4. The first step is to calculate  $q'_{ca}$ , the mean  $q_c$  between  $-a$  and  $+a$ . The second step is to eliminate values higher than  $1.3 q'_{ca}$  along the length  $-a$  to  $+a$ , and the values lower than  $0.7 q'_{ca}$  along the length  $-a$ , which generates the thick curve shown in Figure 6.4. The third step is to calculate  $q_{ca}$ , the mean value of the thick curve.*

*The pile unit side friction,  $f_p$ , is calculated from measured  $q_c$  values divided by a friction coefficient  $\alpha_{lcp}$ . The pile unit end bearing,  $q_p$ , is calculated from the*

calculated equivalent average cone resistance,  $q_{ca}$ , multiplied by an end bearing coefficient,  $k_c$ .

$$f_p = q_c / \alpha_{lcp} \quad (\text{eqn. 6.5})$$

$$q_p = k_c q_{ca} \quad (\text{eqn. 6.6})$$

**Table 6.4** Bearing capacity factors,  $k_c$  (Bustamante and Gianselli, 1982)

Nature of soil	$q_c$ (MPa)	Factors $k_c$	
		Group I	Group II
Soft clay and mud	< 1	0.4	0.5
Moderately compact clay	1 to 5	0.35	0.45
Silt and loose sand	$\leq 5$	0.4	0.5
Compact to stiff clay and compact silt	> 5	0.45	0.55
Soft chalk	$\leq 5$	0.2	0.3
Moderately compact sand and gravel	5 to 12	0.4	0.5
Weathered to fragmented chalk	> 5	0.2	0.4
Compact to very compact sand and gravel	> 12	0.3	0.4

Group I: plain bored piles; mud bored piles; micro piles (grouted under low pressure); cased bored piles; hollow auger bored piles; piers; barrettes.

Group II: cast screwed piles; driven precast piles; prestressed tubular piles; driven cast piles; jacked metal piles; micropiles (small diameter piles grouted under high pressure with diameter < 250 mm); driven grouted piles (low pressure grouting); driven metal piles; driven rammed piles; jacket concrete piles; high pressure grouted piles of large diameter.

Figure 7.1: Table 6.4 from Lunne et al.

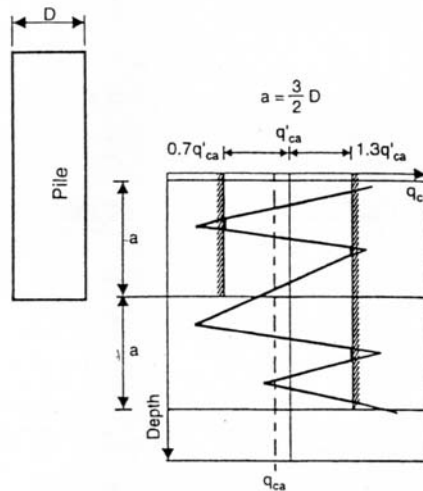


Figure 6.4 Calculation of equivalent average cone resistance (Bustamante and Gianselli, 1982).

Table 6.5 Friction coefficient,  $\alpha$  (Bustamante and Gianselli, 1982)

Nature of soil	$q_c$ (MPa)	Category									
		Coefficients, $\alpha$				Maximum limit of $f_p$ (MPa)					
		I		II		I		II		III	
A	B	A	B	A	B	A	B	A	B		
Soft clay and mud	< 1	30	90	90	30	0.015	0.015	0.015	0.015	0.035	
Moderately compact clay	1 to 5	40	80	40	80	0.035 (0.08)	0.035 (0.08)	0.035 (0.08)	0.035	0.08	$\geq 0.12$
Silt and loose sand	$\leq 5$	60	150	60	120	0.035	0.035	0.035	0.035	0.08	-
Compact to stiff clay and compact silt	> 5	60	120	60	120	0.035 (0.08)	0.035 (0.08)	0.035 (0.08)	0.035	0.08	$\geq 0.20$
Soft chalk	$\leq 5$	100	120	100	120	0.035	0.035	0.035	0.035	0.08	-
Moderately compact sand and gravel	5 to 12	100	200	100	200	0.08 (0.12)	0.035 (0.08)	0.08 (0.12)	0.08	0.12	$\geq 0.20$
Weathered to fragmented chalk	> 5	60	80	60	80	0.12 (0.15)	0.08 (0.12)	0.12 (0.15)	0.12	0.15	$\geq 0.20$
Compact to very compact sand and gravel	> 12	150	300	150	200	0.12 (0.15)	0.08 (0.12)	0.12 (0.15)	0.12	0.15	$\geq 0.20$

Category – IA: plain bored piles; mud bored piles; hollow auger bored piles; micropiles (grouted under low pressure); cast screwed piles; piers; barrettes. IB: cased bored piles; driven cast piles. IIA: driven precast piles; prestressed tubular piles; jacket concrete piles. IIB: driven metal piles; jacked metal piles. IIIA: driven grouted piles; driven rammed piles. IIIB: high pressure grouted piles of large diameter > 250 mm; micropiles (grouted under high pressure). Note: Maximum limit unit skin friction,  $f_p$ : bracket values apply to careful execution and minimum disturbance of soil due to construction.

Figure 7.2: Figure 6.4 & Table 6.5 from Lunne et al.

For determining the bearing capacity factor  $k_c$ , Group II was used since the piles were driven precast piles. The frictional stresses and bearing stresses are then multiplied by the pile side shear area and pile tip area respectively. The bottom tip area used was  $30^2 - \pi (9)^2 = 645 \text{ in.}^2$ . The “a” value described above is equal to  $1.5 * D$  where  $D = 30$  inches. The “a” value is therefore equal to 45 inches or 3.75 ft. (1.14 meters).

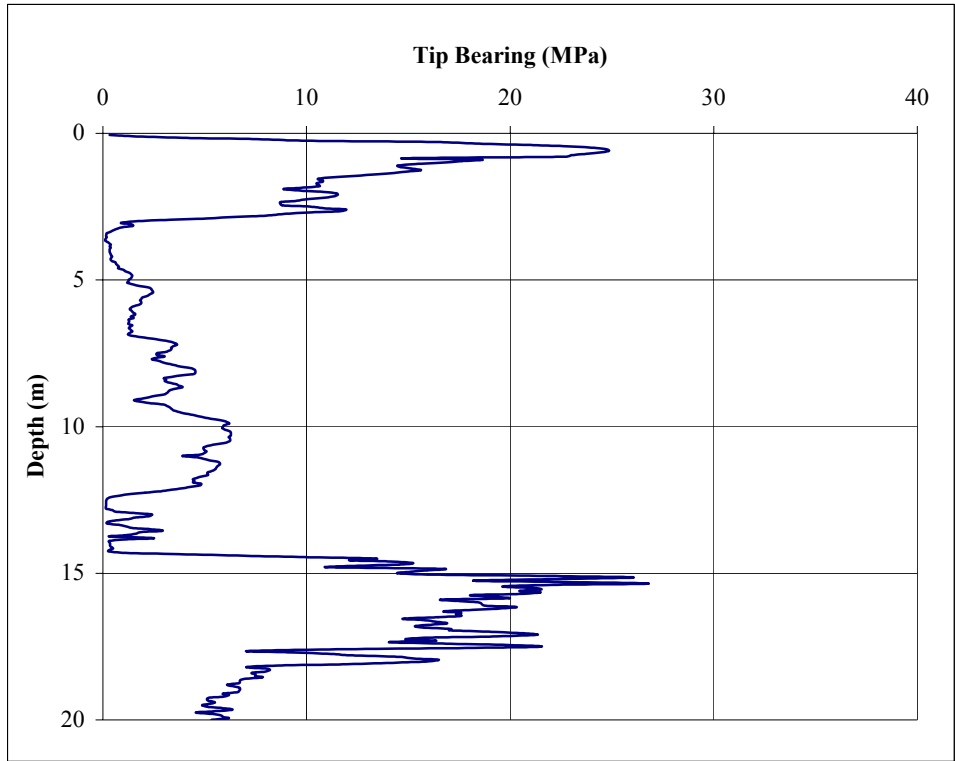


Figure 7.3: West Bay Bridge DTP 1 Tip 1 Bearing vs. Depth

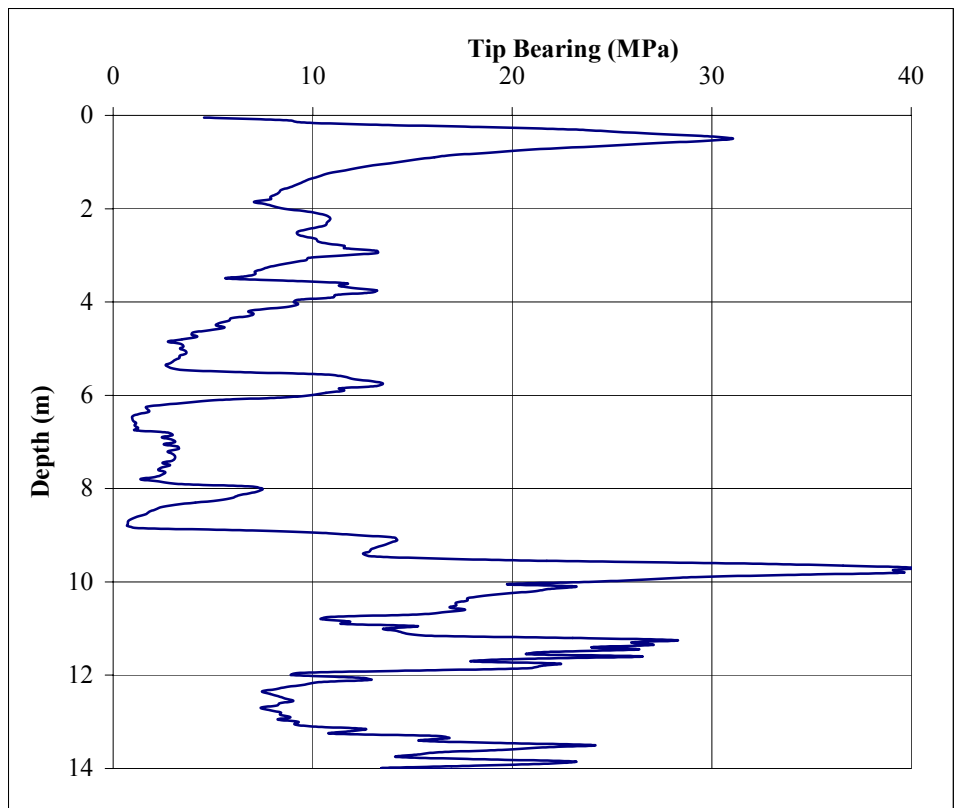


Figure 7.4: West Bay Bridge DTP 2 Tip 1 Bearing vs. Depth

Pile Tip Depth	Ultimate Pile Capacities based on CAPWAP analysis			Ultimate Pile Capacities based on Bustamante & Gianceselli Method using DTP #s 1 & 2 Tip 1 used as $q_c$		
	Total Capacity (kips)	Tip Capacity (kips)	Friction Capacity (kips)	Total Capacity (kips)	Tip Capacity (kips)	Friction Capacity (kips)
39 ft. (11.9 m) TP 5	1125	945	180	1191 (using tip 1 as $q_c$ ) DTP 2	601 (using tip 1 as $q_c$ ) DTP 2	567 (using tip 1 as $q_c$ ) DTP 2
61 ft. (18.6 m) TP 12	1386	1161	225	1054 (using tip 1 as $q_c$ ) DTP 1	361 (using tip 1 as $q_c$ ) DTP 1	693 (using tip 1 as $q_c$ ) DTP 1

Table 7.2: Ultimate Pile Capacities from CAPWAPC and DTP #s 1 & 2 (TP = Test Pile)

The Table above shows the results for the predicted capacities and the capacities determined from the PDA CAPWAPC analysis for test piles 5 and 12. In general the ultimate total capacities agree well with each other for both Test Piles (1125 kips vs. 1191 kips and 1386 kips vs. 1054 kips). The frictional and tip distributions however differ significantly for the piles. Since only DTP tip 1 was used for these calculations the results are equal to the results that would have been determined from using the  $q_c$  bearing values from a standard CPT probe.

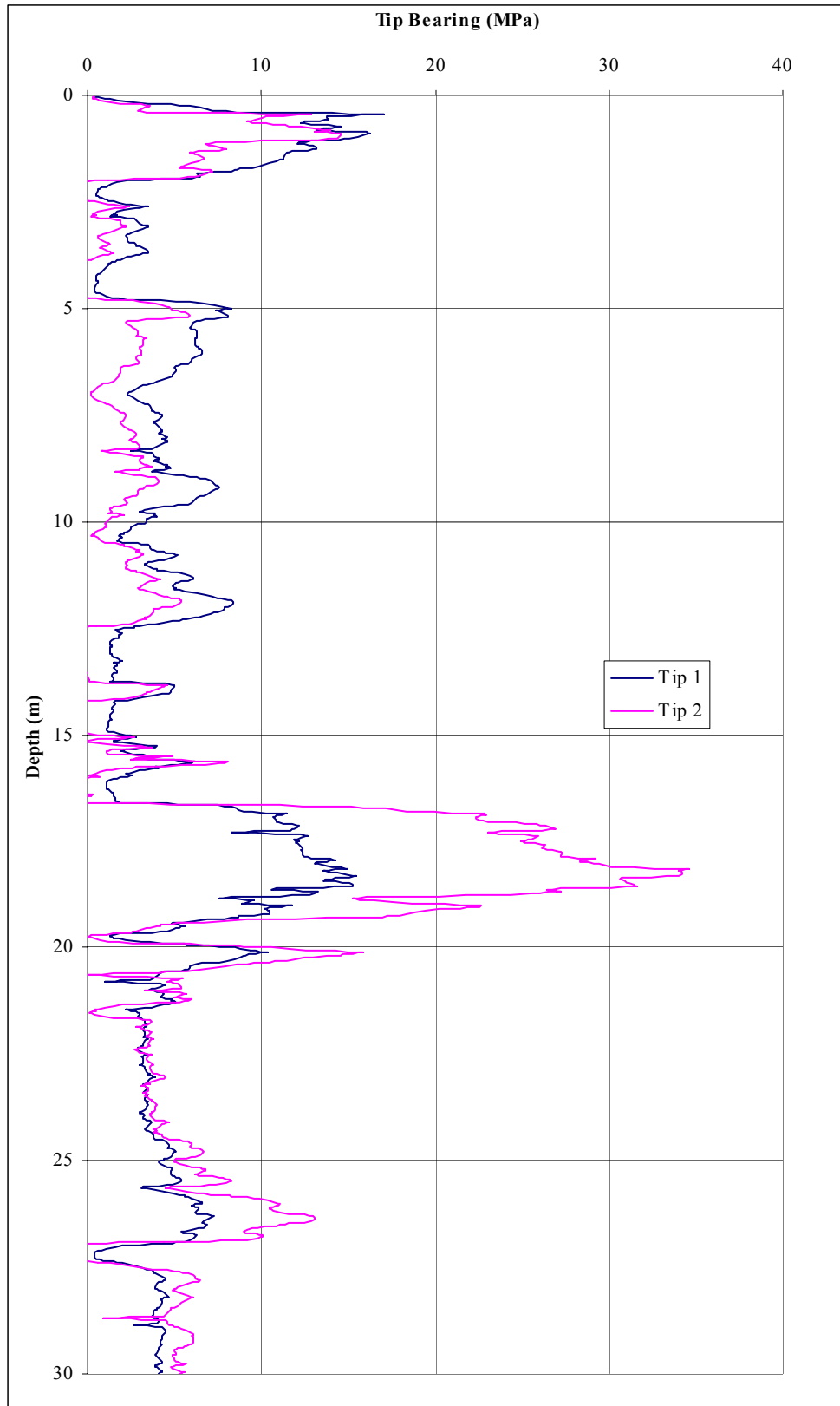


Figure 7.5: West Bay Bridge DTP 4 Tip Bearings vs. Depth

Figure 7.5 above shows the DTP Tip Bearings for DTP 4, performed near Test Pile 4. According to the DTP 2002 soil classification as well as core samplings obtained nearby, it is believed that bearing values at a depth below 16 meters where tip 1 values are over 5 MPa and tip ratios are greater than 1.0, are representative of medium cemented sands. In 1979, SPT testing was performed near DTP 4 and showed that below 16 meters, gray clayey sand with shell was present. It is probably however, that these sands were indeed cemented and then broken up by the SPT sampler. The core samples obtained at DTP 6 (100 feet from DTP 4) contained well-cemented calcareous sand and/or limestone with shell at a depth of 13.7 meters. Unfortunately core samples could not be obtained closer to DTP 4 due to accessibility limits. The limestone located at DTP 6 was not penetrable by the DTP therefore suggesting that the soil at DTP 4 is of lower cementation since DTP 4 was penetrable. Although it is believed that the sands encountered at DTP 4 were cemented it should be reiterated that the DTP is not yet able to distinguish effectively between the effects of density and cementation on bearing strength. It is therefore not possible to conclusively state what the density or degree of cementation was at different depths for DTP 4. However, with further soil sampling and laboratory tests, this constraint should be able to be removed in the foreseeable future.

Test Pile 4 Tip Depth	Ultimate Pile Capacities based on CAPWAPC analysis			Ultimate Pile Capacities based on Bustamante & Ganeselli Method using DTP 4 Tip 1 and Tip 2 used as $q_c$		
	Total Capacity (kips)	Tip Capacity (kips)	Friction Capacity (kips)	Total Capacity (kips)	Tip Capacity (kips)	Friction Capacity (kips)
79 ft. (24.1 m)	94	49	45	951 (using tip 1 as $q_c$ )	179 (using tip 1 as $q_c$ )	772 (using tip 1 as $q_c$ )
79 ft. BOR - 1 hr	294	135	159	821 (using tip 2 as $q_c$ )	209 (using tip 2 as $q_c$ )	612 (using tip 2 as $q_c$ )
80 ft. (24.4 m) BOR - 2 days	578	<b>214</b>	364	821 (using tip 2 as $q_c$ )	<b>209</b> (using tip 2 as $q_c$ )	612 (using tip 2 as $q_c$ )

Table 7.3: Ultimate Pile Capacities from CAPWAPC for Test Pile 4 compared with DTP estimate (BOR = Beginning of Redrive)

From the results above it appears that using the Bustamante & Ganeselli Method for either tip 1 or tip 2 overestimates the capacity, although using tip 2 is better for the BOR = 2 days. This is consistent with the problem statement mentioned in Chapter 1. However, it is strange that test pile 4 reached such a low capacity at a depth of 79 ft. yet test pile 5 (200 ft. away) reached over 10 times as much capacity on the initial drive as test pile 4 at a depth of only 39 ft.

We can nonetheless adjust the total capacities obtained by the Bustamante & Ganeselli method for the DTP 4 to be closer to the ultimate capacities determined from the PDA CAPWAPC analysis for the initial drive to 79 ft. We can do this by averaging the total capacities obtained with DTP tip 1 and tip 2 and then dividing by 9. This would give a total capacity of  $[(951 + 821)/2] / 9$  or 98 kips compared with 94 kips from the CAPWAPC analysis. Of course, division by 9 is simply a factor that has not yet been empirically determined. As is the usual case however, when a new technique and or device is introduced, often the safety factor or “calibration factor” must be artificially higher than warranted. A



case in point was the original pile capacity equation based on energy. The ENR formula required a “factor” of 15 multiplied by its answer to approximate the static load capacity. While this is a “worst case” scenario, it nevertheless illustrates that additional information is required to fine-tune the analysis portion of the DTP. As was mentioned previously, the most promising aspect involves the wavelength analysis proposition. It is very likely that there is a direct correlation between the frequency response of a penetrating probe and the degree of cementation of the material.

This method of adjustment probably will not work in all cases. In the future, a better pile capacity prediction method can be developed through the use of additional DTP data and pile “static” load test data in cemented sands.

## CHAPTER 8: CONCLUSIONS AND RECOMMENDATIONS

### Conclusions

There were three stated goals of this research: 1. to verify that the new Dual Tip Penetrometer was capable of operating in different soil types, 2. have three new probes manufactured and deliver them and the new sounding software to FDOT personnel and 3. attempt to use the DTP to predict the tip capacity of a pile in cemented sand. Based on this effort, the following conclusions can be made:

1. The Dual Tip Penetrometer has been shown to perform in a variety of soils. It can replace the standard CPT penetrometer since the DTP's tip 1 and friction readings obtained are virtually identical (after reducing the friction sleeve values for the DTP). In addition, the tip 2 readings have shown that they can potentially identify cemented sands – although with additional data and corresponding analysis, this ability can be better refined. Fortunately, FDOT has just acquired a state of the art penetrometer rig – located at the State Materials Office in Gainesville Florida, and the new DTP probes have been delivered to their office. It is envisioned that as more data become available, the process of positively identifying cemented sands (as well as the degree of cementation) will be fully implemented. For the short term, the DTP results can be used as a preliminary design tool for driven pile foundations, since tip 1 is identical to the  $q_c$  readings. Thus, it can be used effectively in determining pile capacities in non-cemented sand in conjunction with the Bustamante & Gianselli Method. If CPT friction ratios are required for another geotechnical application, then they can be used from the DTP as long as the DTP friction ratios in sand are divided by a factor of 3.5 to account for the stress bulb effect of tip 2 on the friction sleeve.

2. A preliminary chart, developed to identify cemented sands, is provided below.

Based on the DTP soil criteria for gravelly cemented sands:

$$\begin{array}{rclcl} 0.7 & < & T2/T1 & < & 2.1 \\ 0.2\% & < & FR & < & 1.5\% \\ 5.0 & < & T1 & < & 35 \text{ MPa} \end{array}$$

In addition, the degree of cementation appears to increase with increasing tip 1 bearing and more importantly, the wavelength of the sounding (the number of oscillations of a sounding profile for a given increment of depth) appears to be positively correlated to the presence of cemented sand. Hence, the DTP software will be updated to provide the user with these data as well as analyzing these phenomena. Applying this corroboration methodology in conjunction with the T2/T1 ratio should provide the FDOT engineers with a powerful subsurface analysis tool vis-à-vis cemented sands.

If cemented sands are identified according to the DTP soil classification, then limited soil sampling should be performed at the depth of interest for verification of their location. The Bustamante & Ganeselli Method can then be used to predict the pile tip capacities by averaging tip 1 and tip 2 values. This preliminary design analysis has found that for those piles analyzed, the presence of cemented sand creates a 9-fold over prediction in pile capacity. This is an important finding of this research, i.e., that when the DTP identifies cemented sand, it is prudent to reduce the averaged pile capacities by 9. Of course, division by 9 is simply a factor that has not yet been empirically verified. As is the usual case however, when a new technique and or device is introduced, often the reduction factor or “calibration factor” must be artificially higher than warranted. A case in point was the original pile capacity equation based on energy. The ENR formula required a “factor” of 15 multiplied by its answer to approximate the static load capacity. While this is a “worst case” scenario, it nevertheless illustrates that additional information is required to fine-tune the analysis portion of the DTP. As was mentioned previously, the most promising aspect

involves the wavelength analysis proposition. It is very likely that there is a direct correlation between the frequency response of a penetrating probe and the degree of cementation of the material. This method of reduction may be refined in the future when more data become available. However, it appears that this novel device can tentatively identify cemented sands and subsequently allow for a pile capacity reduction factor. The Dual Tip Penetrometer shows more repeatable tip 2 results in homogeneous soils than in heterogeneous soils. However, this conclusion may also lead to a better method of utilizing the T2/T1 ratio. That is to say, as the standard deviation of these values increases, it may indicate a specific type of soil and or its properties. Any CPT based correlations or pile capacity prediction methods that are based solely on CPT  $q_c$  data are applicable to the DTP where tip 1 bearing is  $q_c$ .

### **Recommendations**

The following is a list of recommendations based on the results of this research:

1. Additional data accumulation is needed to verify the soil trends with respect to DTP data outlined in this report. This will be performed by the Florida Department of Transportation.
2. In the future a better method for determining pile capacities in cemented sand with the DTP should be developed by collecting various case studies of different driven pile “static” load tests in different cemented sands and correlating the results with DTP tests.
3. Until the trends mentioned in this report are observed to occur consistently in the field, the DTP should not be the only insitu device used for preliminary geotechnical site investigations.

## REFERENCES

1. Abdulla, A.A. and Kioussis, P.D., “Behavior of Cemented Sands”. *International Journal for Numerical and Analytical Methods in Geomechanics*, Vol. 21, pp. 533 – 547 (1997).
2. Clough, G.W., Sitar, N., Bachus, R.C. and Rad, N.S., “Cemented sands under static loading”. *Journal of the Geotechnical Engineering Division*, ASCE, 107 (GT6), pp. 799-817 (1981).
3. Durgunoglu, H.T., Mitchell, J.K., “Static Penetration Resistance of Soils 1 – Analysis”. *Proceedings of the Conference on Insitu Measurement of Soil Properties*, June 1-4, 1975, pp. 151 – 171.
4. Graves, R. E., Eades, J. L., and Smith, L.L., “Strength Development from Carbonate Cementation in Silica-Carbonate Base Course Materials”. *Transportation Research Record*, n 1190, 24 - 30 (1988).
5. Hart II, D., “Development of a Modified Friction-Cone Penetrometer for Measuring Strength Reductions in Cemented Sands”. Thesis, University of Florida 1996.
6. Huang, A., Hsu, H. and Chang, J., “The behavior of a compressible silty fine sand”. *Canadian Geotechnical Journal*, 1999.
7. Kiser, S., “Development of a cemented sand device for the electronic cone penetrometer ”. Thesis, University of Florida 2000.
8. Lambe, T.W. and Whitman, R.V., *Soil Mechanics*, John Wiley and Sons, New York, 1969.
9. Lunne, T., Robertson, P.K. and Powell, J.J.M., “Cone Penetration Testing in Geotechnical Practice”, Blackie Academic and Professional 1997.
10. Puppala , A.J., Acar, Y.B. and Tumay, M.T., “Cone Penetration in Very Weakly Cemented Sand”. *Journal of Geotechnical Engineering*, Vol. 121, No. 8 Aug, 1995.
11. Puppala, A.J., Arslan, S., Tumay, M.T. and Yalcin, B.A., “Cone penetration testing in cemented soils: Comparisons between field and laboratory chamber test results”. *Proceedings of the First International Conference on Site Characterization*, Atlanta, Georgia (19-22) April 1998.

12. Rad, N. S. and Tumay, M. T., "Factors Affecting Sand Specimen Preparation by Raining," *Geotechnical Testing Journal*, Vol. 10, No. 1 March 1987, pp. 31-37.
13. Randazzo, A. F., and Jones, D. S., "The Geology of Florida". University Press of Florida 1997.
14. Salgado, R., Mitchell, J.K. and Jamiolkowski, M., "Cavity Expansion and Penetration Resistance in Sand"
15. Schniad, F., Prietto, P. D. M., and Consoli, N.C., "Characterization of Cemented Sand in Triaxial Compression". *Journal of Geotechnical and Geoenvironmental Engineering*, Vol. 27, No. 10 October 2001, 857 – 868.
16. Sweeney, B. P. and Clough, G. W., "Design of a Large Calibration Chamber," *Geotechnical Testing Journal*, Vol. 13, No. 1 March 1990, pp. 36 – 44.
17. Teh, C.I., "An Analytical Study of the Cone Penetration Test". D. Phil. thesis, Oxford University 1987.

**APPENDIX A**  
RESULTS FROM FIELD TESTING

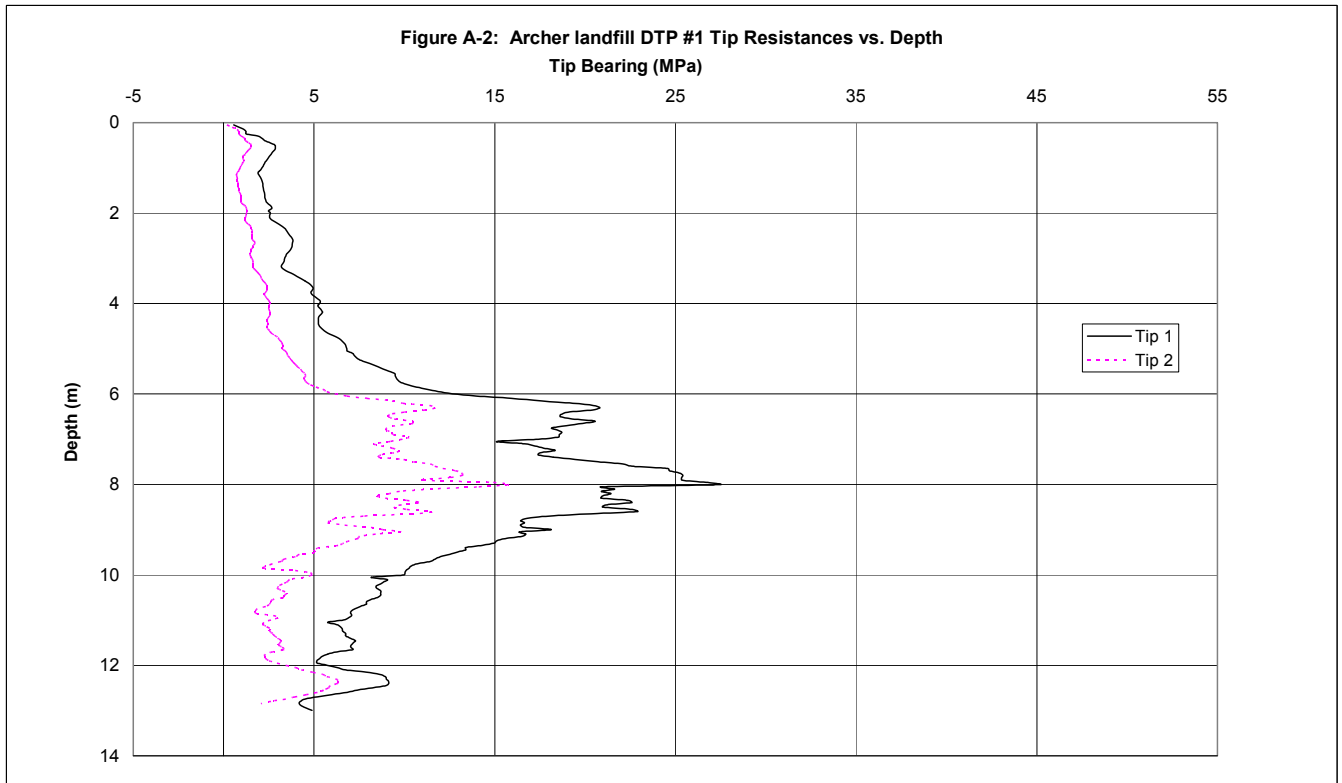
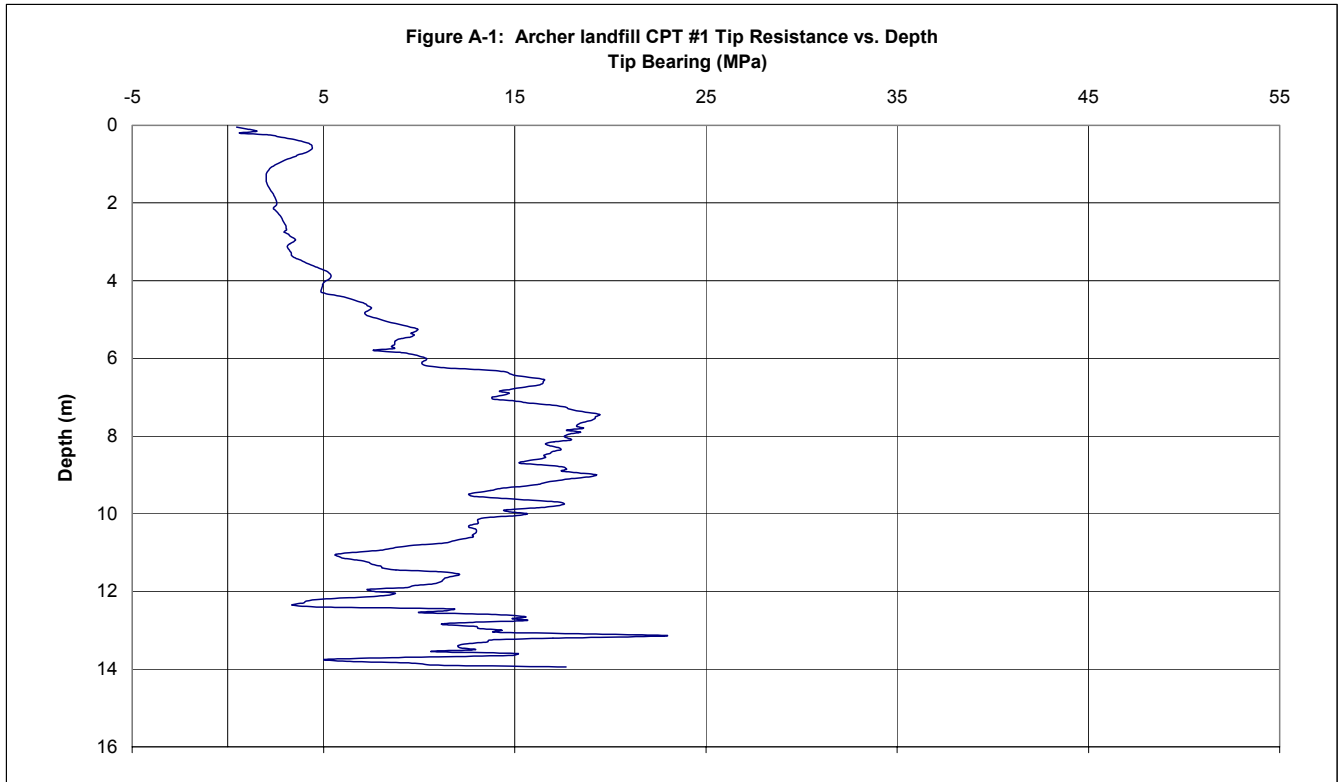




Figure A-3: Archer landfill DTP #2 Tip Resistances vs. Depth  
Tip Bearing (MPa)

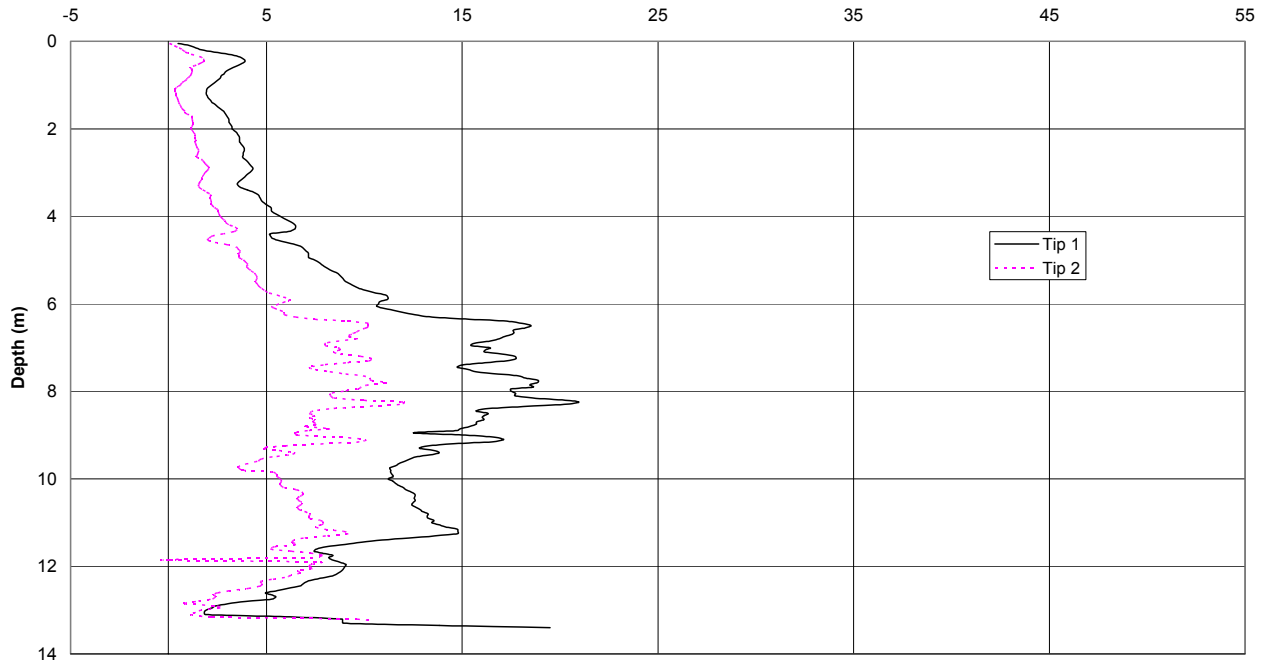


Figure A-4: Archer landfill DTP #3 Tip Resistances vs. Depth  
Tip Bearing (MPa)

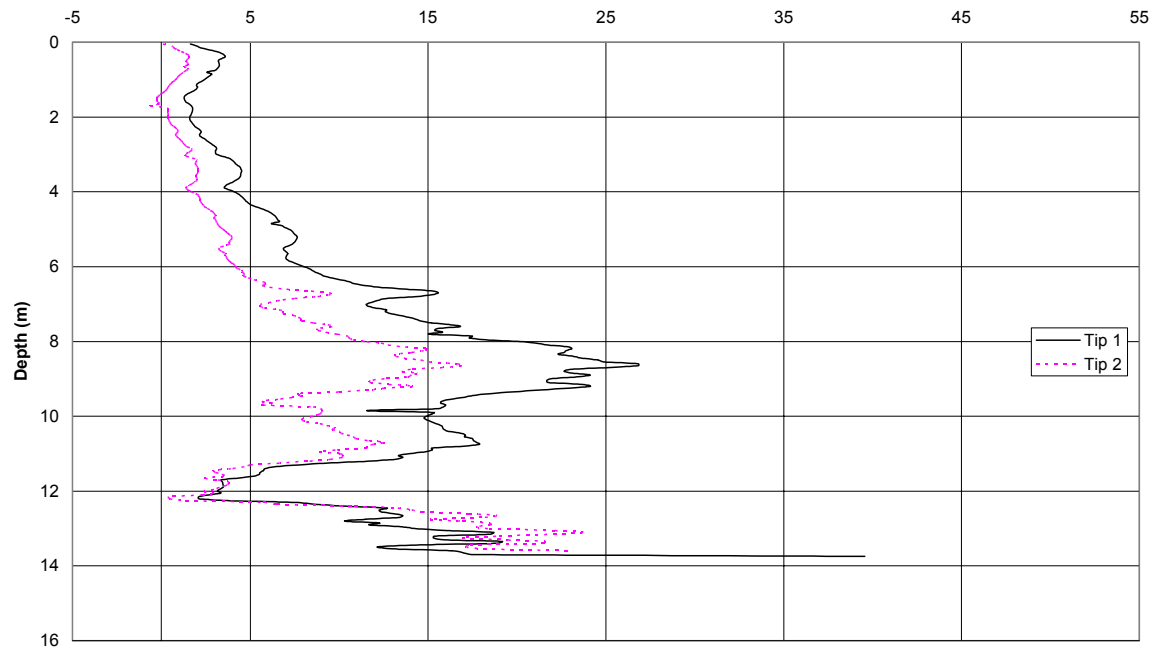


Figure A-5: Archer landfill DTP #1/CPT #1 Friction Ratios vs. Depth

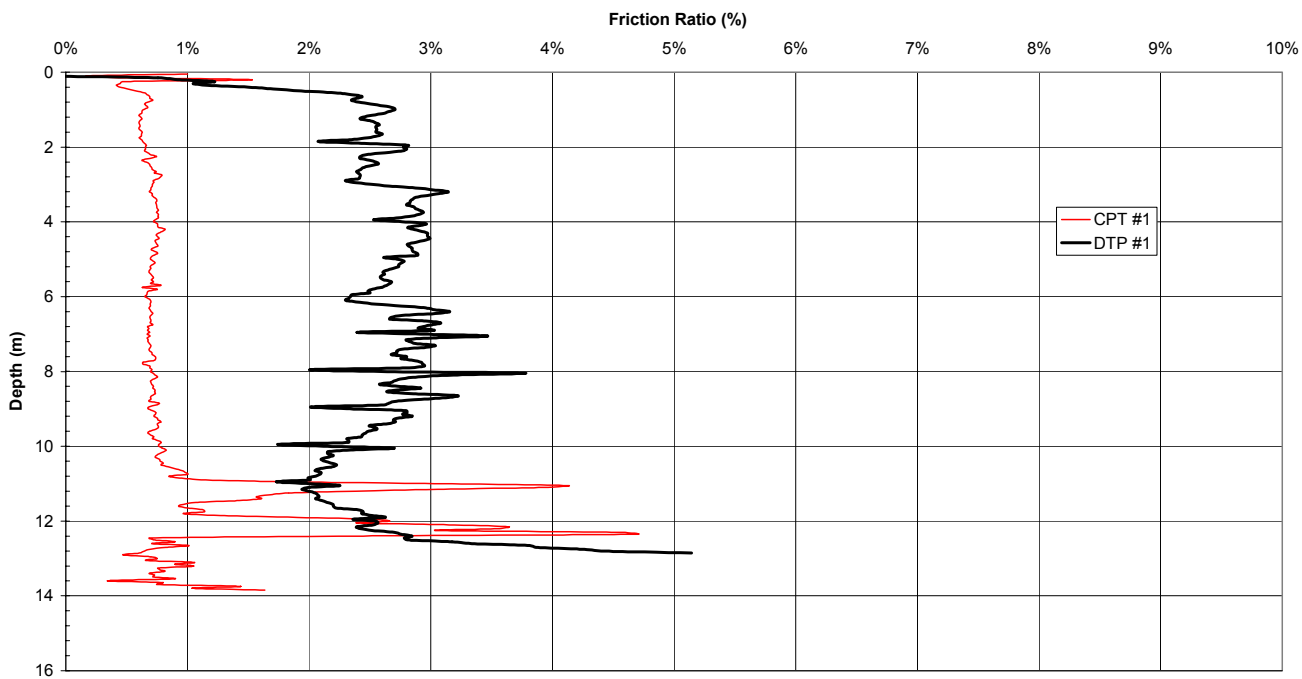


Figure A-6: Archer landfill DTP #2/CPT #1 Friction Ratios vs. Depth

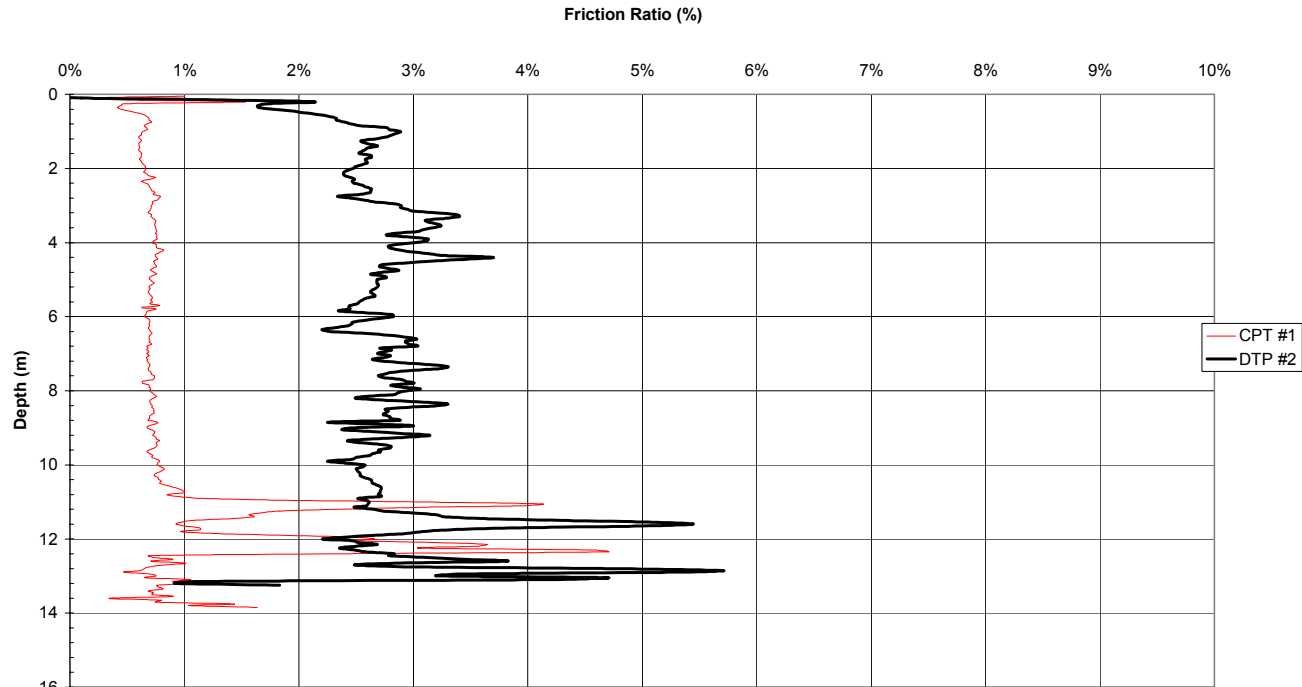


Figure A-7: Archer landfill DTP #2/CPT #1 Friction Ratios vs. Depth

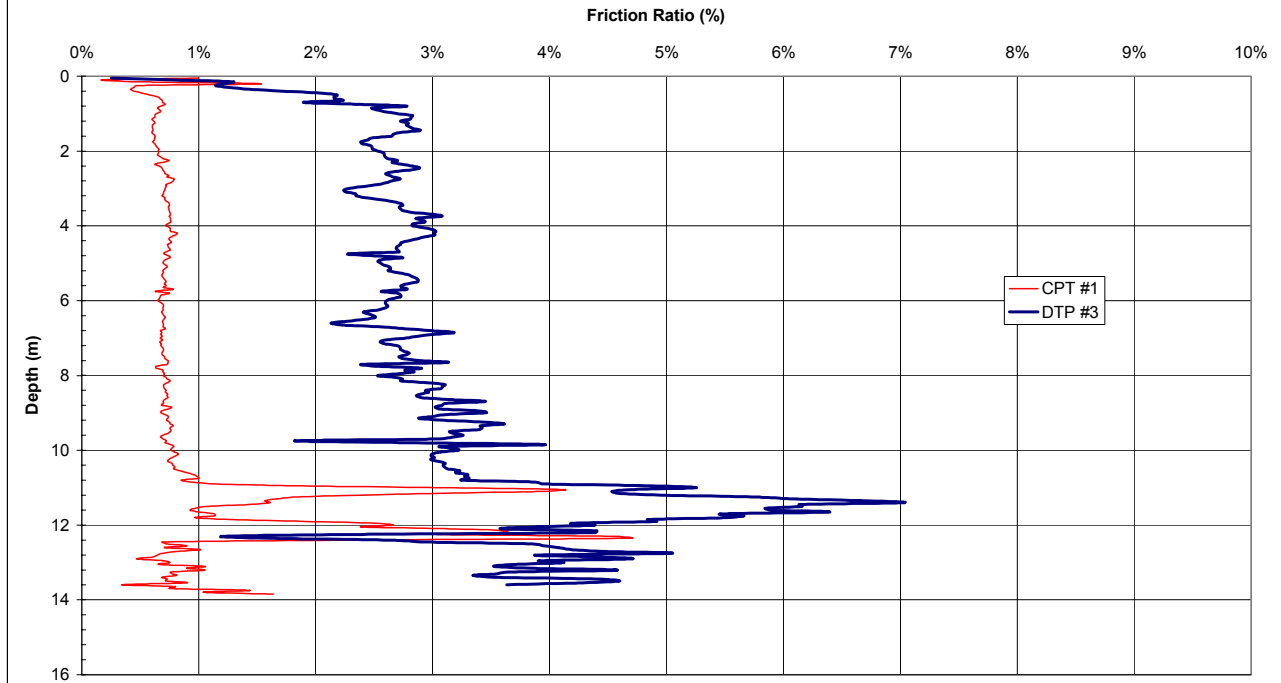


Figure A-8: Archer landfill DTP #1 Tip Ratios vs. Depth

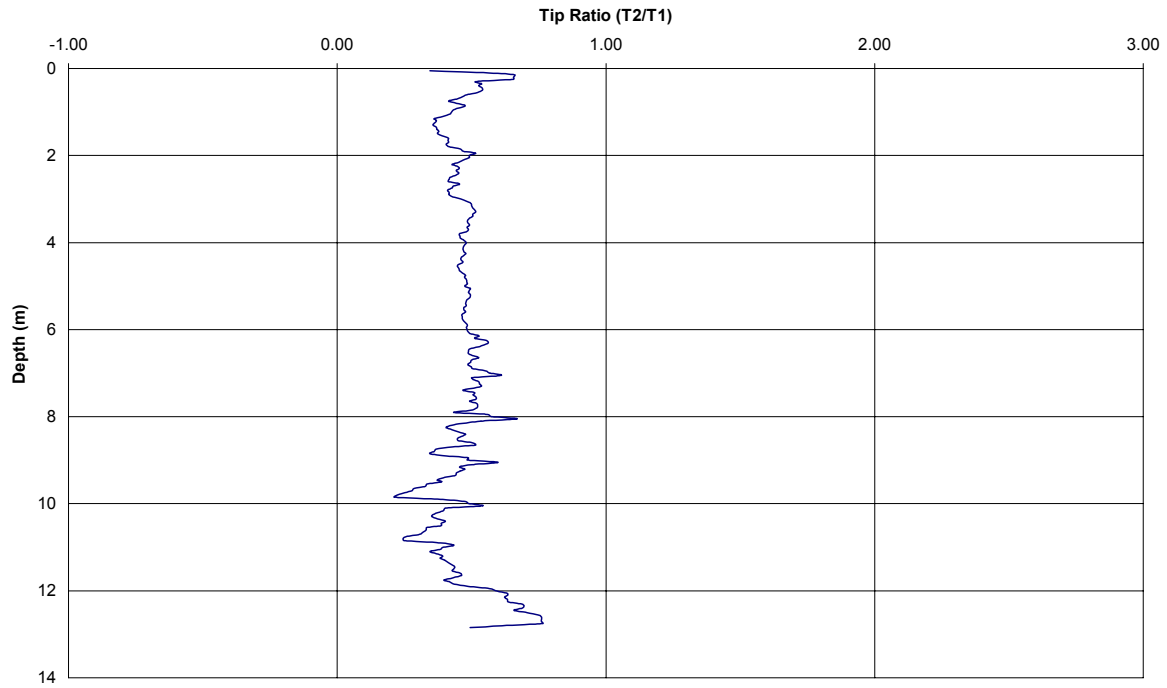


Figure A-9: Archer landfill DTP #2 Tip Ratios vs. Depth

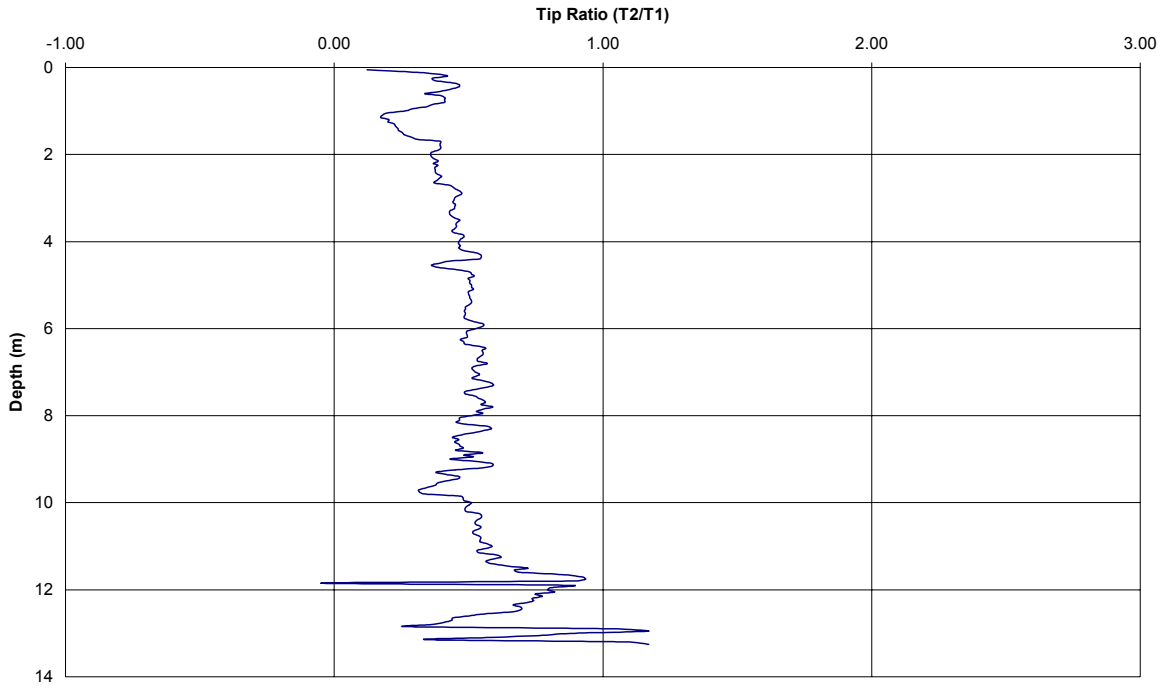


Figure A-10: Archer landfill DTP #3 Tip Ratios vs. Depth

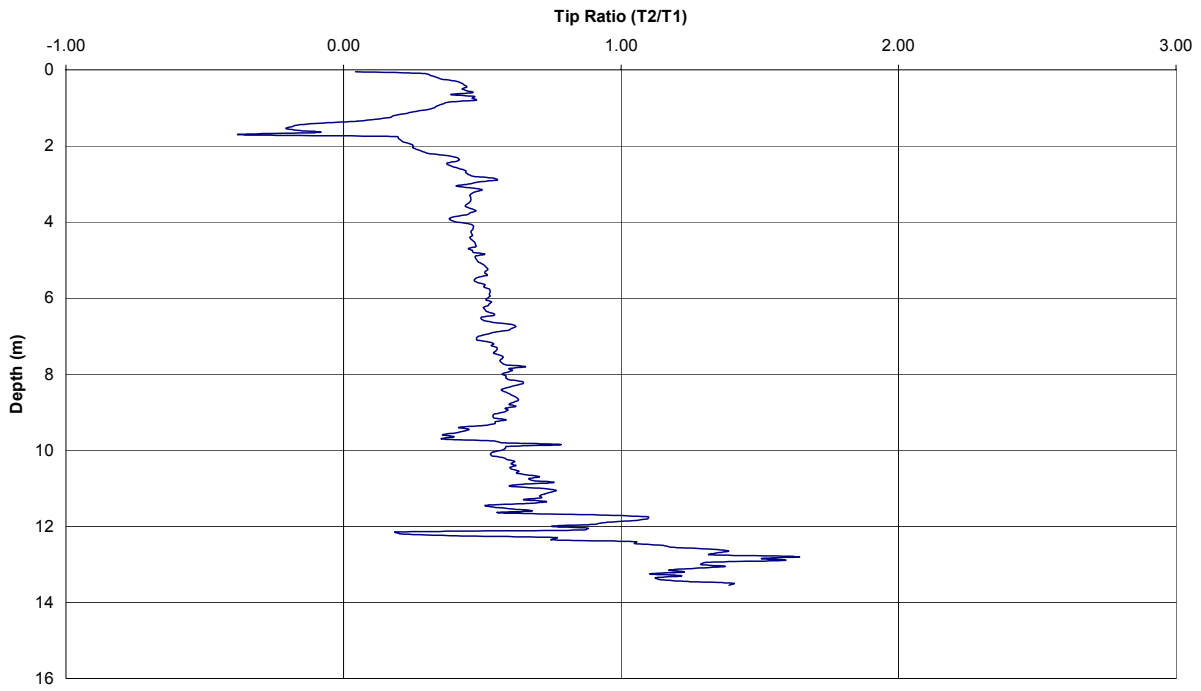


Figure A-11: South West Recreation Center CPT #4 Tip Resistance vs. Depth

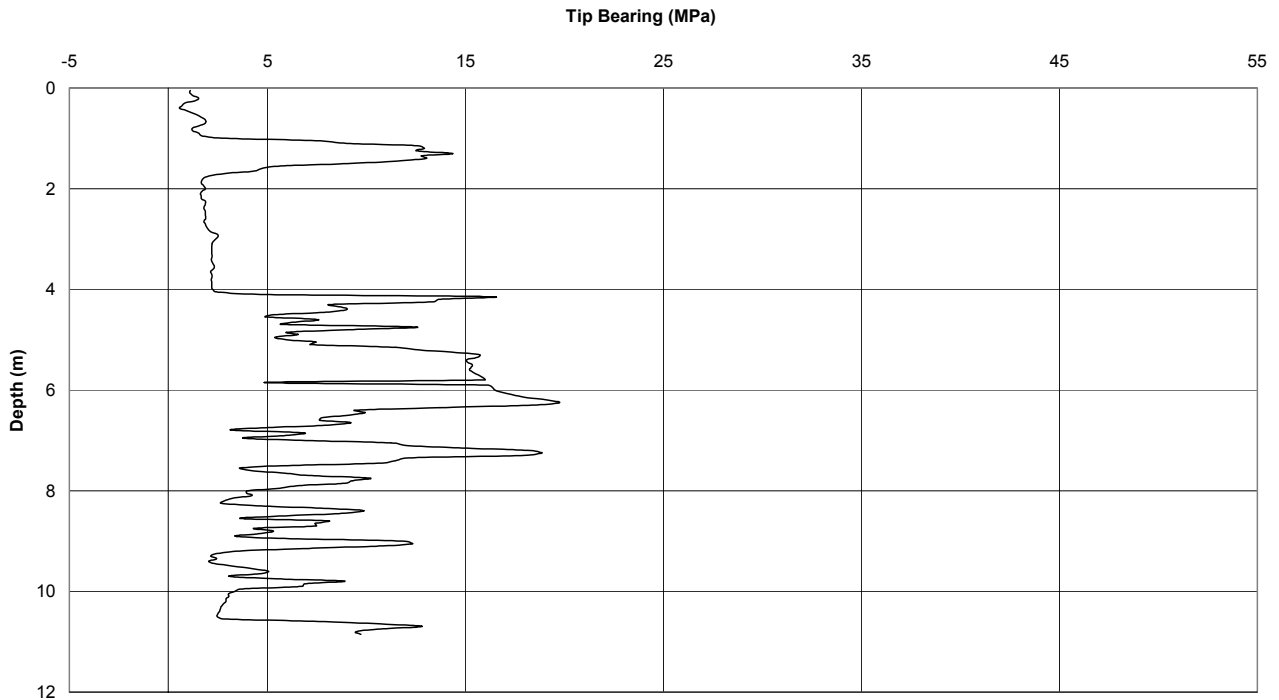


Figure A-12: South West Recreation Center DTP #1 Tip Resistances vs. Depth

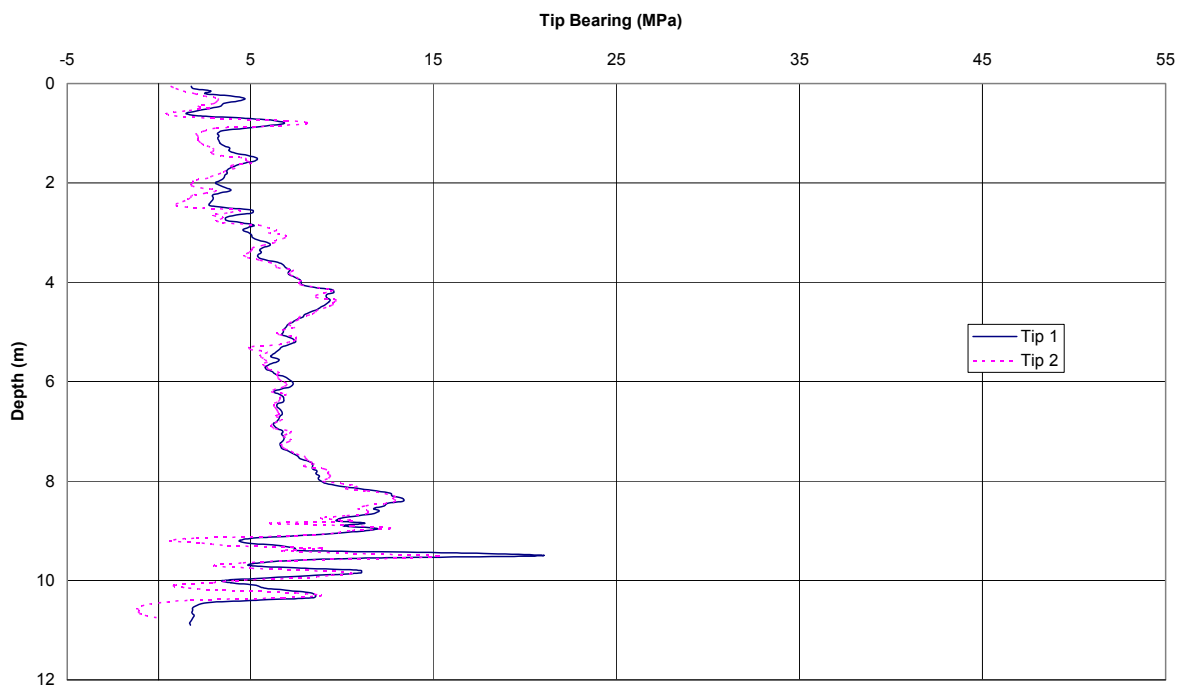


Figure A-13: South West Recreation Center DTP #3 Tip Resistance vs. Depth

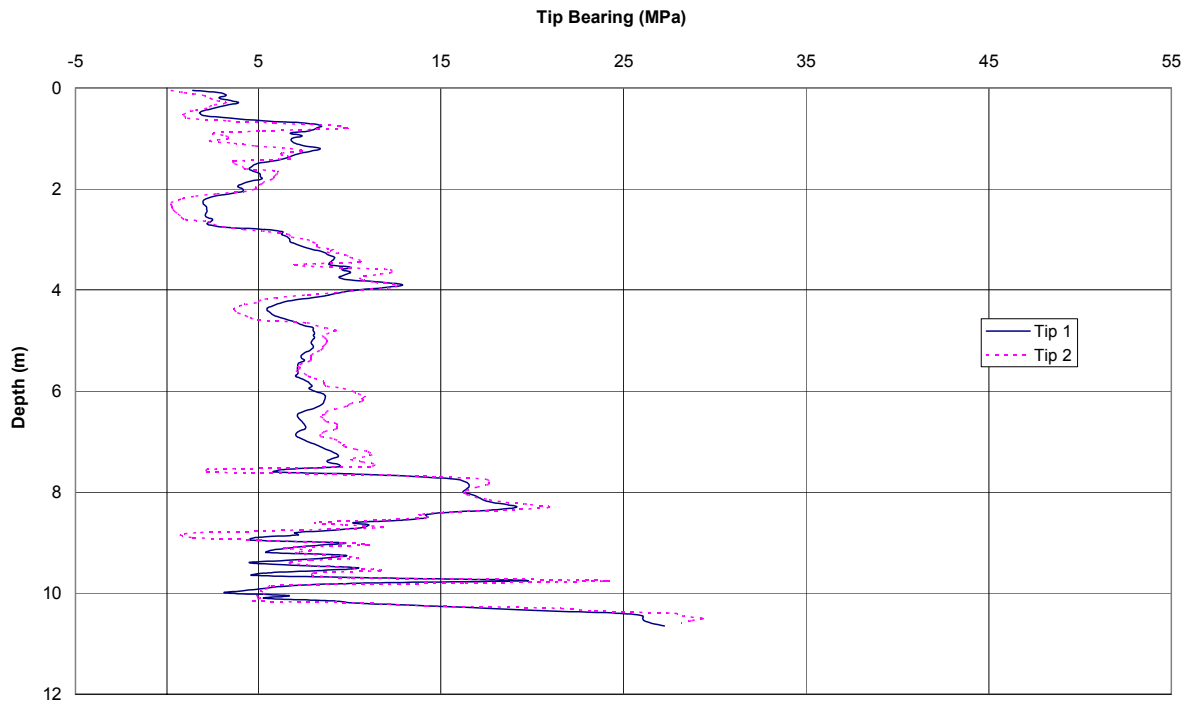


Figure A-14: South West Recreation Center DTP #4 Tip Resistance vs. Depth

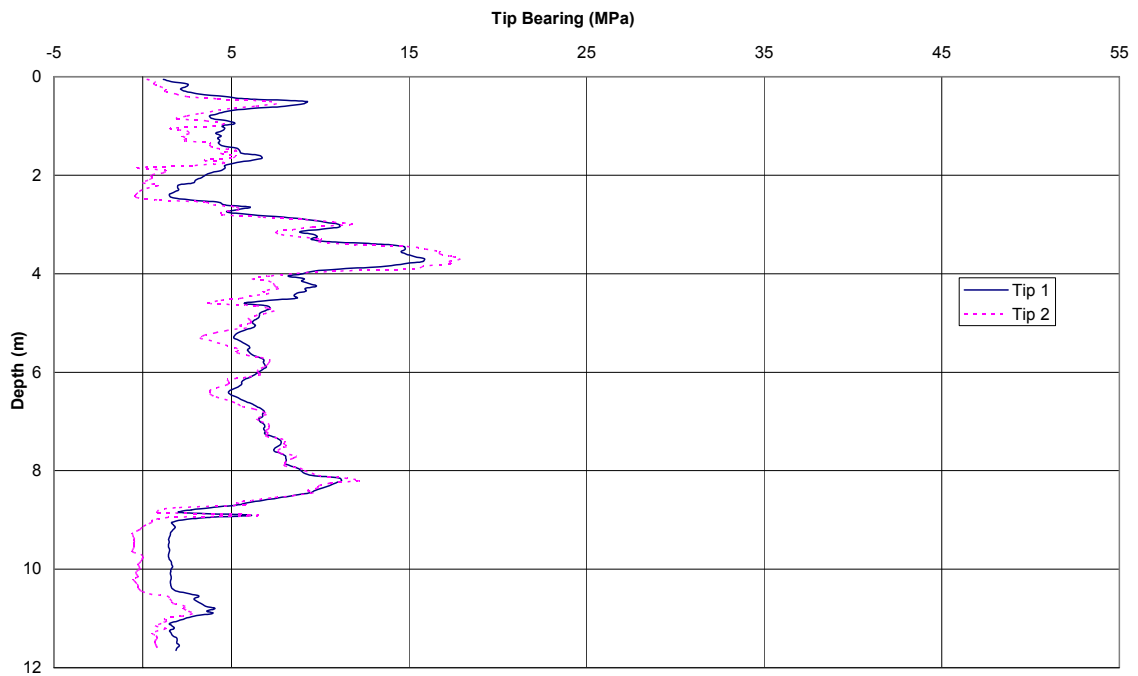


Figure A-15: South West Recreation Center CPT #4/DTP #1 Friction Ratios vs. Depth

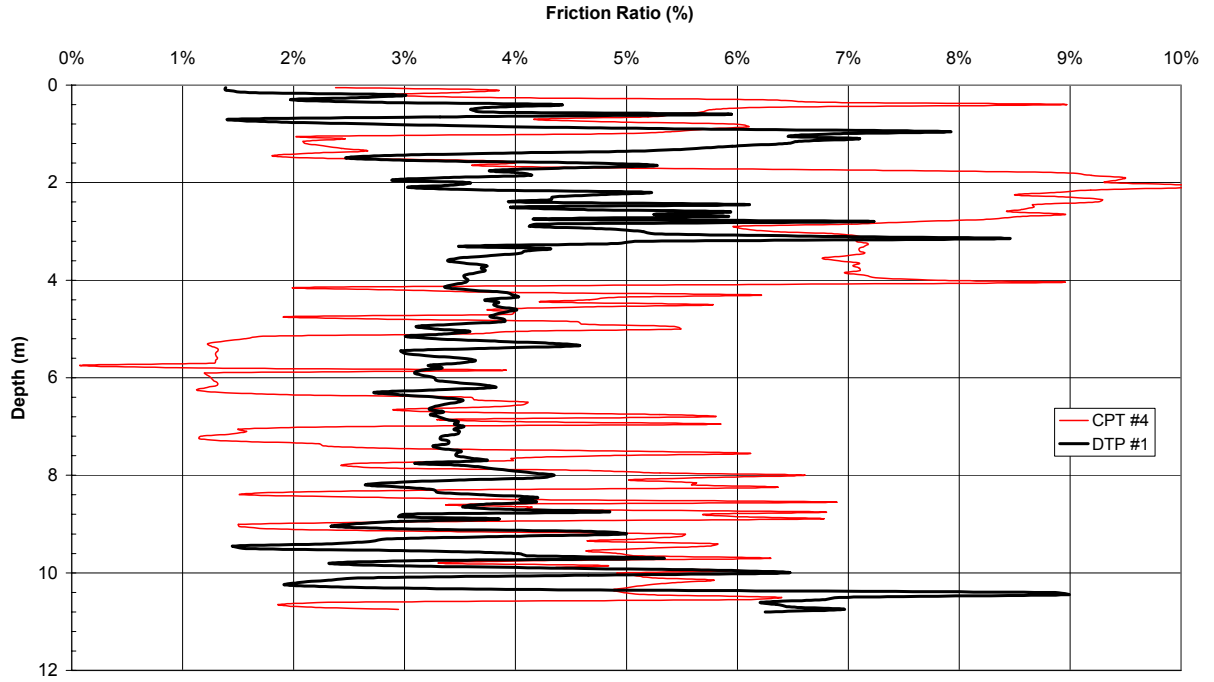


Figure A-16: South West Recreation Center CPT #4/DTP #3 Friction Ratios vs. Depth

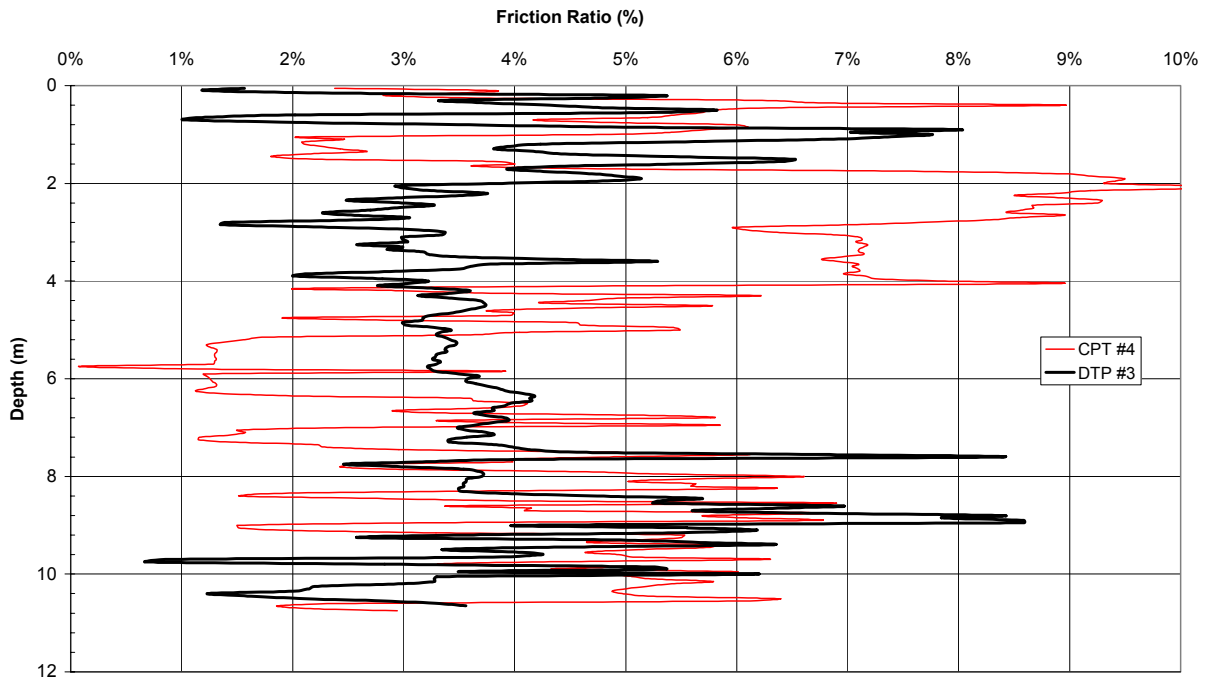


Figure A-17: South West Recreation Center CPT #4/DTP #4 Friction Ratios vs. Depth

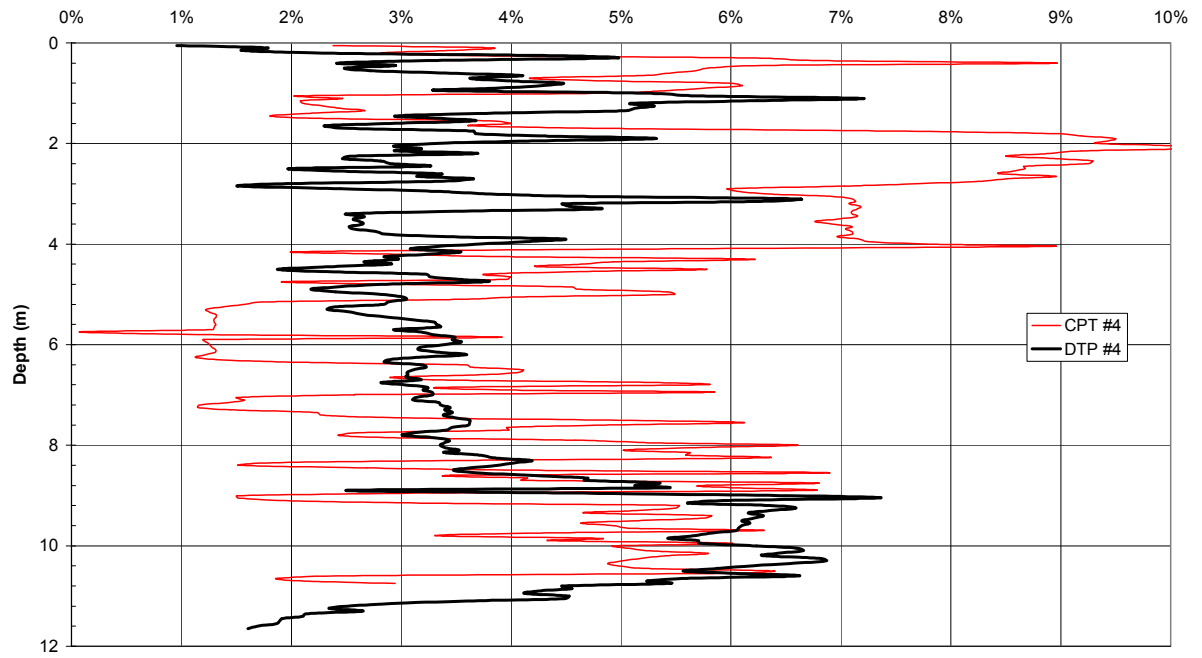


Figure A-18: South West Recreation Center DTP #1 Tip Ratio vs. Depth

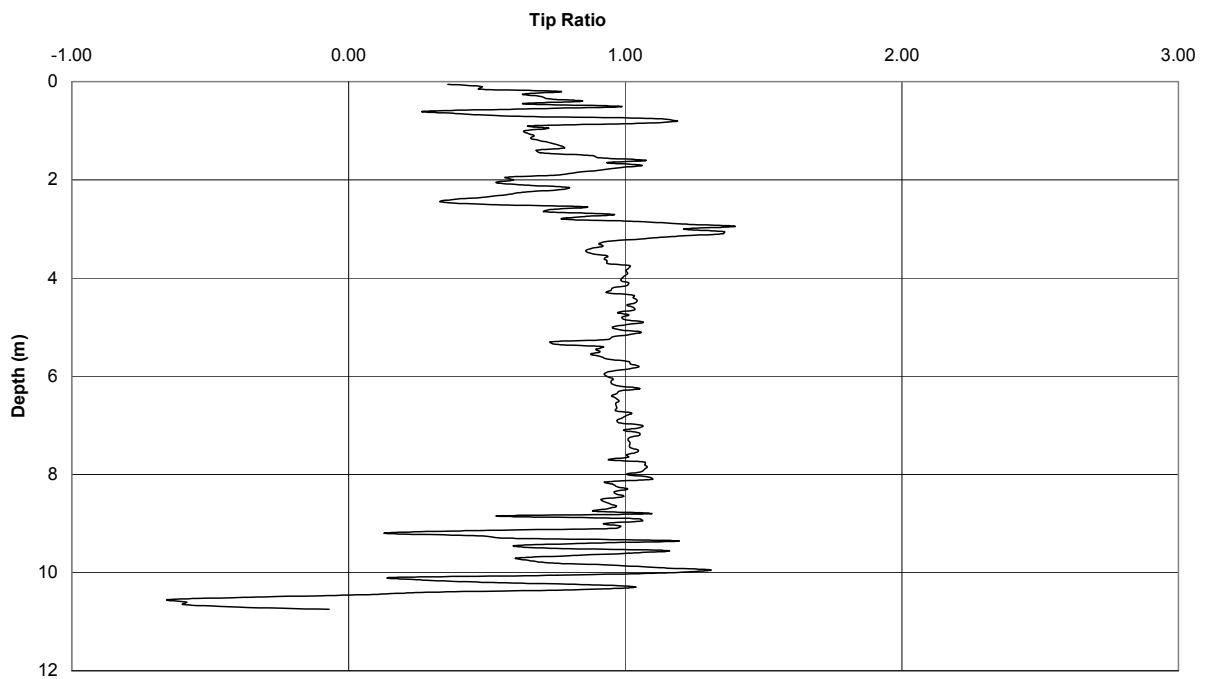




Figure A-19: South West Recreation Center DTP #3 Tip Ratio vs. Depth

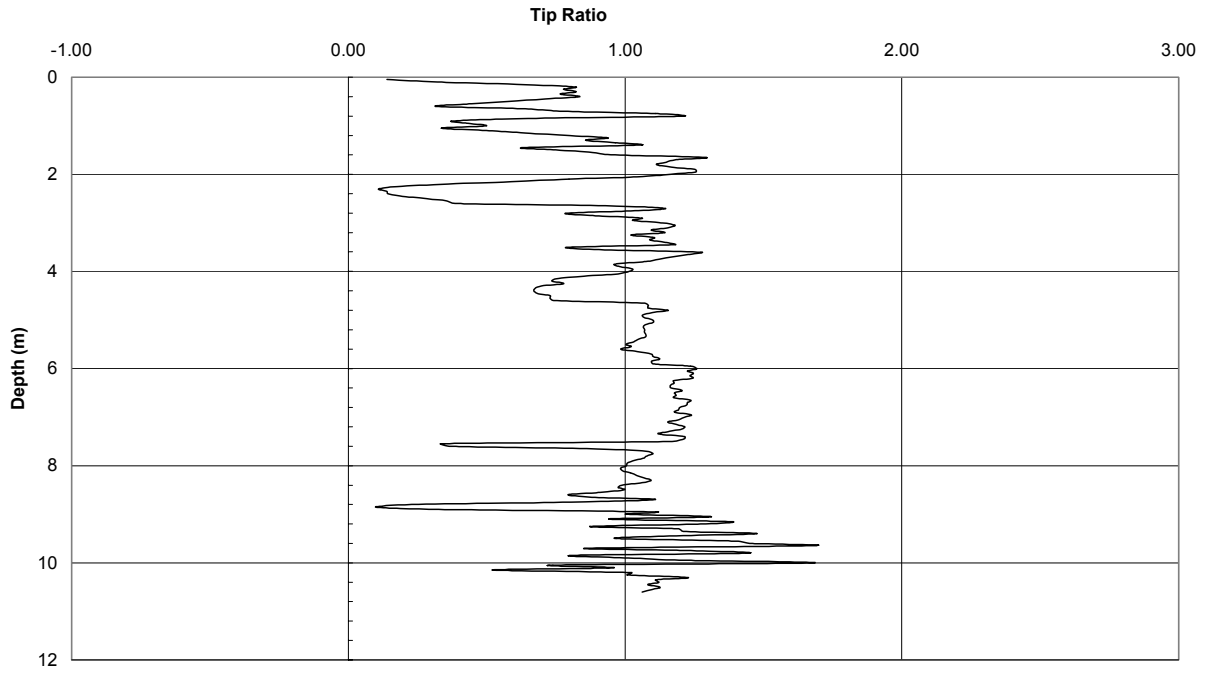


Figure A-20: South West Recreation Center DTP #4 Tip Ratio vs. Depth

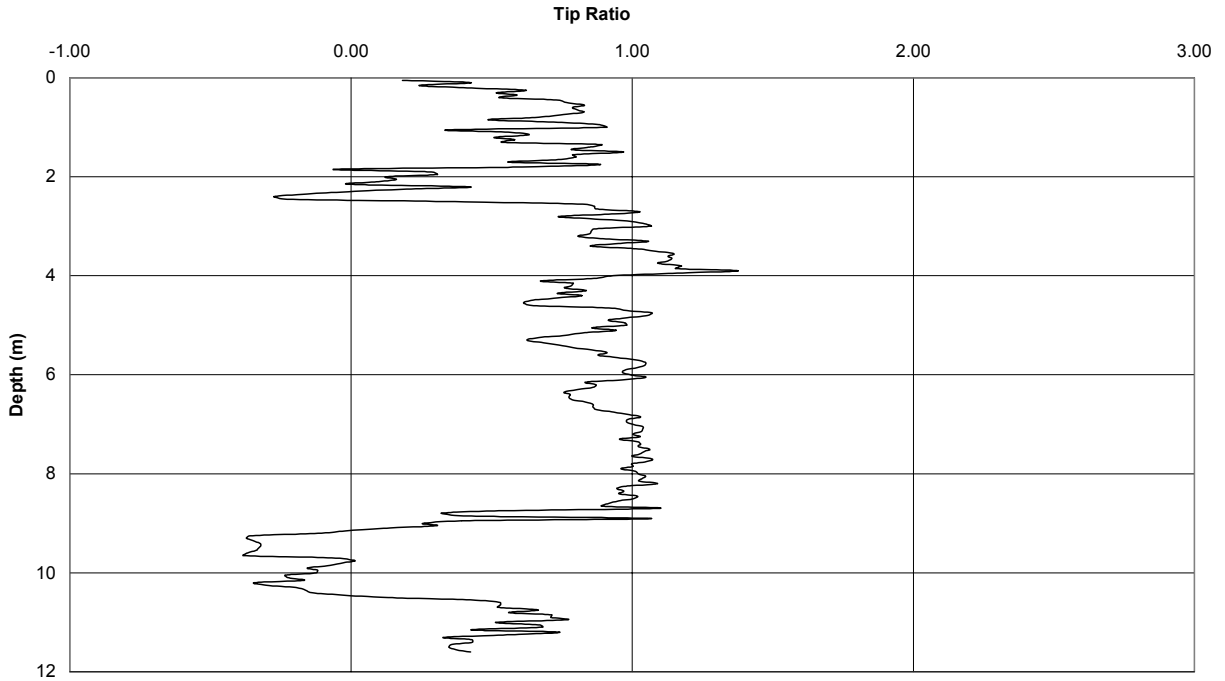


Figure A-21: Vilano Beach CPT #1 Tip Resistance vs. Depth

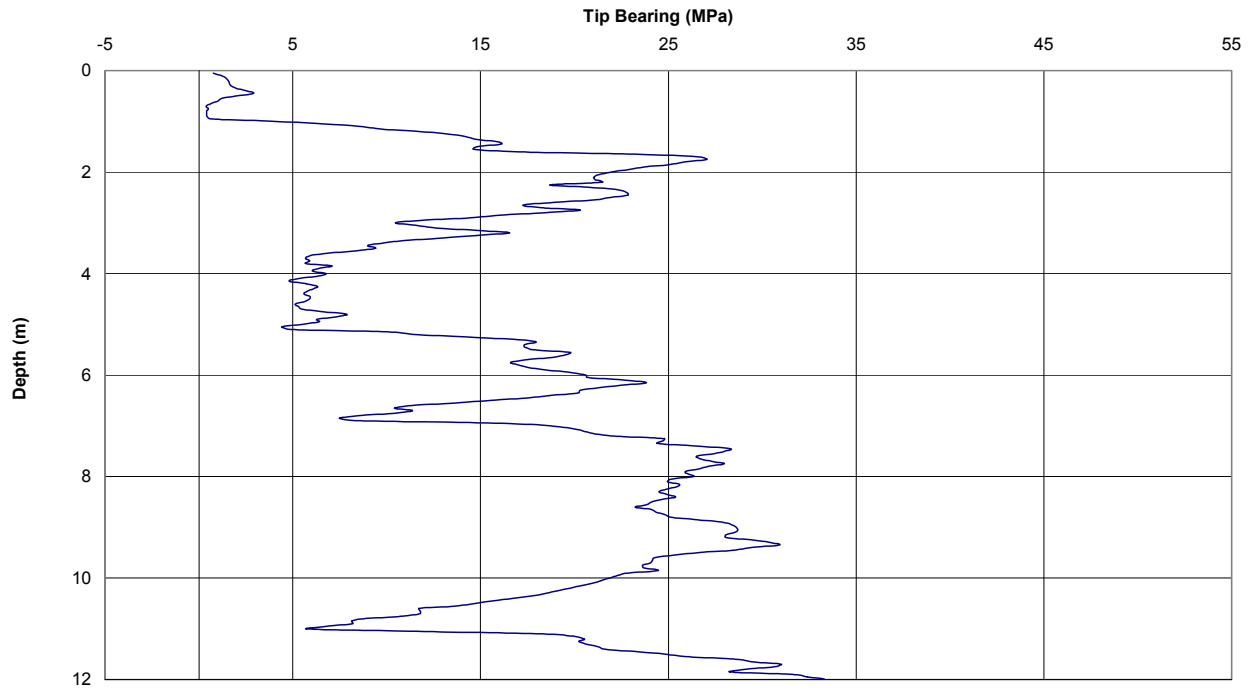


Figure A-22: Vilano Beach CPT #2 Tip Resistance vs. Depth

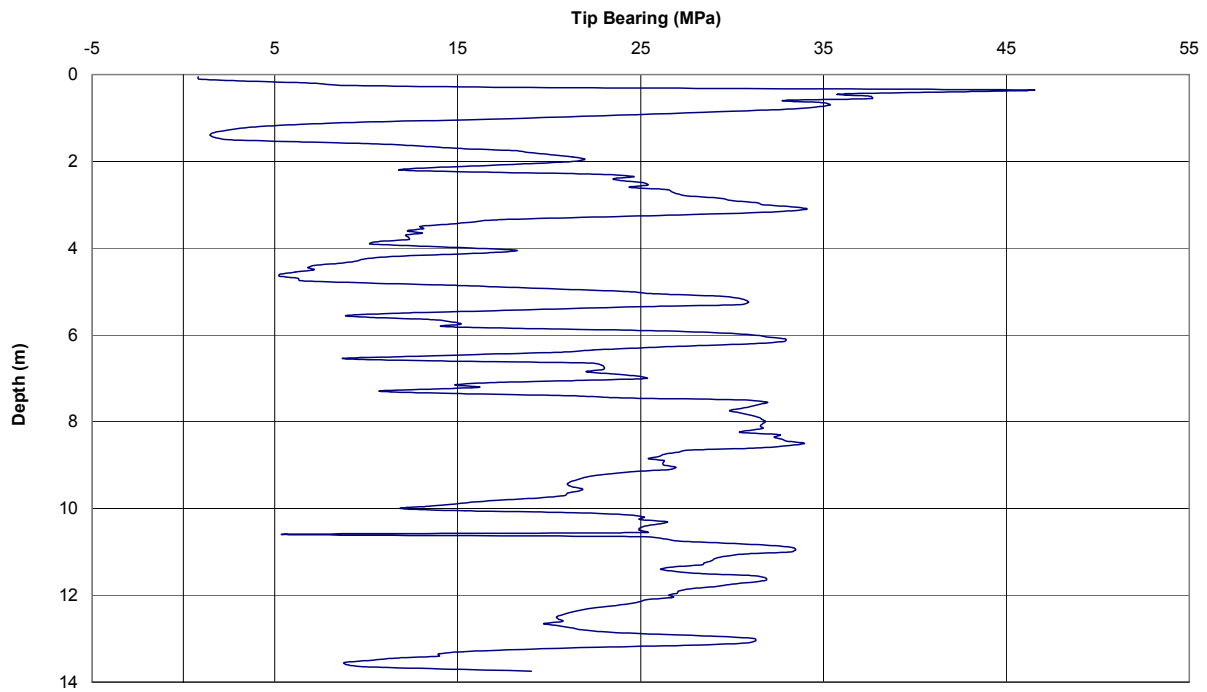


Figure A-23: Vilano Beach DTP #1 Tip Resistance vs. Depth

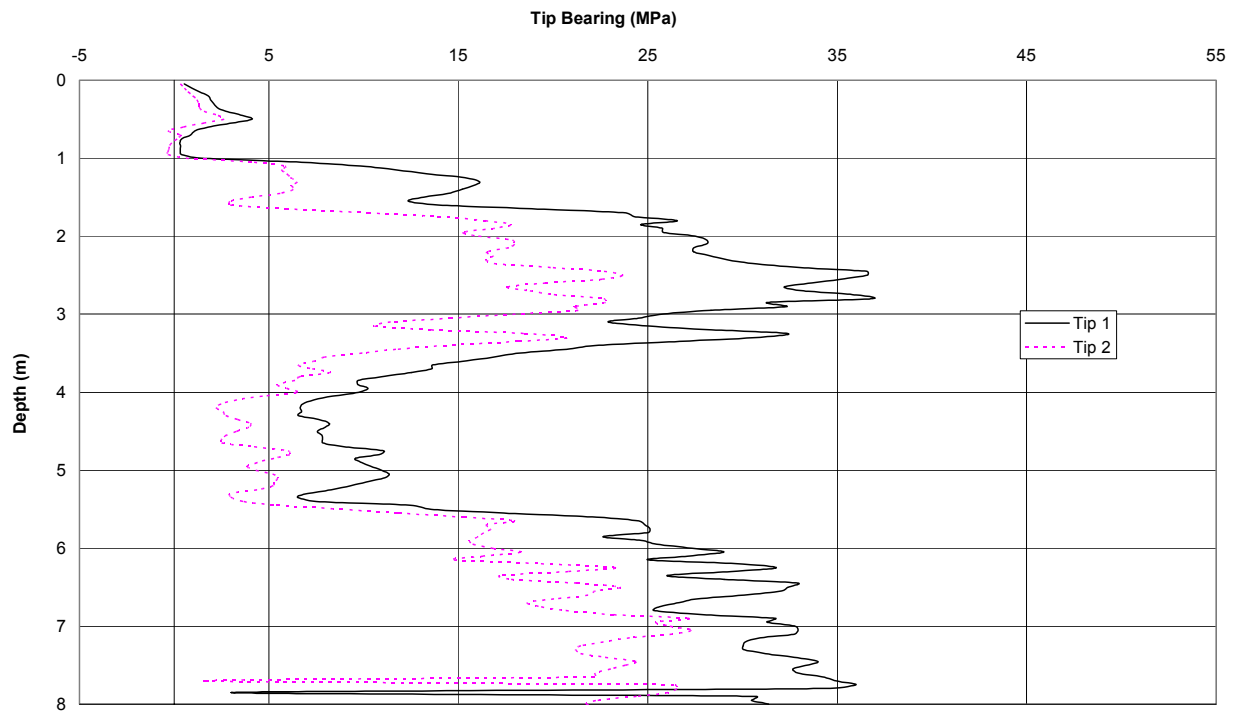


Figure A-24: Vilano Beach DTP #4 Tip Resistance vs. Depth

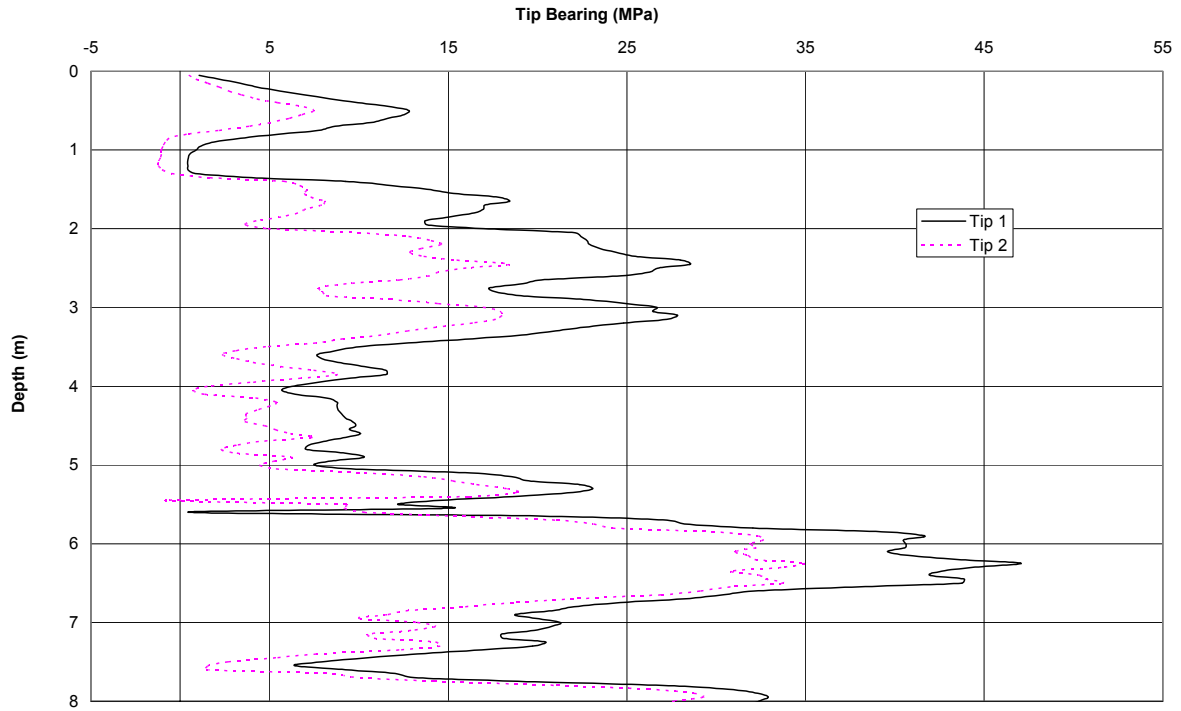


Figure A-25: Vilano Beach DTP #5 Tip Resistance vs. Depth  
Tip Bearing (MPa)

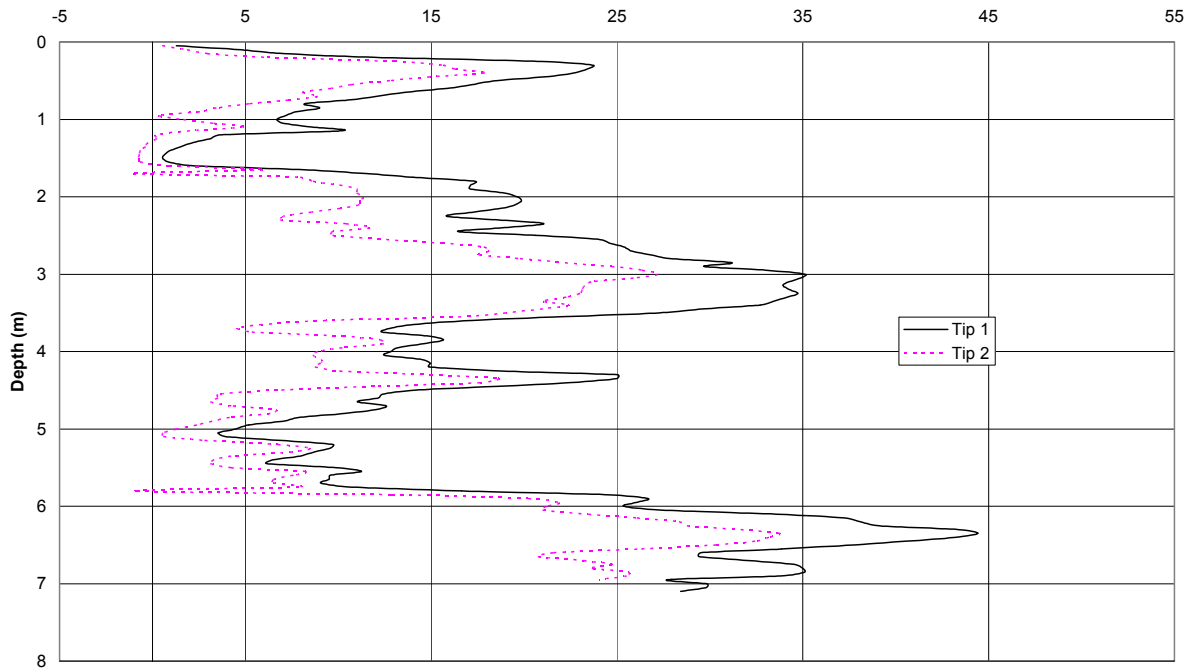


Figure A-26: Vilano Beach CPT #1/DTP #4 Friction Ratios vs. Depth

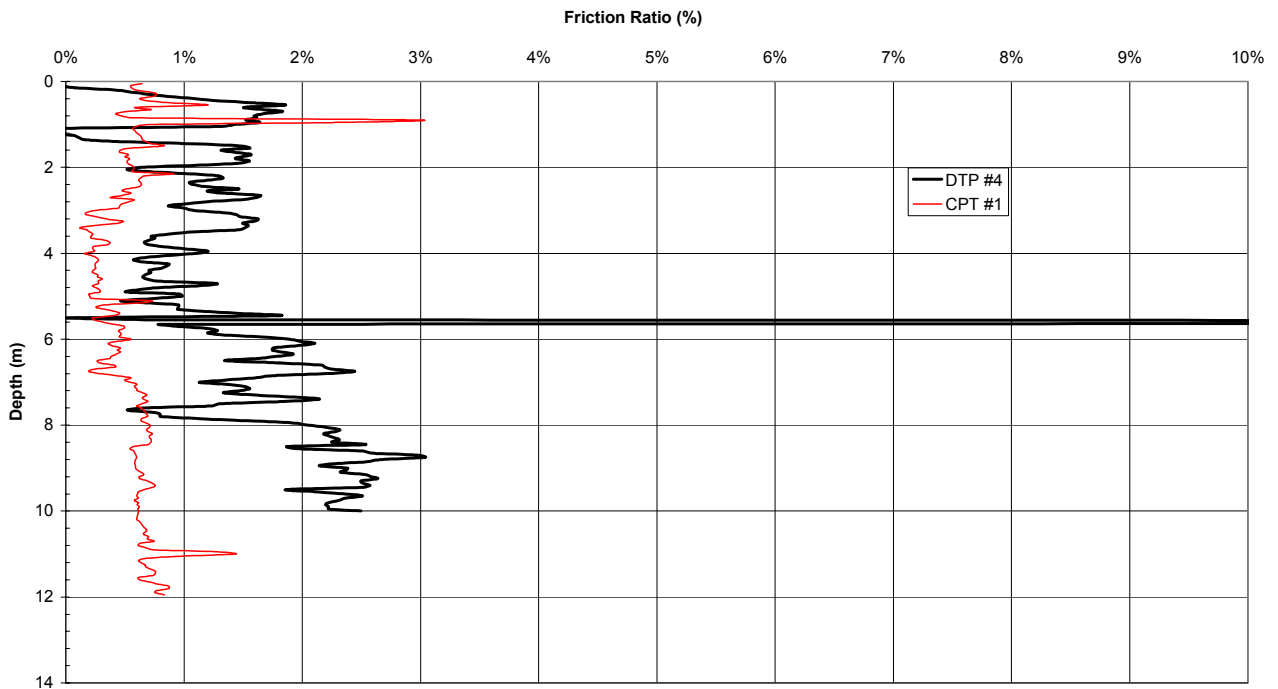


Figure A-27: Vilano Beach CPT #1/DTP #5 Friction Ratios vs. Depth

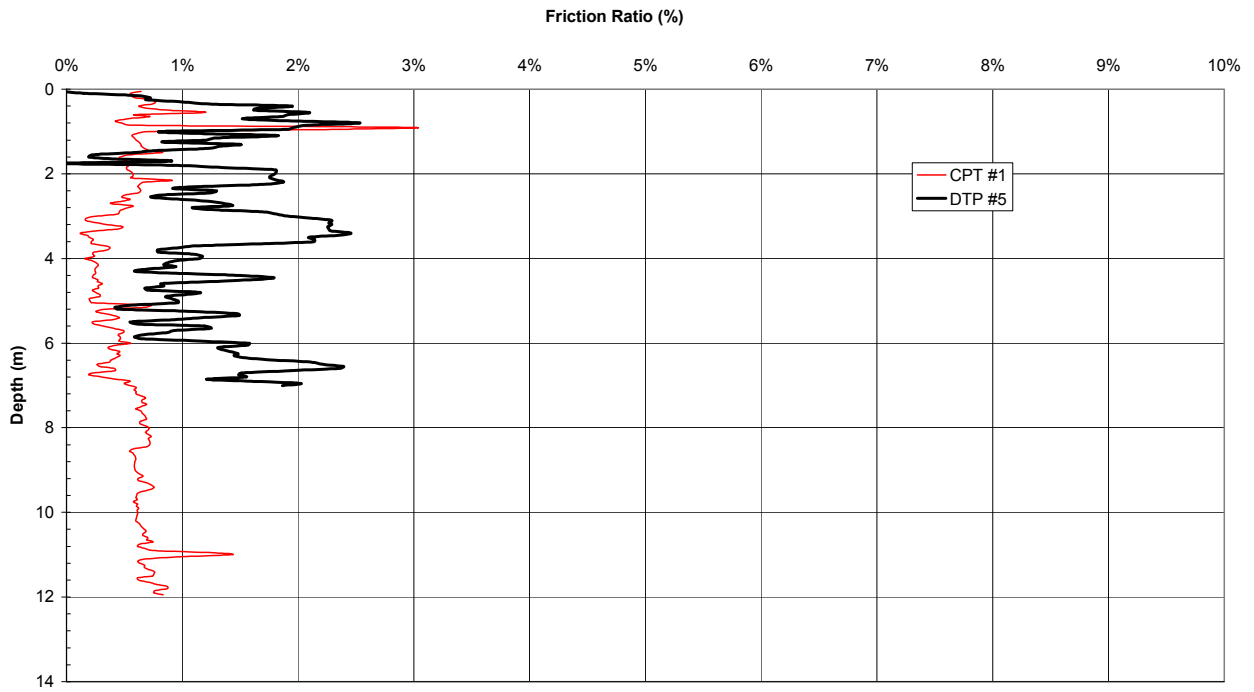


Figure A-28: Vilano Beach CPT #2/DTP #1 Friction Ratios vs. Depth

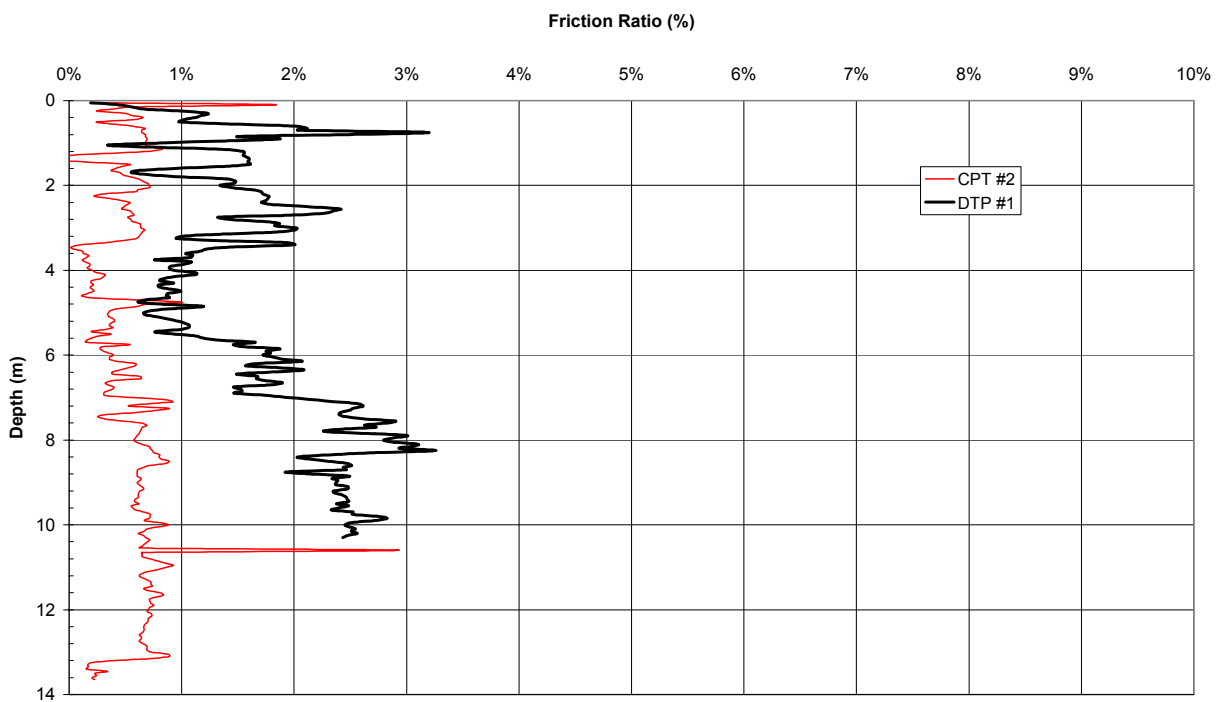


Figure A-29: Vilano Beach CPT #2/DTP #4 Friction Ratios vs. Depth

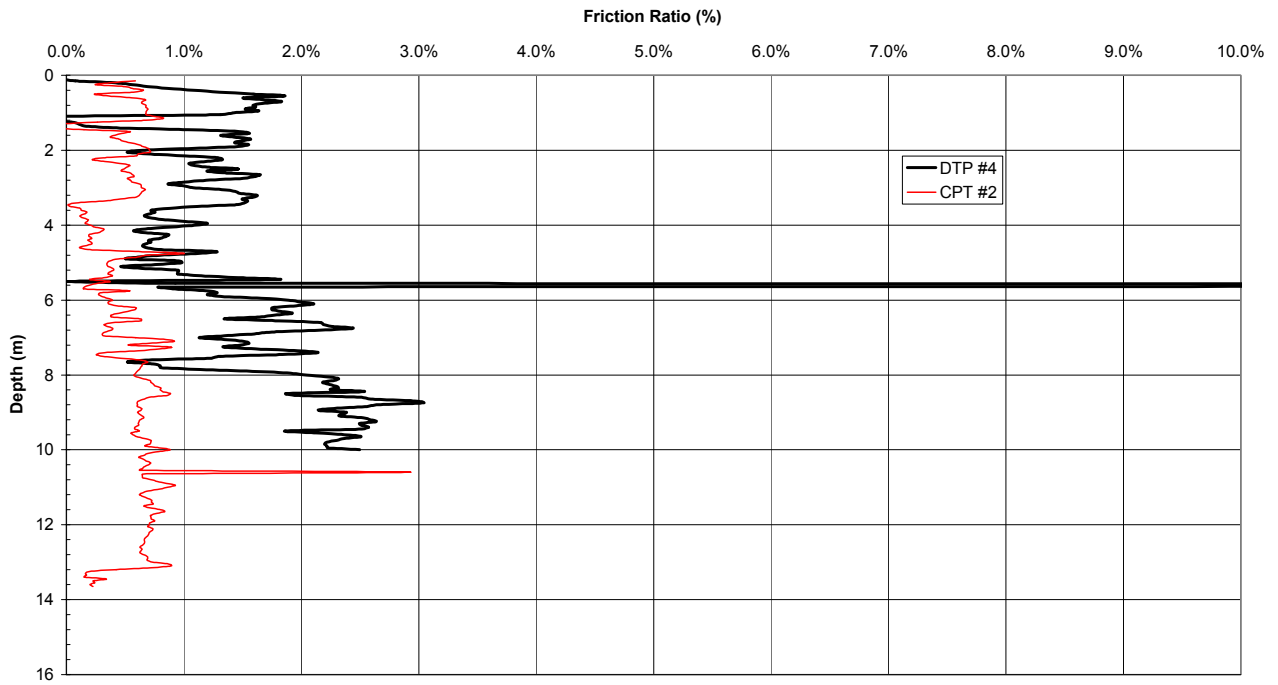


Figure A-30: Vilano Beach DTP #1 Tip Ratio vs. Depth

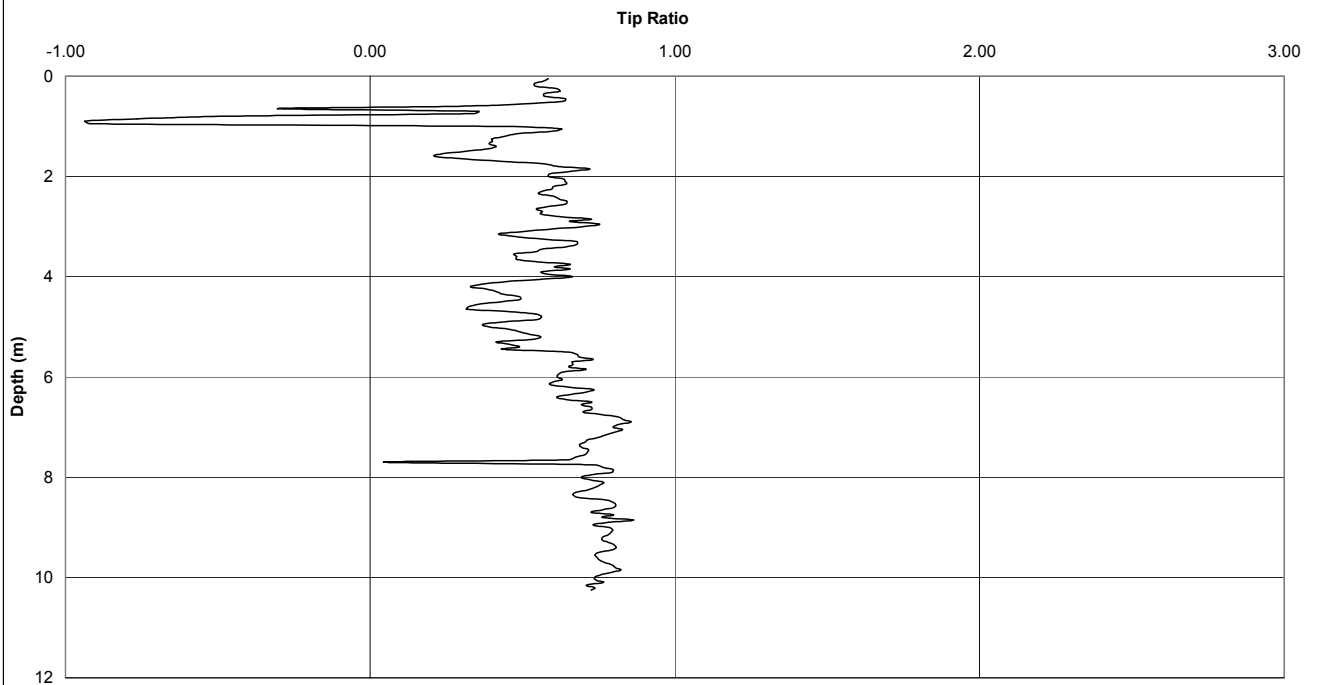


Figure A-31: Vilano Beach DTP #4 Tip Ratio vs. Depth

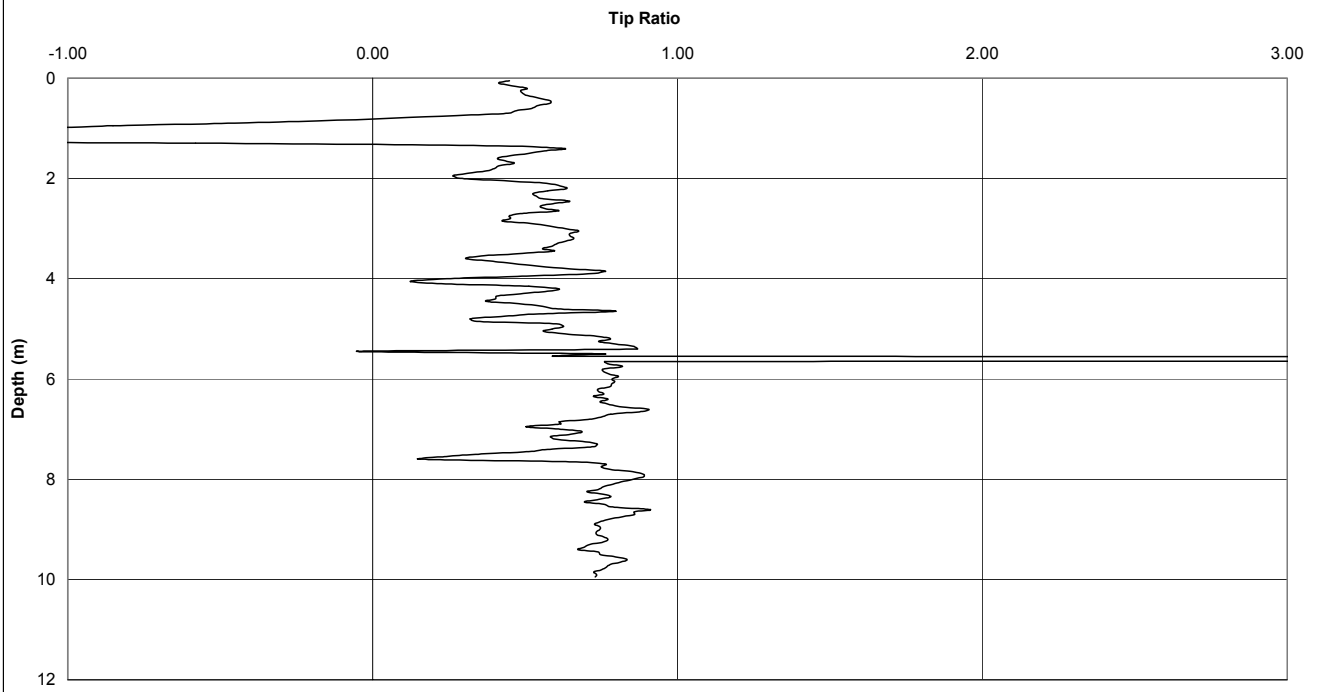


Figure A-32: Vilano Beach DTP #5 Tip Ratio vs. Depth

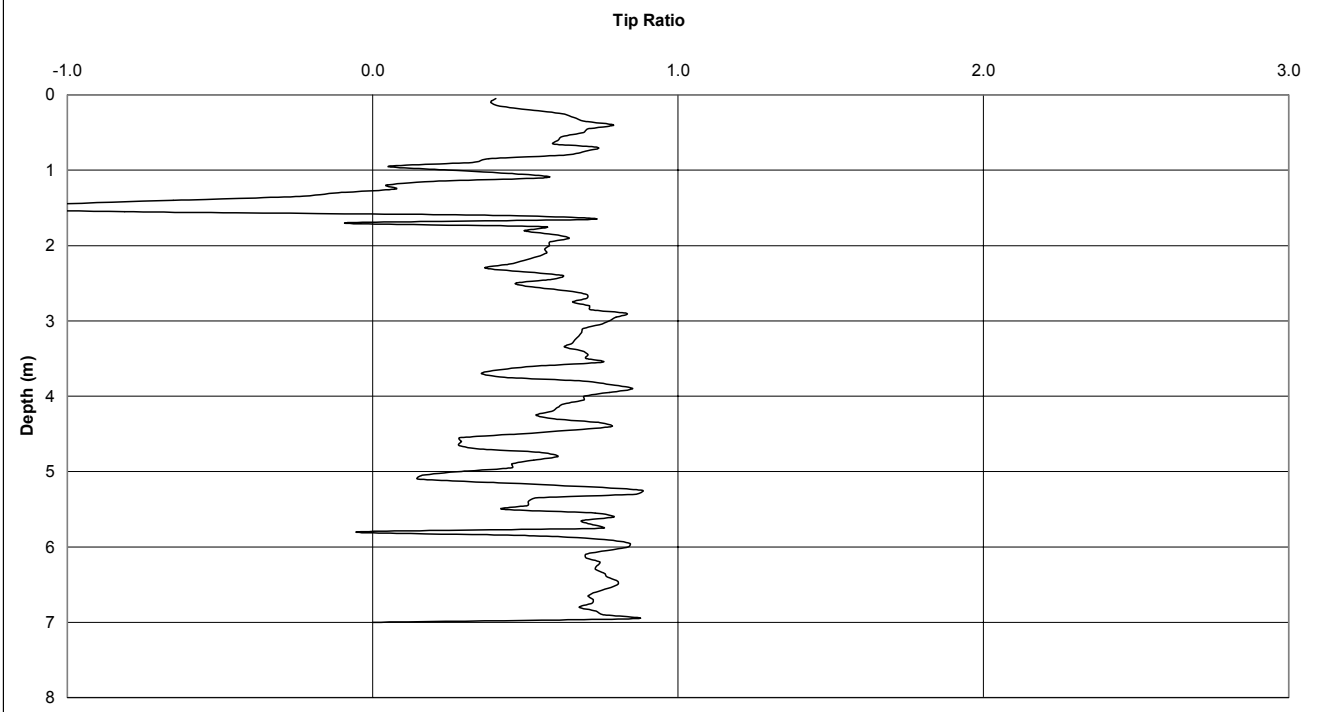


Figure A-33: Vilano Beach West CPT #1 Tip Resistance vs. Depth

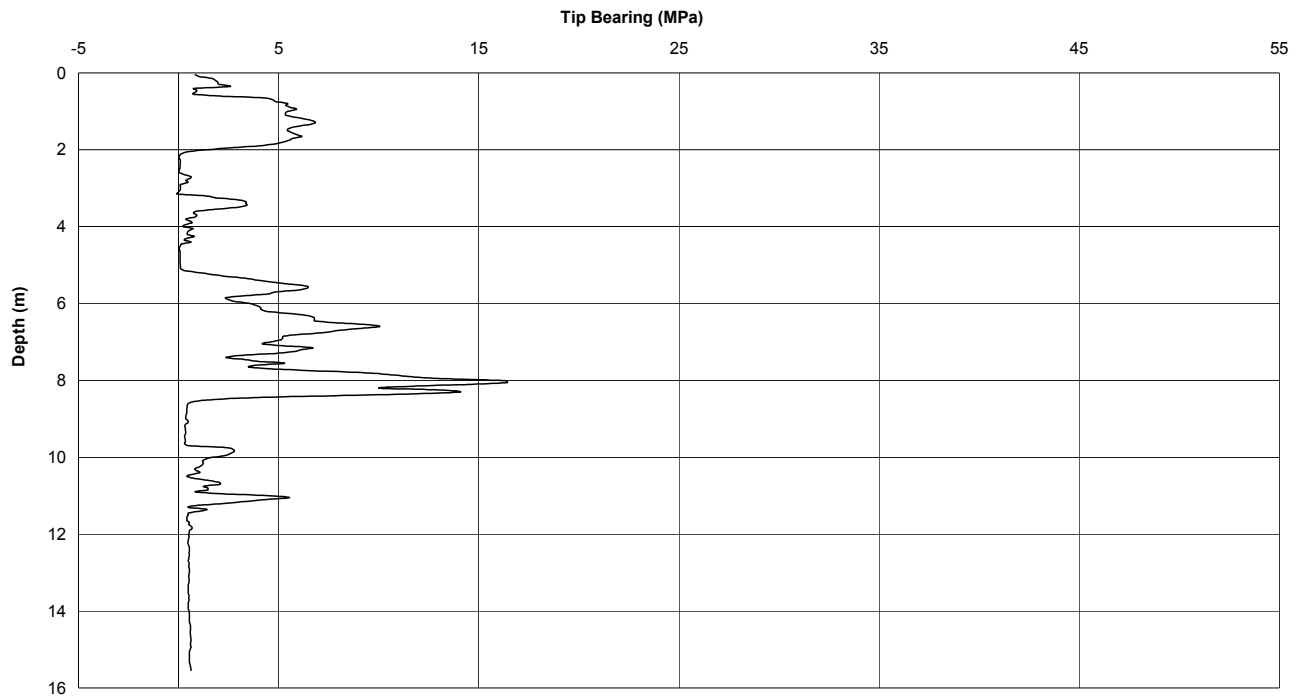


Figure A-34: Vilano Beach West DTP #1 Tip Resistances vs. Depth

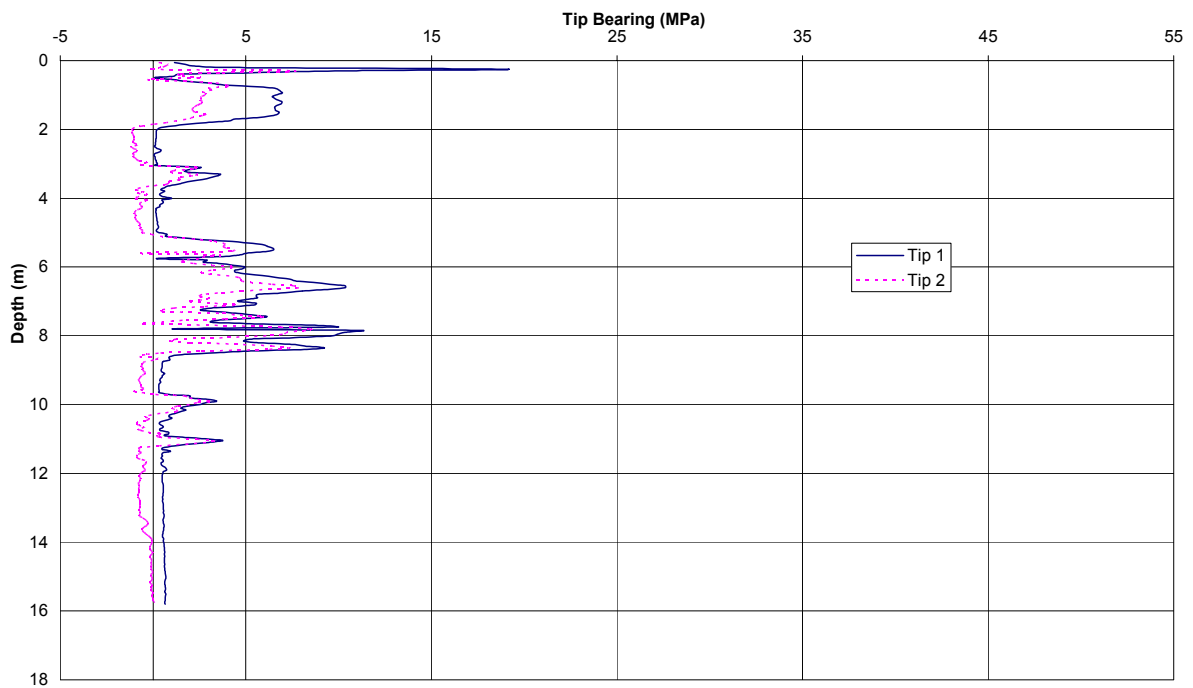




Figure A-35: Vilano Beach West CPT #1/DTP #1 Friction Ratios vs. Depth

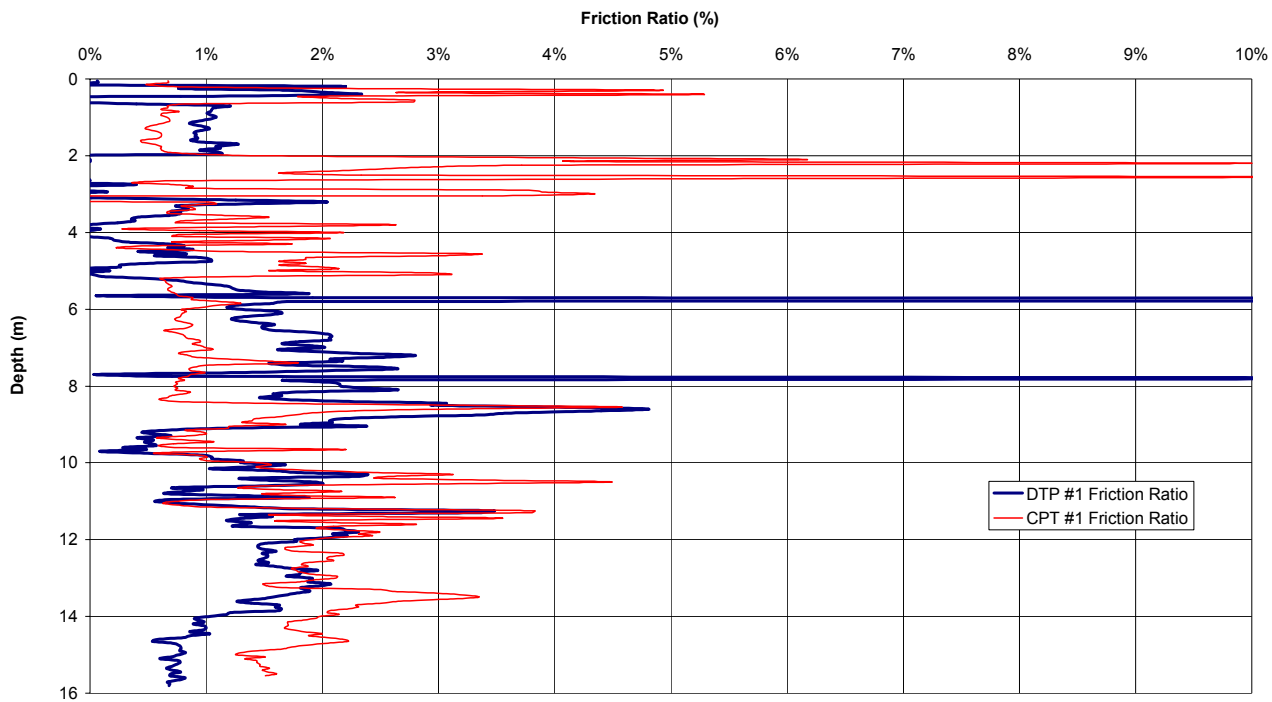


Figure A-36: Vilano Beach West DTP #1 Tip Ratio vs. Depth  
(large variability due to low Tip 1 and negative Tip 2 Readings)

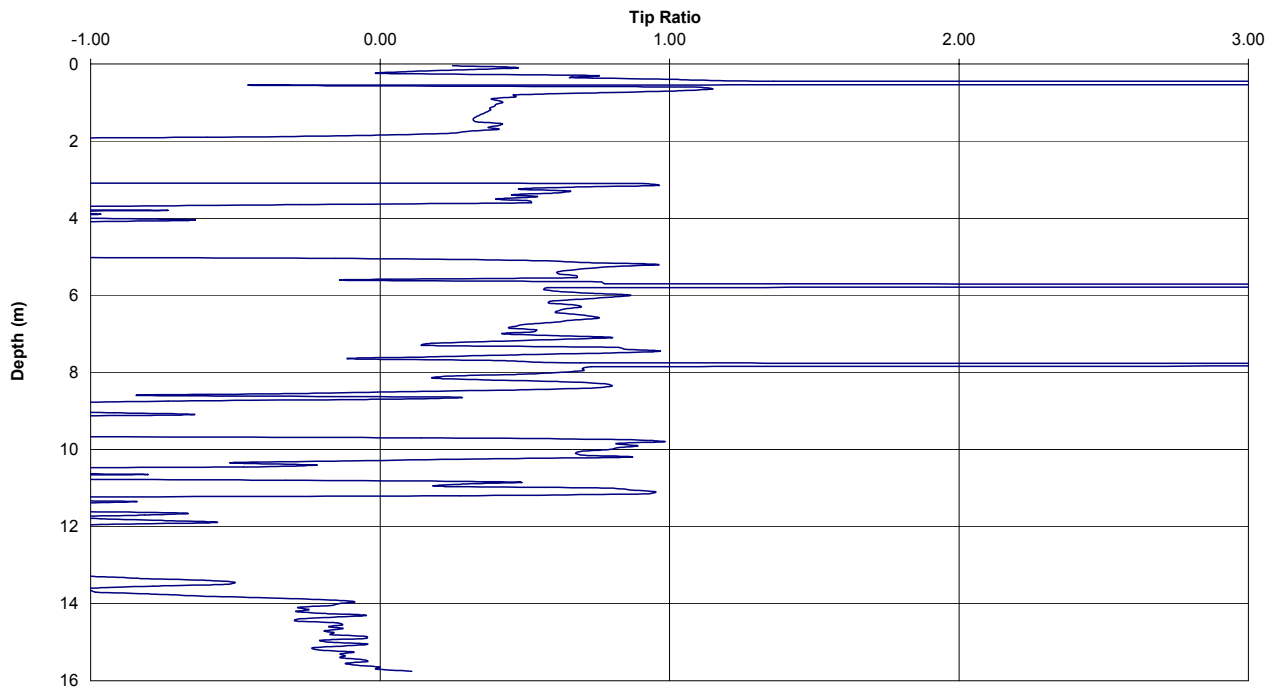


Figure A-37: Lake Alice West Bank CPT #1 Tip 1 Resistance vs. Depth

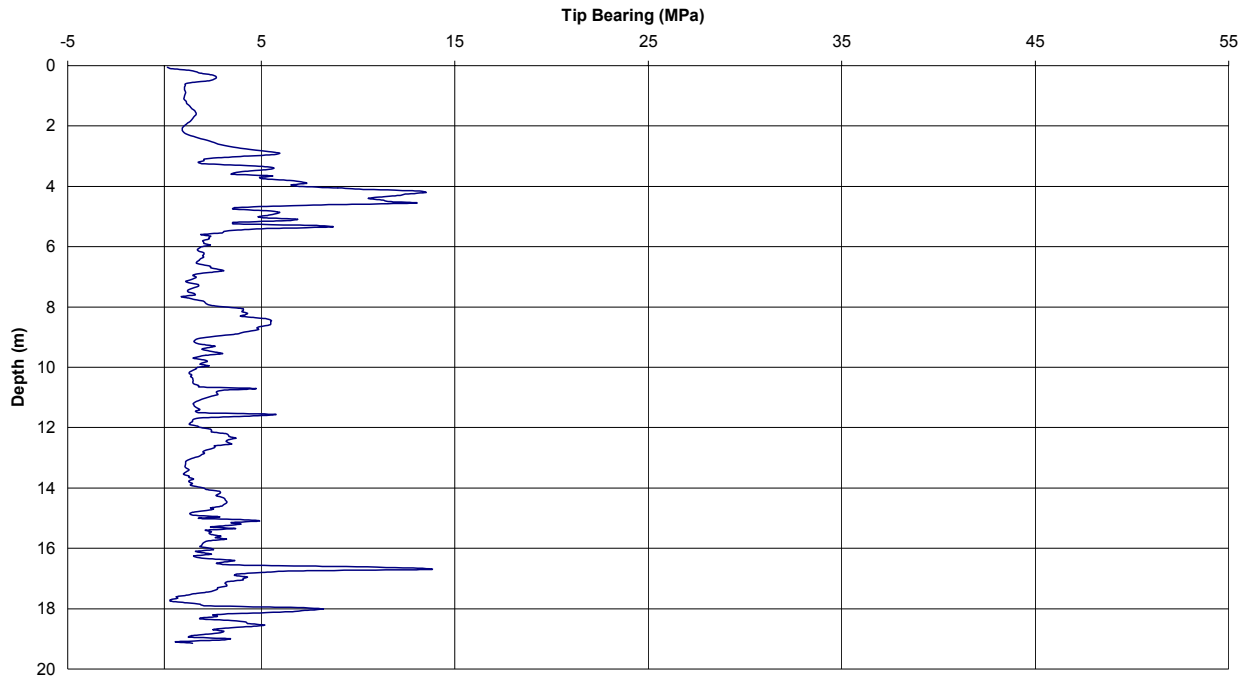


Figure A-38: Lake Alice West Bank DTP #1 Tip Resistances vs. Depth

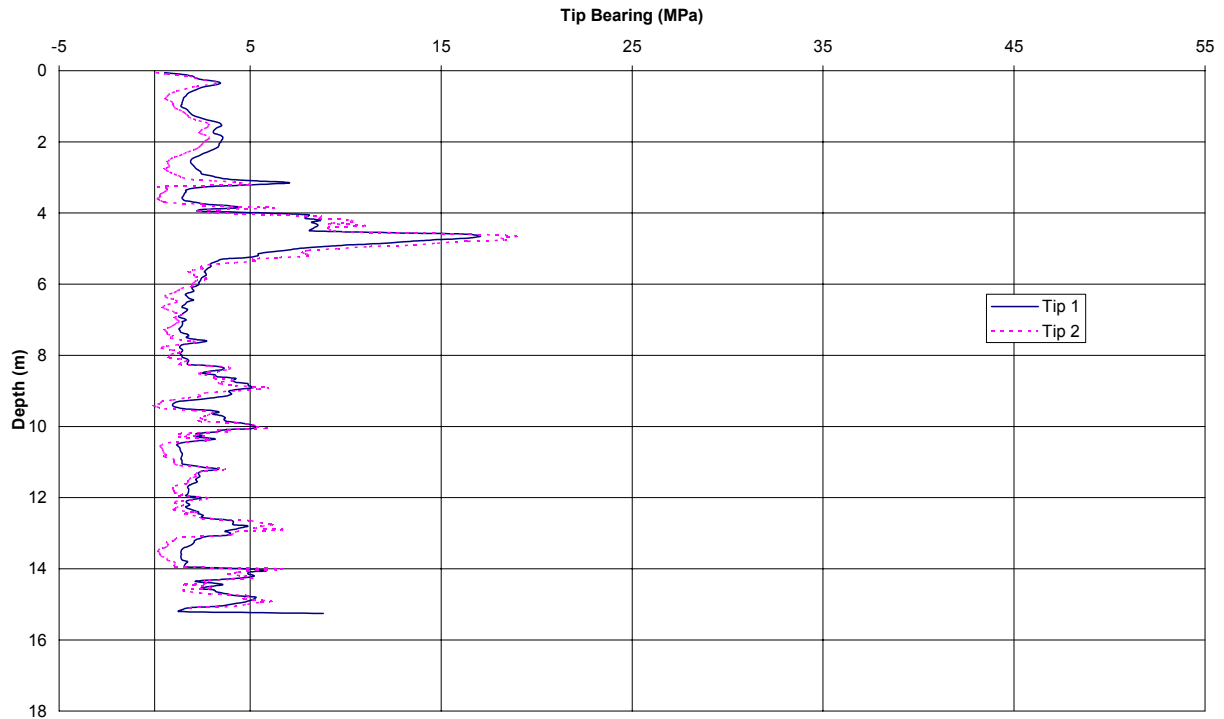


Figure A-39: Lake Alice West Bank CPT #1/DTP #1 Friction Ratios vs. Depth

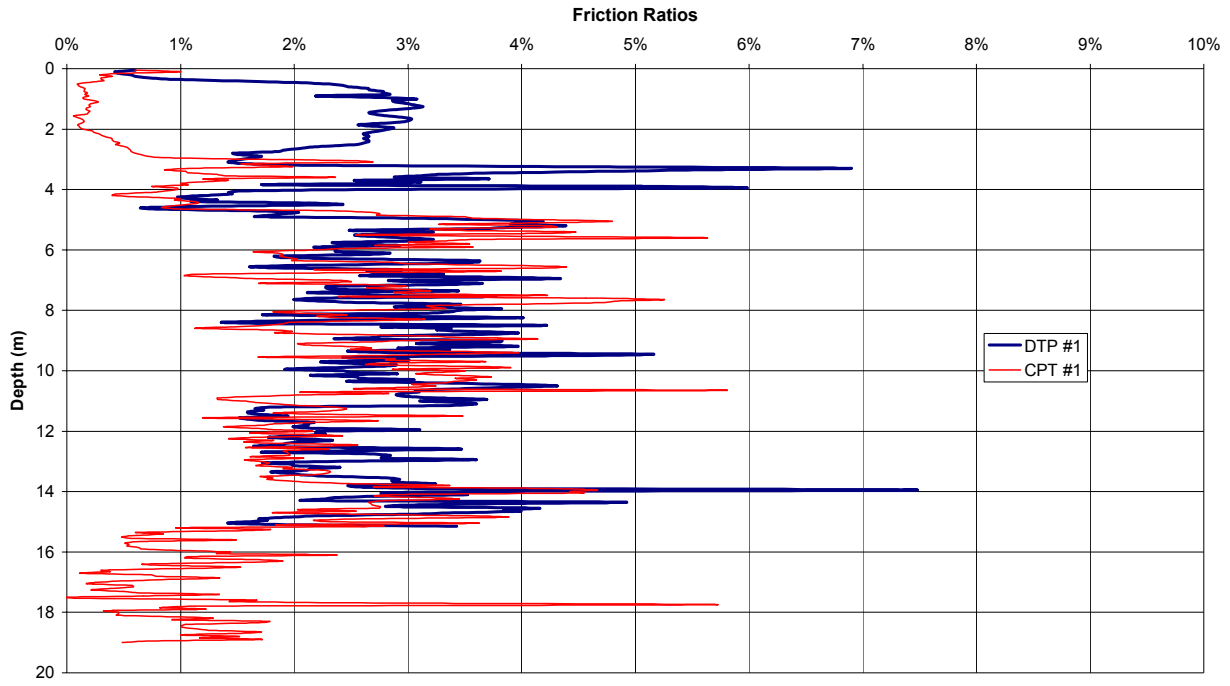


Figure A-40: Lake Alice West Bank DTP #1 Tip Ratio vs. Depth

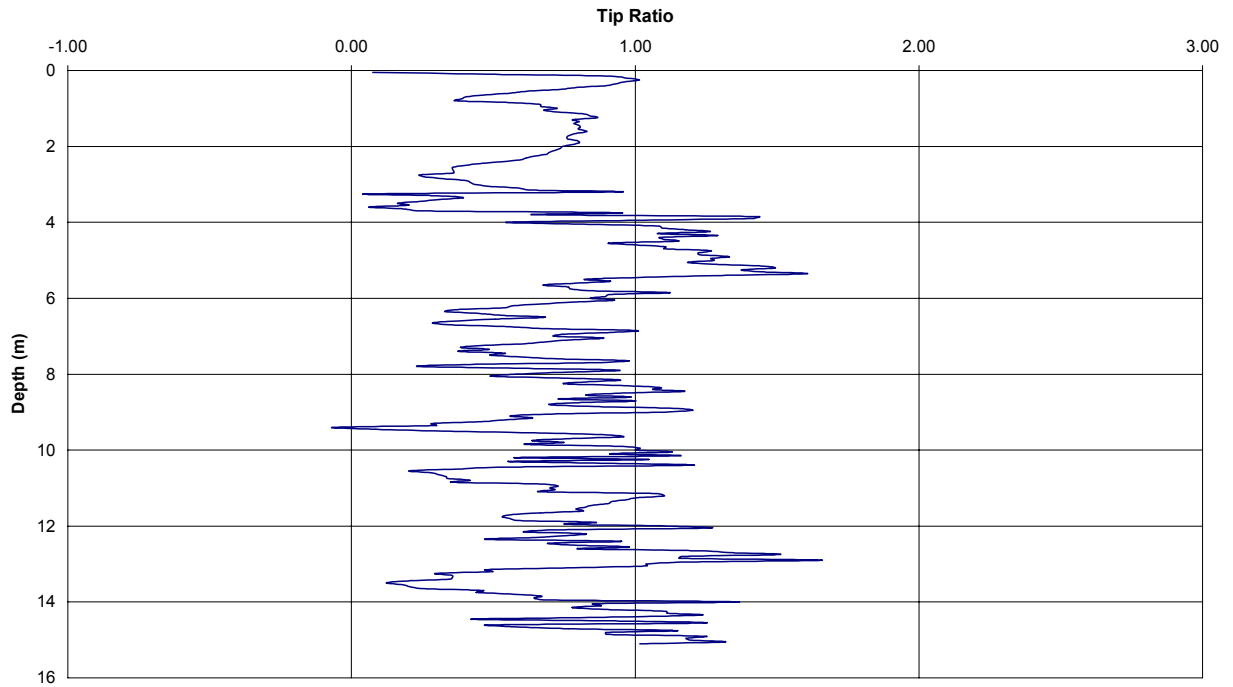


Figure A-41: Green Cove Springs CPT #1 Tip 1 Bearing vs. Depth

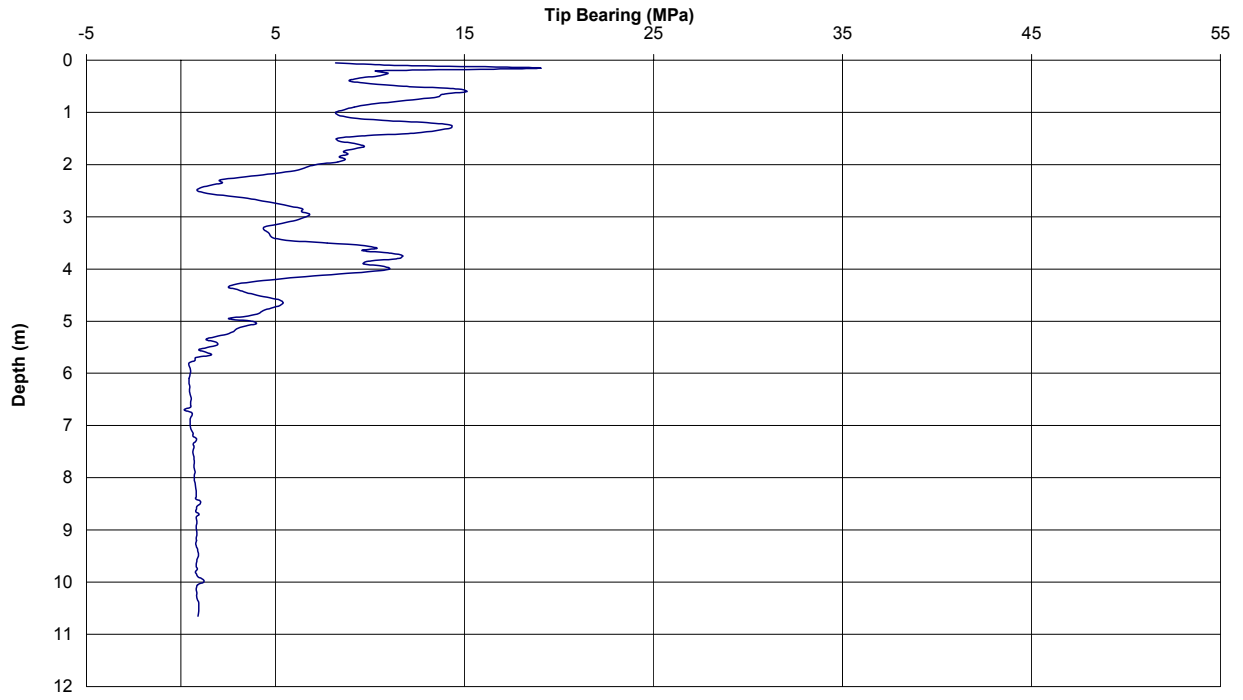


Figure A-42: Green Cove Springs DTP #1 Tip Bearings vs. Depth

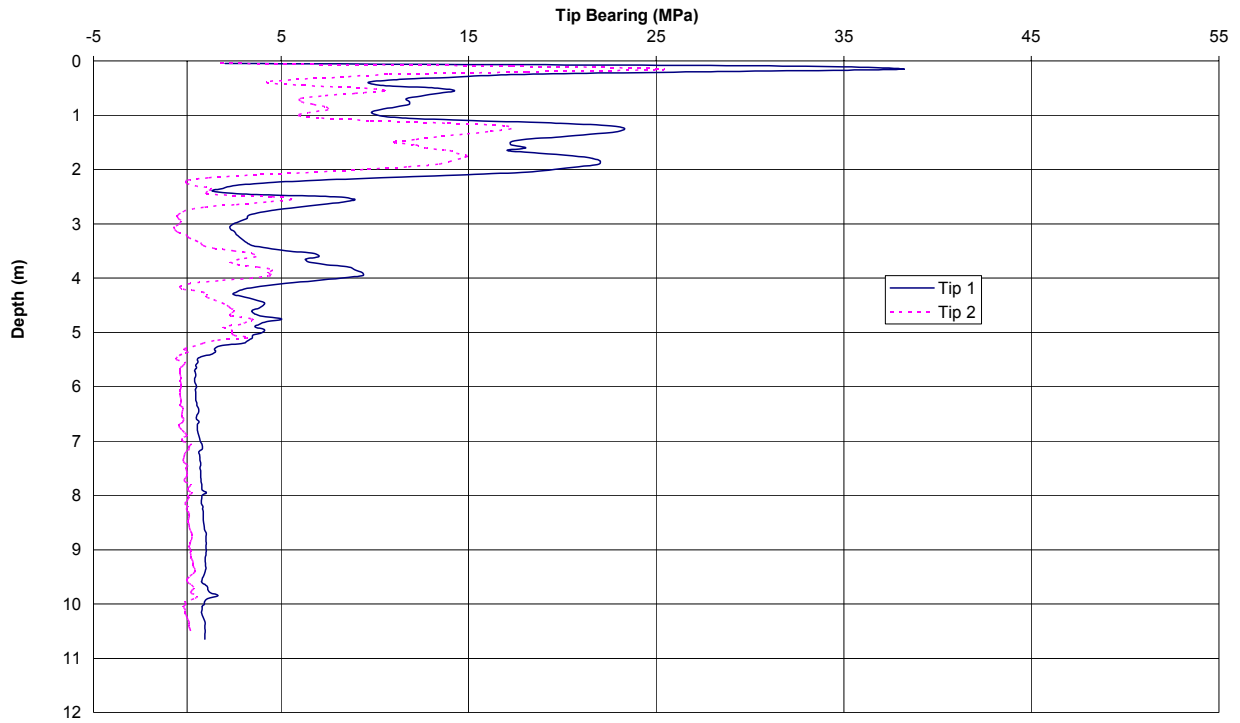


Figure A-43: Green Cove Springs CPT #1/DTP #1 Friction Ratios vs. Depth

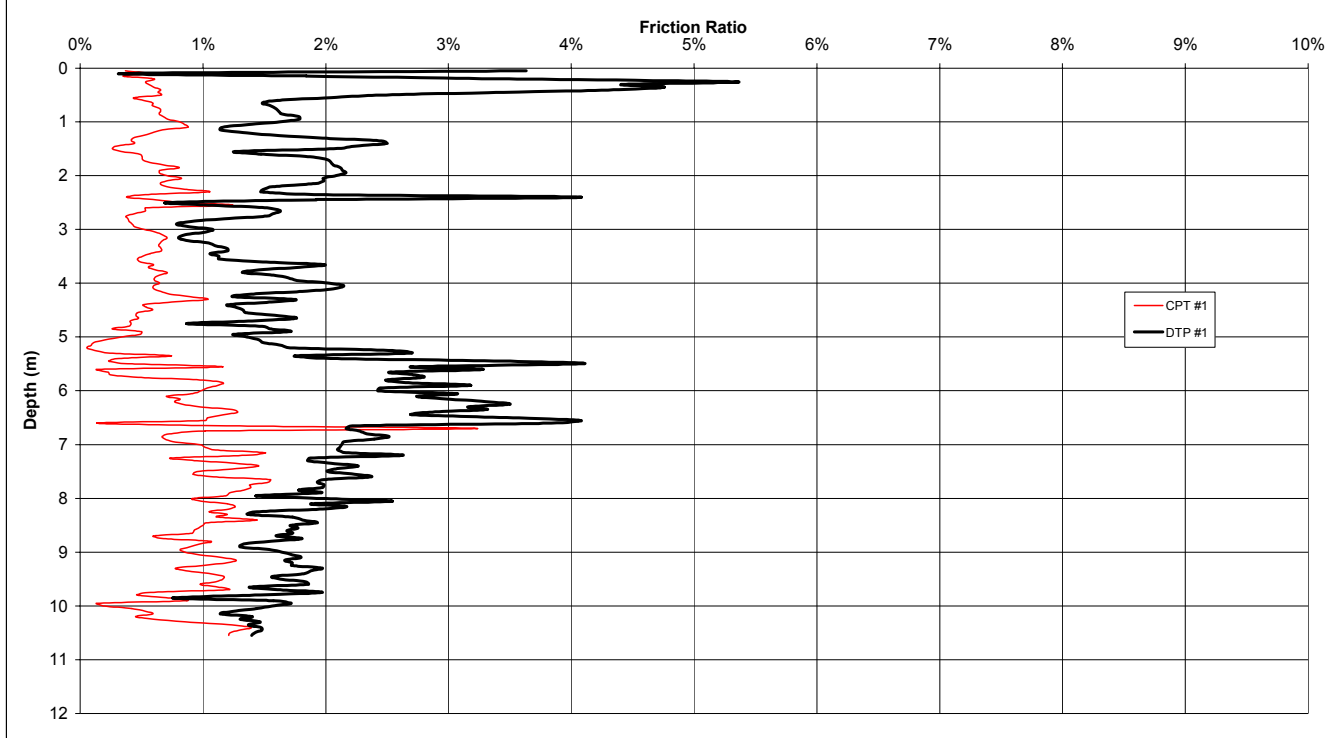
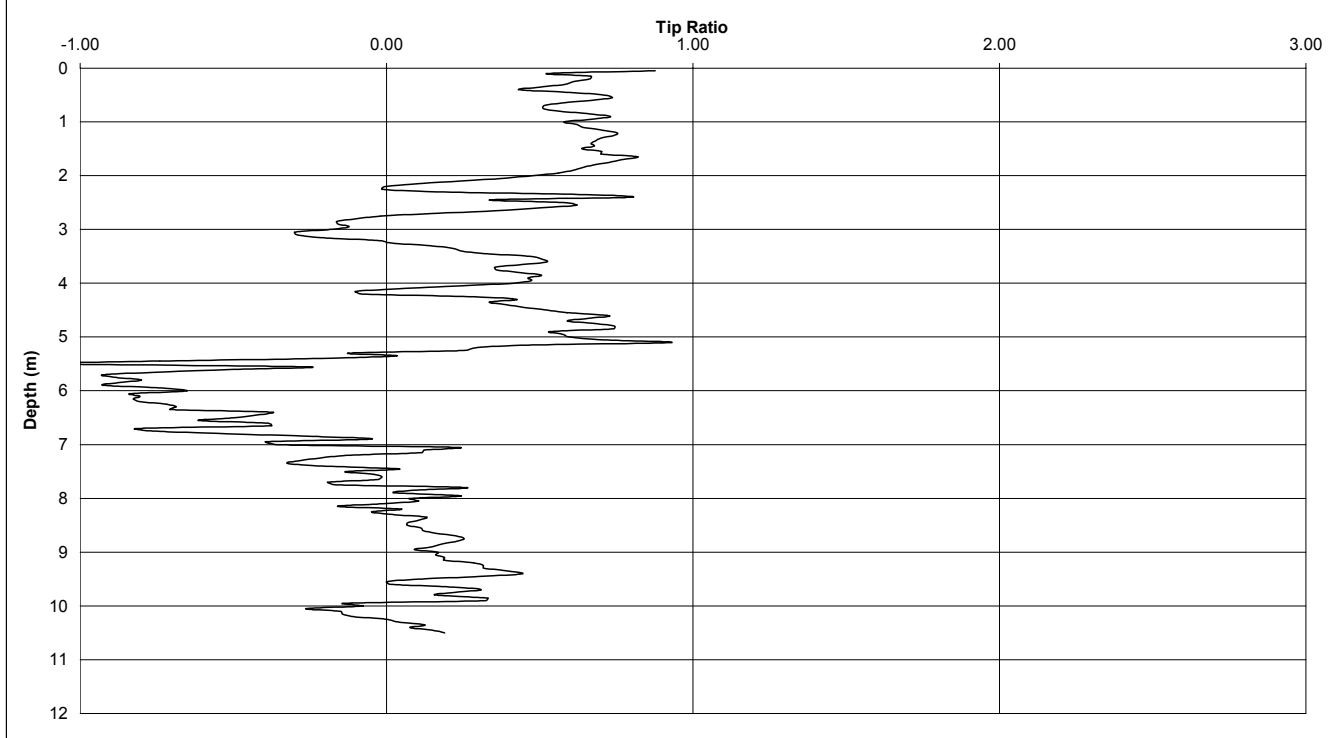


Figure A-44: Green Cove Springs DTP #1 Tip Ratio vs. Depth



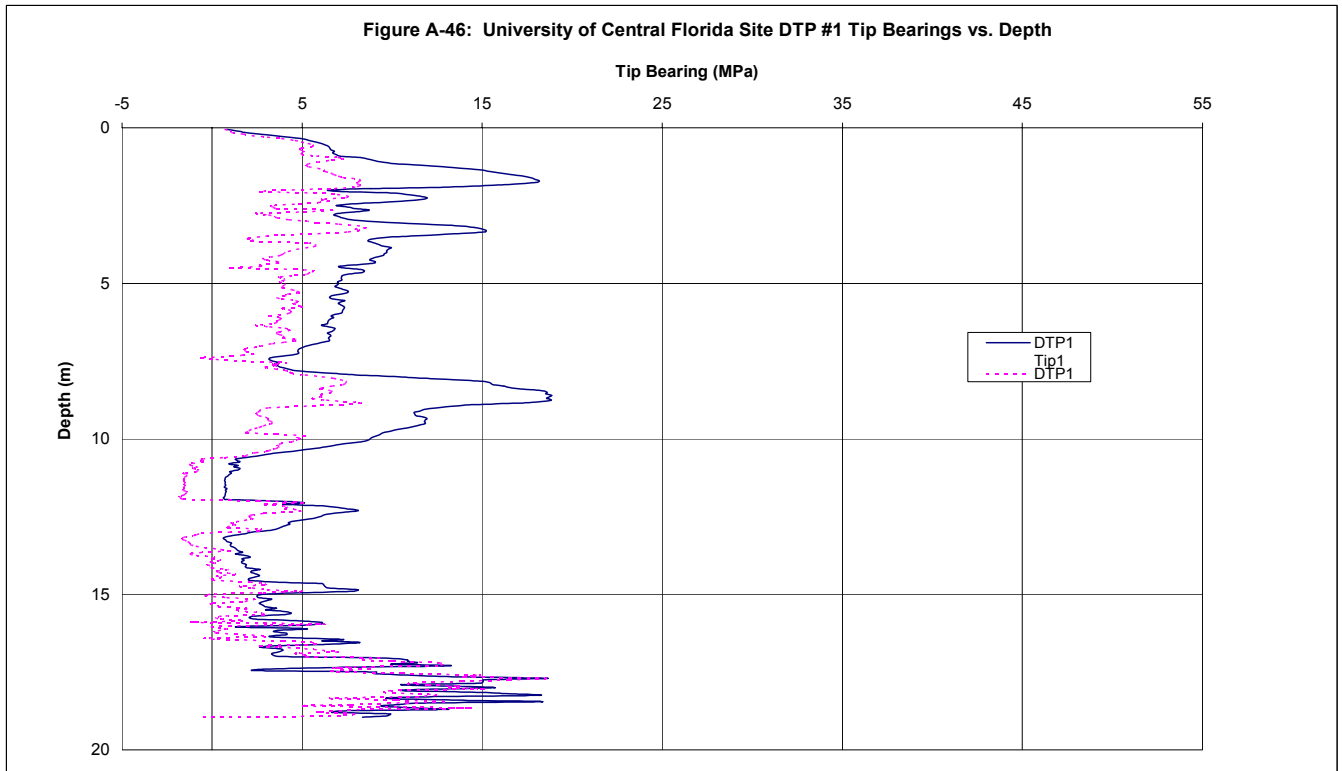
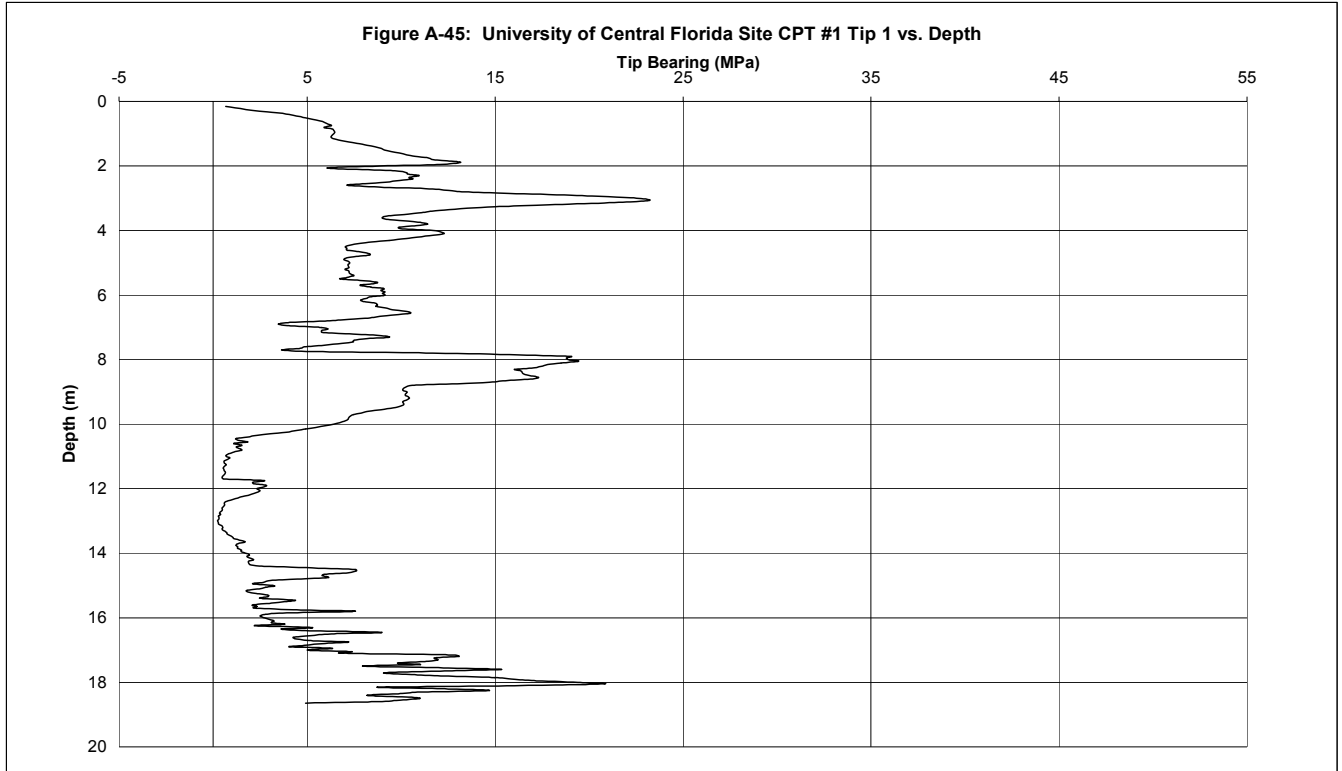


Figure A-47: University of Central Florida Site CPT #2 Tip 1 vs. Depth

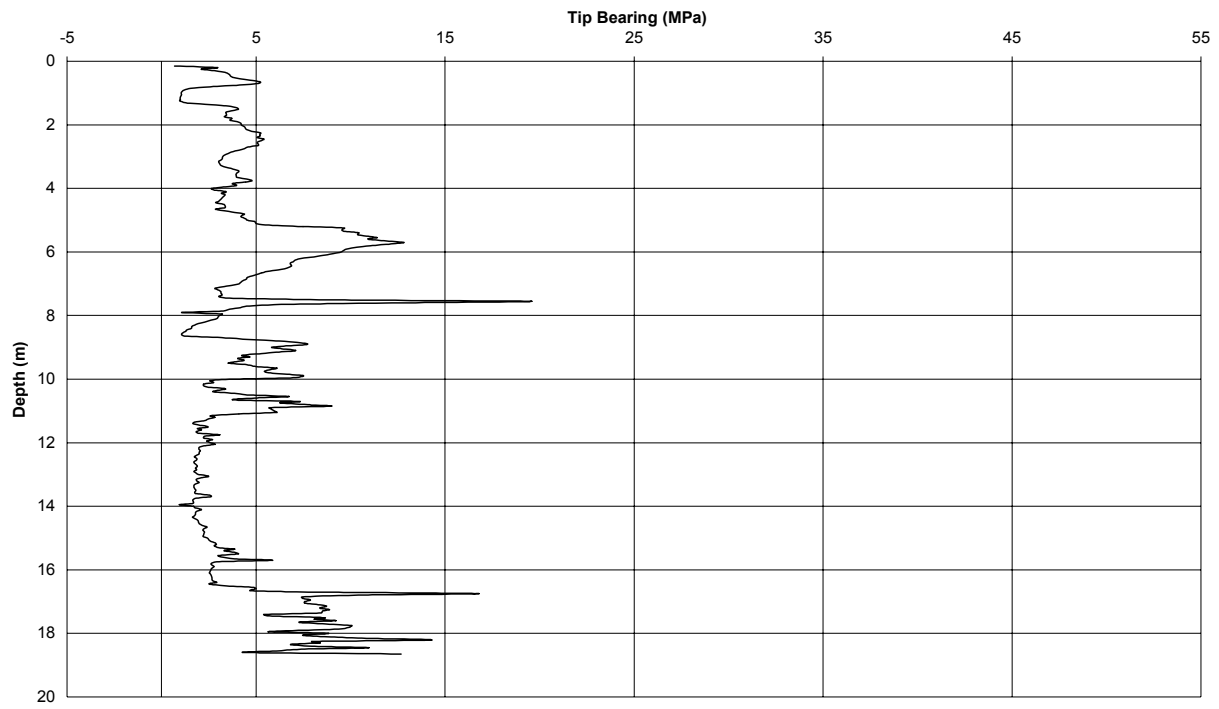


Figure A-48: University of Central Florida Site DTP #2 Tip Bearings vs. Depth

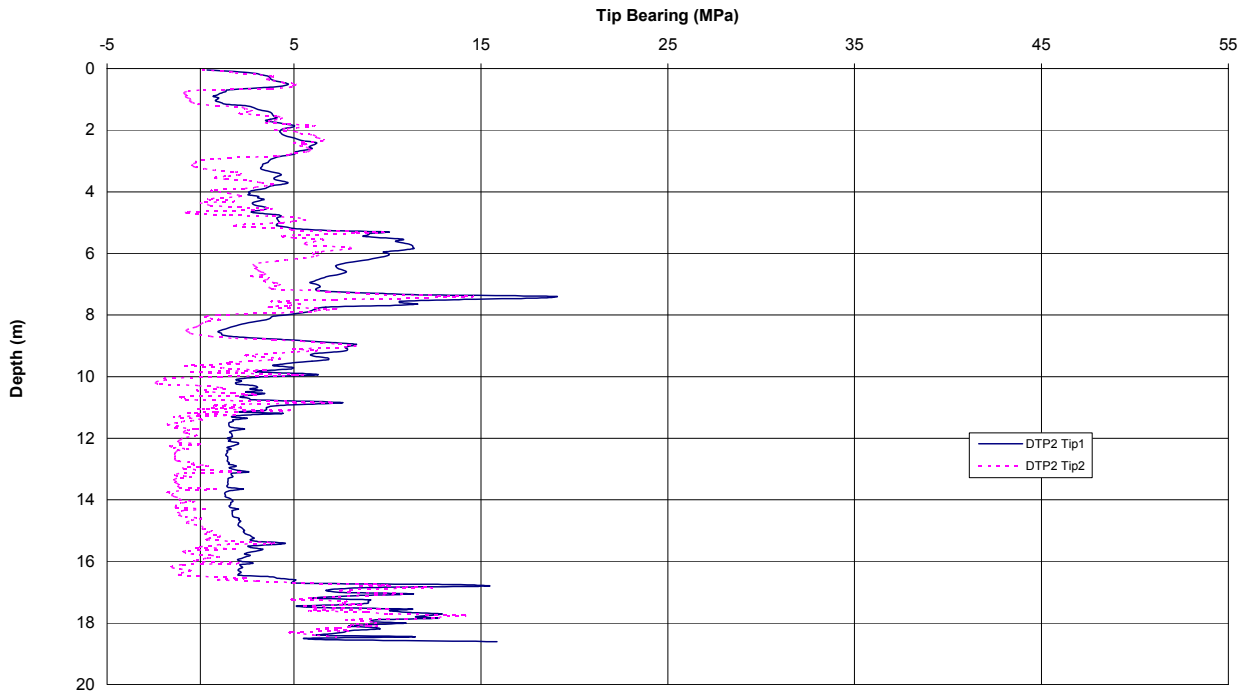


Figure A-49: University of Central Florida Site CPT #3 Tip 1 vs. Depth

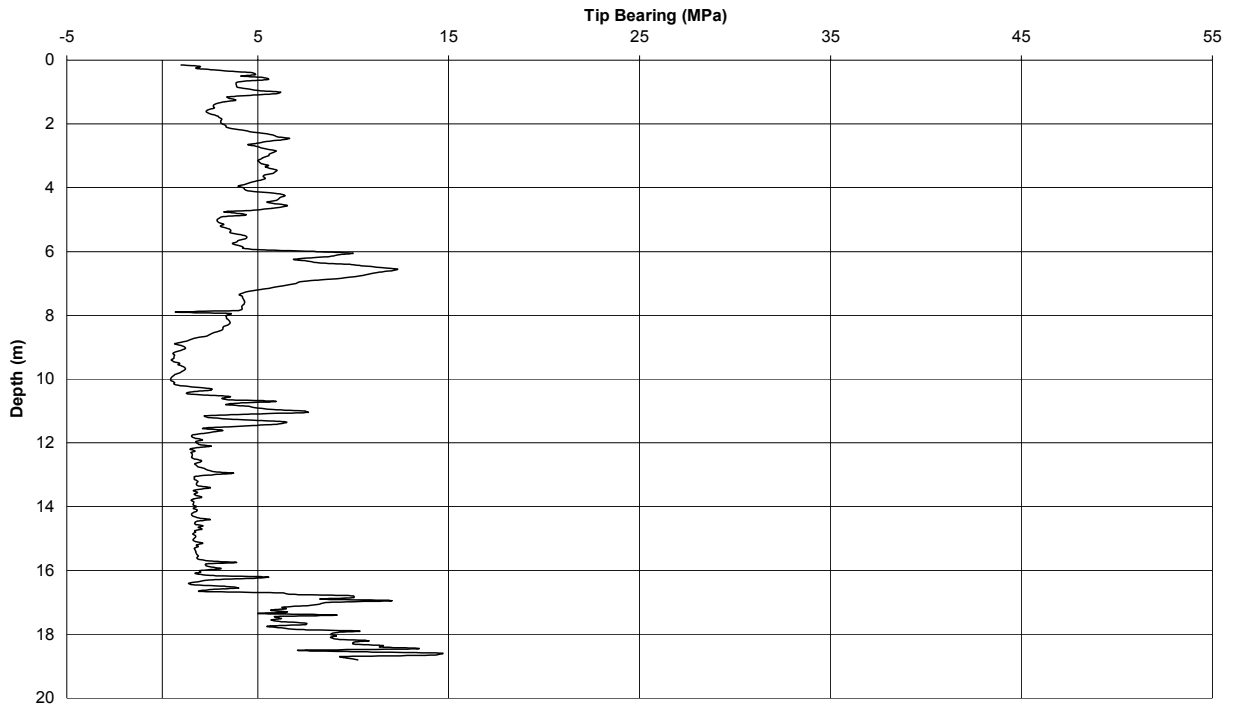


Figure A-50: University of Central Florida Site DTP #3 Tip Bearings vs. Depth

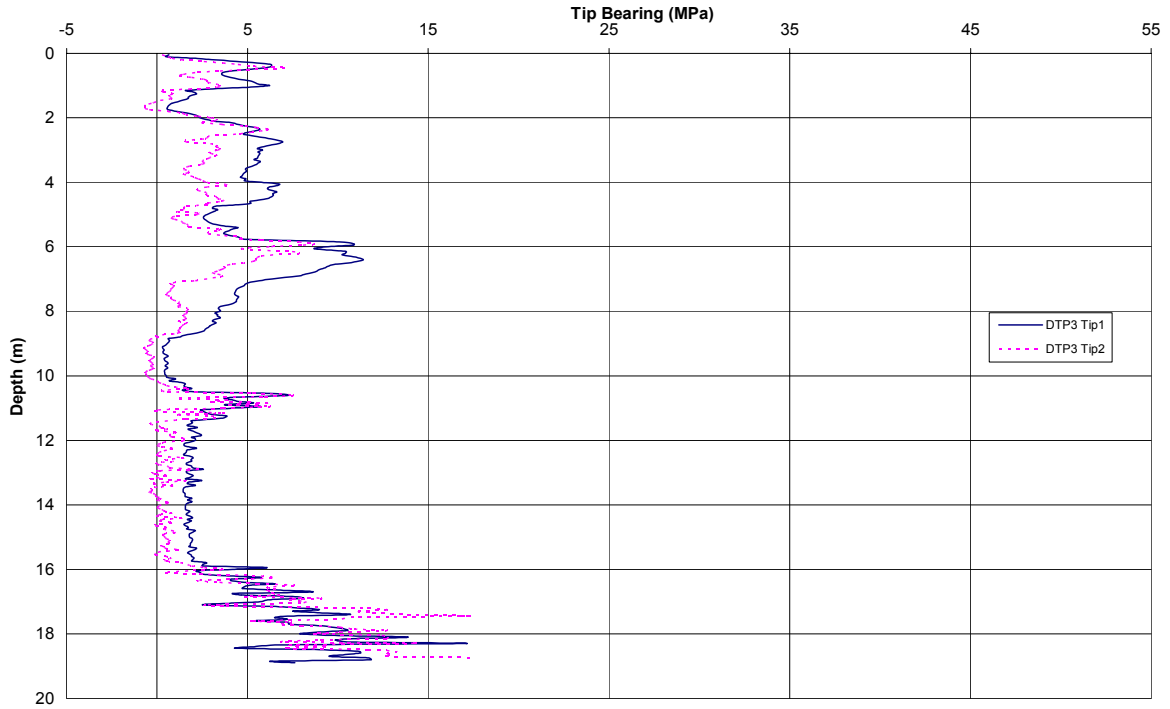




Figure A-51: University of Central Florida CPT #4 Tip bearing vs. Depth

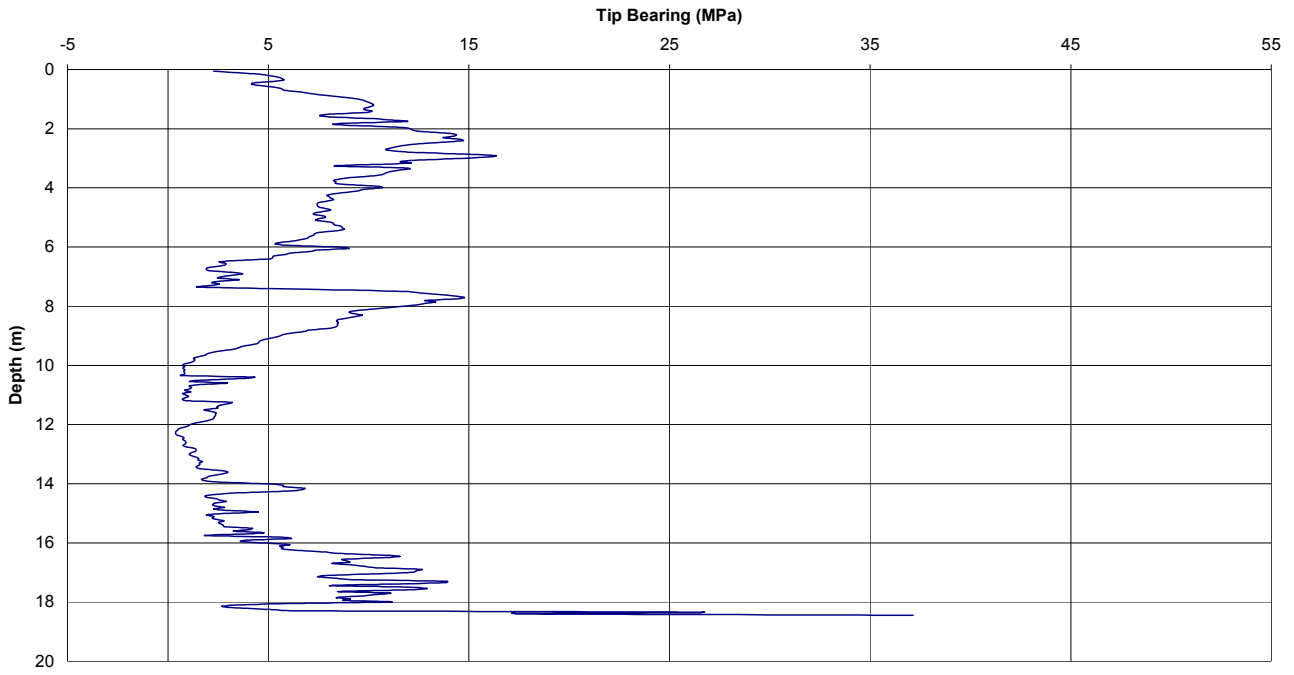


Figure A-52: University of Central Florida DTP #4 Tip Bearings vs. Depth

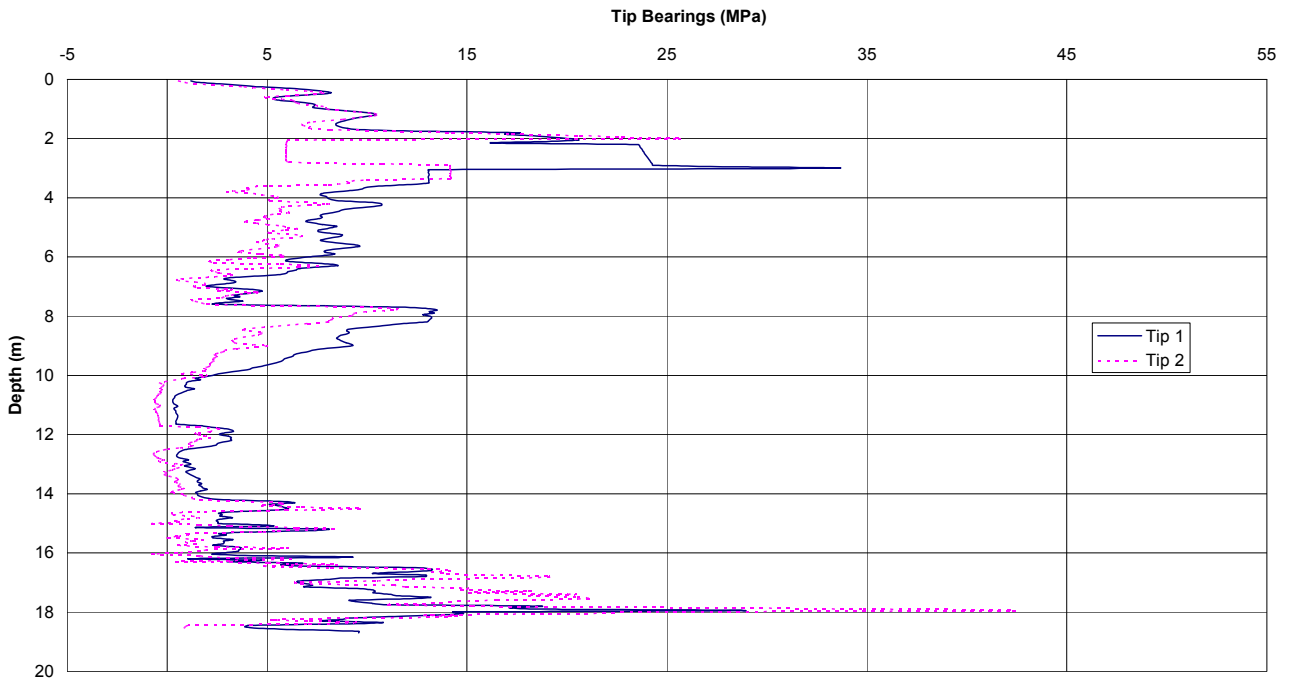


Figure A-53: University of Central Florida Site CPT #1/DTP #1 Friction Ratio Comparisons

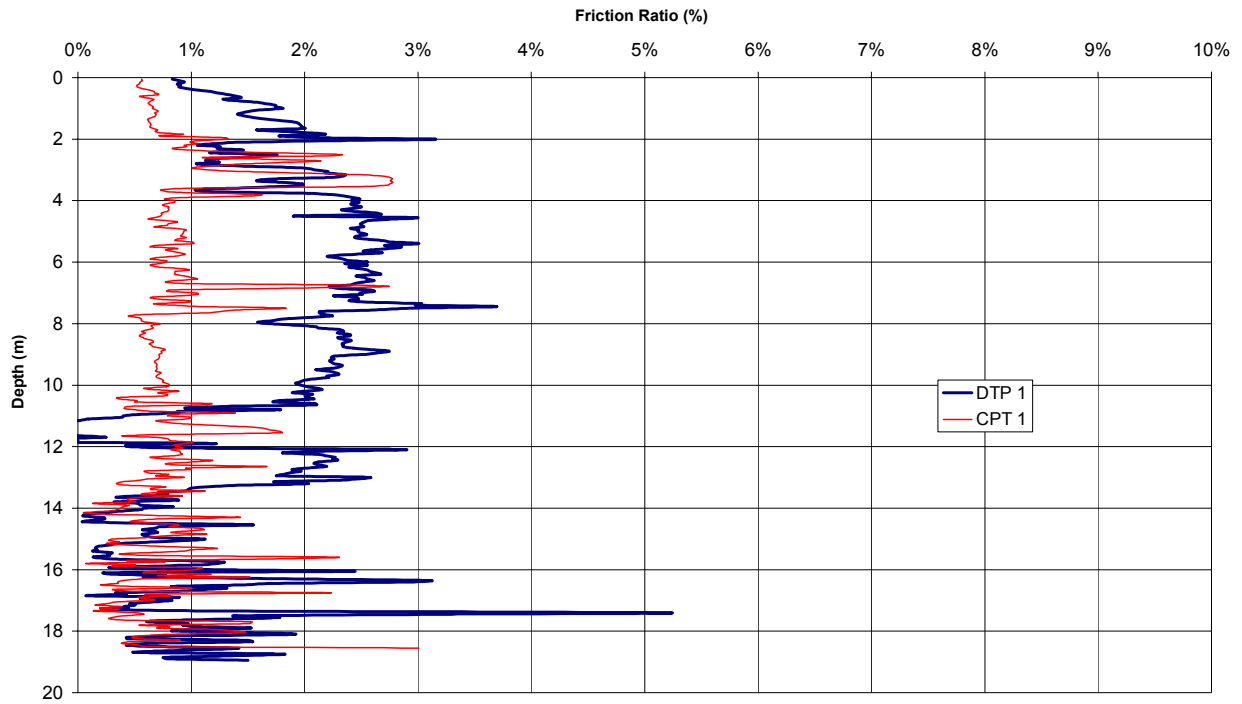


Figure A-54: University of Central Florida Site CPT #2/DTP #2 Friction Ratio Comparisons

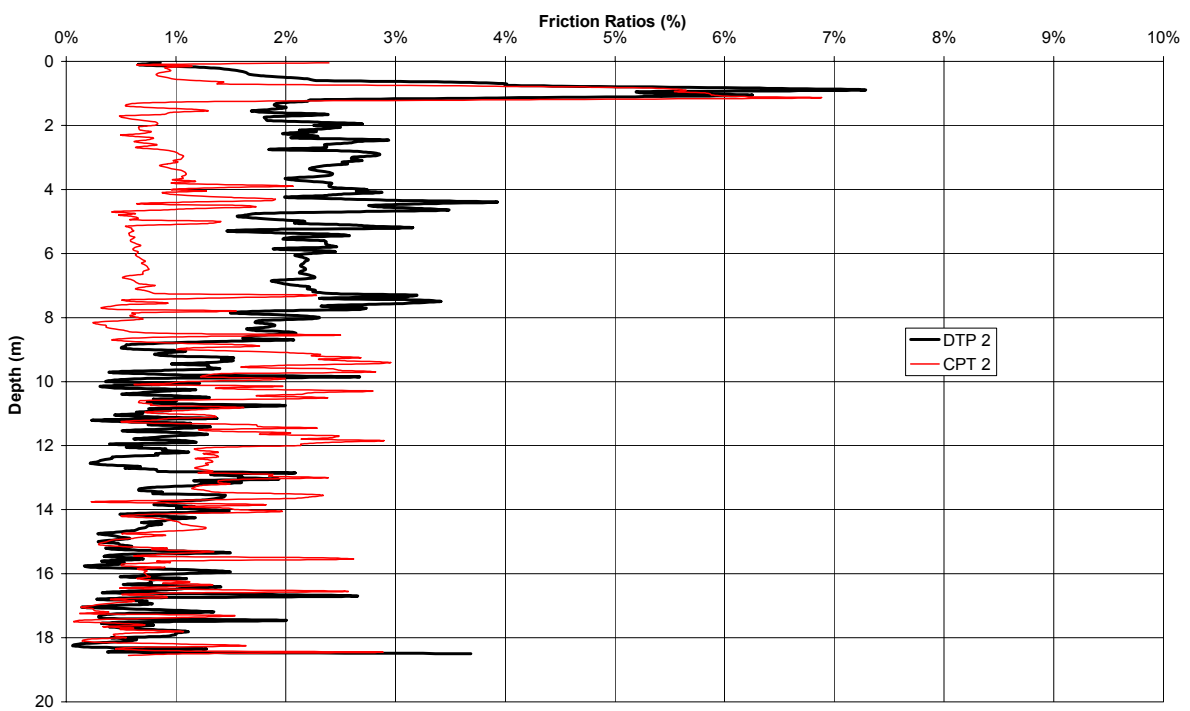


Figure A-55: University of Central Florida Site CPT #3/DTP #3 Friction Ratio Comparisons

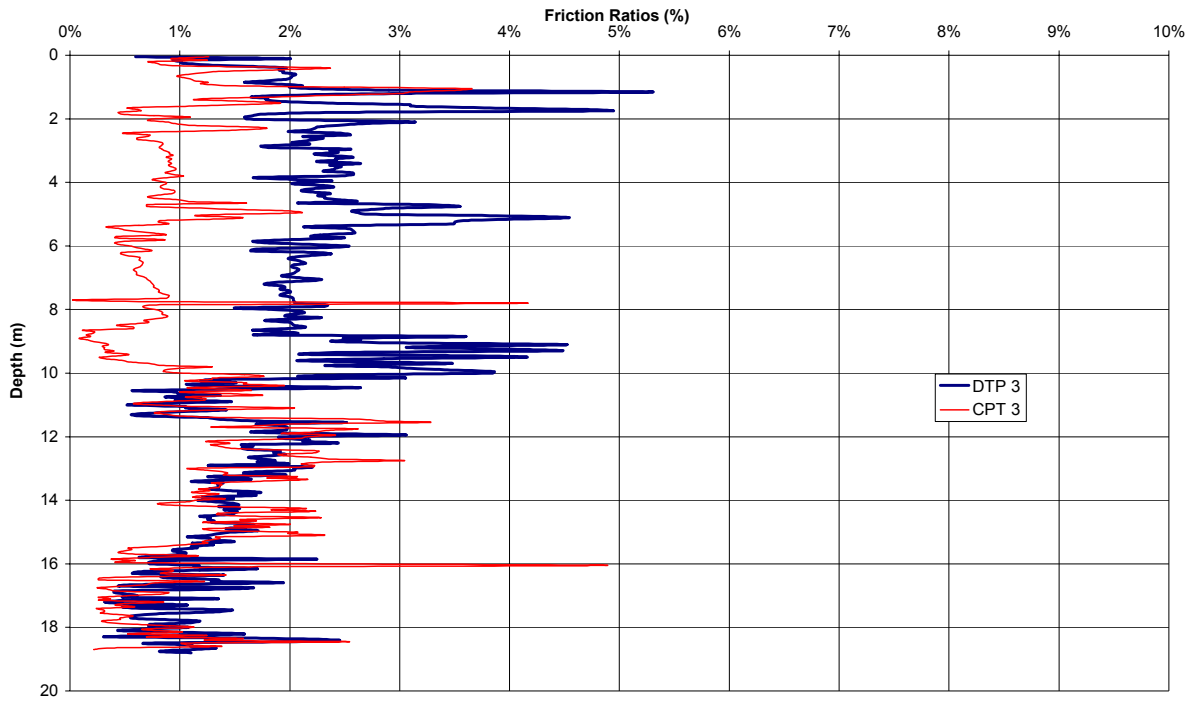


Figure A-56: University of Central Florida Site CPT #4/DTP #4 Friction Ratios vs. Depth

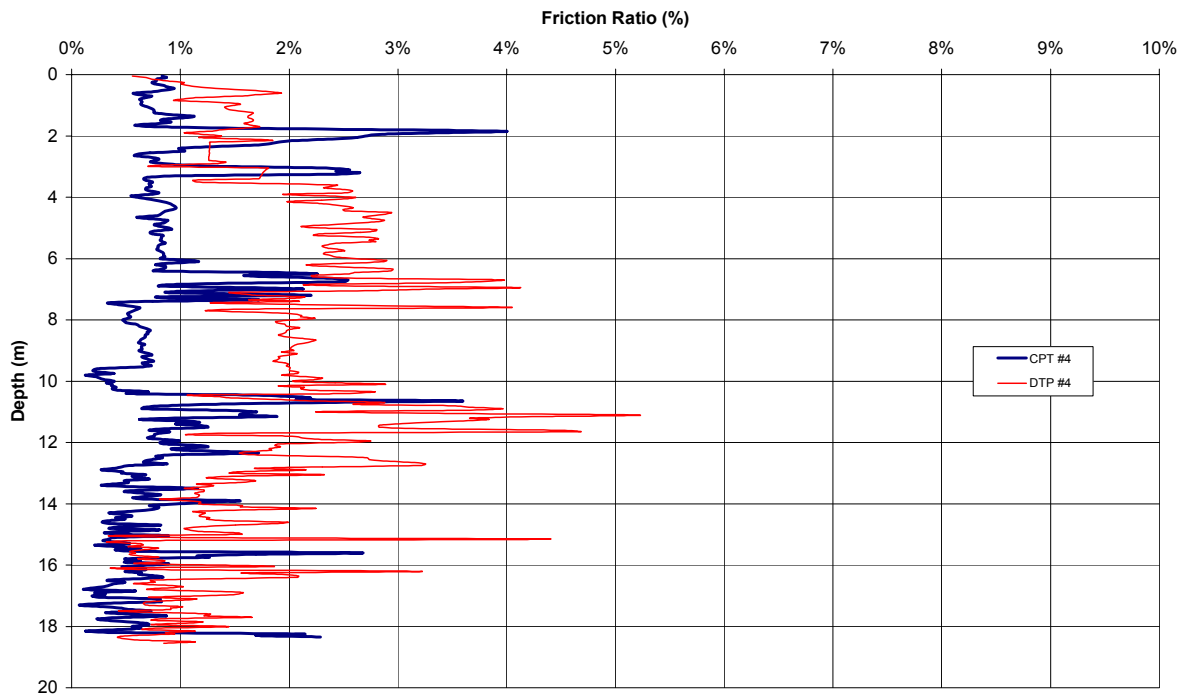


Figure A-57: University of Central Florida Site DTP #1 Tip Ratio vs. Depth

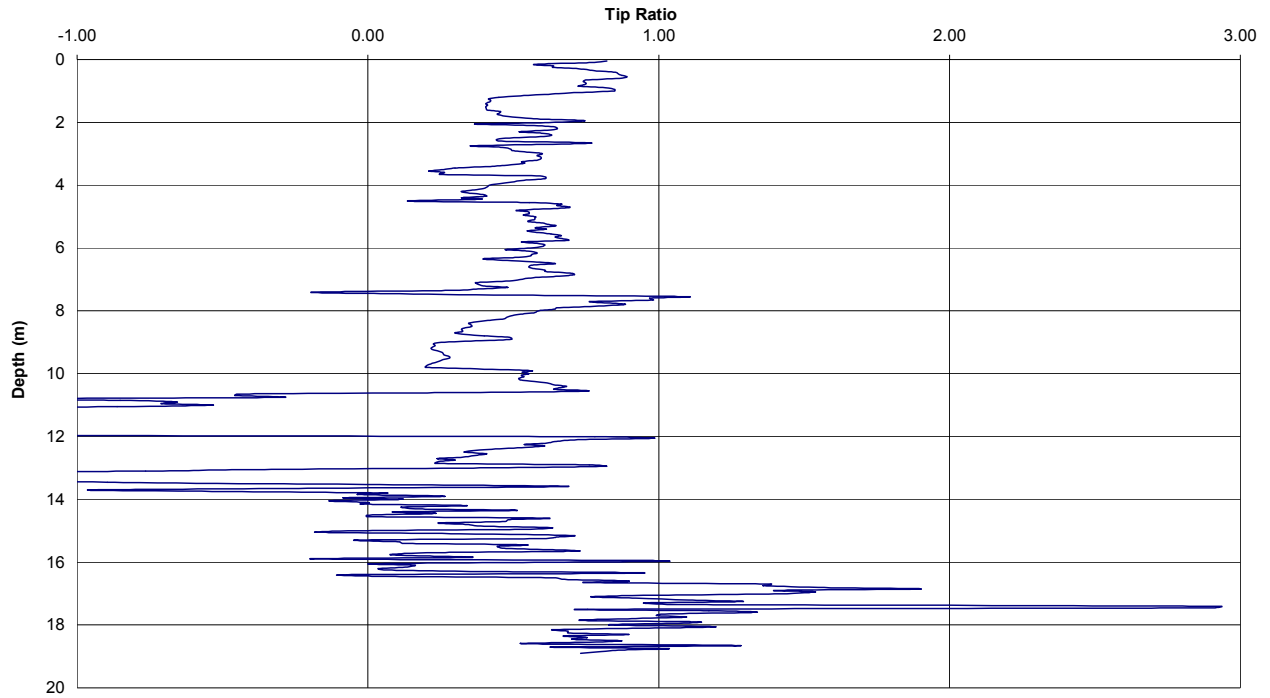


Figure A-58: University of Central Florida Site DTP #2 Tip Ratio vs. Depth

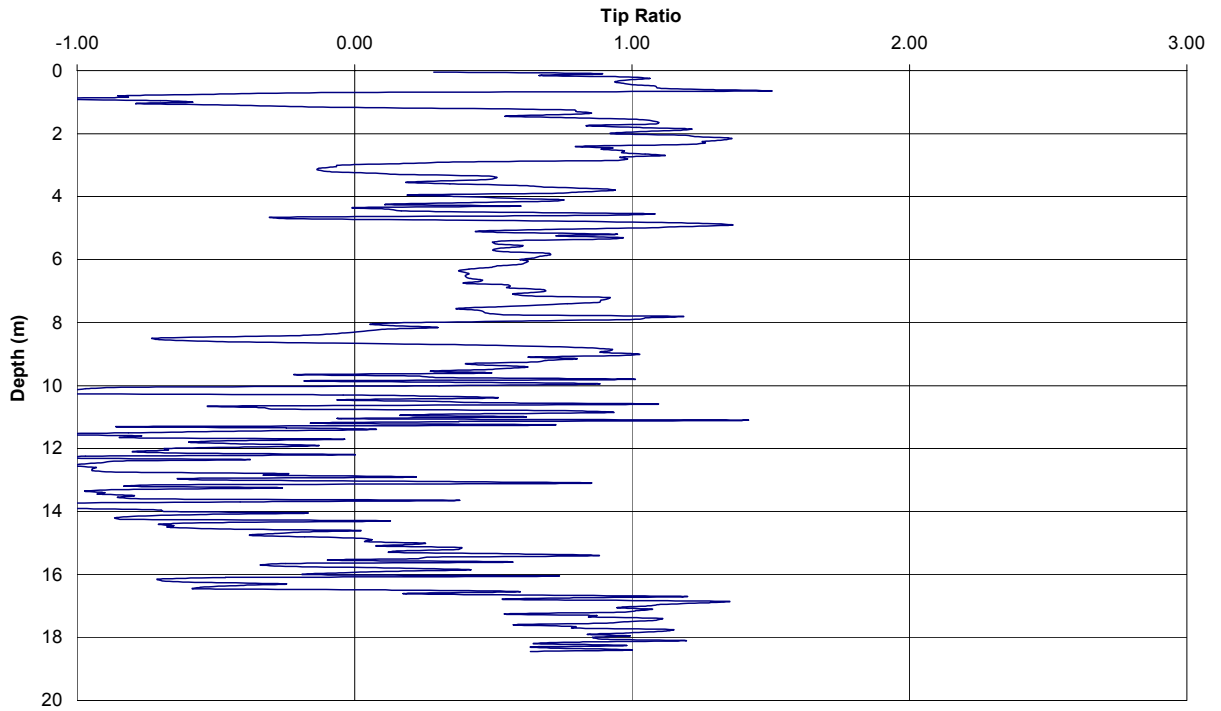


Figure A-59: University of Central Florida Site DTP #3 Tip Ratio vs. Depth

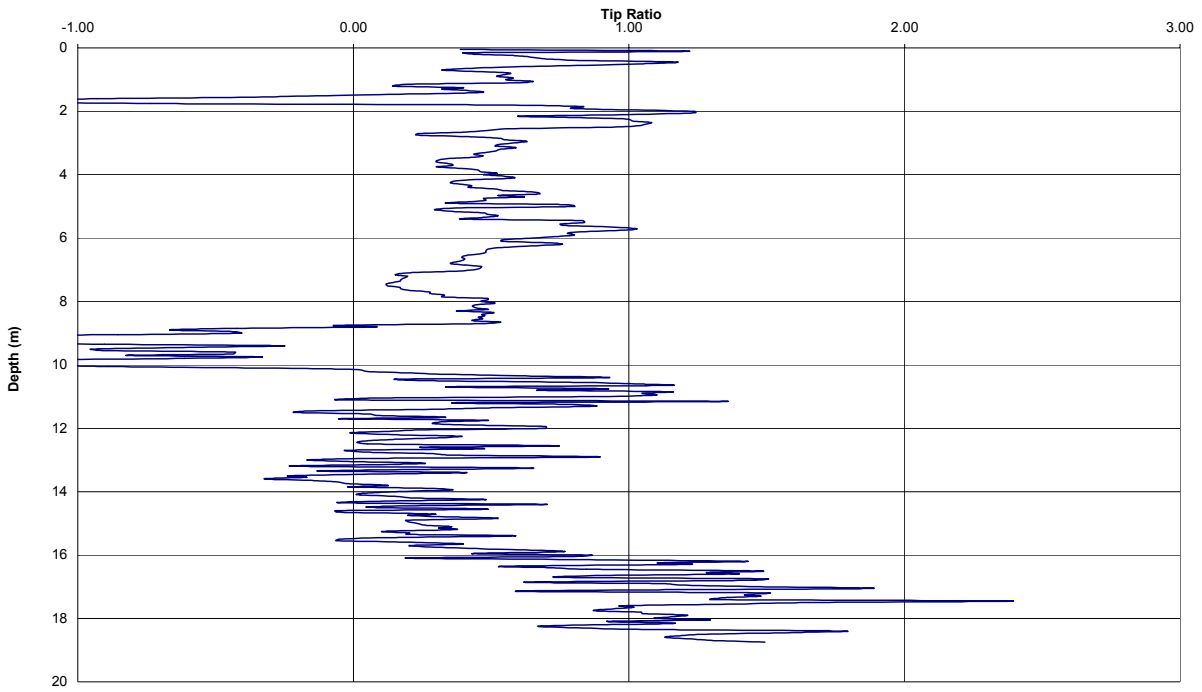


Figure A-60: University of Central Florida Site DTP #4 Tip Ratio vs. Depth

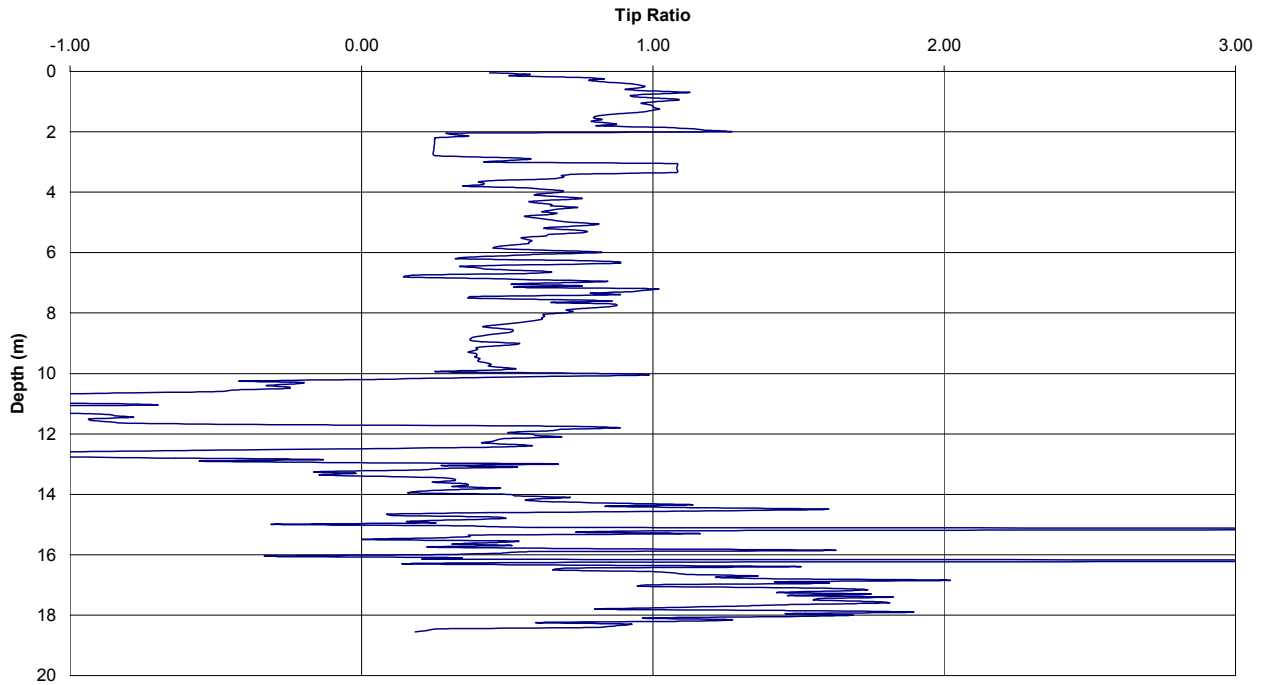


Figure A-61: West Bay Bridge CPT #1/DTP #1 Tip 1 Bearings vs. Depth  
(note: Tip 2 bearings for DTP #1 and DTP #2 were discarded due to errors)

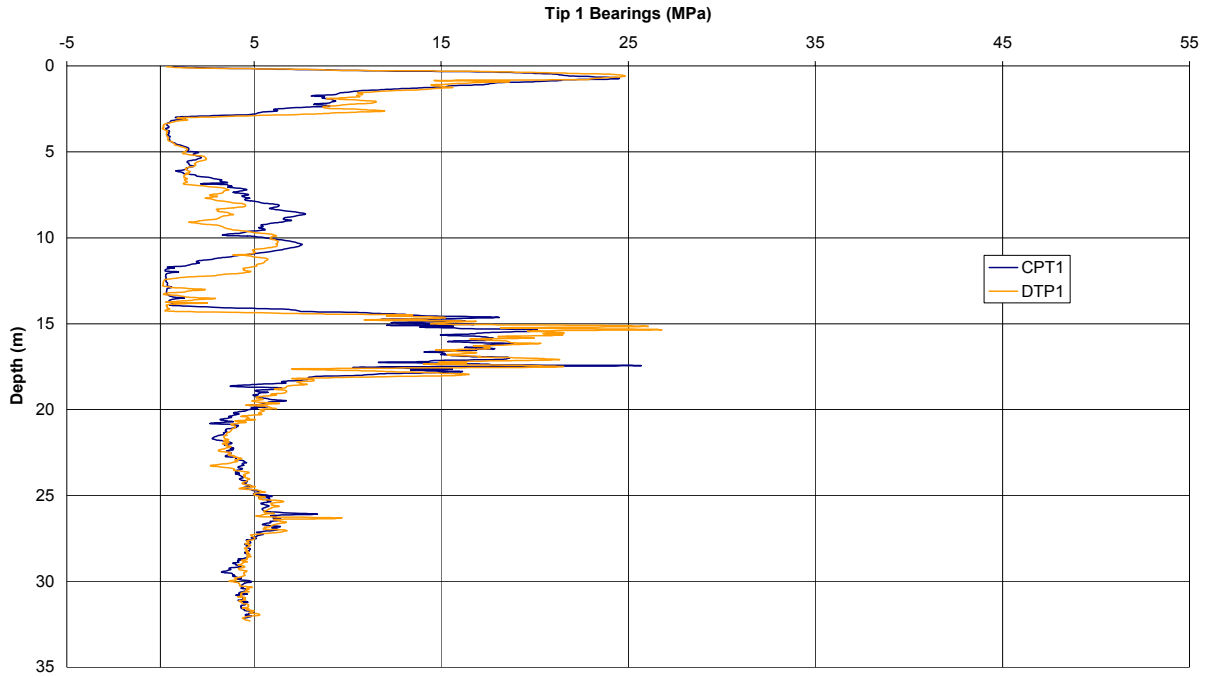
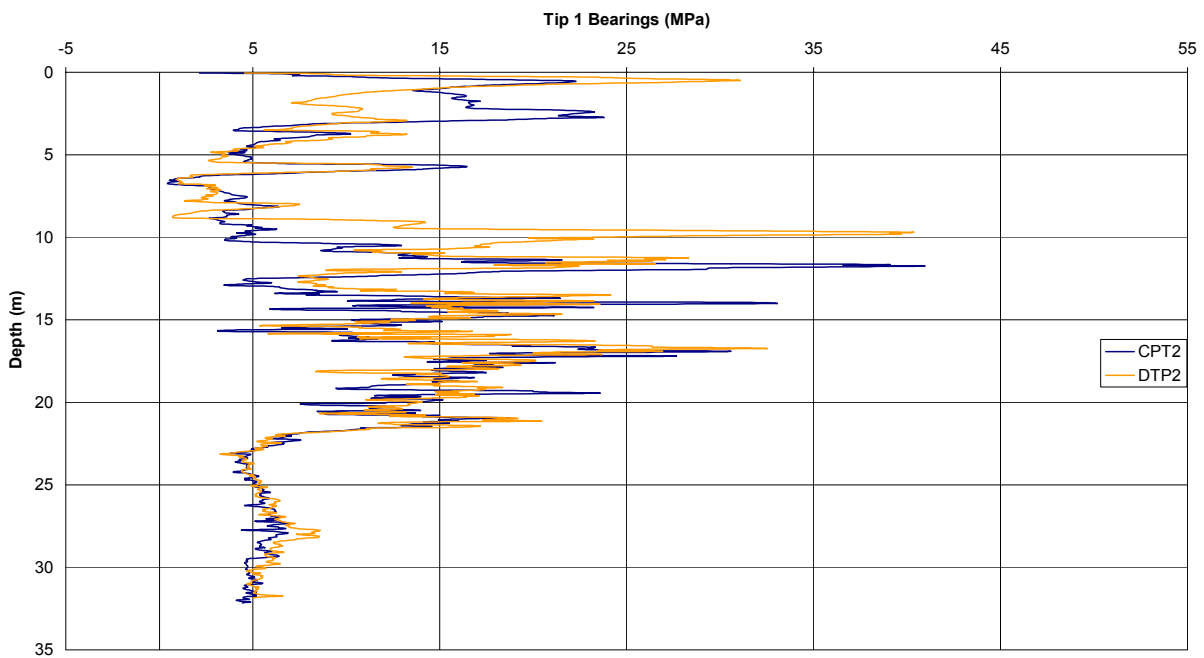


Figure A-62: West Bay Bridge CPT #2/DTP #2 Tip 1 Bearings vs. Depth  
(note: Tip 2 bearings for DTP #1 and DTP #2 were discarded due to errors)



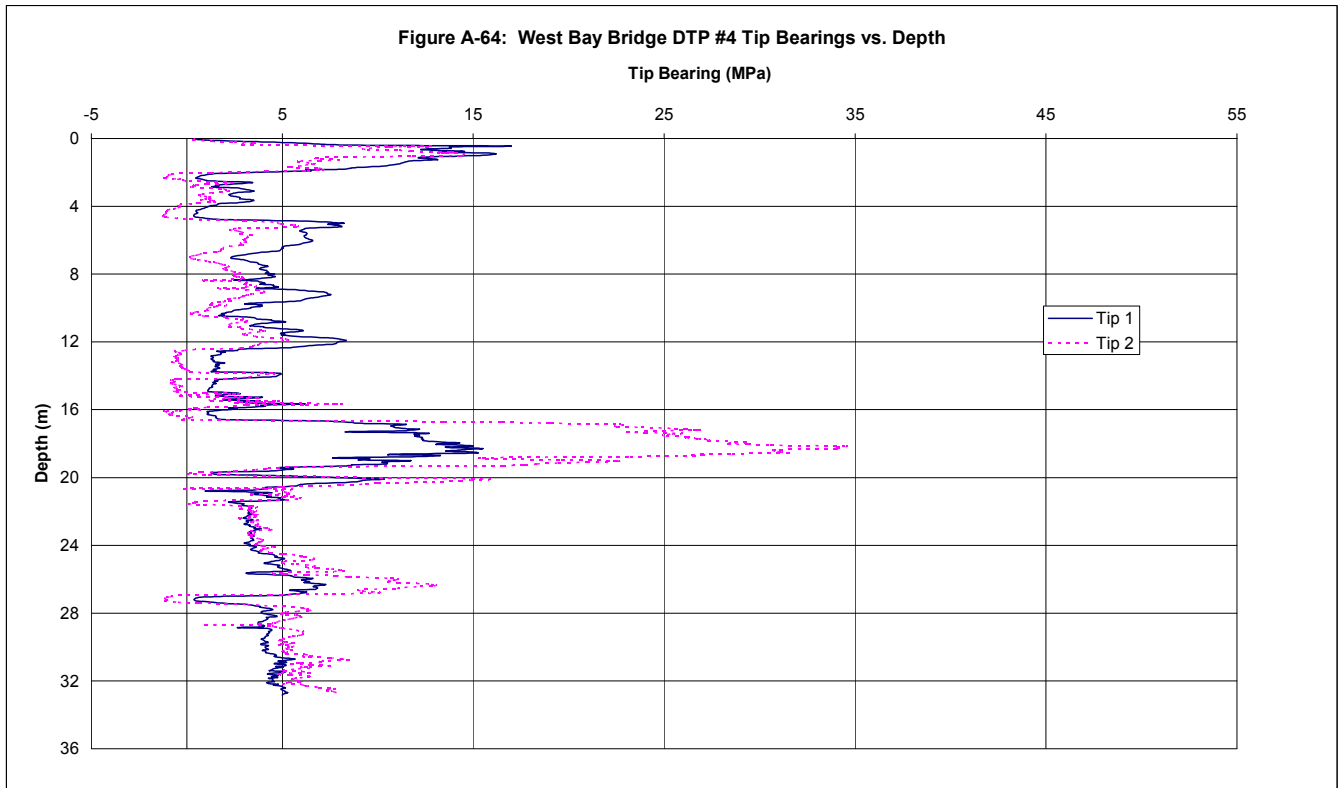
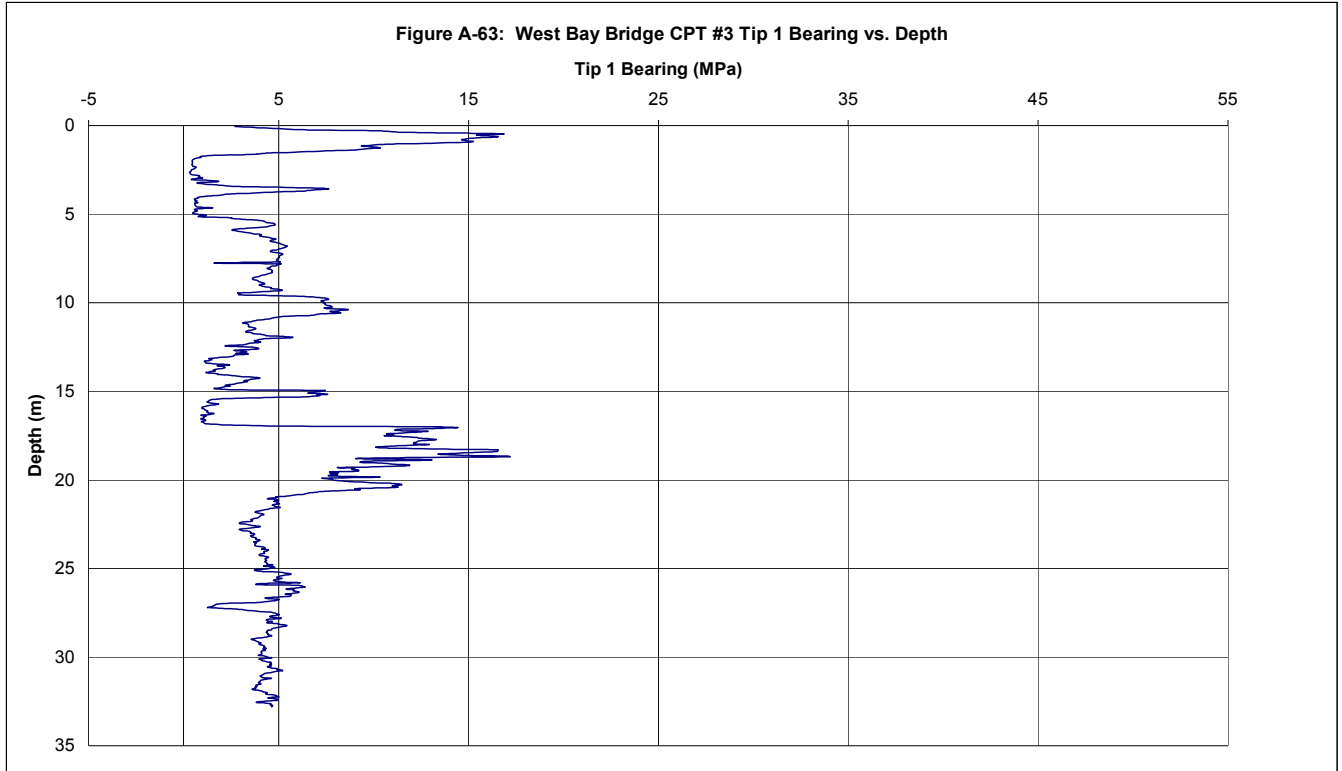


Figure A-65: West Bay Bridge DTP #5 Tip Bearings vs. Depth

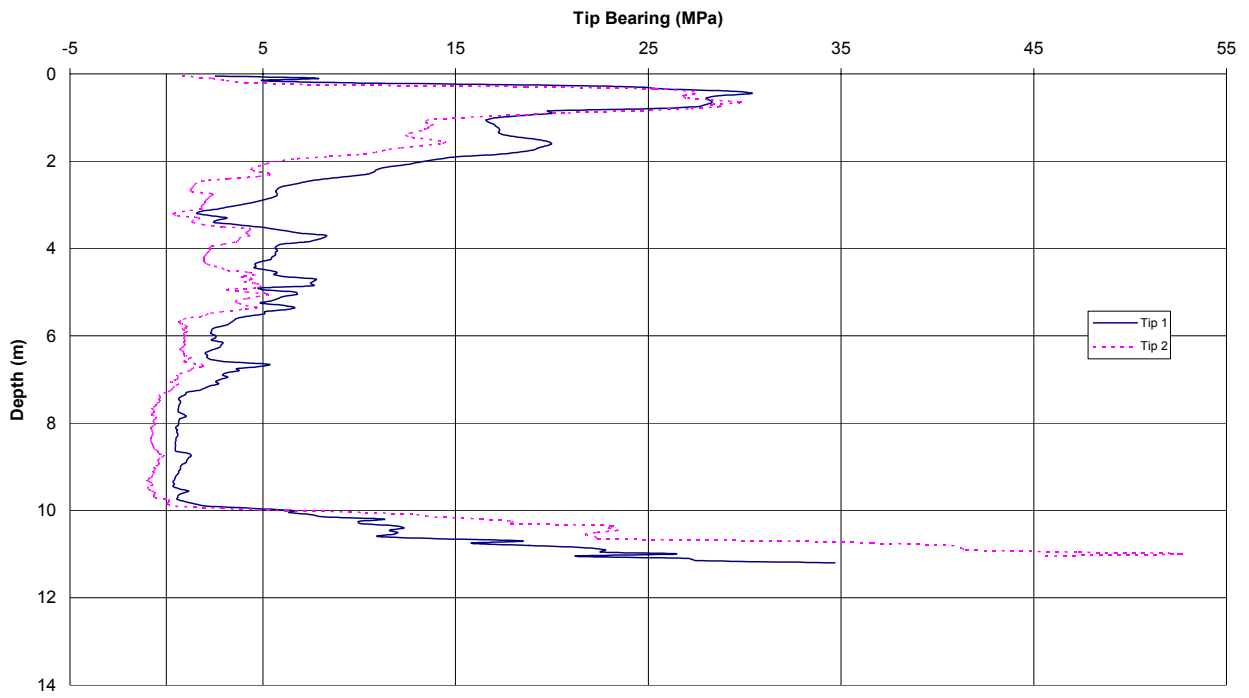


Figure A-66: West Bay Bridge CPT #1/DTP #1 Friction Ratios vs. Depth

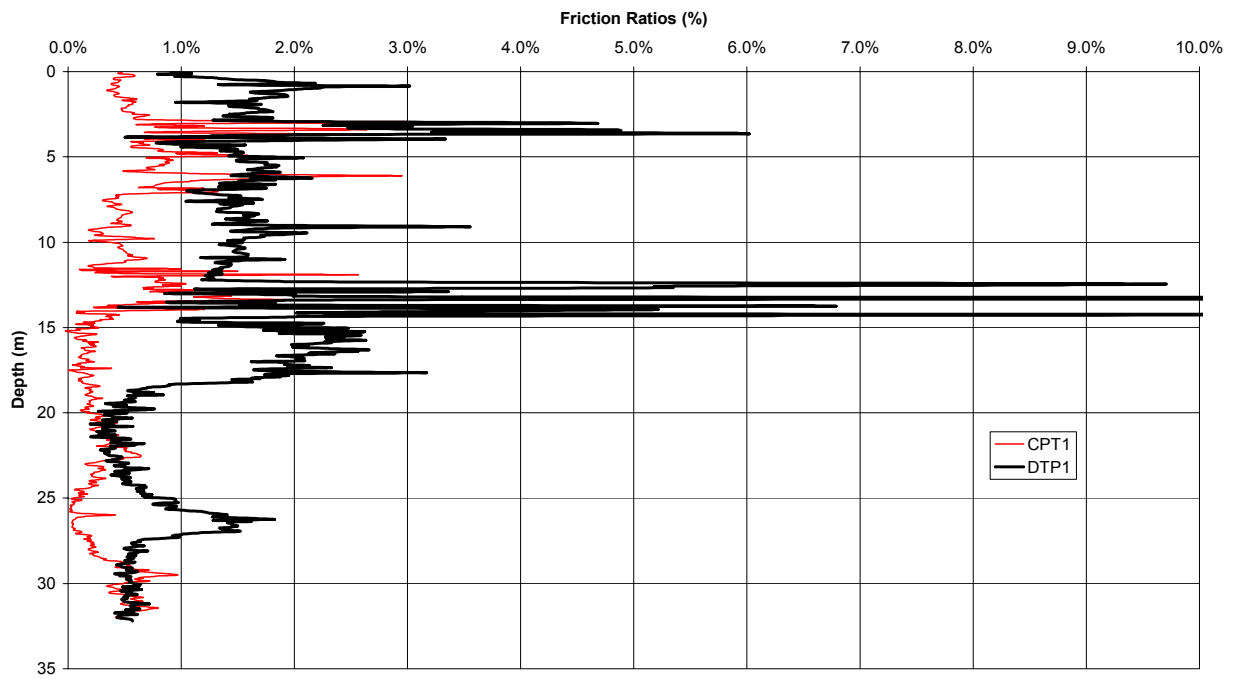




Figure A-67: West Bay Bridge CPT #2/DTP #2 Friction Ratios vs. Depth

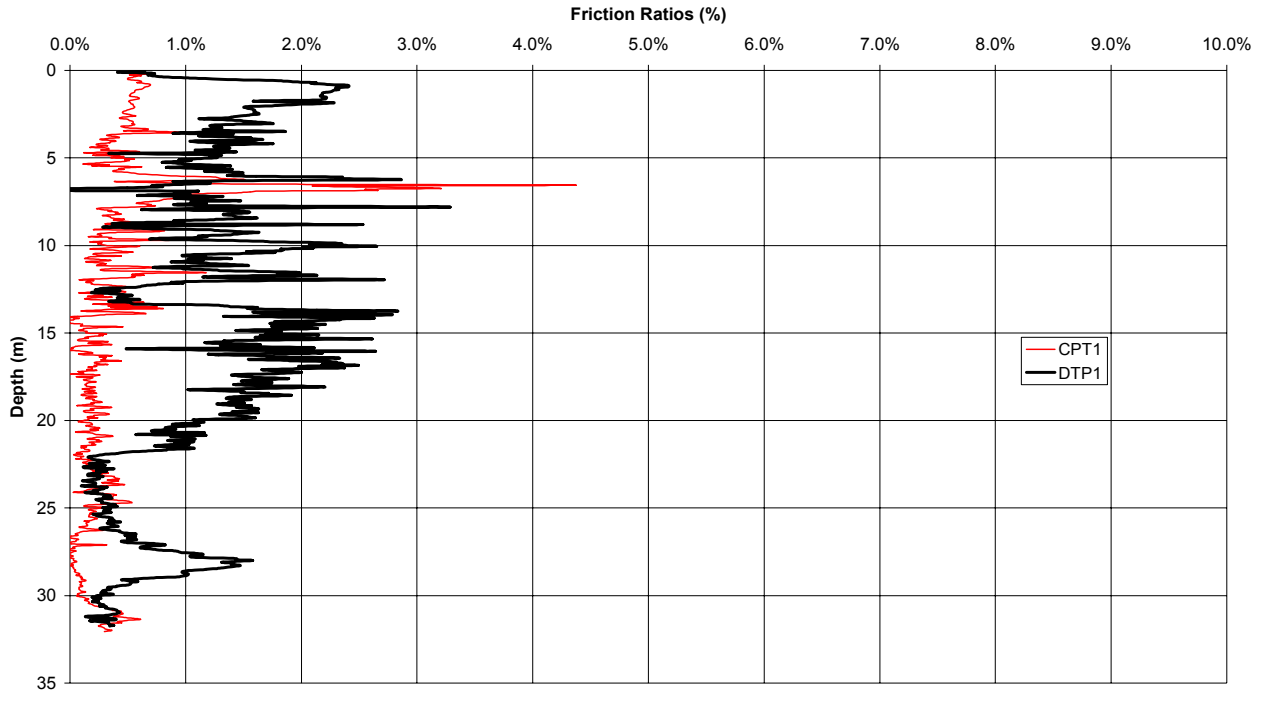


Figure A-68: West Bay Bridge CPT #3/DTP #4 Friction Ratios vs. Depth

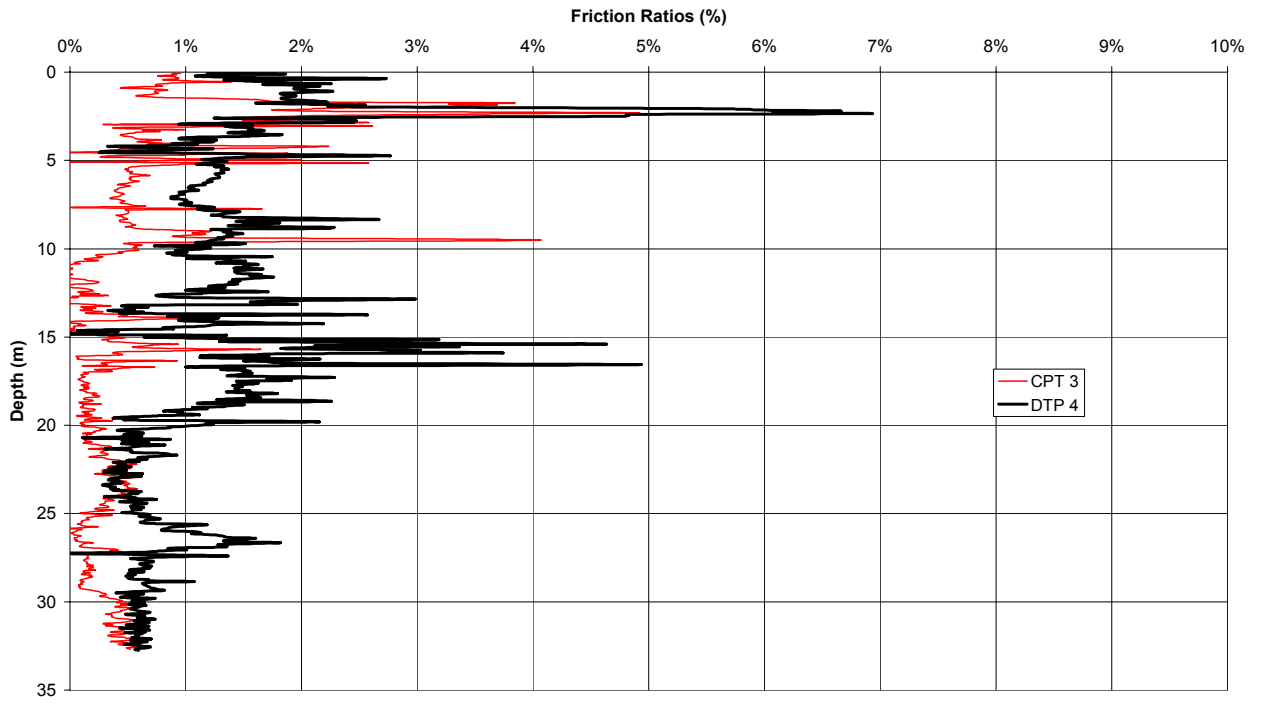


Figure A-69: West Bay Bridge DTP #4 Tip Ratio vs. Depth

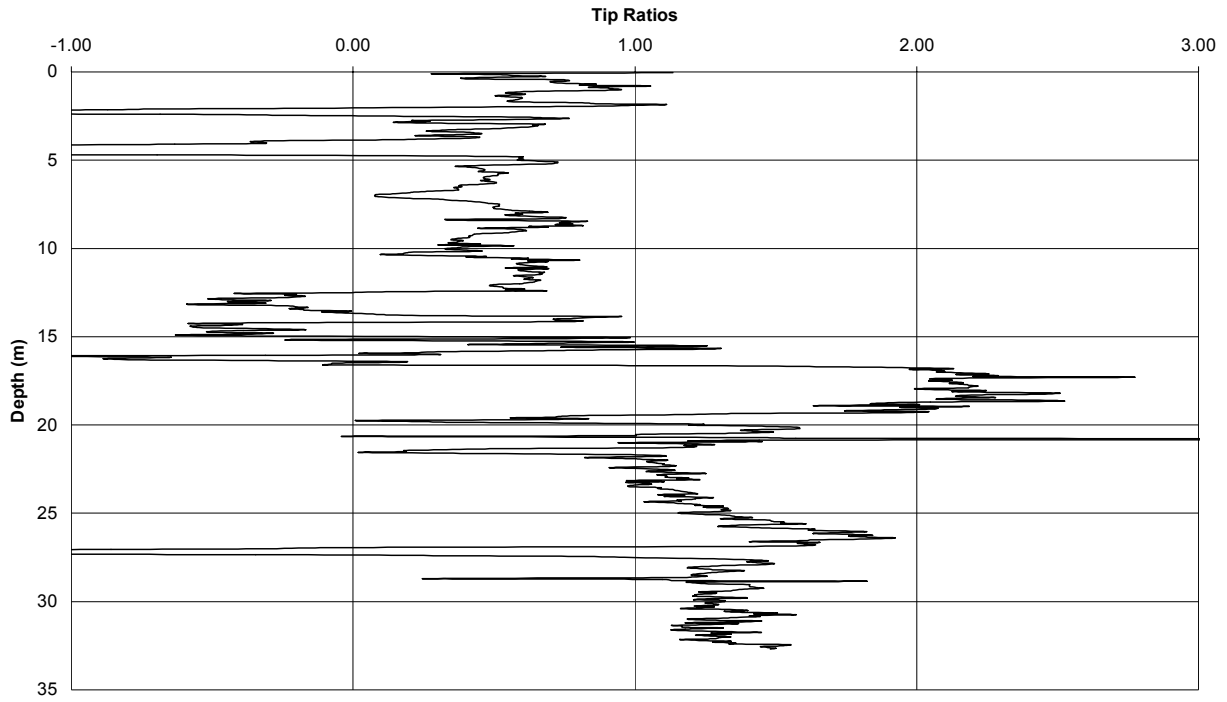


Figure A-70: West Bay Bridge DTP #5 Tip Ratio vs. Depth

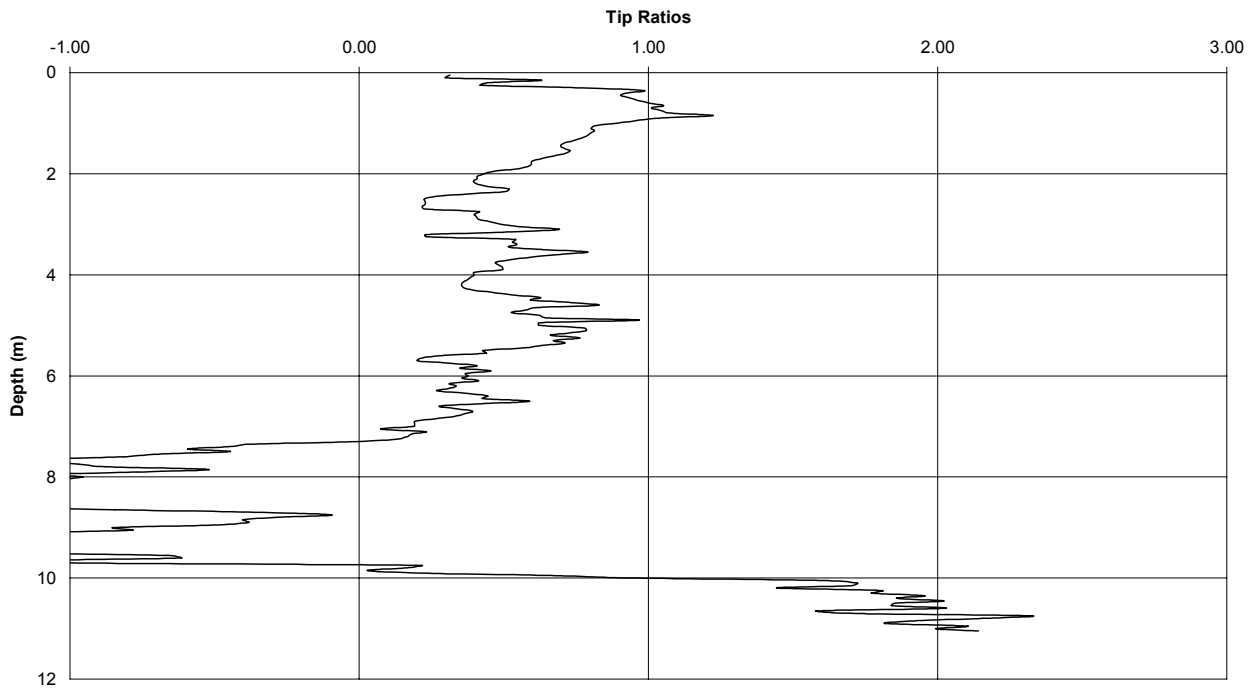


Figure A-71: Port Orange Bridge DTP 1 "CSC 830 TC" Tip Bearings vs. Depth

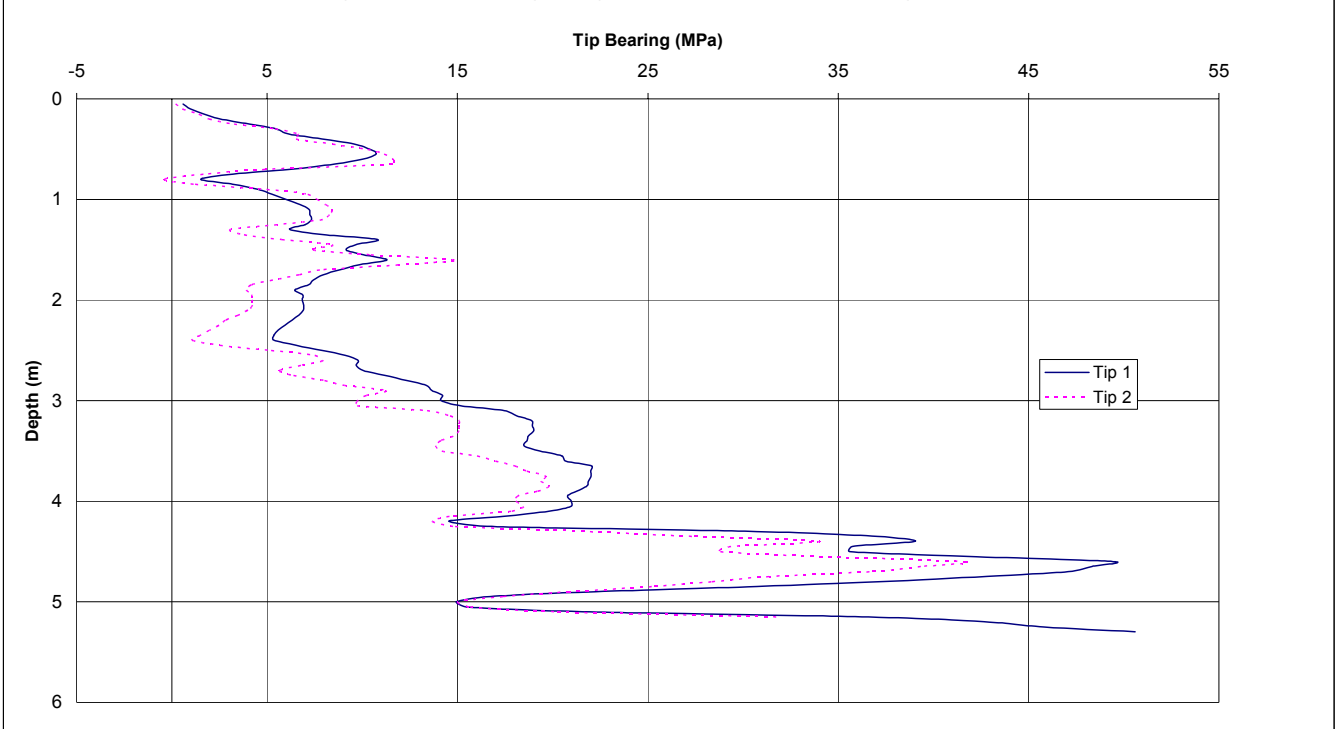


Figure A-72: Port Orange Bridge DTP 2 "CSC 830 TC" Tip Bearings vs. Depth

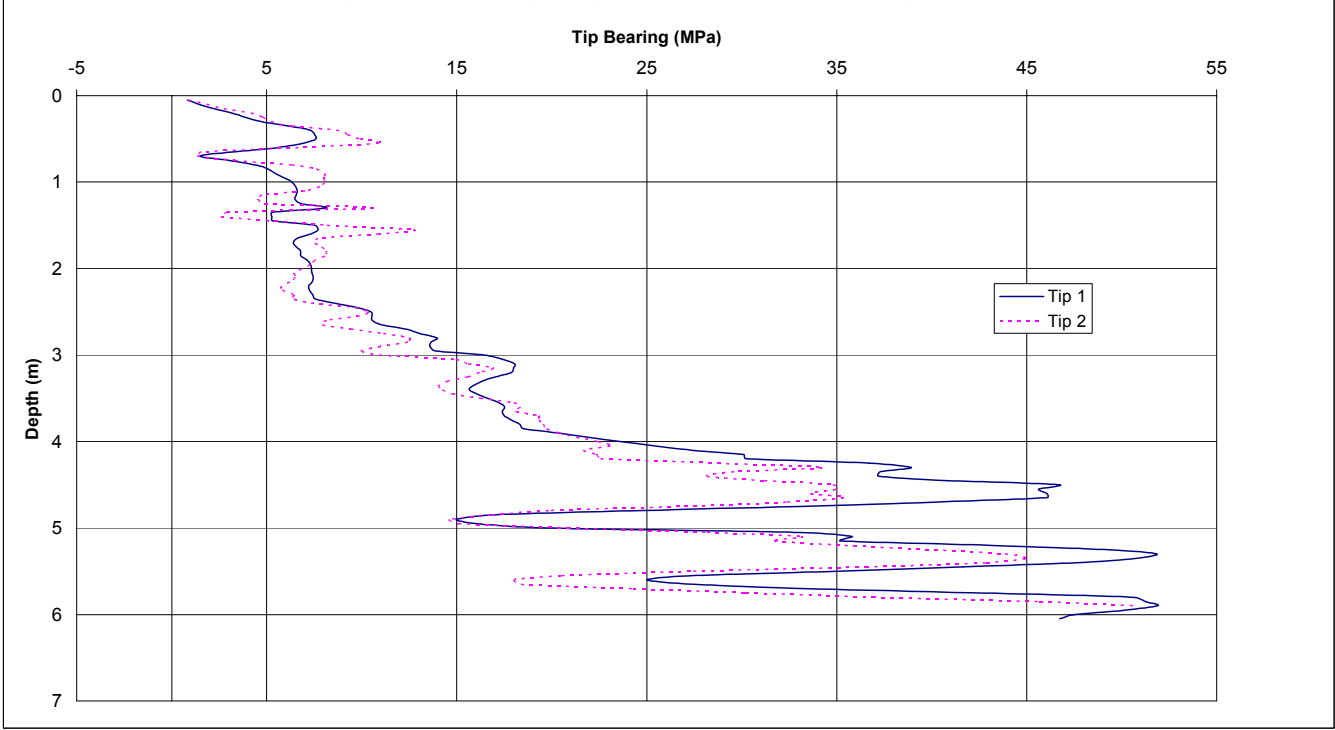


Figure A-73: Port Orange Bridge DTP 3 "CSC 829 TC" Tip Bearings vs. Depth

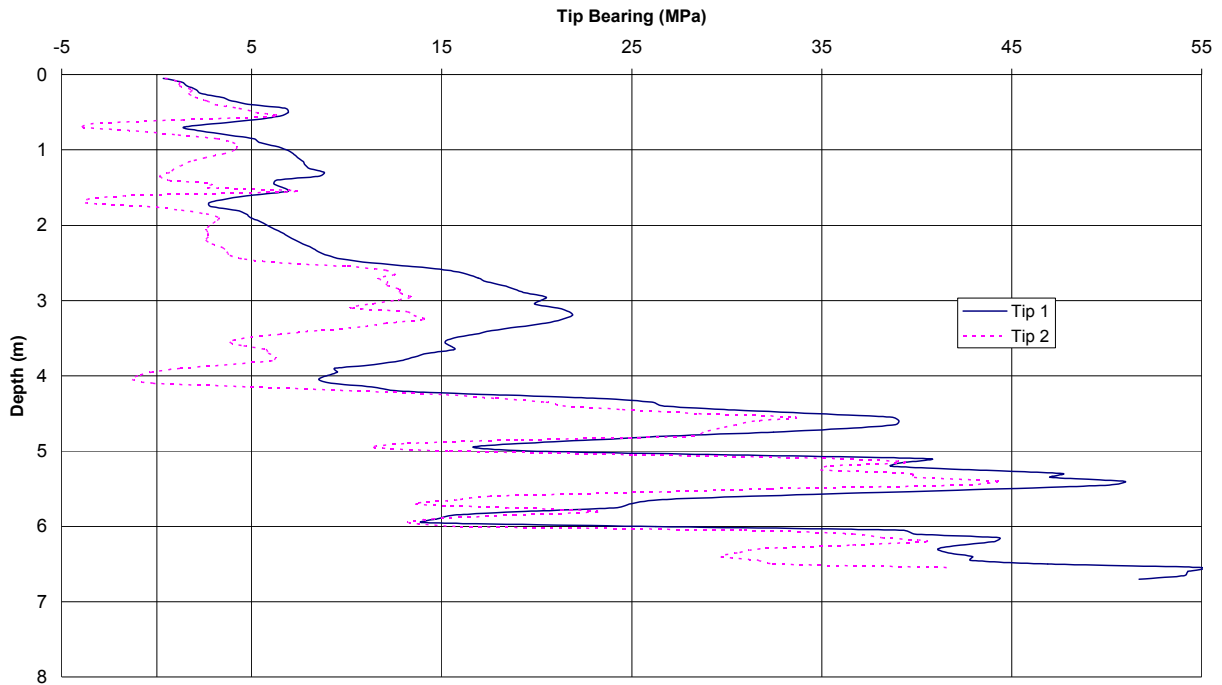


Figure A-74: Port Orange Bridge DTP 4 "CSC 829 TC" Tip Bearings vs. Depth

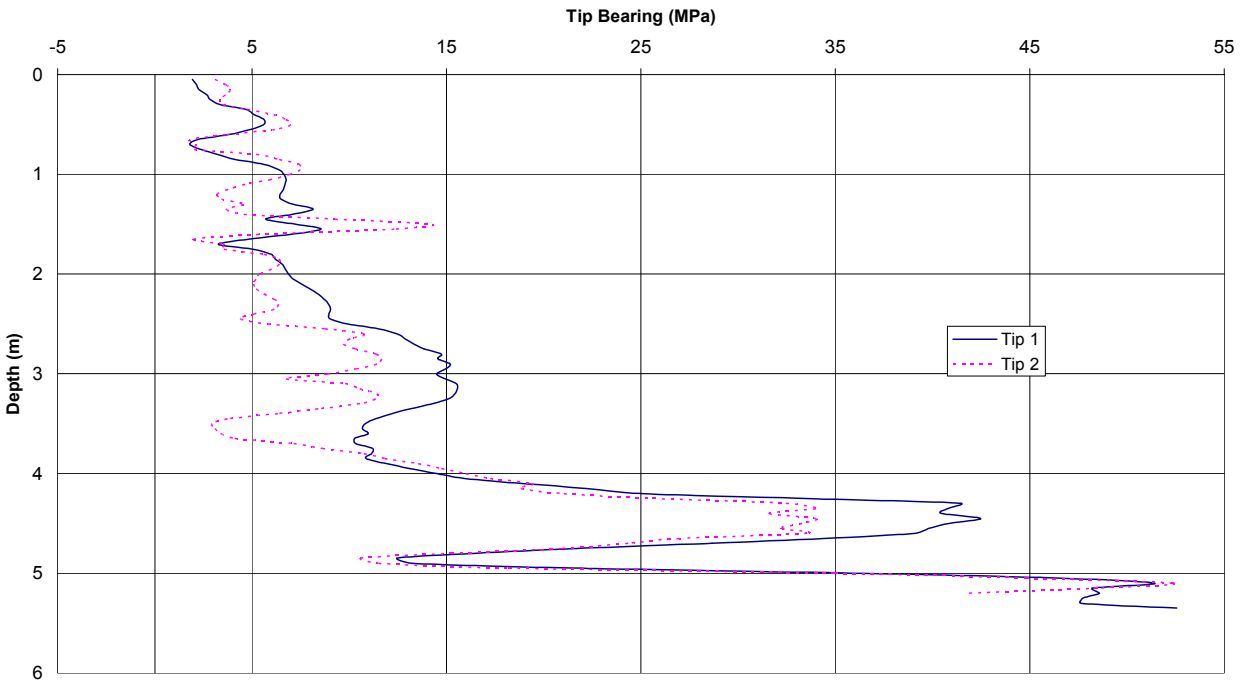


Figure A-75: Port Orange Bridge DTP 5 "CSC 782 TC" Tip Bearings vs. Depth

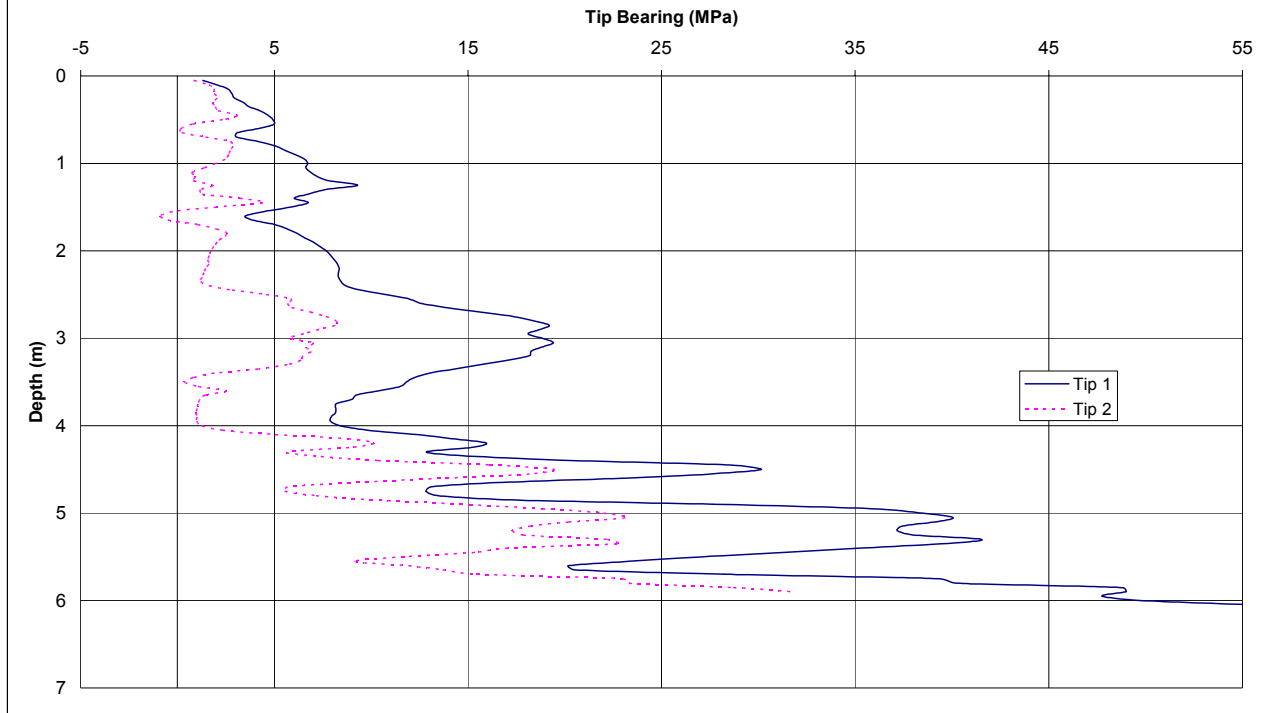


Figure A-76: Port Orange Bridge DTP 2 "CSC 782 TC" Tip Bearings vs. Depth

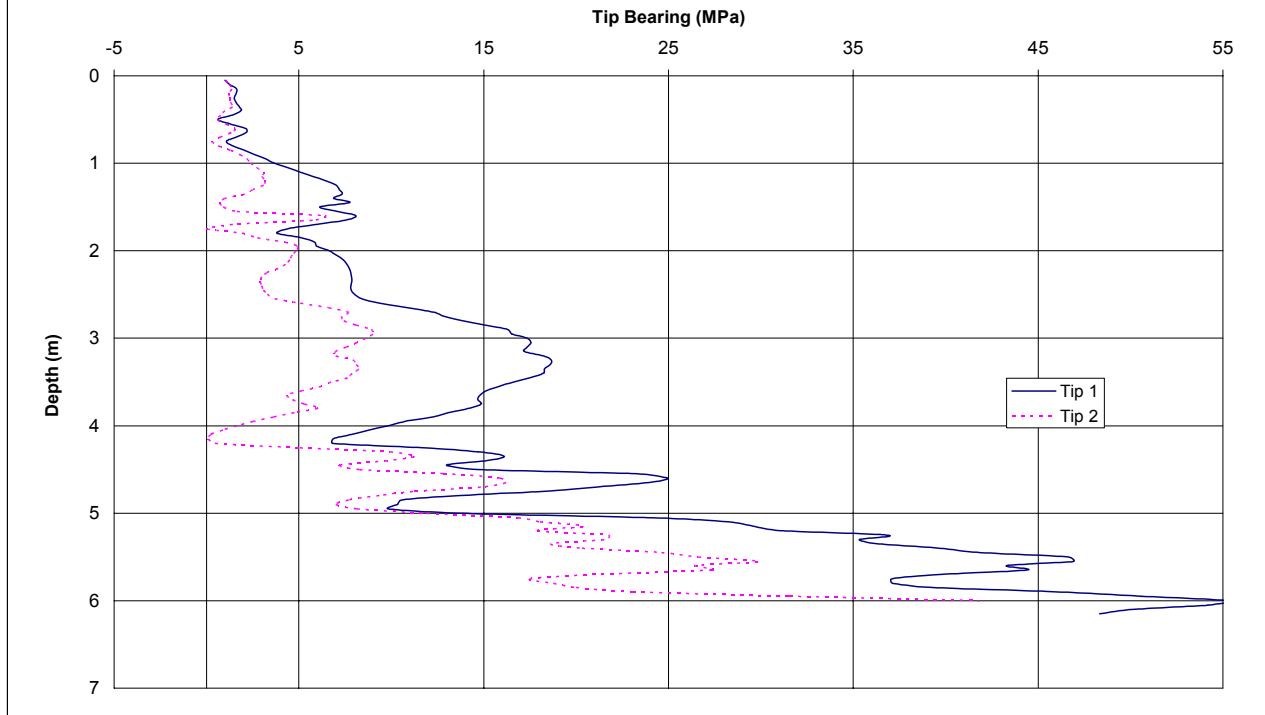


Figure A-77: Port Orange Bridge DTP 1 & 2 Friction Ratios vs. Depth

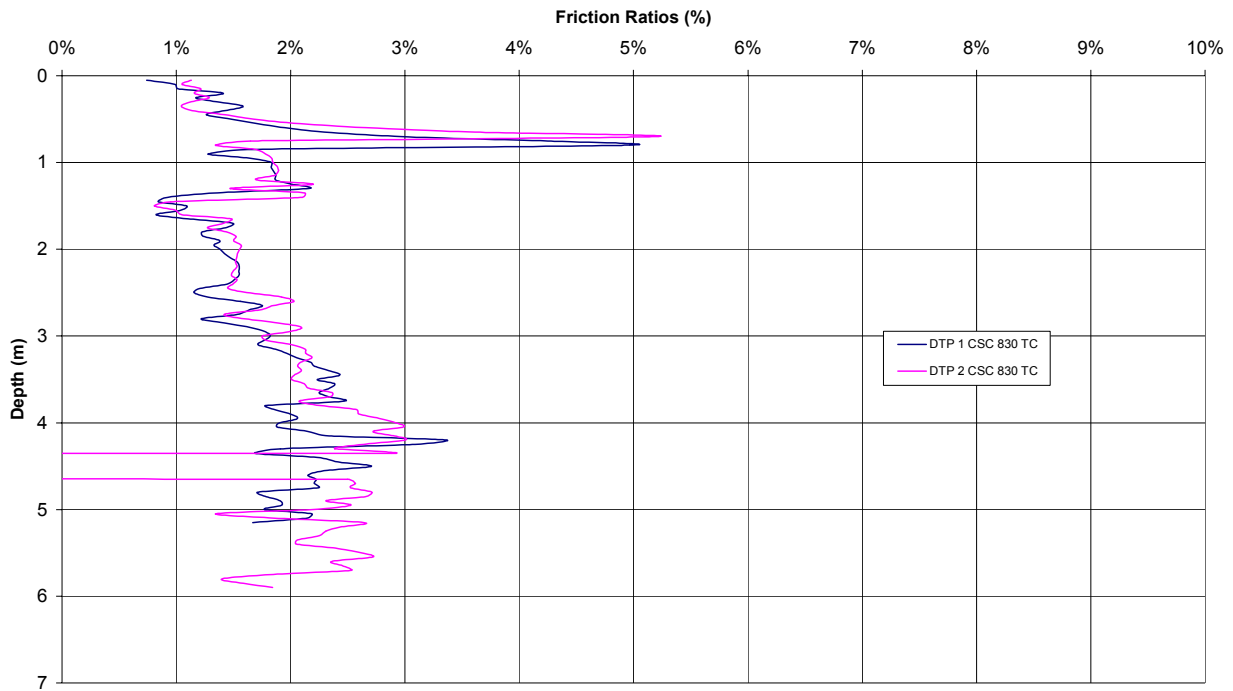


Figure A-78: Port Orange Bridge DTP 3 & 4 Friction Ratios vs. Depth

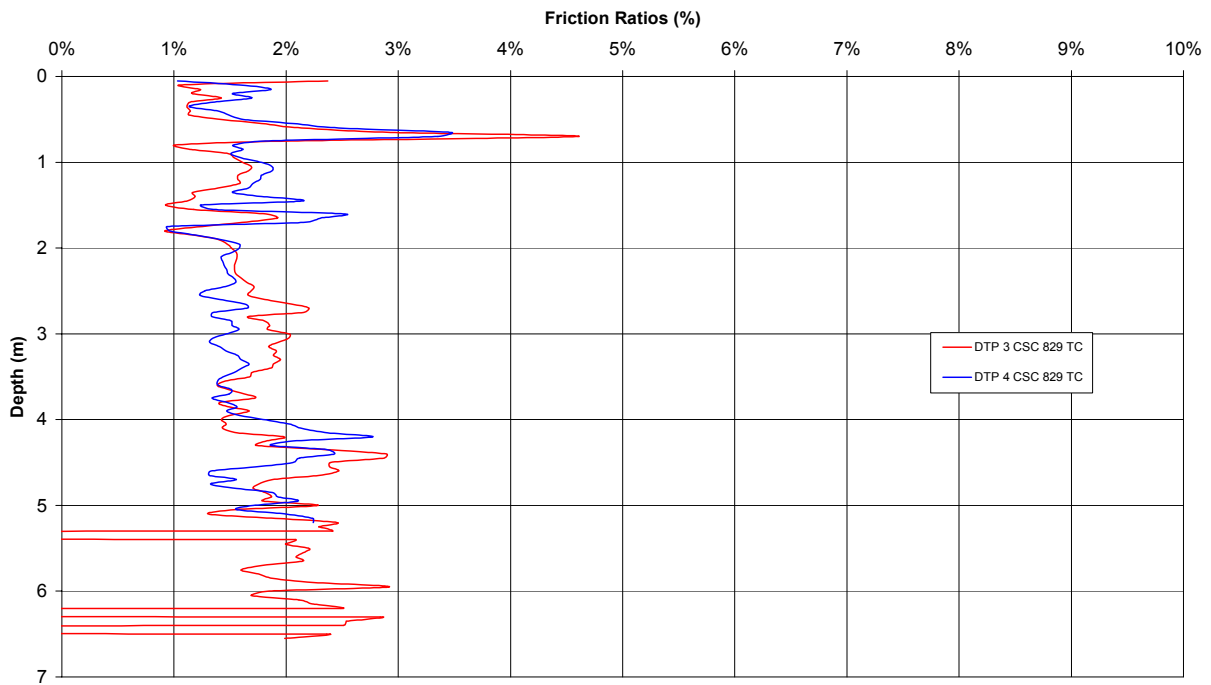


Figure A-79: Port Orange Bridge DTP 5 & 6 Friction Ratios vs. Depth

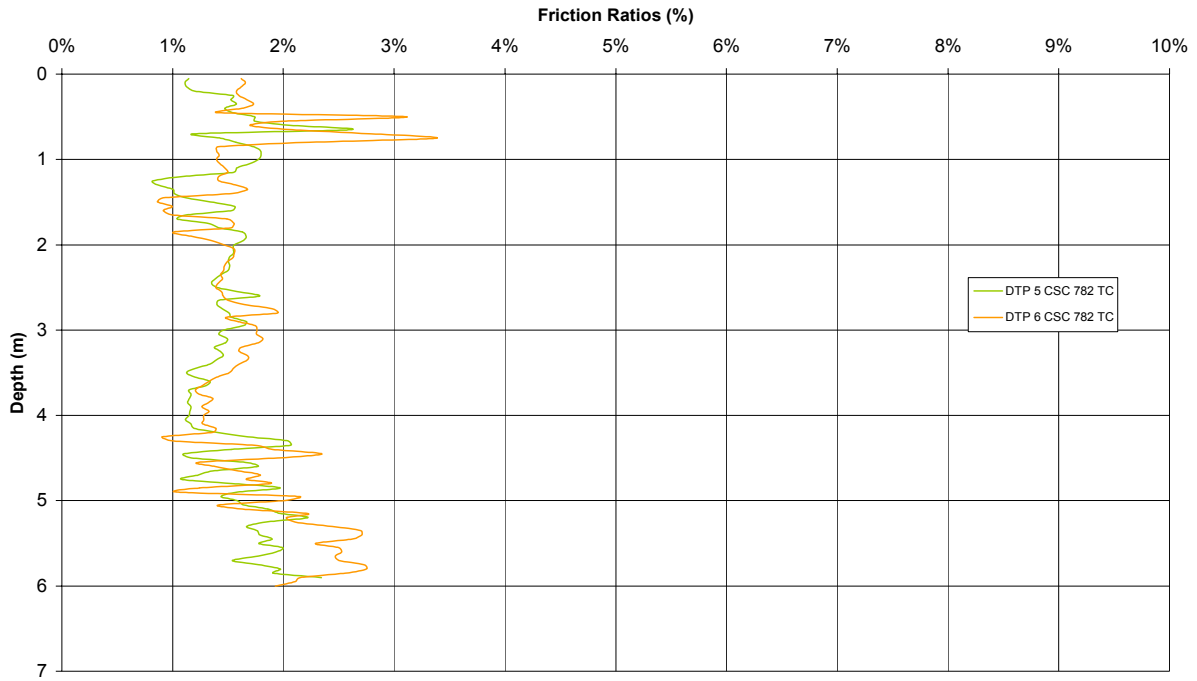


Figure A-80: Port Orange Bridge DTP 1 & 2 Tip Ratios vs. Depth

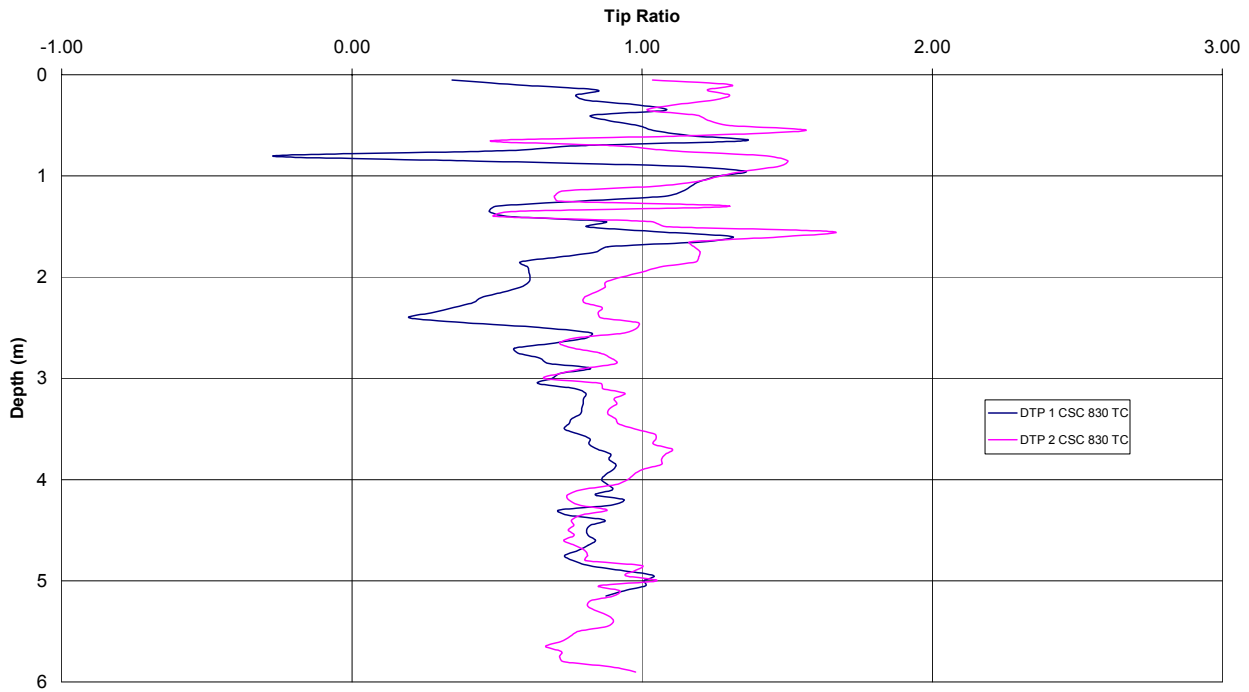


Figure A-81: Port Orange Bridge DTP 3 & 4 Tip Ratios vs. Depth

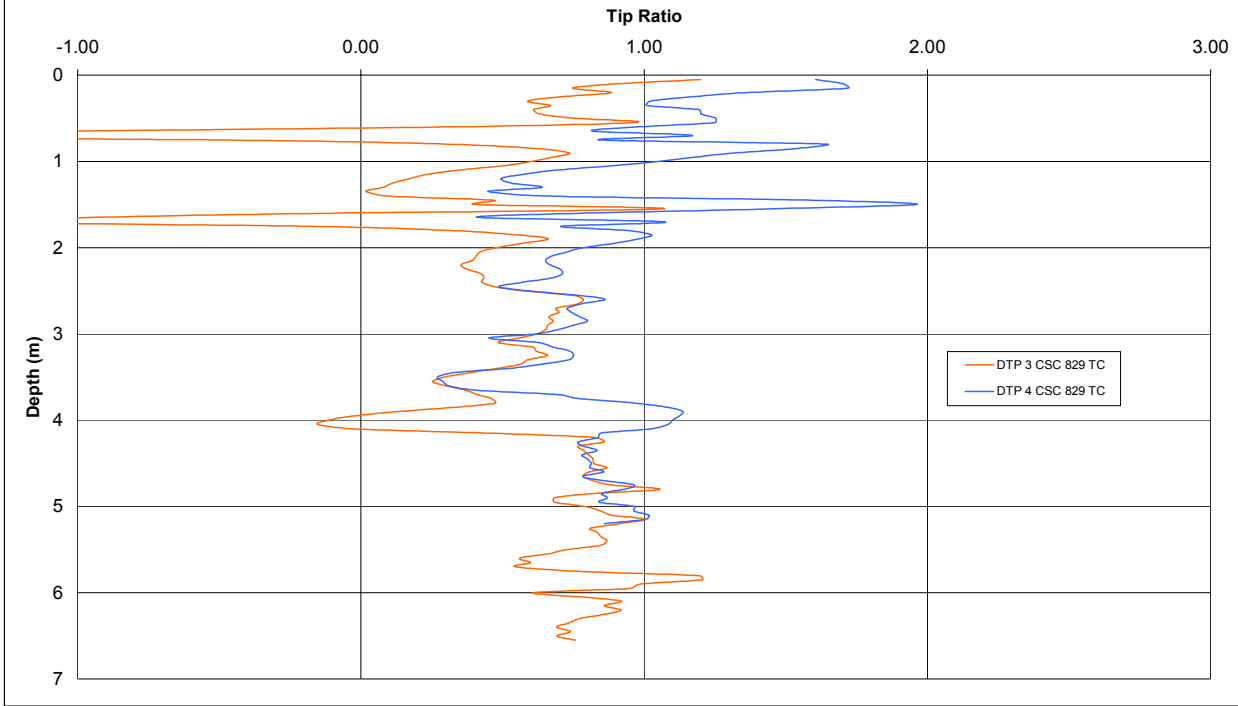
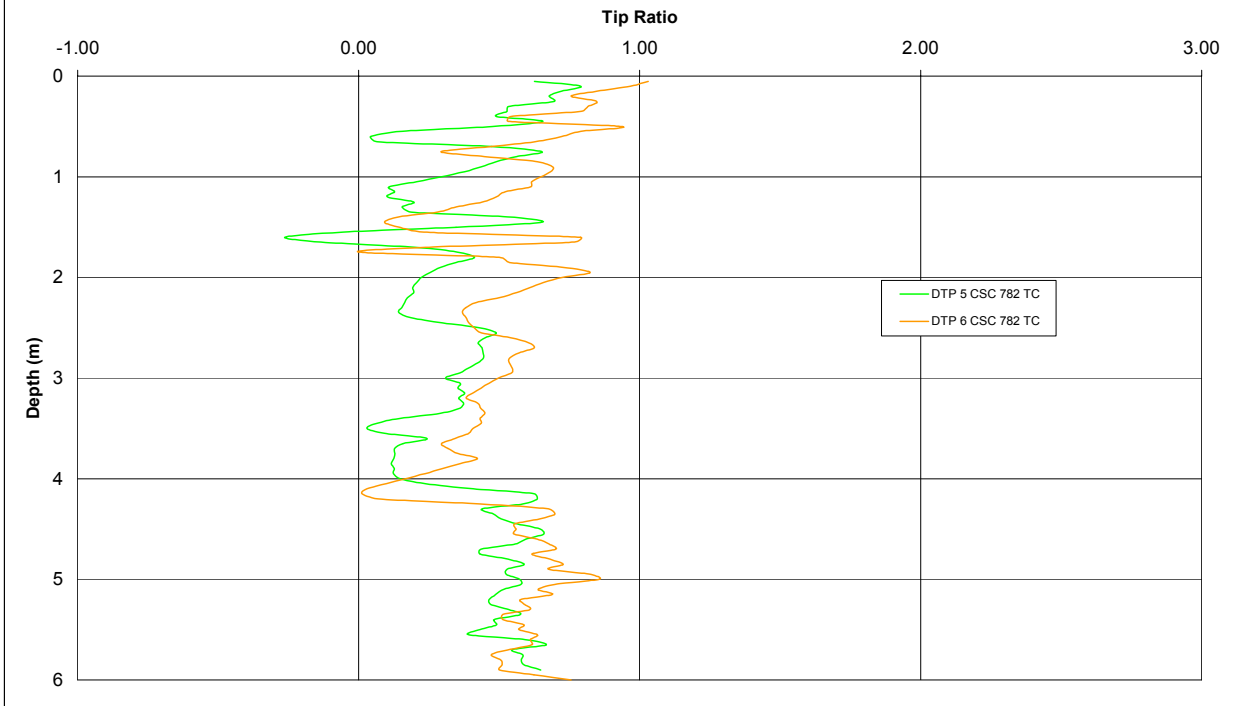


Figure A-82: Port Orange Bridge DTP 5 & 6 Tip Ratios vs. Depth





**APPENDIX B**  
BUSTAMANTE & GIANESELLI VALUES FOR WEST BAY  
BRIDGE DTPSOUNDINGS 1, 2 AND 4









DTP #1		2-Jan		15:54 JV/CK		M[S]T2		Bustamante & Gianaselli Method															
West B&FI		CSC782TC		1		3 1 .05 .1		Determining Tip Capacity						Determining Friction Capacity									
Depth		Tip 1		F. Slve		Inc.		Tip 2*		FR (%)		Tip		Tip 1		Tip 2*		Tip 1		Tip 2*			
(m)		(MPa)		(Kpa)		(deg)		(MPa)				Ratio		Q'ca		Q'ca		α/cpc		α/cpc			
														Qca		Qca		fp		fp			
														Tip 1		Tip 2*		Fs		Fs			
														Tip 1		Tip 2*		(MN)		(MN)			
18.85	6.41	37.4	6.27	10.91	0.58%	1.70								6.41	10.91	645 sq.in.							
18.9	6.7	47.1	6.27	12.84	0.70%	1.92								6.7	12.84	##### sq.m.							
18.95	6.75	56.8	6.39	13.72	0.84%	2.03								6.75	13.72								
19	6.695	35.7	6.42	12.44	0.53%	1.86								6.695	12.44								
19.05	6.64	38.9	6.57	11.02	0.59%	1.66								6.64	11.02								
19.1	5.9	35.2	6.57	11.04	0.60%	1.87								5.9	11.04								
19.15	6.2	35.5	6.58	11.03	0.57%	1.78								6.2	11.03								
19.2	5.94	33.9	6.63	9.99	0.57%	1.68								5.94	9.99								
19.25	5.18	25.9	6.63	8.92	0.50%	1.72								5.18	8.92								
19.3	5.11	28.8	6.63	9.48	0.56%	1.86								5.11	9.48								
19.35	5.17	30.6	6.63	9	0.59%	1.74								5.17	9								
19.4	5.5	24	6.63	9.17	0.44%	1.67								5.5	9.17								
19.45	5.22	17.2	6.63	7.91	0.33%	1.52								5.22	7.91								
19.5	4.88	19.4	6.64	7.58	0.40%	1.55								4.88	7.58								
19.55	5.14	26.6	6.68	8.22	0.52%	1.60								5.14	8.22								
19.6	5.84	23.2	6.69	8.97	0.40%	1.54								5.84	8.97								
19.65	6.37	26.5	6.7	10.27	0.42%	1.61								6.37	10.27								
19.7	5.45	30.5	6.99	9.16	0.56%	1.68								5.45	9.16								
																		Total Skin Capacity		#####		5.7E+05 lbs	
																		Tip Area					
																		Total Tip Capacity Tip 1		Tip 2*		Qb	
																						1.61 2.39 MN	
																						##### 2.4E+06 N	
																						##### 2.4E+05 kg	
																						##### 5.4E+05 lb	
																						361 536 kips	
																		Note: Tip 2 Results for DTP 1 not usable since Cone CSC 782 TC had problems.					









DTP #2-Feb		11:15 JV/CK		M[	SIJT2				Bustamante & Gianaselli, Method														
West FI		CSC782TC1			3	2	.05	1	2	3	4	Determining Tip Capacity						Determining Friction Capacity					
Depth (m)	Tip 1 (MPa)	F. Slve (Kpa)	PW (Kpa)	Inc. (deg)	Tip 2* (MPa)	FR (%)	Tip Ratio	Modified				Tip 1				Tip 2*							
								Tip 1 q'ca	Tip 2* q'ca	Tip 1 (MPa)	Tip 2* (MPa)	Tip 1 Qca	Tip 2* Qca	Tip 1 qlcpc	Tip 2 qlcpc	Tip 1 fp (MPa)	Tip 2* fp (MPa)	Tip 1 Fs (MN)	Tip 2* Fs (MN)				
12	8.92	170.9	-85	7.21	5.52	1.92%	0.62	18.64	11.1	8.92	5.52					Total Skin Capacity				2.628	1.065	MN	
12.1	12.3	148.3	-84.7	7.07	6.25	1.21%	0.51					12.3	6.25	kc =	0.50	for Pile Type Group II				2.6E+06	1.1E+06	N	
12.1	12.92	113.9	-84.8	7.11	7.4	0.88%	0.57					12.92	7.4	6.43	3.83	qp				2.7E+05	1.1E+05	kg	
12.2	10.31	100.9	-85.3	7.12	7.12	0.98%	0.69					10.31	7.12	645 sq.in. Tip Area				5.9E+05	2.4E+05	lbs			
12.2	9.6	73.9	-85.4	7.11	5.69	0.77%	0.59					9.6	5.69	0.4161 sq.m.				590	239	kips			
12.3	8.71	64.2	-85	7.07	5.3	0.74%	0.61					8.71	5.3										
12.3	8.17	52.7	-84.2	7.2	4.26	0.65%	0.52					8.17	4.26										
12.4	7.45	45.2	-84.2	7.2	3.42	0.61%	0.46					7.45	3.42										
12.4	7.87	42.7	-83.5	7.32	3.82	0.54%	0.49					7.87	3.82										
12.5	8.27	23.9	-82.8	7.32	4.29	0.29%	0.52					8.27	4.29										
12.5	8.6	21.1	-81.8	7.4	5.05	0.25%	0.59					8.6	5.05										
12.6	9.03	20	-82.3	7.41	5.72	0.22%	0.63					9.03	5.72										
12.6	8.35	36.1	-81.1	7.59	5.17	0.43%	0.62					8.35	5.17										
12.7	8.21	24.4	-80.5	7.62	4.5	0.30%	0.55					8.21	4.5										
12.7	7.4	13.6	-79.7	7.8	3.96	0.18%	0.54					7.4	3.96										
12.8	7.87	29.2	-79.3	7.8	7.51	0.37%	0.95					7.87	7.51										
12.8	8.41	36	-90	7.8	8.33	0.43%	0.99					8.41	8.33										
12.9	8.37	45.1	-81.4	7.81	6.99	0.54%	0.84					8.37	6.99										
12.9	8.89	38.5	-51	8.22	6.1	0.43%	0.69					8.89	6.1										
13	8.24	35.7	-41.3	8.22	6.4	0.43%	0.78					8.24	6.4										
13	9.28	38.1	-27.6	8.22	6.49	0.41%	0.70					9.28	6.49										

Note: Tip 2 Results for DTP 1 not usable since Cone CSC 782 TC had problems.















DTP #4 2-Sep		05:51 JV		M[S]T2		Bustamante & Gianaselli, Method														
WestBay		CSC765TC		1		3		.05		.1		Determining Tip Capacity				Determining Friction Capacity				
Depth (m)	Tip 1 (MPa)	F. Slve (kpa)	Inc. (deg)	Tip 2 (MPa)	FR (%)	Tip Ratio	Modified				Soil Nature	Tip 1		Tip 2		Tip 1 Fs (MN)	Tip 2 Fs (MN)			
							Tip 1 q <sub>ca</sub>	Tip 2 q <sub>ca</sub>	Tip 1 (MPa)	Tip 2 (MPa)		Tip 1 q <sub>ca</sub>	Tip 2 q <sub>ca</sub>	αlcpc	αlcpc			fp (MPa)	fp (MPa)	
23.9	3.03	15.4	2.68	3.7	0.51%	1.22						60	60	0.035	0.035	0.0053	0.0053			
23.95	3.31	17.3	2.68	3.58	0.52%	1.08						60	60	0.035	0.035	0.0053	0.0053			
24	3.23	14.3	2.68	3.8	0.44%	1.18						60	60	0.035	0.035	0.0053	0.0053			
24.05	3.59	10.8	2.68	3.97	0.30%	1.11						60	60	0.035	0.035	0.0053	0.0053			
24.1	3.66	20.7	2.68	4.67	0.57%	1.28	785	4.56	3.66	4.67	3.83	4.47	60	60	0.035	0.035	0.0053	0.0053		
24.15	3.55	18.1	2.68	4.31	0.51%	1.21	550	3.19	3.55	4.31			Total Skin Capacity		3.4411	2.7252	MN			
24.2	3.39	25.3	2.68	4.12	0.75%	1.22	1021	5.93	3.39	4.12					3441100	2725202	N			
24.25	3.34	17.3	2.69	3.84	0.52%	1.15			3.34	3.84	kc =	0.50 for Pile Type Group II			351133	278082	kg			
24.3	3.43	16.5	2.69	3.99	0.48%	1.16			3.43	3.99	1.92	2.23	qp		772492	611780	lb			
24.35	3.66	15.9	2.69	3.78	0.43%	1.03			3.66	3.78	645	sq.in. Tip Area			772	612	kips			
24.4	3.78	25.2	2.69	4.26	0.67%	1.13			3.78	4.26	0.4161	sq.m.								
24.45	3.75	24.7	2.69	4.35	0.66%	1.16			3.75	4.35										
24.5	4.13	22.7	2.69	5.08	0.55%	1.23			4.13	5.08										
24.55	4.52	25.1	2.69	5.49	0.56%	1.21			4.52	5.49										
24.6	4.59	24	2.69	6.03	0.52%	1.31			4.59	5.93					0.79754	0.92954	MN			
24.65	4.73	30.1	2.69	5.88	0.64%	1.24			4.73	5.88					797540	929541	N			
24.7	4.61	24.5	2.69	6.12	0.53%	1.33			4.61	5.93					81382	94851	kg			
24.75	4.95	30.6	2.69	6.59	0.62%	1.33			4.95	5.93					179040	208672	lb			
24.8	5.13	28.3	2.69	6.7	0.55%	1.31			4.99	5.93					179	209	kips			
24.85	4.91	26.6	2.7	6.58	0.54%	1.34			4.91	5.93										
24.9	4.78	25.5	2.7	6.19	0.53%	1.29			4.78	5.93										
24.95	4.46	20	2.7	5.19	0.45%	1.16			4.46	5.19										
25	4.35	24.7	2.7	5.01	0.57%	1.15			4.35	5.01										
25.05	4.04	27.9	2.7	4.96	0.69%	1.23			4.04	4.96										
25.1	4.35	27.8	2.71	5.73	0.64%	1.32			4.35	5.73										
25.15	4.63	27.5	2.71	6.24	0.59%	1.35			4.63	5.93										
25.2	4.86	33.3	2.79	6.63	0.69%	1.36			4.86	5.93										
25.25	4.76	34.4	2.8	6.74	0.72%	1.42			4.76	5.93										

**APPENDIX C**  
INSTRUCTIONS FOR PERFORMING DTP SOUNDINGS

## DTP SOUNDING INSTRUCTION

### Data Acquisition Equipment

Before performing a sounding the data acquisition system must be adjusted so that it can recognize the Dual Tip Penetrometer. The data acquisition equipment is the same as that used for cone penetration soundings, consisting of a computer, a keyboard and a printer. Most cone soundings performed today at the University of Florida make use of 4 of the channels within the cone penetrometer. These channels collected readings for tip resistance, friction sleeve resistance, inclination, and pore pressure. The Dual Tip Penetrometer uses a fifth channel for recording tip 2 resistance. The CPTSND program used for standard cone penetration tests must be altered by adding four new files: a new cone file (with the extension .cnf) to identify the new cone as the DTP, and three new units files containing unit conversions for data collection in both Metric (kg/square cm. and mpa) and English (tons/square ft.) units.

### Testing Procedure

The following instructions for performing DTP soundings applies to testing using the University of Florida's cone truck. Any testing performed with other insitu soil testing mobile units may require somewhat altered instructions than those that follow.



Figure C - 1: University of Florida Cone Truck

Once the truck is driven to the appropriate testing location, the Dual Tip Penetrometer soundings can begin. The first step is to level the truck using the two rear pads and front plate, which are advanced using four hydraulic levers. A simple carpenter's level, placed on the chuck assembly, can be used to ensure that the truck is horizontal in both the front-to-back and side-to-side directions. Next, the Dual Tip Penetrometer is prepared for a sounding. The screw threads near the end of the DTP should be lubricated with a small amount of gray silicon grease. The cone cable is what connects the penetrometer to the cone computer. The cone cable is threaded through the cone rods and placed through the friction reducer where it connects into the penetrometer. Before threading the end through the friction reducer the half-moon shaped metal clip and metal ring with threads must be removed. After threading through the friction reducer these pieces are placed again on the electronic end. The electronic connection is then pushed into the end of the Dual Tip Penetrometer until the cable

electronics are seated snugly into the penetrometer's housing. The metal ring with the screw threads is wrench tightened to the female portion of the penetrometer. The friction reducer must be hand tightened to the large male-end screw threads at the end of the tip, while taking care, at ALL TIMES, TO NOT TURN THE PENETROMETER when it is plugged into the cable. Rather, the penetrometer should be held still while turning the friction reducer. Failure to do so could result in expensive damage to the internal connections of the penetrometer. The friction reducer and tip should be placed into the vise grips on-board (the tip should never be in the actual clamps of the vise), and the first push rod wrench tightened to the friction reducer.

Once the tip, friction reducer, and initial rod are securely connected, the rod guide is slid onto the first rod. The entire assembly is lowered slightly (tip first) into the hole in the floor of the truck, then raised until the push rod rests on the chucks in the hydraulic ram. The assembly should be hanging above the ground by the chucks. If this is not the case, the assembly should be removed from the chucks, the chuck position reversed, and the assembly replaced inside the chucks.

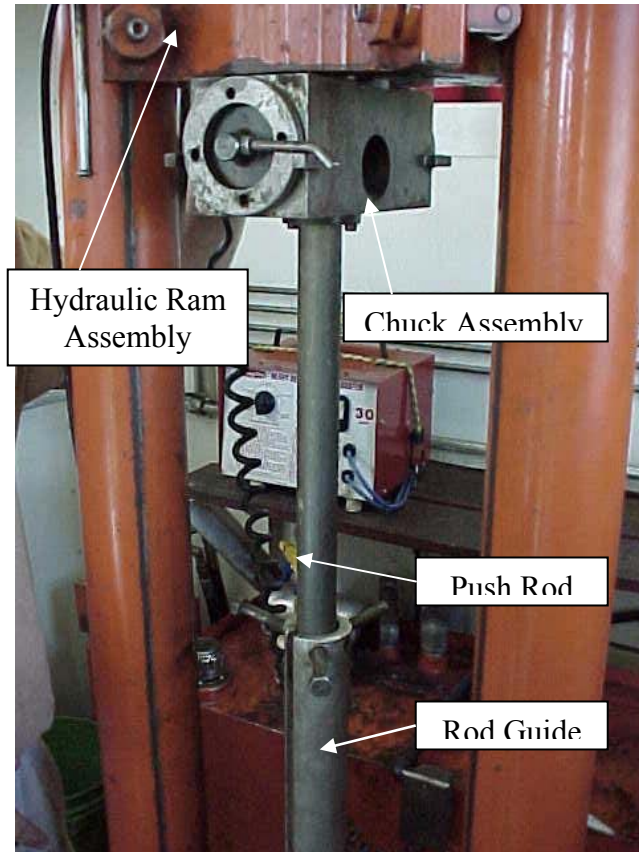


Figure C – 2: Hydraulic Ram Assembly with Rods and Rod Guide

With the penetrometer hanging from the chucks several feet above the ground surface, the computer acquisition system can be started. The computer could have been started earlier as long as the cone cable is connected to the penetrometer and all the connections for the computer and printer are correctly attached. The DTP is supposed to be used with the CPTSND software. After selecting the appropriate cone identification (designated “10T T2” for 10-ton, with a tip 2), and active channels (tip 1, tip 2, inclination, pore pressure (optional) and friction sleeve) the correct project information should be entered. After the DTP has warmed up for about 10 to 15 minutes a baseline should be recorded with the penetrometer still hanging slightly above the ground. The sounding should

be started on the computer. However, data acquisition will only begin once there is a load on tip 1.

With the system still in place in the chucks, another push rod should be hand tightened into the first push rod. The assembly is raised in the chucks by lifting the push rods by hand, and reversing the chuck position. The push rods should be lowered SLOWLY until the tip touches the ground. The ram is next raised with the fast lever until the chucks “click” into position in the groove at the top of the last push rod. The penetrometer is then advanced with the slow lever at 2 centimeters per second. When the ram assembly nears the lower end of its range of motion, some WD-40 should be sprayed into the female end of the advancing push rod, and a new rod hand tightened into this end. The ram is then raised with the fast lever, stopping again when it “clicks” into the groove at the top of the newly-added push rod. Advancing is resumed with the slow lever. This process is repeated until the desired depth is reached or significant resistance/ inclination is encountered. Excessive loads or inclinations could lead to damage of the DTP or rods.

During advancement the computer displays a plot of tip 1 resistance versus depth, as well as the magnitudes of tip 1, friction sleeve, friction ratio, inclination, and tip 2 for the last 4 depths recorded. This plot should be monitored at all times during advancement to ensure the penetrometer was not being pushed into soil that produced readings outside of normal operating ranges. The software also contains an automatic safety shut-off device to protect the penetrometer. If the tip 1 resistance or inclination rises too sharply, the system recognizes the presence of a stiff layer and shuts down the penetration. The DTP can be

advanced further by pressing the override button. This should be done using extreme caution due to the risk of damaging the penetrometer or rods.



Figure C - 3: On-Board CPT Data Acquisition Computer

Upon reaching the desired depth the sounding should be ended by pressing the correct button on the computer keypad. The system of push rods and penetrometer tip must then be removed from the ground. To do this, the ram is raised just above the last push rod and the chuck position reversed. The ram must be carefully lowered (with the slow lever) until it “clicks” into the groove on the push rod. Once in place, the ram is raised near its topmost position, then lowered back down with the fast lever. Once the ram clicks into position on the next lower rod, the upper rod is free to be removed and stacked into the rod housing. The ram must be raised again, and this procedure repeated until the entire assembly is removed from the ground. When raising the rods the friction of the soil keeps the rods from sinking



under its own weight. However, near the surface there is usually not enough friction between the rods and the surrounding soil to keep the rods from sinking and a wrench should therefore be placed on the push rod near the floor of the truck to keep the rods from falling. A second baseline should be taken when the penetrometer is out of the ground and still hanging, similar to its position when the initial baseline is recorded. The penetrometer and its connections should be taken apart by following the construction instructions in reverse, taking note to never turn the tip when the cable is plugged in. The data is automatically saved into the default directory on the hard drive, and should be saved to a 3.5-inch floppy disk. The truck can then be lowered from the leveling pads, and moved to a new location for more testing. The output file is a .cpd file and can be analyzed with the DTP 2002 software. The output file data can also be reduced with microsoft excel or viewed with notepad.